

# **INTERNATIONAL HARMONISED RESEARCH ACTIVITIES SIDE IMPACT WORKING GROUP STATUS REPORT**

**Craig Newland**  
**Chairman**  
**On behalf of IHRA Side Impact Working Group**

Paper Number 05-0460

## **ABSTRACT**

This paper reports on the status of work of the International Harmonised Research Activities (IHRA) Side Impact Working Group (SIWG) as at its 23<sup>rd</sup> meeting prior to the 19<sup>th</sup> ESV conference in Washington in June 2005. This includes decisions made and the reasons for them and represents a final report on this phase of the IHRA work.

## **INTRODUCTION**

At the 2003 ESV conference, the International Harmonised Research Activities (IHRA) Side Impact Working Group (SIWG) reported a suite of draft test procedures designed to enhance safety in real world side crashes.

The draft test procedures proposed in 2003 represent a complementary suite of procedures designed to provide a range of test conditions encompassing a range of occupant sizes, seating positions and impact conditions to minimise the incentive for sub-optimisation of vehicle designs to specific test conditions. Hence, a mobile deformable barrier (MDB) to vehicle test with fifth percentile female dummies has been proposed to address vehicle to vehicle side impact crashes and a vehicle to pole test with a fiftieth percentile male dummy has been proposed to address vehicle to narrow object crashes. In addition, an interior surface headform impact test has been proposed to reduce head injury risk that may arise under different impact configurations than those specified by the MDB and pole impact test procedures. To ensure that no detrimental effects are generated by design changes to meet the testing requirements, a set of out of position test procedures are also proposed.

The IHRA SIWG undertook to coordinate an evaluation program by members of these test procedures over the period 2003-2005, with the aim of reporting recommended test procedures to enhance real world safety in side crashes at ESV 2005. The

IHRA SIWG provides a crucial framework for targeting studies and research efforts. Currently, no other global framework exists under which this collaborative research effort may be conducted.

## **BACKGROUND**

A steering committee was set up at the 15th Enhanced Safety of Vehicles (ESV) conference in Melbourne in 1996 to work towards a harmonised vehicle safety research agenda to avoid duplication of research. This is the International Harmonised Research Activities (IHRA) Steering Committee comprising government representatives including vehicle safety regulators from around the world. It was agreed that IHRA be responsible for overseeing research activities in six key areas.

One of the original key areas, functional equivalence, was replaced by side impact following the 16th ESV conference in Windsor, Canada in 1998. The six working groups under IHRA after the 16th ESV are shown below with each group chaired by the country in parenthesis:

- Side impact (Australia)
- Advanced frontal crash protection (Italy)
- Vehicle compatibility (United Kingdom)
- Biomechanics (USA)
- Pedestrian safety (Japan)
- Intelligent Transport Systems (Canada)

At the 17th ESV in Amsterdam, progress was again reviewed and it was decided to amalgamate the Advanced Frontal and Vehicle Compatibility Working Groups with the resulting five groups tasked for a further 4 years with a review at each ESV. The Steering Committee also agreed to a revised set of Terms of Reference for the Side Impact Working Group (SIWG).

The various IHRA working groups generally consist of about 10 members to ensure that progress is as

speedy as possible. Although IHRA is essentially a government group, industry has been invited with a total of three representatives in each working group, one each from North America, Europe and Asia-Pacific regions. This maximises outcomes by engaging vehicle manufacturers in the research process so that countermeasures can be designed into vehicles as soon as possible.

## SIWG MEMBERSHIP

The current members of the IHRA Side Impact Working Group are:

Craig Newland	Department of Transport and Regional Services, Australia (Chair)
Mark Terrell / Duncan Lockie	Department of Transport and Regional Services, Australia. (Secretaries)
Dainius Dalmotas	Transport Canada
Suzanne Tylko	Transport Canada
Adrian Roberts	EC/EEVC
Michiel van Ratingen	EC/EEVC
Joseph Kianianthra	National Highway Traffic Safety Administration, USA
Hideki Yonezawa	National Traffic Safety and Environment Laboratory, JMLIT
Minoru Sakurai	JARI
Atsushi Hitotsumatsu	OICA Asia-Pacific/JAMA
Michael Leigh / Stuart Southgate	OICA North America/AAM
Christoph Mueller	OICA Europe/ACEA
Keith Seyer	OICA Asia Pacific/FCAI

Past members:

Robert Hultman	OICA North America/AAM
Haruo Ohmae	JARI
Takahiko Uchimura	OICA Asia-Pacific/JAMA
Rainer Justen	OICA Europe/ACEA
Richard Lowne	EC/EEVC
Akihisa Maruyama	OICA Asia-Pacific/JAMA
Keith Seyer	DOTARS (Chair)
Mark Terrell	Department of Transport and Regional Services, Australia (Secretary)

## TERMS OF REFERENCE

At its 12<sup>th</sup> meeting, the SIWG finalised the revised Terms of Reference which states the objectives of the group, the outcomes of its first 2-year term, the

activities to be undertaken in the future and a timeframe for these. These are summarised below.

### Objective

Co-ordinate research worldwide to support the development of future side impact test procedure(s) to maximise harmonisation with the objective of enhancing safety in real world side crashes.

### Scope

In its first 2-year term, the Side Impact Working Group (SIWG) concluded that new test procedures to address the side impact problem should include:

- A mobile deformable barrier to vehicle test
- A vehicle to pole test
- Sub-systems head impact test
- Out of position airbag evaluation

In its next term, the SIWG will also coordinate research to examine the feasibility of improving side impact protection for occupants on the non-struck side and develop a test procedure to evaluate such protection.

### Activities

The SIWG is working towards achieving these goals by:

1. Reviewing any new real world crash data to prioritise injury mechanisms and identify associated crash conditions taking into account likely future trends.
2. Taking into account the need to protect both front seat and rear seat(s) adult and child occupants.
3. Interaction with the IHRA Biomechanics Working Group to monitor the development of harmonised injury criteria.
4. Interaction with the IHRA vehicle compatibility working group to ensure solutions in one area do not degrade safety in another.
5. Monitoring and, as appropriate, providing input to the development of WorldSID and any other side impact dummy.
6. Determining the greatest degree of harmonisation feasible and the design and vehicle safety performance implications of adopting different levels of test severity or the worst case condition.
7. Coordinating the evaluation of proposed test procedures subject to availability of test dummies and injury criteria.

## Timeframe

While the progress of the group will be reviewed every 2 years, it is expected that:

- The target date for draft final proposal of test procedure(s) is 2003 ESV
- The target date for final proposal of test procedure(s) is 2005 ESV with validation in the intervening 2 years.

The test procedure(s) would include the best available dummies as recommended by the IHRA Biomechanics Working Group (BWG) (for example, the harmonised test dummy being developed by the ISO WorldSID Task Group ([www.worldsid.org](http://www.worldsid.org))). The BWG will also advise on availability of any other suitable test dummies and the injury criteria to be used.

Members noted that there are differences in fleet compositions around the world but were hopeful that research could be focused on these differences to determine whether they had a quantifiable effect on the injury risk in side impacts.

## SUMMARY OF RESEARCH

### Methodology

To determine the side impact trauma problem that needed to be addressed, the group began by examining real world crashes in the 3 major geographical regions, North America, Europe and Asia-Pacific, to identify the:

- types of side impact crashes occurring
- injuries being sustained by body region
- causes of these injuries, where possible
- characteristics of the drivers and passengers most at risk (gender, size, seating position, etc)

For vehicle to vehicle crashes, members were asked to report on any research that examined the effects on injury risk of mass, stiffness and geometry of striking vehicles together with any other parameters that were considered important for side impact protection.

There has been close cooperation and communication between the SIWG and other IHRA WGs on advanced frontal, vehicle compatibility and biomechanics, and with the WorldSID Task Group.

## Real World Crash Studies

As part of the IHRA Biomechanics Working Group (BWG) task to define the real world side impact safety problem, Transport Canada analysed the real world crash data submitted by the various regions. This study, to be reported by the IHRA BWG, indicated that:

- Collectively, side impacts involving vehicle to vehicle crashes and vehicle to narrow object crashes constitute about 90% of the side impact trauma. However, the frequency of involvement of specific vehicle types and narrow objects varied from region to region.
- Most of the trauma in side impacts occurs to struck side occupants.
- Up to 40% of the trauma to occupants of the struck car in side crashes occurs to non-struck side occupants depending on the geographical region.
- The head and chest were consistently the most frequently injured body regions.
- The frequencies of abdominal, pelvic and lower extremity injuries were also significant, but varied with geographical region.
- The main contact points causing injury to struck side occupants were door structure, exterior object and B-pillar.
- Depending on the region, the proportions of male and female severely or fatally injured occupants in vehicle-to-vehicle crashes were either similar or slightly predominated by females (up to 60%).
- Young males predominated in vehicle to narrow object crashes.
- Elderly occupant casualties were over-represented in vehicle to vehicle crashes.
- Rear occupants account for less than 15% of road trauma in side impacts.

The above research, combined with the need to ensure enhanced side impact protection for all adult occupants, would indicate the importance of using a small adult female test device in the front driver position in an MDB to vehicle test and using a mid sized adult male test device in a vehicle to pole test. Regulators may wish to specify requirements for other dummy sizes, if crash statistics indicate such a need for a particular region.

## **Parametric Studies on Effect of Mass, Stiffness and Geometry on Dummy Response**

Research conducted within IHRA found differences in the makeup of the vehicle fleets in each of the global regions.

Since a mobile deformable barrier (MDB) represents a striking vehicle, it was noted that it may be difficult to propose a single MDB representative of striking vehicles from all global vehicle fleets. Jurisdictions in which the striking vehicles are predominantly passenger cars felt that it may not be appropriate for them to consider an MDB representing an SUV.

A number of parametric studies have been conducted to examine the effect on injury risk of the mass, stiffness and geometry of the striking vehicle in side impacts. The data presented to the SIWG included results from:

- A computer simulation by the UK Transport Research Laboratory
- A cooperative project of full-scale tests by the Australian Department of Transport and Regional Services and Transport Canada.
- A full-scale test series by the US Insurance Institute for Highway Safety (IIHS).
- Full scale tests by Transport Canada.
- A computer simulation by the NHTSA.
- Full-scale tests and FEM simulations of front-end structures of impacting vehicles for the comparison with current European MDB face by JAMA.
- Full scale tests by JMLIT.

Based mainly on single parameter variations, these data supported the following conclusions on the factors that increased dummy response:

- Raising ground clearance of the striking vehicle/trolley had the greatest effect (mainly due to a reduction in engagement of the side sill of the struck vehicle).
- Increasing the mass and stiffness of the striking vehicle/trolley has a lesser effect.
- A perpendicular impact of the striking vehicle/trolley maximises the loadings to the driver when compared to crabbing the vehicle/trolley.
- Non-homogeneous barriers generate more “punch-through” than homogeneous ones.

It was also noted that:

- In high frontal profile striking vehicles such as 4WDs/Light Trucks and Vans (LTVs) there is typically less engagement of the sill and floorpan of the struck vehicle and these striking vehicles are more likely to load the head (from contact with the high hood/bonnet) and chest (from the higher intrusion profile).
- Typically, injuries occur (40-50 msec after impact) before momentum transfer to the struck vehicle occurs (around 70 msec).
- The stiffness ratio between the front and side structure of vehicles is so high that, for the same geometry, variation in front structure stiffness has little effect on dummy response.

Some of these studies also included increasing impact speed which was found to have an effect similar to increasing ground clearance. For example one of the studies showed that increasing the speed from 50 to 60 km/h had the same or similar effect on dummy responses as increasing the ground clearance from 300 mm to 400 mm.

Compound variations of mass, stiffness, geometric and velocity parameters were not investigated.

### **Non-Struck Side Test Research**

Members agreed that there should be a test to evaluate injuries to non-struck side occupants because real world crash data attributed up to 40% of road trauma to this group depending on the geographic region. In the US, FMVSS201 addresses this problem to some extent.

The SIWG received information regarding preliminary research and a work plan for a collaborative program between General-Motors Holden's, Monash University, George Washington University, Virginia Tech, DOTARS and Autoliv. This work showed that current dummies are unlikely to provide correct kinematics but that WorldSID's design showed promise. This work is reported elsewhere in this ESV. However, there is much more to be done in this area and should be given a higher priority in the SIWG's considerations in the future.

### **CONCLUSIONS**

After reviewing further research data, members confirmed that the IHRA Side Impact test procedure should comprise:

1. A mobile deformable barrier to vehicle test to simulate the vehicle to vehicle crash condition.
2. A vehicle to pole test to simulate the vehicle to narrow object crash condition.
3. Sub-systems interior surface head impact test to address the risk of head injury under crash conditions other than the specific MDB and pole tests.
4. Out-of-position side airbag evaluation test(s).

Draft test procedures were proposed in the status report from the IHRA Side Impact Working Group at ESV 2003. During 2003-2005, a number of organisations have commenced validation of these draft test procedures.

Since a recommendation for suitable test device(s) and injury criteria has not been made by the IHRA Biomechanics Working Group, the validation work has been undertaken using a range of existing side impact dummies and injury criteria. It is anticipated that further verification testing may be required when test dummies and criteria are recommended.

The following sections will discuss the progress and status of work conducted by the IHRA SIWG on each of these tests.

## **MOBILE DEFORMABLE BARRIER (MDB) TEST**

Defining the parameters of the Mobile Deformable Barrier (MDB) test has proven to be the most challenging task for the group. While the group was hopeful of recommending only one MDB test, it became clear that this would be difficult because of the fleet differences between regions around the world.

In North America, LTVs currently account for approximately 50% of all new light vehicle sales (cars, light trucks and vans). In other regions there has been an increase in the popularity of “soft-roaders”/small 4WDs, although not to the same extent as North America. While smaller and lighter than traditional 4WDs, their high geometry front structures present similar problems to vehicles they strike.

Therefore, the group agreed to consider two MDB test procedures to be taken into the validation phase which may result in further refinements:

1. An MDB test using a barrier based on a passenger car/small 4WD-type bullet vehicle.

This will initially be the Advanced European (AE)-MDB test procedure currently being developed by the EEEVC.

2. An MDB test using a barrier based on a LTV type vehicle. This will initially be the Insurance Institute for Highway Safety (IIHS) MDB test procedure currently being used by the IIHS.

The group noted that:

- A single “worst case” test would be the ideal for harmonisation. However, this could only be achieved if the proposed more severe test could be guaranteed to provide at least the same degree of protection for all significant body regions as generated by the less severe test.
- By taking at least 2 draft test procedures (eg the new draft AE-MDB and the IIHS MDB) into the validation phase, there would be some latitude to develop and select appropriate tests for the different fleet mixes and to examine whether the worse case test option is feasible.
- The accident data indicated that, at a minimum, a small female dummy should be used in the MDB tests and a mid-sized dummy should be used in the pole test.

A number of side impact parametric studies were reported to the group, including both physical testing and computer simulation, evaluating the influence of MDB characteristics on injury risk and vehicle structural behaviour. These concluded that the ground clearance of the front of the MDB (and consequent reduction in engagement of the side sill of the struck vehicle) had a major effect on injury risk, whilst MDB mass and stiffness has only a minor effect. This formed the basis for the proposed MDB mass of 1500kg - probably lighter than a typical striking vehicle in some jurisdictions, but heavier than a typical striking vehicle from other jurisdictions, but with the effect of mass not such an important factor. Further, the perpendicular impact mode provided more severe load conditions for the driver, while the force – deflection response of etched (progressive) honeycomb barriers was different in the crabbed mode to perpendicular mode. For these reasons, perpendicular impact is the preferred impact mode as reported in the previous IHRA SIWG status report. Since this report, NHTSA has expressed some concerns regarding this position.

Accident studies from Asia-Pacific, North America and Europe have shown that 50 km/h would be an appropriate perpendicular impact speed for the MDB.

The geometric and stiffness requirements for a proposed MDB were not as easy to reconcile. Since the Insurance Institute for Highway Safety (IIHS) had already finalised a specification for its side impact assessment, the IHRA SIWG agreed to consider this test procedure as a potential candidate procedure on the basis that this barrier had been designed to represent a large SUV striking vehicle. In parallel, EEVC Working Group 13 had been developing a new MDB (known as the AE-MDB) to represent small SUVs and passenger car striking vehicles.

### **Advanced European (AE)-MDB Test Procedure**

The AE-MDB is designed to provide an impact environment similar to that seen in car-to-car and small 4WD-to-car side impacts. The objective has been to

- (i) provide a sufficiently stringent test condition for the rear seat dummy while maintaining the same level of severity for the front seat dummy
- (ii) provide a perpendicular test
- (iii) provide a severity of test appropriate for a predominantly car-based fleet mix.
- (iv) develop test conditions that would require protection measures that would be effective in real car-to-car impacts (i.e. that could not be overcome by vehicle design changes optimised for the MDB but that would not work in many car-to-car accidents).

The car-based barrier test, to be used within the IHRA SIWG suite of test procedures is being developed by EEVC Working Group 13. A report on the status of this research is being prepared by WG13 (Roberts et al, 2005.) Since the last IHRA SIWG progress report the external shape of the AE-MDB has remained unchanged but its specification has developed to incorporate the manufacturing and build features as is specified in the revised ECE Regulation (R95/02) MDB face and the principle of 'progressive stiffness' honeycomb. EEVC has also developed the dynamic crush certification corridors to reflect the geometric characteristics of the barrier.

It is important that the advanced barrier is appropriate for use in a range of different loading conditions. At the time of the previous ESV report WG13 had been assessing the AE-MDB performance against the results of two struck vehicles being struck by two other vehicles, in moving car to moving car tests. The target cars were the Toyota Camry and the Renault Megane being struck by a Ford Mondeo, which was

considered to be an 'average European family car' with reasonably good EuroNCAP scores and a Landover Freelander, a typical European SUV, also considered equivalent to a large family car. Since 2002 WG13's research has extended the baseline assessment testing to include the Alfa 147 and Toyota Corolla as target vehicles (both three door vehicles). The Freelander has continued to be one of the bullet vehicles. The other bullet vehicles have been the Toyota Corolla and the Renault Megane. Tests with the AE-MDB, to the revised build specification, have also been performed into these new target vehicles and into the rigid load cell wall as part of certification and repeatability studies.

Further information on the stiffness of modern vehicles has been obtained and has generally confirmed that the force deflections previously used are valid, for this particular loading condition, which has traditionally been used to specify the dynamic performance of European barrier faces used in the European standards.

The IHRA MDB test procedures are expected to use more advanced side impact test dummies (possibly the 5th%ile WorldSID) with enhanced injury assessment capability, as recommended by the IHRA Biomechanics group. The IHRA Biomechanics group has not yet made a recommendation for a 5th%ile side impact dummy. Since the previous IHRA SIWG report in 2003, EEVC WG13 has been evaluating the AE-MDB test procedure using the ES-2 dummy, not with the rib extension modification as this has not been approved for regulatory application in Europe or been recommended by EEVC WG12, the EEVC Dummies group.

The latest full scale tests with the AE-MDB are suggesting that the MDB loading into the struck cars may not be as representative as was hoped when compared to the vehicle to vehicle tests. One suggestion for this is due to the fact the AE-MDB is not interacting with some of the more rigid structures of the struck vehicles, e.g. the stiff B posts. It has also been noted that some front structures of modern cars now incorporate lateral stiffening structures, cross beams, which can form a link across the two outer longitudinals. Research is currently taking place by WG13 and within the EC APROSYS project to investigate changes to the AE-MDB to include such attributes. EEVC WG13 is therefore not in a position to recommend that the AE-MDB barrier, described in the former report is sufficiently well developed for it to be considered for wide spread evaluation within the IHRA suite of test procedures.

It is hoped that a design revision will be agreed upon in the next year. At this point in time the IHRA suite of procedures can not be completed with the AE-MDB test procedure. This has resulted in an inability to compare the two candidate MDB test procedures at this time and hence the IHRA SIWG is not in a position to recommend an MDB test at present.

**Japanese Supportive Research** - Japan has been cooperating with the development of the AE-MDB, as a part of international harmonization research. Impact tests of cars have been conducted using this barrier face to compare the profile of deformation in tested vehicles (crashed vehicles) with the deformation resulting from crashes involving actual vehicles.

Impact tests were performed car-to-car (passenger car to passenger car), AE-MDB-to-car, SUV-to-car, MPV-to-car, etc. Unlike the EEVC WG13 tests, most of these tests were conducted with the centre of the

barrier aimed at the R-point at that time. The results showed that the amount of deformation in test vehicles when crashed against AE-MDB tended to be greater than when crashed against passenger cars, but was likely to be smaller than in crashes with SUVs or MPVs. These results almost satisfied the specification target of the barrier face that simulates vehicles including compact SUVs. Regarding particular parts of crashed vehicles, there were some differences in the profile of deformation around B-pillar in test vehicles when crashed against actual vehicles and when impacted against the barrier face (Fig. 1). When tested with the barrier face, the deformation was smaller at the B-pillar than at the door, with the barrier face itself undergoing significant deformation in the centre. When crashed against actual cars, on the other hand, the amount of deformation was similar at the door and at B-pillar, with the front end of crashed cars showing extensive deformation. The difference is suspected to be due to the influence of the bumper beam that connects the right and left sections of the vehicle's front end.

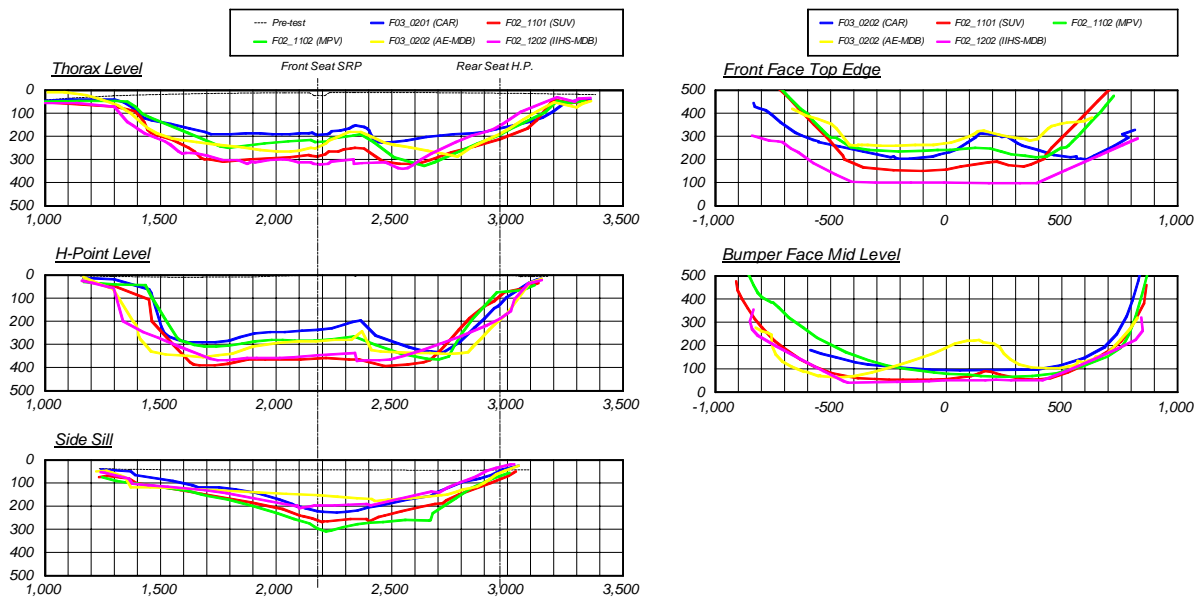


Figure 1. Deformation Profiles of Struck Vehicles (left) and Striking Vehicles (right)

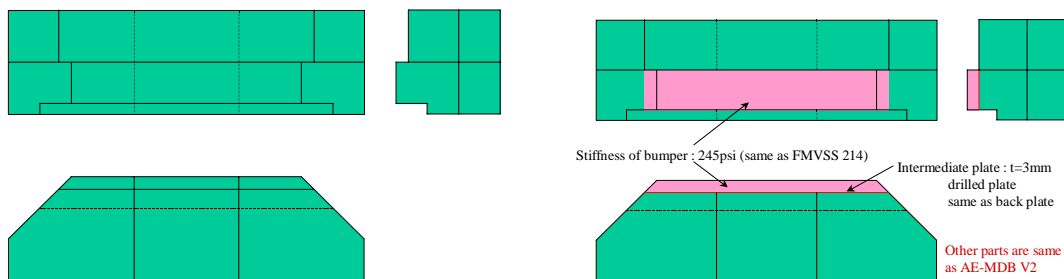


Figure 2. AE-MDB (left) and Japanese Prototype AE-MDB (right)

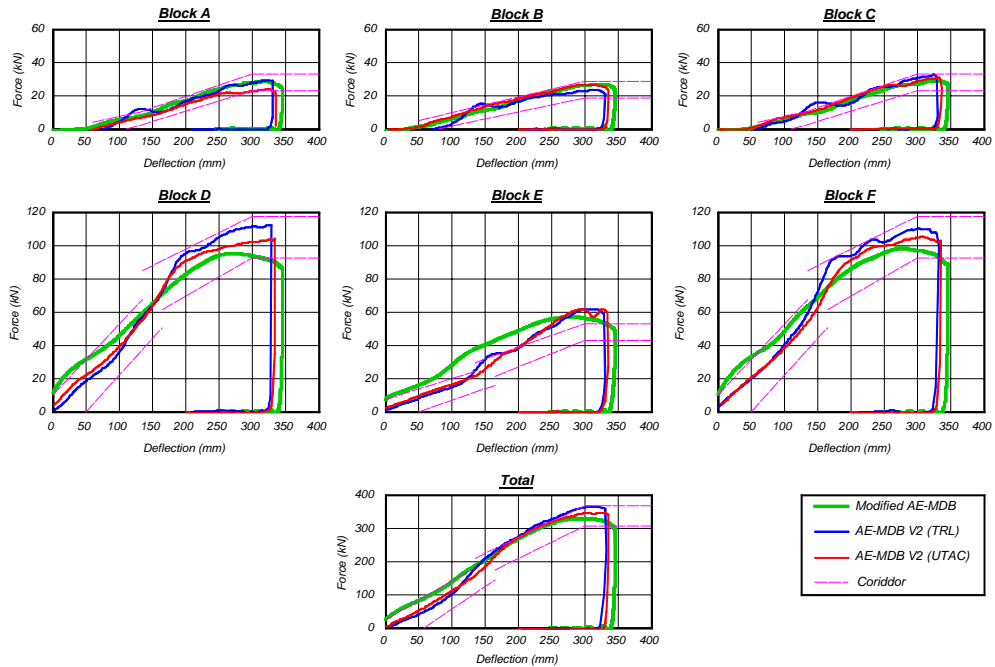


Figure 3. Characteristics of AE-MDB and Japanese Prototype AE-MDB

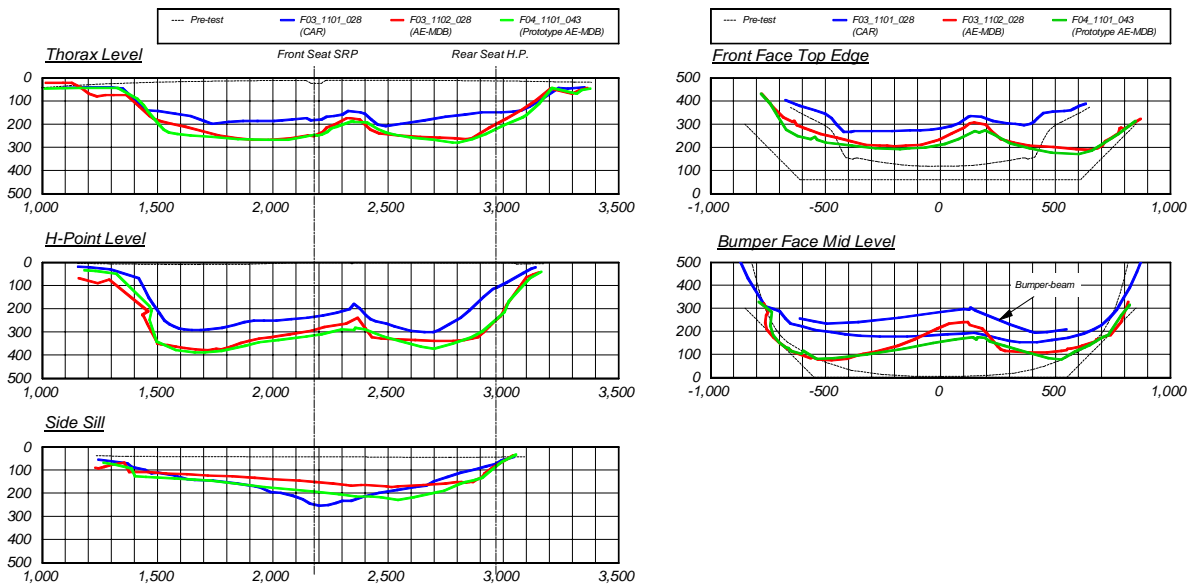


Figure 4. Deformation Profile of Struck Vehicles (left), AE-MDB and Japanese Prototype AE-MDB (right)

In order to decrease this variance, it was suggested to add a bumper to the barrier face. The improved barrier face was trial manufactured and tested for barrier characteristics verification test and for MDB-to-car crashes. The barrier face was improved by replacing the honeycomb sandwich structure at the protrusion of the bumper in the front end of the lower block with stiffer honeycomb to simulate the bumper (or bumper beam) that connects the left and right sections of the vehicle's front end (Fig. 2). This barrier face (modified AE-MDB) is characteristically stiffer at the entire lower block, as the malleable section in the lower block has been replaced with stiffer honeycomb. The lower centre section was found to be even stiffer due to the connection with the right and left blocks (Fig. 3).

Results of modified AE-MDB-to-car crash tests showed that deformation of the struck vehicle was closer to the deformation caused by car-to-car impact tests than that from the conventional AE-MDB. The absolute value of the amount of deformation, however, increased due to the greater stiffness of the barrier face (Fig. 4). The deformation profile of the bumper in the barrier face was similar to the deformation profile of bumper beam in the impacting vehicle in car-to-car tests.

Based on the above results, Japan believes that the next-generation barrier face for side-impact tests could be the AE-MDB with a simulated bumper (or bumper beam). The characteristics of the modified AE-MDB (with a simulated bumper) manufactured here will need to be improved to simulate the stiffness more appropriately within the corridor.

### **IIHS MDB Test Procedure**

The IIHS MDB test consists of a stationary test vehicle struck on the driver's side by a moving barrier fitted with an IIHS side impact deformable face (version 4) ballasted to 1500 kg. The barrier has an impact velocity of 50 km/h (31.1 mph) and strikes the test vehicle on the driver's side at a 90-degree angle. The impact point of the barrier is dependent on the wheelbase of the test vehicle. For a vehicle struck on the left side, the impact point is defined as the distance rearward from the struck vehicle front axle to the left edge of the deformable barrier face when the deformable barrier face makes first contact with the struck vehicle.

The impact point is calculated as follows:

- If wheelbase < 250 cm, then impact reference distance (IRD) = 61 cm
- If  $250 \text{ cm} \leq \text{wheelbase} \leq 290 \text{ cm}$ , then impact reference distance =  $(\text{wheelbase} \div 2) - 64 \text{ cm}$
- If wheelbase > 290 cm, then impact reference distance = 81 cm

The horizontal and vertical impact tolerances at the point of contact between the MDB and the vehicle shall be less than  $\pm 25 \text{ mm}$ .

The moving deformable barrier (MDB) is accelerated by the propulsion system until it reaches the test speed (50 km/h) and then is released from the propulsion system 25 cm before the point of impact with the target vehicle. The impact speed is clocked over a 1 m length of vehicle travel ending 0.5 m before the vehicle's release from the propulsion system.

The MDB braking system, which applies the test cart's service brakes on all four wheels, is activated 1.5 seconds after it is released from the propulsion system. The brakes on the struck vehicle are not activated during the crash test.

APROSYS plans to conduct an evaluation test program of the IIHS MDB and the AE-MDB, specifically investigating the possibility that one of these could be considered a worst case condition. This work is delayed due to specification of the AE-MDB not being finalised.

Transport Canada has conducted an extensive evaluation of the IIHS barrier for comparison with various vehicle to vehicle crashes. Residual deformation and dummy responses from the IIHS barrier were consistent with vehicle to vehicle tests (Arbelaez et al 2002). In addition to the IIHS barrier, Transport Canada evaluated the feasibility of the use of the SIDIIs dummy and concluded that the SIDIIs was suitable (Tylko et al, 2004).

**NHTSA position** - NHTSA decided early on that the barrier research would entail considerable amount of work before an acceptable design could evolve. However, in the interest of a quick evaluation of the suitability of the IIHS test, comparison testing was undertaken. NHTSA conducted five crash tests to compare the FMVSS No. 214 barrier to the IIHS barrier at FMVSS No. 214 and US NCAP speeds. Initial findings from this research concluded that the IIHS barrier stiffness distribution was not representative of pickups and SUVs analysed and the stiffness was relatively high compared to the Ford F-

150. It was also concluded that a higher profile is essential to simulate the then existing fleet in the early 2000.

NHTSA also noted in the early testing, the front-end design may not be quite suitable for crabbed test procedure and the sill engagement was totally absent which had the potential for making the side structures excessively stiff. However much research was necessary to properly design a barrier that would accurately simulate the characteristics of the fleet involved and at the same time not drive vehicle designs that will overly increase their side stiffness. NHTSA noted that AE-MDB and other designs would have to be looked at in more detail and a considerable amount of testing would have to be undertaken before zeroing in on an acceptable design.

#### **VEHICLE TO NARROW OBJECT (POLE) TEST**

The real world crash data clearly indicated that vehicle impacts into narrow objects was an area that needed to be addressed. There was considerably more consensus on the requirements of a vehicle to pole test procedure than for the MDB test. The following has been proposed:

- Moving vehicle to pole test.
- Oblique impact @ 75 degrees to the longitudinal plane of the test vehicle
- Speed of 32 km/h.
- Pole impact to evaluate at least head and thorax protection.
- Mid-sized adult male test device.
- Rigid pole diameter of 254 mm.
- Pole to span at least below sill height to above roof height.

The main area of discussion has been the diameter of the pole and how this relates to the wish to load the head and thorax simultaneously. These two body regions were identified as being the main causes of trauma in impacts into narrow objects. A larger diameter pole was expected to better achieve head and thoracic loading at the same time as well as resulting in a more repeatable test. All regions except the USA initially supported a 350 mm diameter pole. The current FMVSS 201 dynamic pole test utilises a 254 mm diameter pole as does the consumer crash testing procedure used in various countries.

APROSYS has analysed four pole tests with a Subaru Legacy vehicle (equipped with thorax and curtain side airbags) using WorldSID and ES-2re at 90 degrees and 75 degrees. The oblique condition for WorldSID resulted in reduced head and neck responses, while thorax and abdomen responses were generally higher than the 90 degree condition. For ES-2re all responses were generally lower in the oblique condition than in the perpendicular condition. The experimental program was extended by virtual testing study conducted by Subaru. This study found the pole diameter had negligible influence on dummy responses and structural deformations. The Subaru study found that dummy responses were more sensitive to variations impact characteristics under the oblique condition than in the perpendicular impact condition.

As reported elsewhere in this ESV, Transport Canada has conducted three paired tests comparing WorldSID dummy responses in oblique and perpendicular pole tests. Two additional paired tests in the oblique condition were also performed with ES-2re and WorldSID.

While WorldSID dummy responses were generally higher in the oblique condition, head responses were dependent on airbag effectiveness and head positioning. Increased thoracic and abdominal responses in the oblique test were found to be due to a forward shift in impact location and increased impact energy rather than impact angle.

It was observed that during oblique pole impacts the geometry of the ES-2re shoulder, by design, prevented compression of the shoulder and encouraged the shoulder and arm complex to rotate forward, leading to reduced rib deflection readings. WorldSID in contrast has a compliant shoulder which compresses laterally under load, the WorldSID ribs are consequently loaded more severely than the ES-2 ribs.

In the abdominal region, high abdominal deflections in WorldSID were not matched with high abdominal force readings in ES-2re.

**NHTSA Position** - A recent test program by the USA has shown that an oblique impact using a 254 mm diameter pole was able to load the chest and head simultaneously. NHTSA believes that an oblique impact angle would serve the safety need because the test is likely to result in wider inflatable head protection systems and thus protect occupants over a wider range of impacts with narrow objects

and improve crash sensing for air bag inflation. In addition, NHTSA has determined that air curtain systems could be effective in preventing or reducing complete and partial occupant ejection through side windows.

NHTSA has found the oblique pole test to be beneficial for enhancing side crash safety because of the necessity of advanced air bag and window curtain designs that will become necessary to meet the oblique pole test requirements. NHTSA found the test procedure to be very repeatable in terms of impact line and closing speed. Additionally, in comparison to the FMVSS 201P procedure (perpendicular pole impact), the oblique procedure consistently produced significantly higher head injury measures. The head air bag system designed for the 201P test was found to be sensitive to seat track position and seat back angle changes. In one tested model, a failure to deploy the side airbags was observed. NHTSA contends that the sensors designed for the perpendicular test could not detect narrow object impact against the door when forward of the specified seating position.

This test procedure is intended to simulate real world side crashes with narrow objects such as trees and poles. The goal is to utilize an oblique pole side impact test procedure to evaluate countermeasures for head and chest protection in higher severity side crashes.

In narrow object side crashes, half of the seriously injured occupants are in crashes of delta-Vs 32 km/h or higher. Only 16% are in crashes with a principal direction of force around 90° while 63% are in frontal oblique narrow object crashes. The optional FMVSS No. 201, rigid pole side impact test is at 90° and an impact speed of 18 mph (29 km/h) while the oblique pole test is at 75° and 20 mph (32 km/h).

### **INTERIOR HEADFORM IMPACT TEST**

The real world crash data indicated that head injuries were a significant part of side impact trauma even though the results of current regulatory MDB tests do not show a head injury risk. Consequently it was proposed that the IHRA harmonised side impact test procedures include a supplementary interior surface headform test to ensure that the potential contact points for head impact are evaluated.

The proposed IHRA interior surface test procedure is being based on research being carried out by EEVC WG13. The outline of the developing test procedure

was presented by EEVC WG13 at the 2003 ESV conference. The key research that has taken place since the previous IHRA report has been a quest to have a highly repeatable test procedure with minimal scope for misinterpretation and have one that can adequately assess active head protection systems and give credit for them if they can be shown to give good all round protection. This research has now progressed to a point where EEVC WG13 has been able to release it for wider evaluation. WG13 has noted that some issues in the procedure will require confirmation as there are differing ways of trying to achieve the same goal neither of which appears to be significantly better than the other. It is acknowledged that the best way of clarifying these issues is via a wider evaluation, in a range of different vehicles and with different types of head protection system. These issues will need to be resolved before the procedure could be considered fit for consideration as a regulatory test procedure.

The headform used is the same as that specified for use in the US FMVSS 201 standard, using a free flight projection system. Key impact points are selected in a similar way to that used in FMVSS201 but defined within an area bounded by horizontal and vertical planes, based on defined limits of occupant seating position. In a desire to test 'worse case' impact positions the prime target positions can be moved based on structural considerations and the ability to test the particular point. The headform is a non-symmetrical impactor and the potential exists to incur multiple or secondary impacts with uncertified parts of the headform. Procedures are included to try and minimise these risks in a repeatable manner. It is noted in the procedure that it defines strategies to manipulate the headform, to reduce the risk of secondary impact and the fact that the use of a symmetrical headform could potentially reduce some of these noted problems. The potential of adopting an alternative impactor is mentioned but is not discussed, even though such a device is now included in other regulatory test procedures (EC pedestrian impact). It is noted that some restrictions are needed in defining potential contact zones and impact vectors to areas of the car that can be realistically contacted by an occupant's head and ones that are 'sensible to evaluate'. The EEVC procedure now includes 'test limitation zones' and recommendations of impact vectors, based on simulations of a range of impacts. These will need to be validated.

The headform procedure, as proposed by EEVC WG13, includes a perpendicular pole test to evaluate active head protection systems. Currently it uses the

ES-2 dummy, without the rib extension modification. This procedure is based on that used by the EuroNCAP consortium which in turn is based on the optional pole test included in the existing FMVSS201. The IHRA suite of procedures includes an oblique pole test. Since WG13 has no experience with the oblique pole test the perpendicular pole test is included in this procedure 'until it can be shown that the oblique pole test is at least as stringent as is the perpendicular one'. Further details of this procedure are reported in the EEVC WG13 status report (Langner et al, 2005).

The biggest change and extension to the EEVC procedure, since the previous report, relates to proposals to evaluate deployed head airbags to ensure that protection is encouraged at all realistic occupant head contact positions, in addition to the single contact position evaluated in the full scale pole test. If adequate protection can be proven the procedure will allow reduced level (lower velocity testing) to vehicle structures that are covered by an active system, provided that full severity protection can be proven for all possible head positions when the system is deployed. An outline procedure had been detailed but will need to be validated before it could be recommended for regulatory application.

The EEVC work confines impact zones to those that are contactable by restrained occupants in side impacts. With front seatbelt wearing rates approaching 80% in the USA, NHTSA has agreed to look at the EEVC's "restrained-only zones" in the validation phase.

NHTSA FMVSS201 interior surface headform compliance testing for recent model vehicles shows very few test results exceeding the HIC(d) of 1000, the highest of these results only being around 1100.

APROSYS will evaluate two vehicles under the proposed interior headform test, with a focus on the rear seating position. BAST and German vehicle manufacturers will evaluate performance of rigid roof convertible interiors and supported structures.

## **OUT-OF-POSITION SIDE AIRBAG EVALUATION**

Initially, it was agreed that NHTSA and Transport Canada would draft the evaluation procedure based on ISO TR 14933 and the NHTSA/Transport Canada research. Later it was agreed that the recent work under the chairmanship of the Insurance Institute for

Highway Safety (IIHS) would also be taken into consideration.

In August 2000, the Side Airbag Out-of-Position Injury Technical Working Group (TWG) chaired by the IIHS released the "*Recommended Procedures for Evaluating Occupant Injury Risk from Deploying Side Airbags*". The procedures were developed in response to a request by the National Highway Traffic Safety Administration (NHTSA) that industry develops public standards which their member companies would adhere to in the design of future side airbags. The TWG procedures recommend Anthropomorphic Test Devices (ATDs), instrumentation, test procedures, and performance guidelines that should be used for assessing the injury risk of interactions between a deploying side airbag and a vehicle occupant. The IHRA SIWG agreed to take these test procedures into the validation phase which may result in further refinements.

The TWG recommendations are intended to minimise the risk of out-of-position injury for that segment of the population believed to be at greatest risk, namely small women, adolescents and children. As such the ATDs deemed most appropriate by the TWG for the evaluation of risk include the SID-IIs, the Hybrid III 5<sup>th</sup> percentile female and the Hybrid III 6 and 3-year old child ATDs. A series of test procedures has been developed for each of the following inflatable system types: seat mounted airbags, door or quarter panel mounted airbags and roof-rail mounted inflatable systems. Each test is intended to quantify the level of risk to a designated body region and/or to evaluate the risk of a specific injury mechanism.

The fundamental premise of the TWG recommendations requires that the full complement of tests for a given system be carried out to ensure that a thorough evaluation of the system has been completed. The use of sound engineering judgment is strongly recommended to guide additional tests perhaps with slight variations, for systems demonstrating elevated risks.

NHTSA has been monitoring the risks to children both by closely analyzing real world crash data and also by undertaking statically testing side air bags with child dummies placed out-of-position in the test vehicles. To-date no serious injuries have been reported to children and small adults in the crash cases that have been investigated under NHTSA's special crash investigations. Since finalizing the test

procedures and requirements developed by the TWG, many manufacturers have been following those procedures to check voluntarily if there are any such risks from their air bag designs. While no real world injuries have been observed, it is necessary to continue to monitor side air bag designs since changes are likely to occur as manufacturers change their designs to meet various requirements such as the IIHS and NCAP ratings and other requirements.

Some members of the IHRA SIWG are unconvinced of the benefit of OOP side airbag testing, particularly if they do not have any reported cases of serious injury attributed to this condition. IHRA SIWG members have not proposed any test conditions in addition to those developed by the TWG. Further evaluation of OOP side airbag tests is planned within the APROSYS programme.

#### **DEVELOPMENT OF HARMONISED TEST DEVICE**

The WorldSID Task Group initially had funding and development resources for the mid-sized adult male test device only. ISO Working Group 5 has now given a mandate for the development of a small adult female test device. APROSYS is contributing to the development of this dummy. Production 50<sup>th</sup> percentile WorldSID dummies have been available since March 2004.

#### **CONCLUSION**

Overall, the IHRA SIWG has made significant progress in harmonising research and drafting a set of side impact test procedures to maximise harmonisation with the objective of enhancing safety in real world side crashes.

The IHRA Side Impact Working Group has been successful in fostering a great deal of cooperation between members who have contributed resources and research outputs to specific objectives set by the working group. Most members aligned their research programmes with the work activities of the IHRA Side Impact Working Group.

Delays in some of the contributory work programs for the IHRA SIWG have limited the group's ability to make strong recommendations on detailed test procedures at this time. However, the large body of research data that has been generated and the basic principles of the proposed suite of test procedures are valuable outputs. There are several research programs already underway that will progressively

yield data that may form the basis for decisions regarding suitable test procedures.

#### **RECOMMENDATIONS**

In its 7-year term, the group has drafted and partially evaluated a set of test procedures that might form the basis of a harmonised side impact regulation. The members believe that there needs to be:

- Completion of the evaluation work already in progress and an assessment of the suitability and efficacy of the proposed suite of test procedures.
- Continued coordination with the WorldSID Task Group and the IHRA BWG to evaluate harmonised test device(s).
- Recommendations for appropriate test devices and injury. This may require further validation testing to ensure that the recommended test procedures remain practical and that any test redundancies are identified and eliminated.
- Continued coordination with the IHRA Vehicle Compatibility group to ensure that solutions in one area do not result in disbenefits in another.
- Examination of the feasibility of improving side impact protection for occupants on the non-struck side and develop a test procedure to evaluate such protection.

As before, the success of this work is contingent upon the commitment of resources from IHRA members.

Subject to endorsement by the IHRA Steering Committee, it is anticipated that the test procedures could be submitted to the WP29 regulatory process and may be used as a basis to develop a new harmonised side impact regulation.

## REFERENCES

Arbelaez, R.A.; Dakin, G.J.; Nolan, J.M.; Dalmotas, D.J.; and Tylko, S. *IIHS side impact barrier: development and crash test experience*, IMechE Conference Transactions: International Conference on Vehicle Safety 2002, 73-88. London, United Kingdom: Professional Engineering Publishing Ltd.

Dakin, G et al, *Insurance Institute for Highway Safety Side Impact Crashworthiness Evaluation Program: Impact Configuration and Rationale*, Paper No. 172, 18<sup>th</sup> ESV Conference, Nagoya, 2003.

Insurance Institute for Highway Safety, *Crashworthiness Evaluation Side Impact Crash Test Protocol (Version IV)*, December 2004

Langner, T; van Ratingen, M.R.; Versmissen, T; *EEVC Research in the Field of Developing a European Interior Headform Test Procedure*, Paper No 05-0158, 19<sup>th</sup> ESV Conference, Washington DC, 2005

Lund, A (Chairman, The Side Airbag Out-of-Position Injury Technical Working Group - A joint project of Alliance, AIAM, AORC, and IIHS), *Recommended Procedures for Evaluating Occupant Injury Risk from Deploying Side Airbags*, July 2003

Roberts, A; Ellway, J; *The Development of an Advanced European Mobile Deformable Barrier Face (AE-MDB)*; Paper No 05-0239, 19<sup>th</sup> ESV Conference, Washington DC, 2005

Roberts, A. et al, *The Development of the Advanced European Mobile Deformable Barrier Face (AE-MDB)*, Paper No. 126, 18<sup>th</sup> ESV Conference, Nagoya, 2003.

Samaha, R.R. et al, *NHTSA Side Impact Research: Status and Update*, Paper No. 492, 18<sup>th</sup> ESV Conference, Nagoya, 2003.

Seyer, K., *International Harmonised Research Activities Side Impact Working Group Status Report*, Paper No. 579, 18<sup>th</sup> ESV Conference, Nagoya, 2003

Tylko, S; Dalmotas, D, *SID-IIS Response In Side Impact Testing*, SAE Paper Number 2004-01-0350

Van Ratingen, M.R. et al, *Development of a European Side Impact Interior Headform Test Procedure*, Paper No.138, 18<sup>th</sup> ESV Conference, Nagoya, 2003.

Yonezawa, H et al, *Investigation of New Side Impact Test Procedure from Japan*, Paper No. 328, 18<sup>th</sup> ESV Conference, Nagoya, 2003.

## ACKNOWLEDGMENTS

APROSYS is a European Commission funded project TIP3-CT-2004-506503.

The IHRA Side Impact Working Group wishes to acknowledge the support of all manufacturers and organisations that supported programs with vehicles, parts and other resources:

Audi

Daimler-Chrysler

Fiat

Ford

Renault

Subaru

TMC Europe

Volkswagen

Volvo

WorldSID Task Group

European governments supporting the EEVC

## APPENDIX

### TEST PROCEDURE SPECIFICATIONS

The IHRA Side Impact Working Group has been evaluating a draft suite of complementary test procedures aimed at improving side impact safety.

The group has not yet concluded its work and is not in a position to provide recommended detailed test procedures. This appendix is intended to provide some information on the test procedures being considered and evaluated by the group.

It should be noted that, in many cases, tests may not have been conducted in strict accordance with the specifications described below. Most notably, different dummies may have been used. Other deviations from the nominal procedures may also have been used to investigate sensitivity of test results to changes in test parameters.

#### MOBILE DEFORMABLE BARRIER TO VEHICLE TEST

Two candidate procedures are under evaluation by the IHRA SIWG:

- the AE-MDB which is designed to represent a car or small SUV; and
- the IIHS MDB which is designed to represent a large SUV.

#### AE-MDB

The specification for the AE-MDB has not yet been finalised by EEVC WG 13. Further detail on the development of this barrier may be obtained from the EEVC WG13 status reports from ESV 2003 and ESV 2005 (Roberts et al, 2003 and Roberts et al 2005). AE-MDB tests conducted to date have been based on early drafts of this test procedure, with some deviations including different dummies and modifications to the deformable barrier face.

#### IIHS

The base specification used for evaluating the IIHS barrier has been the Insurance Institute for Highway Safety Crashworthiness Evaluation Side Impact Crash Test Protocol (Version IV). This procedure is available from the IIHS website [www.iihs.org](http://www.iihs.org). Dummies other than the SID-IIs (specified in the IIHS protocol) have been used in testing.

#### VEHICLE TO POLE TEST

The IHRA SIWG has evaluated a range of pole impact conditions using both physical tests and computer simulation. The group agreed to consider the oblique pole test proposed recently by the NHTSA, but has also conducted perpendicular pole tests in an attempt to understand the advantages of the oblique configuration.

The oblique vehicle to pole impact procedure under evaluation was that proposed by the NHTSA in their recent Notice of Proposed Rulemaking (NPRM) [Docket No. NHTSA-2004-17694] available from the NHTSA website.

<http://www.nhtsa.dot.gov/cars/rules/rulings/SideImpact/index.html>.

Oblique pole tests have been conducted with various dummies including ES-2re, ES-2 and WorldSID.

In addition, perpendicular pole tests have been conducted, with test specifications based on the EuroNCAP or FMVSS 201P procedures, again with some deviations from these specifications including the use of various dummies.

#### INTERIOR SURFACE HEADFORM TEST

The interior surface headform test being considered by the IHRA SIWG was developed by EEVC WG13 and is reported in detail at this conference (Langner et al, 2005).

#### OUT-OF-POSITION TESTS

The out-of-position test procedures under consideration by the IHRA SIWG are those prepared by The Side Airbag Out-of-Position Injury Technical Working Group (Lund, 2003). These procedures are available from the IIHS website [www.iihs.org](http://www.iihs.org).

# THE DEVELOPMENT OF AN ADVANCED EUROPEAN MOBILE DEFORMABLE BARRIER FACE (AE-MDB)

**J D Ellway**

TRL Limited (UK) on behalf of EEVC WG13  
Paper Number 05-0239

## ABSTRACT

The European Enhanced Vehicle safety Committee (EEVC) Working Group 13 (WG13) is working within the IHRA (International Harmonised Research Activities) Side Impact Working Group (SIWG) assisting in the development of a suite of harmonised test procedures for side impact protection. Included in the procedures will be a full-scale barrier based side impact test. This paper presents the current status of a research programme that has been carried out to develop a more appropriate side impact barrier face for use in an advanced side impact test procedure. The Advanced European Mobile Deformable Barrier Face (AE-MDB) test will reflect the 'car to car type' accident that is typical in Europe and other regions of the world. The latest research performed by EEVC Working Group 13 in the development of an AE-MDB includes reviews of vehicle force distributions, car to car tests as well as the performance of the current specification AE-MDB tests into a range of vehicles.

It is noted that the European vehicle fleet has developed since the UN-ECE Regulation 95 barrier was first conceived, and as a result an improved test procedure is required. The IHRA procedures are being developed to encourage enhanced protection for both the front and rear seat occupants. The AE-MDB should perform in a way that reflects the current accident situation.

## BACKGROUND

The AE-MDB is being developed by EEVC WG13 as part of a contribution to the activities of the IHRA side impact working group, which is co-ordinating worldwide research for various aspects of side impact protection including out of position, interior surface protection, full-scale pole impacts and a full-scale mobile deformable barrier based test procedure. This paper presents the status of the vehicle based AE-MDB test specification and the results of tests performed under the WG13 barrier development programme. It is noted that further research is also being conducted outside of WG13 as part of other research projects including the Advanced Protection Systems (APROSYS) project, and an MDB evaluation in Japan.

There are two MDB based test procedures under consideration by IHRA, one being proposed by the

Insurance Institute for Highway Safety (IIHS) and the other by EEVC WG13. The IIHS MDB is representative of an impact by large sports utility vehicles (SUV) and small trucks, which is more reflective of accident severities seen in the US. The AE-MDB is more reflective of the European accident situation, where the MDB is more representative of car-type impacts which form the largest proportion of the European vehicle fleet when compared to SUV type vehicles.

Analysis has shown that the existing ECE Regulatory side impact test procedure (R95), is becoming less representative of the impact severity observed in recent accident data [1]. Overall vehicle intrusion, as seen in real-life side impact accidents is also greater than that seen in laboratory side impact tests, and therefore it has been recommended that the overall side impact test procedure severity should be increased [2]. Edwards et al [1] subsequently proposed several ways to increase the test severity to be able to encourage enhanced occupant protection, which included increasing the speed and/or mass of the MBD and also an increase in ground clearance as supported by data from vehicle structural analyses.

One of the main considerations made by WG13 alongside that of the barrier face specification was that the MDB should be capable of simultaneously loading both the front and rear occupants. This measure was made to ensure that vehicles offer adequate protection to both front and rear seat occupants. This is in line with the original proposal made by EEVC WG9 during the research that led to the development of ECE Regulation 95 and EU Directive 96/27EC, although this aspect was not finally included.

## PREVIOUS RESEARCH

The initial development stages of the AE-MDB were reported by EEVC WG13 at the 18<sup>th</sup> ESV conference held in Nagoya, Japan, 2003 [3]. The barrier development programme was based upon three specific areas for assessment; these were baseline vehicle test results, test and MDB configuration and barrier specification. The test and MDB configuration proposed by WG13 utilises a stationary target vehicle impacted by the MDB travelling at 50km/h. The centreline of the MDB is perpendicular to that of the target vehicle and is

aligned 250mm rearward of the target vehicle's R-point. This was set to load both front and rear seat occupants and represent a moving car to moving car side impact; where the initial contact point is aimed at the front seat R-point.

### **Test and MDB Configuration**

As reported previously, EEVC WG13 is of the opinion that from a regulatory perspective a perpendicular test (opposed to angled or crabbed) is the preferred option as it minimises shear loading to the forward honeycomb elements of the barrier face and makes for a less variable test. Furthermore, an analysis of the Co-operative Crash Injury Study (CCIS) database for the UK accidents indicated that perpendicular accidents were equally as frequent as angled impacts [4]. The proportion of casualties that were seriously or fatally injured was 60 percent for perpendicular impacts compared with 45 percent for the angled impacts. This highlights the differences that have been seen between the dummy responses observed in crabbed and perpendicular impacts.

WG13 also believes that a perpendicular impact configuration is the most appropriate for the car based test as suggested by accident data, and is reflective of more than half of the side impact accidents within Europe. These reasons, reinforced by the benefits of repeatability and reproducibility of a stationary target vehicle, formed the basis for the impact configuration of the new test procedure.

Current European side impact requirements are limited to front seat occupants only. The inclusion of a rear seat occupant, as proposed by IHRA, aims to ensure that rear seat occupants are also offered a similar level of safety. This measure requires the AE-MDB impact test to load rear seat occupants appropriately without reducing the loading applied to front seat occupants. Previous studies into the geometrical characteristics of vehicle structures performed by EEVC WG13 indicated that the spacing between the lower rails was similar to the distance between the front and rear seating positions [5]. In order to increase the loading applied to rear seat occupants, the MDB centreline is aimed mid-way between the seating positions. The impact point of the MDB is therefore aimed 250mm rearward of the vehicle R-point.

A measure taken to increase the test severity was to increase the mass of the MDB. The proposed trolley mass was increased from the 950kg specified in R95 to 1500kg. This mass is more representative to that of vehicles in the current vehicle fleet, and is also proposed by IHRA for promotion of harmonisation between test procedures.

### **Barrier Specification**

To increase further the test severity, the initial ground clearance of the AE-MDB face was 350mm. The upper surface of the barrier face is at the same height above ground as that of R95, 800mm, as recommended by Edwards, 2000.

Rigid car to load cell wall (LCW) data, collected from vehicle models dated circa 1970-80s, formed the basis of the stiffness distribution for the R95 barrier face. This measure was based upon force-deflection and energy absorption limits for the individual barrier blocks and the barrier total. The same approach has also been taken to date to develop the AE-MDB corridors. The main source of LCW data available to WG13 prior to the 18<sup>th</sup> ESV conference (Nagoya) was provided by the Japan Automobile Research Institute (JARI) [3]. The original AE-MDB corridors were subsequently based around these results, and were described by Roberts, 2003. It was proposed that further LCW tests with European vehicles should be performed and compared to the JARI data. WG13 subsequently collected rigid LCW data from seven different vehicle models.

### **Baseline Vehicle Test Results**

The performance assessment for the AE-MDB was based on the results of the 'baseline vehicle test data'. These tests were moving car to moving car perpendicular side impacts; and represented the type of impact that the AE-MDB should be able to replicate. Two different bullet vehicles were used to provide a range of impact scenarios, one being a family sized car and the other a small off road vehicle. Previously, only two target vehicles, a Renault Megane and Toyota Camry, had been used by WG13. It was proposed that the AE-MDB should undergo further evaluation using different vehicle models.

The results from those earlier baseline tests indicated that the AE-MDB performed differently when impacting the Megane than when impacting the Camry. Comparison of the post test vehicle intrusion profiles from the AE-MDB tests with those from the baseline tests indicated that when impacting the Megane, the AE-MDB appeared to be a suitable representation of the European accident situation. However, with the Camry the AE-MDB results were less conclusive suggesting that it may be more suitable for Europe than the IIHS barrier face.

Further baseline car to car and AE-MDB to car tests have been performed since the previous WG13 report. A range of target and bullet vehicles were used in order to provide a broader assessment for the barrier face.

## VEHICLE TO RIGID LCW PROGRAMME

The rigid LCW data provided by JARI, gave a clear indication that the frontal stiffness distribution of modern vehicles has changed significantly since the development of the R95 barrier face. WG13 performed additional car to rigid LCW tests in order to confirm that the stiffness distribution in modern European vehicles was comparable to that of the JARI data.

The stiffness distribution; as indicated by JARI and WG13 LCW results together with the AE-MDB version 2 corridors; is shown in Figure 1. The upper frontal structures of the vehicles tested, which align with blocks A, B and C, show a relatively homogenous stiffness distribution and low levels of loading applied. In contrast, the vehicle structures which align with the lower row of blocks do not show such homogeneity. The outer areas are loaded to a greater extent than any other below 350mm of displacement. This load is most likely to have been transferred through the lower rails of the vehicles tested. The centre area (block E) initially indicated large forces after relatively little deformation, it is suggested that this is due to the inertial response from bumper beams and lower

rail connecting members. This is exaggerated by the effects of data the filtering processes, which caused loading to be shown prior to vehicle displacement. The load applied to the centre area is, for the most part, lower than that of the outer areas. The loading to this area reaches a similar level to that of the outer areas due to engine loading, which becomes apparent at around 300mm of displacement.

It is accepted that rigid LCW data is unable to clearly highlight the presence of significant lateral connections between lower rails. However, the results are able to provide an indication as to the global stiffness of the vehicles tested. It is currently unclear as to the proliferation of such beam structures throughout the European vehicle fleet, and there is currently no equivalent test procedure which can be used to assess and specify such design, either in terms of barrier design or specification. WG13 has analysed data from LCW tests with a 150mm aluminium honeycomb barrier fitted to the wall. These results were deemed unsuitable for the definition of vehicle stiffness, due to the vehicle structural characteristics being obscured by the presence of the deformable element.

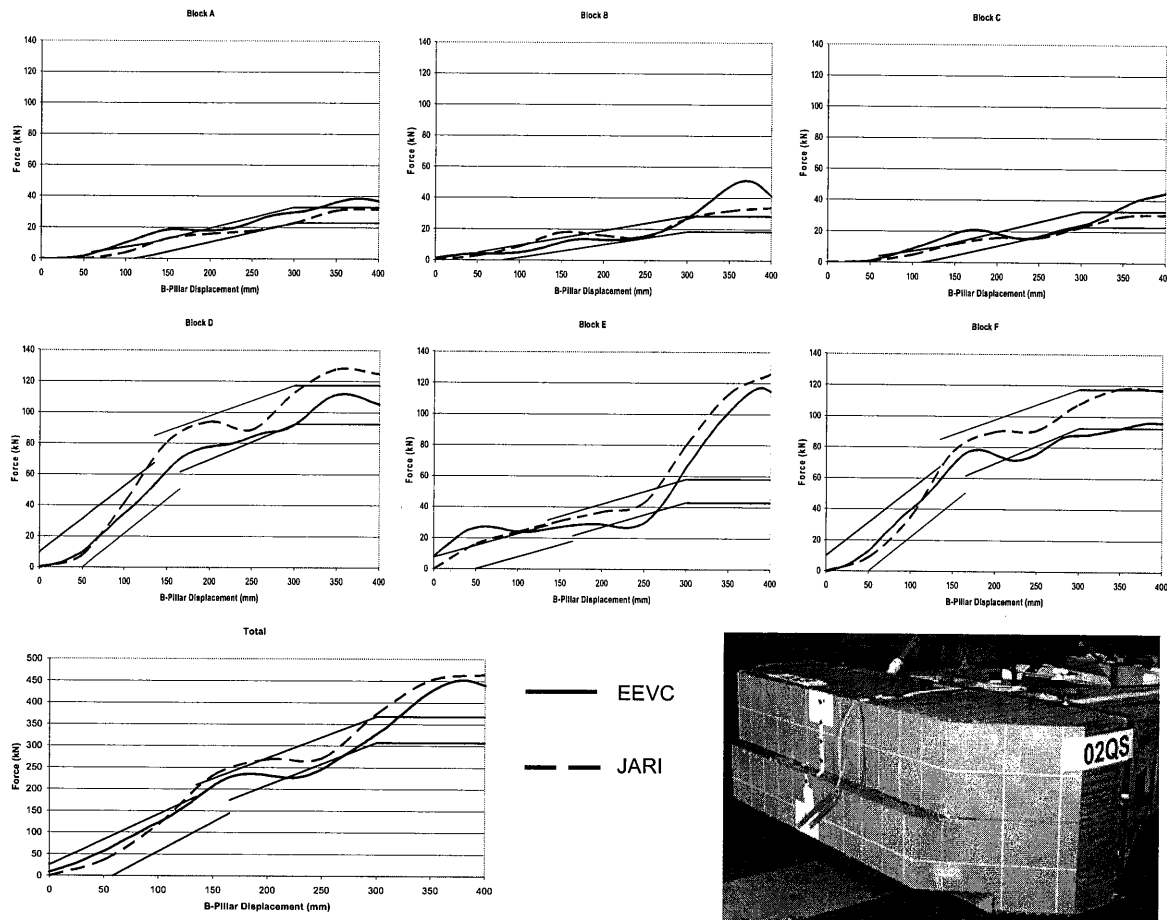


Figure 1 Vehicle to Rigid Load Cell Wall Test Data

Both the Japanese and WG13 data show similar trends across all corridors, and in the case of blocks A, C and E, local and overall force levels are also comparable. For the upper row the WG13 data was slightly above that of the JARI data, whereas the reverse is observed for the lower row. The AE-MDB stiffness corridors have a similar stiffness distribution similar to that of the vehicle data. In general, the total force-deflection traces are very similar and the AE-MDB corridor appears to be a suitable representation of the overall stiffness, up to about 300mm displacement where engine loading becomes apparent.

The information provided by JARI was a 'calculated average' where the force was weighted by vehicle sales data from 1998, with the relative B-pillar displacement normalised. The data was made up from approximately 80 vehicles to LCW tests, and a further analysis based on C-segment vehicle models showed very close similarities between data, which indicated that the full data set was representative of the most common vehicle models. The WG13 data was an averaged force with the relative B-pillar displacement normalised. It was not weighted by vehicle sales, as was the Japanese data, thus any variation could be due to this difference. The WG 13 data was made up of seven vehicle models, and included a small off road model, a multi-purpose vehicle and various D-segment vehicles.

Although the AE-MDB version 2 performance corridors have been modified since those presented at the 18<sup>th</sup> ESV conference (AE-MDB version 1), the modifications have only been included to make allowance for the geometrical characteristics of the AE-MDB. For example, block E of the AE-MDB utilises the same honeycomb as that of the R95 barrier blocks 1 and 3, subsequently it was given the same corridor in version 1. However, due the step in the AE-MDB, the force applied between 0-150mm displacement is less than that of R95. Therefore the corridor was reduced for this period, and at 150mm the full surface of block E is engaged and the corridor returns to that used in R95. It was the intention that the materials to be used in the construction for the AE-MDB should be based upon those which already exist. In the case of AE-MDB blocks A to C, which form the upper row, the honeycomb to be used was the same as that used for the R95 barrier face block 4.

#### **BASELINE VEHICLE TEST PROGRAMME**

Since the previous report at the 18<sup>th</sup> ESV conference, WG13 has performed four additional baseline tests using two other target vehicle models. In total, eight baseline tests have been performed using four different target vehicles and

three different bullet vehicle models. The centreline of each bullet vehicle was aimed at the R-point of each target vehicle, with both vehicle centrelines perpendicular to each other. The speed of each target vehicle was 24km/h, and the bullet vehicles were travelling at 48km/h. This configuration is exactly the same to that of the previous research performed by WG13.

#### **Bullet Vehicle Models**

Ford Mondeo – family size vehicle, five-door hatchback. Mark 1 (pre-1996), 1.6l engine, test mass 1390kg.

Land Rover Freelander – small off road vehicle, typical within the European vehicle fleet and available worldwide. 2000 model year, 2.5l engine, automatic transmission, GS model, test mass 1720kg.

Toyota Corolla – small family size vehicle, four-door saloon. 2002 model year, 1.4l engine, test mass 1340kg.

#### **Target Vehicle Models**

Renault Megane - small family size vehicle, five-door hatchback. 1998 model year, 1.4l engine, 'AIR' model, test mass 1350kg. Equipped with side airbags.

Toyota Camry – executive four-door saloon available worldwide. 1999 model year, 2.2l and 3.0l engine, test mass for both models 1600kg. Equipped with side airbags.

Toyota Corolla - small family size vehicle, three-door hatchback. 2002 model year, 1.4l engine, test mass 1340kg. Not equipped with side airbags.

Alfa Romeo 147 - small family size vehicle, three-door hatchback. Equipped with side airbags.

The recent baseline tests to a Toyota Corolla and an Alfa 147 were performed using a Land Rover Freelander and a Toyota Corolla. These tests were used to gain further experience of impacts with a small off road vehicle and an average family size vehicle, which provide a representation of the real-world impacts that the AE-MDB procedure should be able to reflect. It was also possible to investigate any differences between three and four/five door vehicles, as the Corolla and Alfa were both three door hatchbacks.

#### **Anthropometric Test Devices**

The initial studies by WG13 used the EuroSID-I dummy. Since that research was performed this dummy has been superseded by the ES-2, which is seen as being an improvement over the EuroSID-I. Therefore, WG13 agreed to use the ES-2 and any

direct comparison between these evaluations phases should make note of this change.

### Toyota Corolla Test Observations

The post test struck side vehicle deformation to the Corolla is shown below in Figure 2 and Figure 3. The Frelander applied loading to the Corolla at a higher level to that applied by the Corolla bullet vehicle, this was indicated by the deformation to the roof and door panel visible just below the height of the door handle. The loading applied by the Corolla was concentrated toward the lower edge of the door and around sill level, in these respective areas, were where the B-pillar was seen to receive most of its loading. There was more door deformation visible in the Frelander test where the lower edge over-rode the sill. There was little sill deformation visible after the Corolla test.



Figure 2 Corolla impacted by the Corolla



Figure 3 Corolla impacted by the Frelander

### Alfa Romeo 147 Test Observations

The post test struck side vehicle deformation to the Alfa is shown in Figure 4 and Figure 5. The bullet vehicles applied loading to the Alfa in similar ways to those seen in with the Corolla. Note also that the vertical bend in the door, just rearward of the side mirrors, was pronounced in the Frelander impact, whereas the when impacted by the Corolla this deformation was not present. The form of deformation to the sill and rear panel, beneath the rear window, appeared to be quite similar. In both cases, the lower edge of the driver's door remained engaged with the vehicle sill. But, the visible rotation of the sill about its primary axis and deformation to the underside, suggests that loading

has also been applied to a large proportion of this area.



Figure 4 Alfa impacted by the Corolla



Figure 5 Alfa impacted by the Frelander

All of the vehicles impacted by the Frelander indicated that most of the load was being applied approximately midway up the door(s), from observations of vehicle damage. However, the Mondeo and Corolla mostly loaded the target vehicles toward the lower edge of the door(s). With the Frelander, the presence of a high beam connecting the lower rails was evident on each target vehicle. A pre-test measurement of this beam showed it to be positioned approximately 560mm above ground level. With the family sized vehicles, the presence of such beams was not as clear, but measurements of the Mondeo and Corolla located the beams approximately 430mm and 480mm, respectively, above ground level.

### AE-MDB TEST PROGRAMME

The current specification of AE-MDB face that has been published is version 2. The barrier version evaluated by WG13 and published at the 18<sup>th</sup> ESV conference was version 1, the only difference being the build specification to reflect the changes that had been included in the revised R95 barrier face. Prior to the vehicle tests with the AE-MDB V2, two LCW certification tests were performed at two different laboratories in order to ensure that the barriers used met the specification required. The results from the V2 tests, in bold black lines, are shown in Figure 6 alongside those of the V1 tests performed previously by WG13.

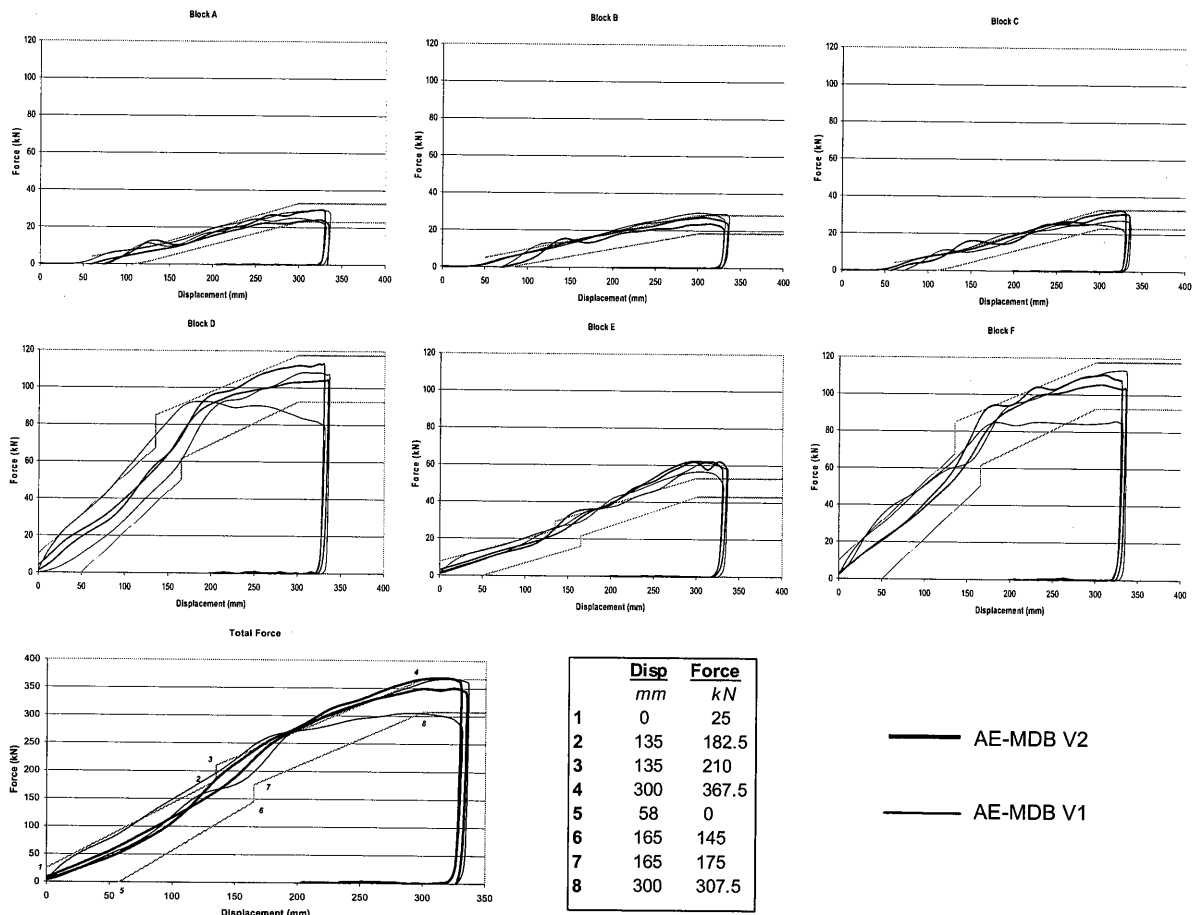


Figure 6 AE-MDB Certification tests

The certification test results showed that the barriers did suitably meet the design specification, although block E was slightly stiffer than desired after approximately 200mm displacement. Further barriers were subsequently constructed and used for assessment of the specification.

#### Toyota Corolla Test Observations

The post test deformation of the Corolla after being impacted by the V2 AE-MDB is shown in Figure 7. There was very little roof and upper B-pillar deformation visible. The loading from the barrier was applied over a greater area than that of the Freelander. The lower edge of the doors were deformed in a manner more like that of the Freelander than the Corolla, and subsequently the door over-rode the sill. The level of sill deformation appears to be between that seen in the baseline tests.

#### Repeatability Evaluation

In an assessment of repeatability; three AE-MDB V2 to Corolla tests were analysed. The results show comparable dummy and deformation results between all of the tests, which were performed at two different laboratories. However, a different trend in door velocity was recorded between

laboratories, which can be attributed to different measurement methods.



Figure 7 Corolla impacted by the V2 AE-MDB

#### Alfa Romeo 147 Test Observations

The post test deformation of the Alfa after being impacted by the V2 AE-MDB is shown in Figure 8. There was less roof and upper B-pillar deformation when compared to that of the Freelander impact, and in this area a closer comparison can be made with the Corolla impact. The most notable differences between the barrier and baseline vehicle impacts is the larger loading to the lower edge of the door, and the lower levels of loading to the sill seen with the AE-MDB. There was no engagement between the door and sill, which did

not rotate as it did in the baseline tests, allowing for greater levels of intrusion. In the area of the rear panel the form of deformation was comparable to that of the baseline tests.



**Figure 8 Alfa impacted by the V2 AE-MDB**

**Vehicle intrusion profiles**

In all of the tests performed by WG13 the geometrical characteristics of each target vehicle were mapped before and after each impact. A grid was applied to each vehicle with rows at a height of 300, 425, 550 675 and 800mm above ground level. Vertical columns, originating from the Driver’s R-point, extended fore and aft at increments of 125mm. The only exception to this was with the AE-MDB to Alfa test, where the grid was measured at 130x200mm increments and do not translate directly to the points measured in the baseline Alfa 147 tests.

**Toyota Corolla**

The marking scheme for the Toyota Corolla prior to impact is shown in Figure 9. The post test intrusion profile for each row is shown in Figure 10 to Figure 15. The data set contains the two baseline results from the Corolla and Freelander impacts, and also three AE-MDB to Corolla tests.

In general, the deformation produced by the AE-MDB was between the levels of the two baseline tests for all rows. The vertical profile at the R-point position showed the AE-MDB to be mid-way between the baseline tests, which also reflected a similar shape. The B-pillar deformation for rows A to C was almost the same as that from the Corolla baseline test. However, the intrusion either side of the B-pillar was mid-way between that of the two baseline tests. The AE-MDB profiles for rows D and E were higher than that of the Corolla, and at the driver’s door the peak intrusion was at a level similar to that of the Freelander. The presence of the stiff B-pillar is clear in all of the AE-MDB profiles, but it is only just visible in the lower Corolla baseline profiles. The B-pillar is not visible for the Freelander profile, which produced ‘square shaped’ intrusion with the maximum level at row C; 550mm above ground level. The peak level of intrusion for the Corolla test was at row D; 425mm

above ground level. The peak level for the AE-MDB tests was at row C; 550mm above ground level.

A comparison between the AE-MDB profiles shows very similar global and local intrusion levels, with similar shaped intrusion.



**Figure 9 Toyota Corolla Map**

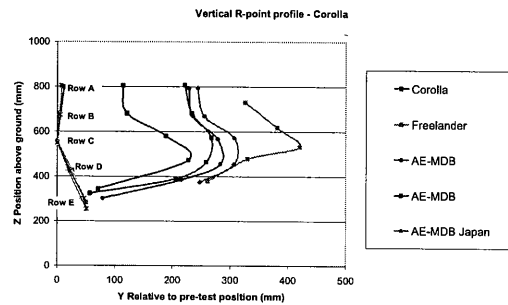


**Figure 10 Corolla R-point profile**

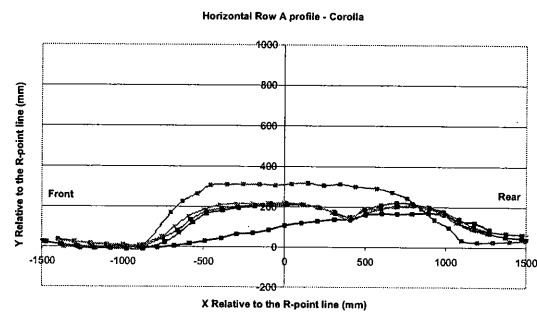


**Figure 11 Corolla Row A profile**

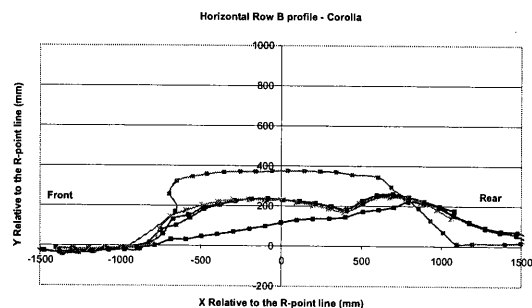


**Figure 12 Corolla Row B profile**

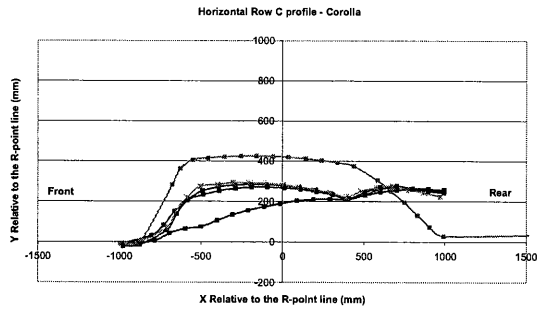


Figure 13 Corolla Row C profile

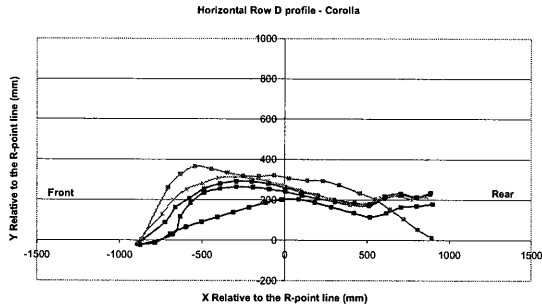


Figure 14 Corolla Row D profile

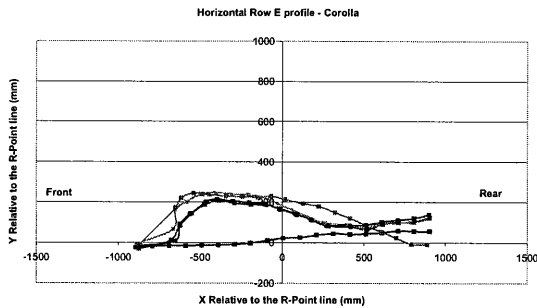


Figure 15 Corolla Row E profile

### Alfa Romeo 147

The marking scheme for the Alfa Romeo 147 prior to impact is shown in Figure 16. The post test intrusion profile for each row is shown in Figure 17 to Figure 22.

Rows A to C show the level of AE-MDB intrusion to be similar to that of the Freelandr along the driver's door. Toward the rear of the vehicle, the stiff B-pillar is visible in the barrier profile with lower levels of intrusion. Rows D and F show a similar level of intrusion between the two baseline tests. Whereas the intrusion from the AE-MDB was larger than both of the baseline tests for the full length of the profile. The largest difference was recorded mid-way along the lower edge of the door by 200mm above that of the Freelandr. The peak intrusion for the Freelandr was at row C; 550mm above ground level, and for the Corolla it was at row D; 425 mm above ground level. The peak intrusion for the AE-MDB was at row D.

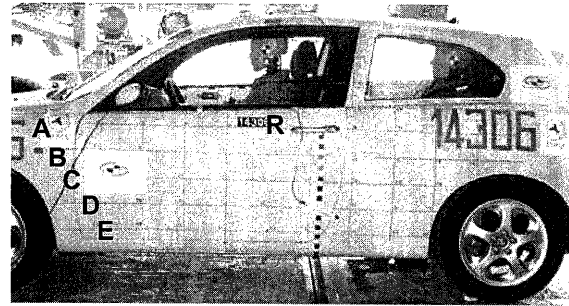


Figure 16 Alfa Romeo 147 Map

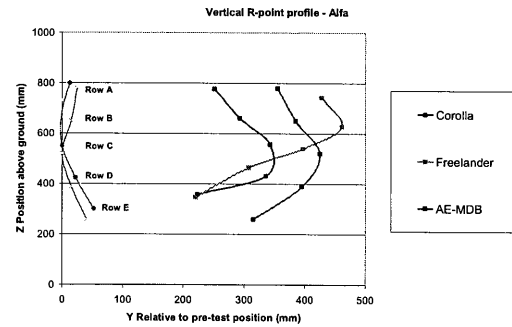


Figure 17 Alfa R-point profile

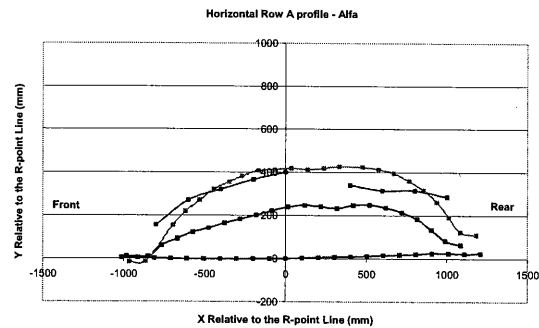


Figure 18 Alfa Row A profile

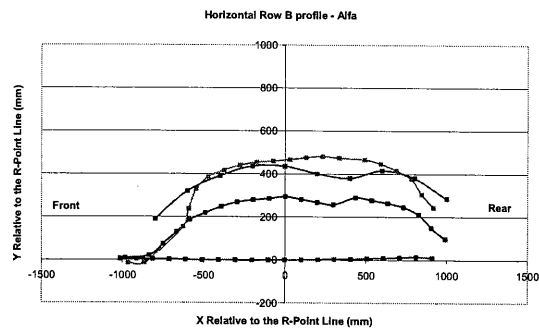


Figure 19 Alfa Row B profile

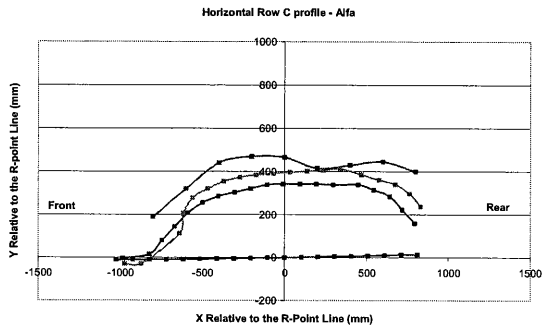


Figure 20 Alfa Row C profile

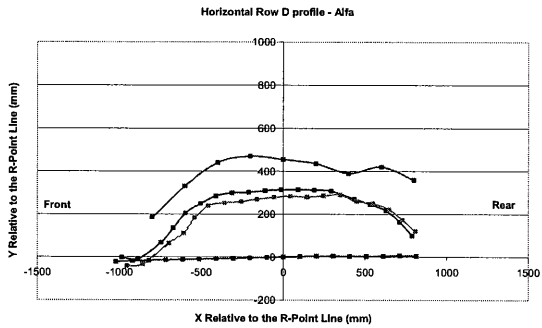


Figure 21 Alfa Row D profile

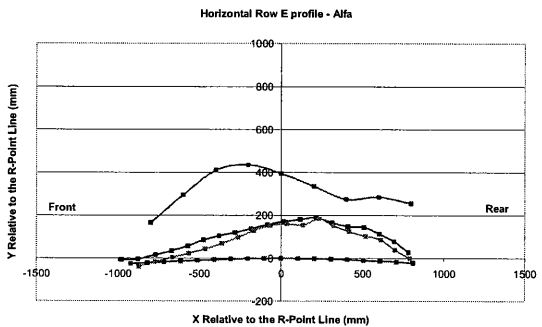


Figure 22 Alfa Row E profile

In reviewing all of the full-scale test data, it is possible to highlight some general trends as assessed by post impact deformation. The baseline tests to all of the vehicles showed that the post impact deformation caused by the Freelander was generally higher than of the Ford Mondeo. In the case of the Megane and Corolla the AE-MDB deformation was between the baseline results. With the Camry the AE-MDB deformation was, in places, above that of the baseline data for rows A, D and E, and for the Alfa this was the case for most rows. Higher levels of door intrusion, in comparison to the B-pillar, were more prominent with the Megane and Camry. A more homogeneous profile was observed with the Corolla and Alfa.

The Freelander has been seen to induce peak intrusion levels at a height of around 550-675mm above ground level on all target vehicles, which is due to the higher level of frontal load paths.

Conversely, the family sized vehicles generally loaded around 300-425mm above ground level. The height of AE-MDB peak loading was between that of the baseline vehicles at approximately 425-550mm.

**Door intrusion velocity**

The importance of door intrusion velocity has previously been highlighted by WG13 as an important measure in determining impact severity as it is the generally door which contacts the occupant and causes injury.

The measurement technique was changed from acceleration based measurement to suitable linear potentiometers, which are believed to be more accurate. Tests to the Megane and Camry used acceleration based measurements, apart from those with the AE-MDB V2, which used potentiometers. The baseline Corolla tests were also acceleration based, and all other Corolla and Alfa tests used potentiometers. One particular characteristic seen with the acceleration based data was higher levels of residual velocity toward the end of the impact. The measurements were taken from the inner door skins at positions close to the driver and rear seat passenger (RSP) dummy thoraxes, but not in a position to interfere with the dummy kinematics. No comparable data was available from the AE-MDB to Alfa 147 test.

The comparative door velocities for all impacts can be seen in Figure 23 to Figure 30. The velocities recorded in the Megane driver and Corolla driver doors show the AE-MDB velocities to be higher than those recorded in the baseline tests. Whereas, in all other positions the AE-MDB V2 barrier was generally between or lower than those of the baseline tests. Peak driver door velocities were not much above 12m/s in the baseline tests and the peak recorded with the AE-MDB V2 was approximately 9m/s using these techniques. For the rear seat passengers, again the largest velocity was recorded at around 12m/s, and 8m/s was recorded with the AE-MDB V2.

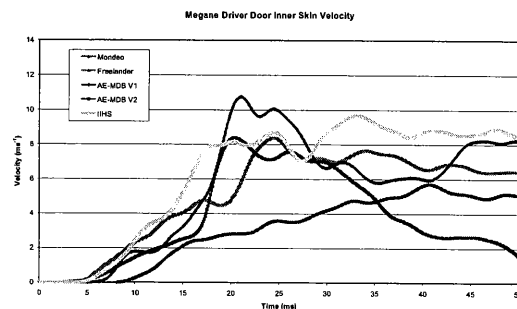


Figure 23 Megane driver door velocities

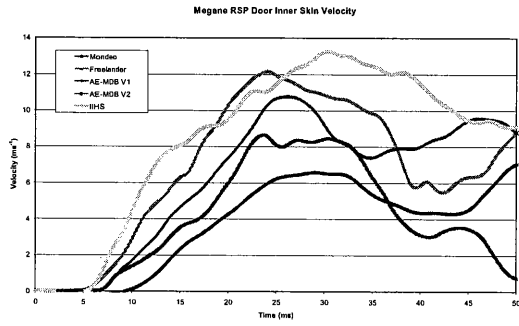


Figure 24 Megane RSP door velocities

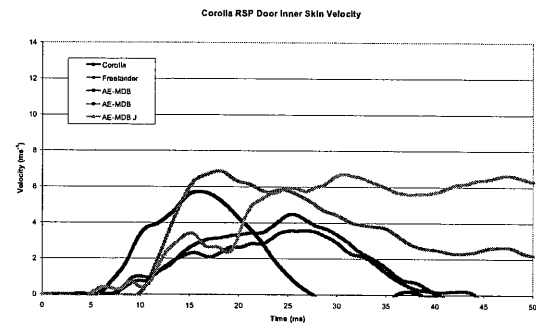


Figure 28 Corolla RSP door velocities

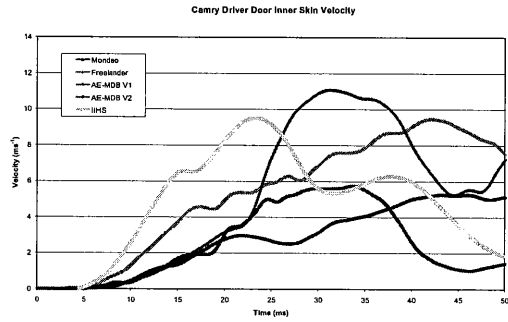


Figure 25 Camry driver door velocities

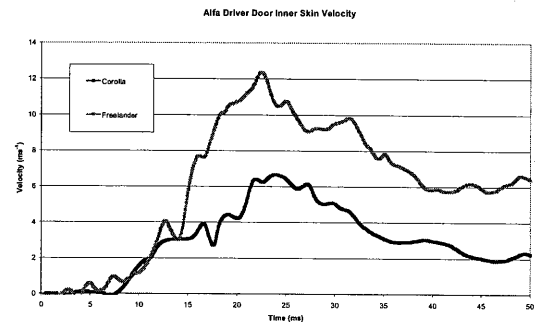


Figure 29 Alfa driver door velocities

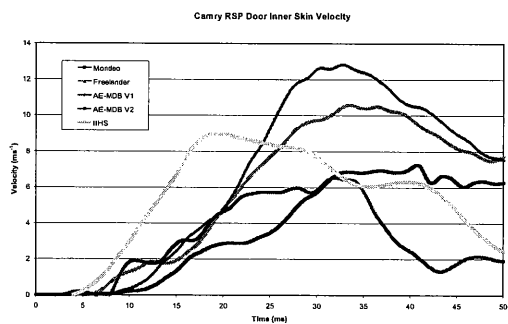


Figure 26 Camry RSP door velocities

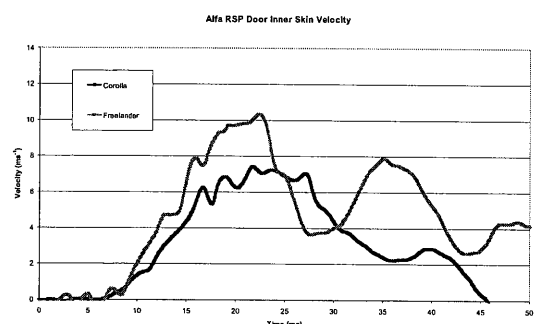


Figure 30 Alfa RSP door velocities

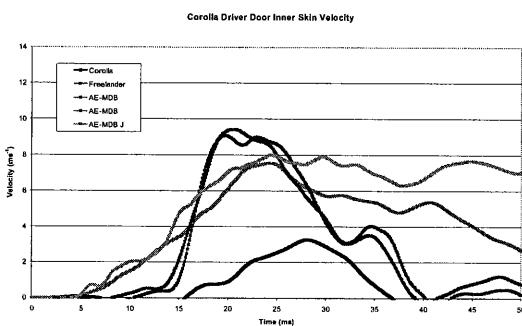


Figure 27 Corolla driver door velocities

### Driver and passenger dummy responses

The test procedure is aimed at encouraging enhancements in occupant protection and reduction in injury risk. It is hoped that if the procedure were to move into a regulatory framework, improved dummies and associated injury criteria would also be adopted.

Throughout the research programme WG13 have used the best 'tools' available. In the Megane and Camry tests WG13 used the EuroSID-I and for the latter tests, to the Corolla and Alfa 147, the ES-2 was used. In the case of all Alfa tests, the ES-2RE dummy was used in the driver's seat and the ES-2 in the rear. These measures can be used to predict the severity of the test based upon current predictions of injury risk. A summary of all WG13 results is shown in Table 1.

		Renault Megane Target Vehicle (EuroSID-1)				Toyota Camry Target Vehicle (EuroSID-1)			
DRIVER HEAD (HIC)		Mondeo	Freelander	AE-MDB V1	IIHS	Mondeo	Freelander	AE-MDB V1	IIHS
Rib Deflection (mm)		72	250	214	454	98	144	121	266
Upper	6	25	24	45	7	24	20	33	
	7	25	18	48	13	25	24	29	
	10	24	15	49	19	30	31	30	
Viscous Criterion	0.02	0.22	0.27	1.16	0.03	0.15	0.18	0.4	
	0.03	0.22	0.12	1.18	0.06	0.23	0.24	0.29	
	0.07	0.17	0.05	1.27	0.10	0.42	0.40	0.31	
Abdomen (kN)		1.2	2.4	1.1	1.6	1.3	2.0	2.2	1.5
Pelvis (kN)		4.3	4.6	4.7	4.5	4.3	4.6	6.2	5.4
Rear Seat Passenger HEAD (HIC)		Mondeo	Freelander	AE-MDB V1	IIHS	Mondeo	Freelander	AE-MDB V1	IIHS
Rib Deflection (mm)		706	107	38	60	476	39	53	446
Upper	7	7	21	31	8	14	19	25	
	6	4	5	11	4	7	17	16	
	6	11	3	12	4	4	15	14	
Viscous Criterion	0.02	0.02	0.10	0.32	0.06	0.07	0.16	0.27	
	0.01	0.02	0.01	0.06	0.01	0.02	0.12	0.13	
	0.02	0.09	0.01	0.09	0.02	0.00	0.12	0.10	
Abdomen (kN)		2.4	4.4	1.6	2.3	1.8	1.7	2.3	2.7
Pelvis (kN)		6.6	7.2	6.4	9.6	4.0	3.3	6.3	5.1

		Toyota Corolla Target Vehicle (ES-2)					Alfa Romeo 147 Target Vehicle (ES-2RE/ES-2)		
DRIVER HEAD (HIC)		Corolla	Freelander	AE-MDB V2	AE-MDB V2	AE-MDB V2 J	Corolla	Freelander	AE-MDB V2
Rib Deflection (mm)		138	444	353	309	144	68	361	230
Upper	6	21	21	27	23	5	51	50	
	1	11	10	14	12	7	38	39	
	3	3	3	6	6	18	44	47	
Viscous Criterion	0.01	0.24	0.16	0.29	0.20	0.01	0.67	0.61	
	0.00	0.11	0.05	0.09	0.07	0.03	0.65	0.75	
	0.00	0.01	0.01	0.04	0.04	0.17	1.05	0.97	
Abdomen (kN)		0.6	2.0	1.3	1.6	1.3	0.7	1.9	1.3
Pelvis (kN)		0.9	5.7	3.7	3.6	3.4	2.5	4.6	4.3
Rear Seat Passenger HEAD (HIC)		Corolla	Freelander	AE-MDB V2	AE-MDB V2	AE-MDB V2 J	Corolla	Freelander	AE-MDB V2
Rib Deflection (mm)		183	215	394	294	209	86	253	177
Upper	21	29	24	24	25	25	21	12	
	11	24	14	17	14	18	9	3	
	0	13	13	10	11	10	3	9	
Viscous Criterion	0.14	0.15	0.15	0.23	0.21	0.12	0.12	0.07	
	0.04	0.16	0.08	0.14	0.08	0.08	0.03	0.01	
	0.00	0.06	0.07	0.07	0.08	0.03	0.01	0.04	
Abdomen (kN)		1.4	0.8	2.3	1.9	2.1	0.1	1.2	1.4
Pelvis (kN)		1.1	1.7	3.2	3.5	3.7	1.7	4.0	5.4

**Table 1 EuroSID-I and ES-2 Dummy Results**

The driver and rear seat passenger dummy injury parameters for the Corolla and Alfa target vehicles are shown in Figure 31 to Figure 34. These have been calculated as percentages of the critical values as defined in ECE Regulation 95. These levels are as follows:

- HIC 1000
- Rib deflection 42mm
- V\*C 1.0m/s
- Abdomen force 2.5kN
- Pelvic force 6.0kN

The head injury criterion (HIC) recorded by the driver dummy in the Corolla tests showed the response of the AE-MDB tests to be between that of the two baseline tests. This was also the case for abdomen and pelvis. The maximum rib deflection and viscous criterion were at a similar level to that of the Freelander baseline test. For the rear seat passenger, the maximum rib deflection was

between that of the baseline tests and the viscous criterion was slightly above. In the case of the abdomen and pelvis, the barrier results were above those of the baseline tests.

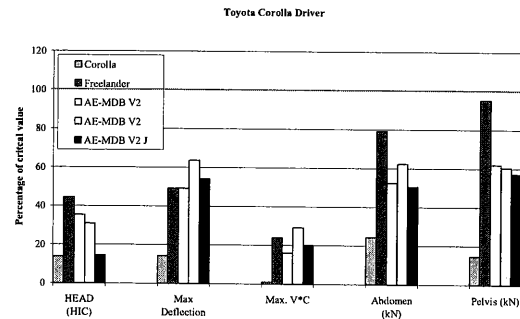


**Figure 31 Corolla driver dummy response**

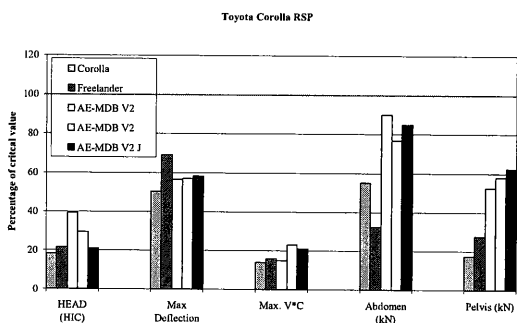


**Figure 32 Corolla RSP dummy response**

In the Alfa tests, the response of the driver dummy, when impacted with the AE-MDB, was always between the baseline car test results and generally closer to those of the Frelander. The chest deflection was above the critical level specified by R95, signifying a 30% risk of injury  $\geq$  AIS3. For the rear seat passenger, the HIC, rib deflection and viscous criterion of the barrier test were between or below the baseline values, whereas the abdomen and pelvis results were higher.

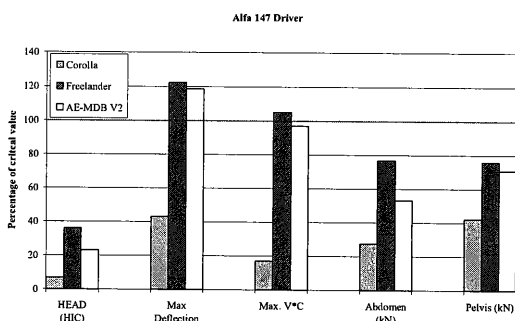


**Figure 33 Alfa driver dummy response**

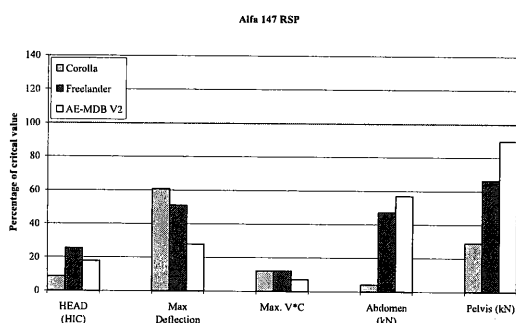


**Figure 34 Alfa RSP dummy response**

## DISCUSSION

The post test intrusion characteristics seen with the AE-MDB show that the barrier is able to replicate, to some extent, the form of deformation seen with the baseline vehicle tests. In the case of the Megane and Camry reported by Roberts et al, which were five and four door vehicles respectively, more

intrusion was caused to the front and rear doors than to the B-pillars of the target vehicles. This trend was visible in both the barrier and baseline tests. However, the door deformation with the AE-MDB was generally at a similar level to that of the most severe baseline test, whereas the loading to the B-pillar was similar to that of less severe baseline test. The tests to some of the target vehicles also showed that the form of intrusion with AE-MDB was similar to that of the baseline tests. Similar trends were visible to the deformation and the doors and B-pillar.

In reviewing the biomechanical data from all of the available driver dummy results, the AE-MDB data was often between or slightly higher than that of the baseline data. The areas where the barrier results exceeded the baseline data, and in the case of the Alfa the critical value, were the pelvis in the Megane, the abdomen and pelvis in the Camry and the ribs in the Corolla and Alfa.

For the rear seat passenger, the higher loading was generally seen in the abdominal and pelvic areas. The velocity profiles of all vehicles, where measured, suggest that the AE-MDB loaded the target vehicles at a similar rate to those of the Frelander baseline test, and in the case of the Corolla the peak velocity with the AE-MDB was slightly higher by approximately 1m/s. It should be borne in mind that the measurement method used for the Corolla baseline tests were different to those with the barrier, thus the magnitude of this difference may be less or greater than that recorded.

Based upon the results seen so far, WG13 believes that modifications to the AE-MDB design specification may be needed in order to reduce the post test 'differential intrusion' between the doors and B-pillar. The severity of the AE-MDB test procedure was either between that of the baseline tests. In some areas slightly more severe than the baseline tests, but this was not a trend that could be observed in all of the target vehicles.

## FUTURE RESEARCH

In order to increase the amount of loading applied by the AE-MDB to the B-pillar, WG13 is considering various modifications to the design specification.

One modification is based upon the application of a 'beam' type element being applied across the lower row of blocks. The beam element would be constructed from high strength honeycomb sandwich, which would try to replicate the presence of significant lateral connections between

longitudinal frontal structures that are present in some vehicles.

An alternative modification, would be to change the stiffness of block E to be more reflective of the rigid LCW data. The initial block stiffness could be increased along with the stiffness toward the end of the current corridor.

Further modifications that have been discussed are based upon a change in stiffness distribution for the lower row of blocks, along with the inclusion of a beam element as described above.

At the time of this report some numerical simulation of different AE-MDB modifications has taken place to provide guidance to future plans, but no barriers to a revised specification have been manufactured or tested.

## CONCLUSIONS

1. The completed review of the stiffness of modern vehicle frontal structures has complemented the previous data studied and presented by WG13, which lead to the current stiffness distribution for the AE-MDB.
2. From baseline vehicle testing, the AE-MDB has been shown to be representative of the baseline deformation profiles in some areas.
3. The deformation produced by the AE-MDB is, in some cases, above that of the baseline tests in the softer areas of the target vehicles (mid doors).
4. In the stiffer area of the target vehicles (B-pillar), the deformation caused by the AE-MDB was less than that applied by the most severe baseline test.
5. Most of the dummy injury parameters were well below the critical values used in the current European regulatory procedure, even when localised intrusion is greater than that of the severe baseline test.
6. The ongoing research may lead to some revisions of the existing AE-MDB design specification. However, no firm direction was available at the time of writing this paper.

## REFERENCES

- [1] Edwards M, Hobbs A, Davies H and Lowne R. 2000. *Review of the Frontal and Side Impact Directives: Final Report*. PR/SE/095/00, TRL Unpublished report.
- [2] EEVC Committee. 2000. *EEVC report to EC DG Enterprise regarding the revision of the frontal and side impact directives*. EEVC Committee.
- [3] Roberts A K, van Ratingen M R, (on behalf of EEVC WG13). 2003. *Progress on the development of the Advanced European Mobile Deformable*

*Barrier face (AE-MDB)*. The 18th International Technical Conference on the Enhanced Safety of Vehicles (ESV), Nagoya, Japan. Paper No. 126.

[4] Lowne R, (on behalf of EEVC WG13). 2001. *Research progress on improved side impact protection: EEVC WG13 progress report*. The 17th International Technical Conference on the Enhanced Safety of Vehicles (ESV). Amsterdam, The Netherlands. Paper No. 47.

[5] INSIA. 1997. *Structural Survey of Car. Definition of the main resistant elements in the car body*. EEVC WG15 Document. Doc No 20.

## ACKNOWLEDGEMENTS

The support and guidance of the WG13 members and its Japanese guests is gratefully acknowledged. The research impact testing was carried out by TNO, UTAC, BAST, TRL, INSIA and Fiat with the support of the respective governments and the Department of Transport and Regional Services (DoTaRs, Australia). Test vehicles were supplied by Toyota MEM and Fiat MC.

Current members of EEVC WG13 are:

A K Roberts TRL (chairman)

National representatives:

T Langner	Germany, BAST
M van Ratingen	The Netherlands, TNO
L Martinez	Spain, INSIA
J-P Lepretre	France, UTAC
G Antonetti	Italy, Fiat
J Ellway	United Kingdom, TRL (secretary)

Technical support members:

S Southgate	United Kingdom, Ford
J Faure/D Pouget	France, Renault
T Versmissen	The Netherlands, TNO
C Müller	Germany, DaimlerChrysler
P Janevik	Sweden, Volvo

# INVESTIGATION OF NEW SIDE IMPACT TEST PROCEDURES IN JAPAN

**Hideki Yonezawa**  
**Naruyuki Hosokawa**  
**Hiroko Minda**

National Traffic Safety and Environment Laboratory  
**Masao Notsu**  
Ministry of Land, Infrastructure and Transport

Japan

Paper No. 05-0188

## ABSTRACT

Various countries are independently conducting side impact tests with actual vehicles, resulting in extensive revisions of safety measures for accidents involving side collisions. However, the number of people injured and killed in these collisions remains high, and so more effective overall measures, including those for the vehicle itself, are urgently needed. The IHRA is actively conducting research toward enacting laws to standardize future methods of side impact tests as one way to realize international harmonization projects. This has led to MDB improvements as well as the improvement and development of dummies.

This report is intended to be useful for IHRA research activities. Tests were conducted using the improved dummies (ES-2, ES-2re) and AE-MDB in order to provide research results for comparison with body and dummy responses obtained in conditions complying with current regulations in Japan and Europe, and proposed regulations in the US.

## INTRODUCTION

Japan introduced a side impact regulation in 1998 for occupant protection in side collisions. As a result, the number of fatal and serious injuries in side collisions has reduced. However, there are still many side collision accidents, and further effective countermeasures are needed to reduce fatalities and serious injuries in side impacts. It is known that occupants in cars are inclined to sustain serious injuries when struck by vehicles with high front stiffness and high ground clearance such as SUVs (sport utility vehicles), MPVs and minivans. It is also necessary to consider improving the protection of occupants against side collisions with narrow objects such as trees and poles in single collisions.

In this paper, new side impact test procedures were investigated, which have been discussed in IHRA SIWG (International Harmonized Research

Activities Side Impact Working Group), and are proposed by the United States. These tests consist of (1) AE-MDB test in which the current vehicle specifications and front stiffness are taken into consideration and (2) Pole impact.

These test procedures were compared with the current regulation (ECE/R95). In the tests of the present research, new side impact dummies such as ES-2, SID-IIs and ES-2re were used in addition to the EuroSID-1.

## TEST CONDITIONS

### Test Conditions

Table 1 shows the test configurations and conditions in the present research. In the tests, two types of Japanese bonnet-type 4 door sedans as car A and car B were used. These two cars are representative models of the vehicle fleet in Japan. From Test No.1 to 4, car A was used as the target car. From No.5 to 7, car B was used.

Test No.1, 2, 3, 4 and 5 were conducted on the basis of the ECE/R95 test configuration. In Test No.1, the ECE/R95 moving deformable barrier (MDB) was used, and the EuroSID-1 was placed in a front seat and SID-IIs in a rear seat. In Test No.2, only ES-2 was placed in a front seat. In Test No.3 and 4, the AE-MDB was used as an MDB, and the ES-2 was placed in a front seat and SID-IIs in a rear seat. In Test No.3, the center line of the AE-MDB was in alignment with the front seat reference point (SRP) of the test car. On the other hand, in Test No.4, the center line of the AD-MDB was 250 mm behind the SRP. From Test No.1 to 4, injury criteria of dummies in front and rear seats were compared. In Test No.5, ES-2 was placed in the front seat of car B, and SID-IIs in the rear seat, and the injury criteria of the dummy were compared with the pole test using the same car model (Test No.6 and 7).

**Table 1.**  
**Test conditions in full-scale side impact test**

Test No.	1	2	3	4	5	6	7
Test config.							
Impact velocity	50km/h	50km/h	50km/h	50km/h	50km/h	32km/h	32km/h
Impact point	Striking vehicle C/L Front seat SRP of struck vehicle	Striking vehicle C/L Front seat SRP of struck vehicle	Striking vehicle C/L Front seat SRP of struck vehicle	Striking vehicle C/L Front seat SRP-250mm of struck vehicle	Striking vehicle C/L Front seat SRP of struck vehicle	Pole center to Front Dummy Head center	
MDB	Type	ECER95	ECER95	AE-MDB	AE-MDB	ECER95	Pole
	Mass	950kg	950kg	1503kg	1503kg	950kg	
	Ground Height	300mm	300mm	Barrier:300mm Bumper:350mm	Barrier:300mm Bumper:350mm	300mm	
Struck Vehicle	Front Dummy	EuroSID-1	ES-2	ES-2	ES-2	ES-2	1194kg
	Rear Dummy	SID-1ls	-	SID-1ls	SID-1ls	SID-1ls	-

Test No.6 and 7 are a pole test which was conducted based on the pole test proposed by NHTSA (FMVSS214 Draft). This pole test was conducted according to the proposal by NHTSA in the FMVSS 214 Draft where the impact velocity is 32 km/h, the impact angle is 75° and the pole diameter is 254 mm. In Test No.6 and 7, a curtain airbag was installed in car B. The ES-2 was placed in the front seat in Test No.6, and the ES-2re in Test No.7. In both tests, the center of gravity of the dummy head in a front seat was in alignment with the center of the pole.

### Moving deformable barrier

In ECE/R95 test conditions, the impact velocity of the MDB was 50 km/h and the ground clearance was 300 mm. The front face of the MDB in the tests was a barrier with a progressively changing crush pressure. The AE-MDB is an MDB that was developed based on the car dimensions, mass and front stiffness in the current vehicle fleet (Figure 1). It also considers both-vehicle traveling and loading of the rear seat occupants. The AE-MDB tests were conducted under two conditions: Center line of AE-MDB was in alignment with the front seat SRP (Test No.3), and it was 250 mm behind the front seat SRP (Test No.4).

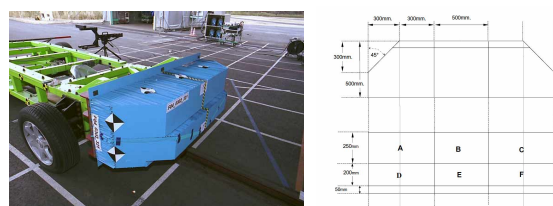


**Figure 1. Dimensions of AE-MDB.**

## TEST RESULTS

### Vehicle and MDB Deformation

The deformations of test car A (outer and inner panel) and MDB in Test No.1, 2, 3 and 4 are presented in Figure 2a and 2b. The deformation of

car B and MDB are also presented in Figure 3a and 3b. Velocity-time histories of car A at the side sill and front door, the MDB, and the lower spine of the ES-2 were compared in Test No.2, 3 and 4, and are shown in Figure 4.

The common velocity and its time of MDB and test car A (side sill) are different with various deformations of test car. Especially, there are differences of velocity at the front door among Test No.1, 2, 3 and 4, which can cause different injury criteria of the dummy.

### Exterior



### Interior



### MDB



Test No.1 (ECE/R95, EuroSID-1)      Test No.2 (ECE/R95, ES-2)

**Figure 2a. Deformation of test car and MDB (Test No.1 and 2).**

Exterior



Interior



MDB



Test No.3  
(AE-MDB)

Test No.4  
(AE-MDB, SRP-250mm)

Figure 2b. Deformation of test car and MDB (Test No.3 and 4).

Exterior



MDB



Interior



Test No.5  
(ECE/R95, ES-2)

Figure 3a. Deformation of test car and MDB (Test No.5).

Exterior



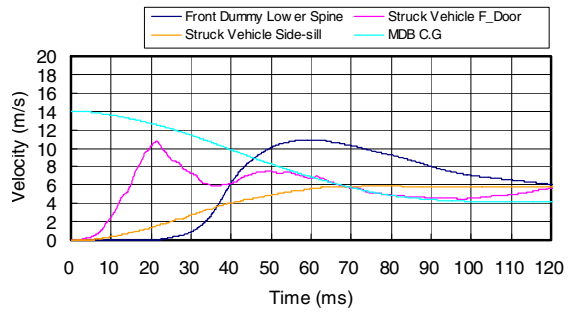
Interior



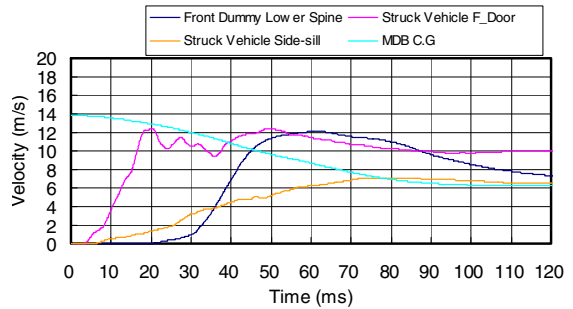
Test No.6  
(ES-2)

Test No.7  
(ES-2re)

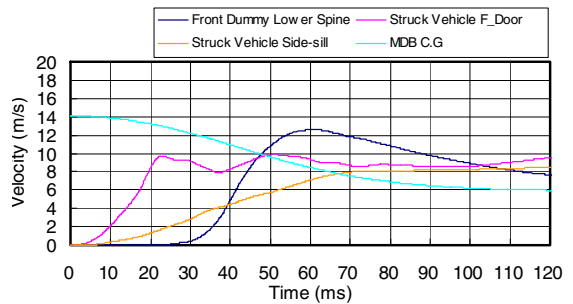
Figure 3b. Deformation of test car and MDB (Test No.6 and 7).



(a) Test No.2 (ECE/R95)



(b) Test No.3 (AE-MDB)



(c) Test No.4 (AE-MDB, SRP-250mm)

Figure 4. Velocity-time histories of car A and MDB.

## Dummy Injury Criteria in Car A

### Front seat dummy (EuroSID-1, ES-2)

Using the test results of Test No.1, 2, 3 and 4, the injury criteria of EuroSID-1 and ES-2 in car A impacted by AE-MDB were compared with those in the test condition using ECE/R95 MDB (Test No.2).

Injury criteria of the dummy were compared for ECE/R95 MDB and AE-MDB. Figure 5 shows the HPC (head performance criteria) of ES-2 in Test No.2, 3 and 4. The HPC of the dummy were higher in the AE-MDB tests than the ECE/R95 MDB test. In Test No.4 (SRP-250) where the AE-MDB target location was 250 mm behind the SRP, the head of the front seat dummy interacted with the B-pillar and HPC was above 600.

Figure 6 compares thorax upper, middle and lower rib deflections of the ES-2 dummy in Test No.2, 3 and 4. The thorax deflections are in descending order of upper, middle and lower rib, and there are no significant differences of dummy thorax deflection between ECE/R95 MDB and AE-MDB. The thorax deflection was slightly smaller in Test No.3 (AE-MDB center was in alignment with the target car front seat SRP) among the three tests.

The thorax V\*C of ES-2 is compared in Figure 7. The V\*C in upper, middle and lower rib was highest in the ECE/R95 MDB test (Test No.2), and lowest in the AE-MDB test (Test No.3).

The abdominal force and pubic force of ES-2 are compared in Figure 8. The abdominal force shows similar values among the three tests, whereas the pubic force is higher in the AE-MDB tests (Test No.3 and 4) than the ECE/R95 MDB test (Test No.2). In Test No.3, the abdominal force and pubic force are highest, though the thorax rib deflection and V\*C were smallest among the three tests.

Injury criteria of front seat dummies are compared between EuroSID-1 (Test No.1) and ES-2 (Test No.2) in Figure 9. The thorax rib deflection and V\*C are higher for ES-2 than EuroSID-1. However, the abdominal force and pubic force are similar between the two dummies. Due to a modification of the back plate of ES-2 from EuroSID-1, interaction between the dummy back and the seat back was changed, which significantly affects the thorax injury criteria.

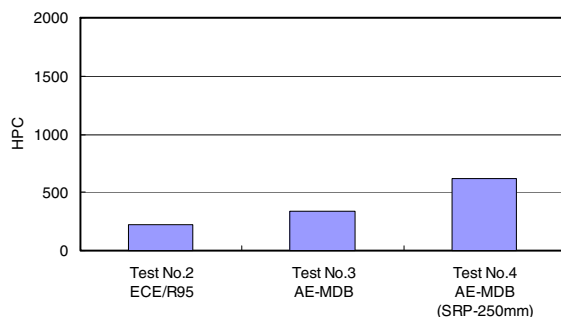


Figure 5. HPC of ES-2 in car A.

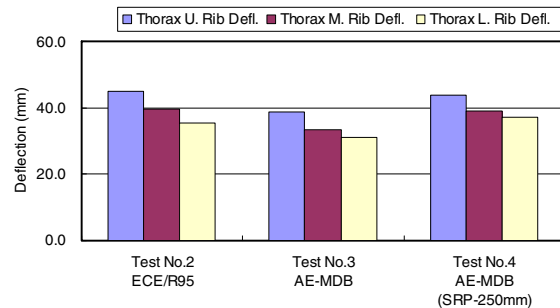


Figure 6. Thorax rib deflection of ES-2 in car A struck by ECE/R95 MDB or AE-MDB.

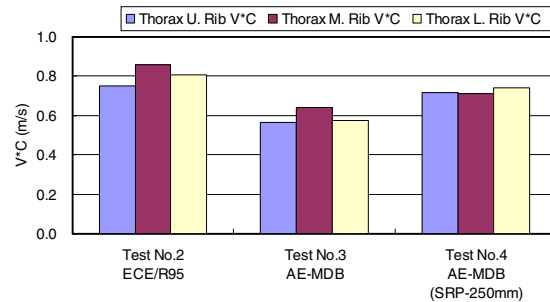


Figure 7. Thorax Rib V\*C of ES-2 in car A struck by ECE/R95 MDB or AE-MDB.

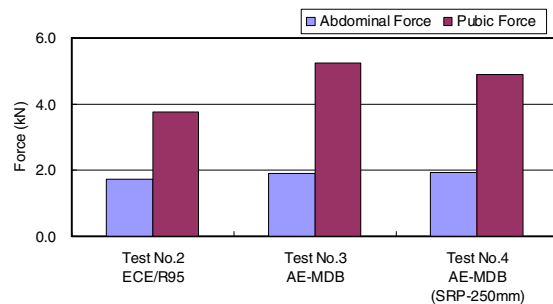
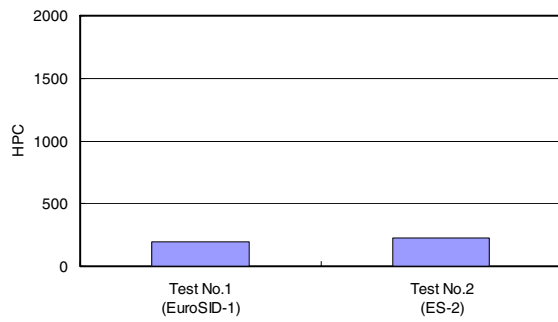
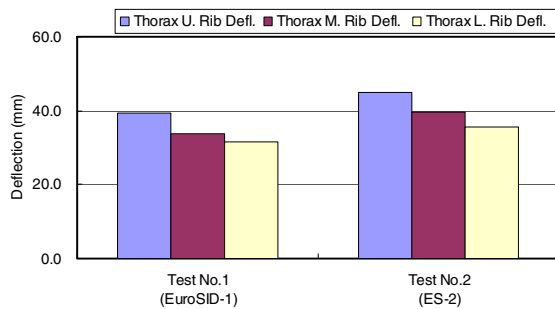


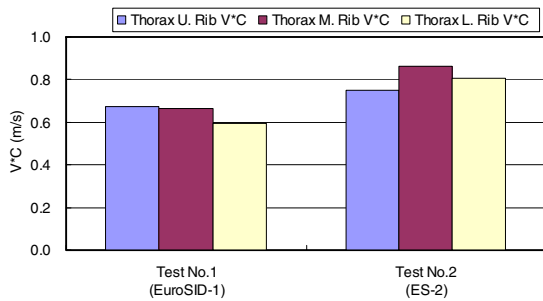
Figure 8. Abdominal and Pubic Force of ES-2 in car A struck by ECE/R95 MDB or AE-MDB.



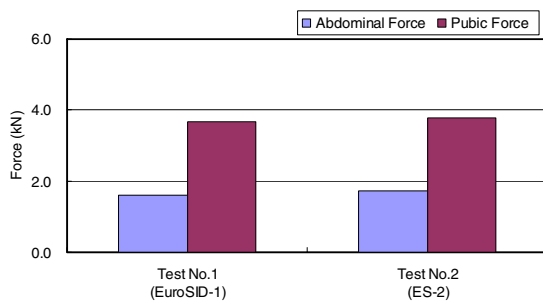
(a) HPC



(b) Thorax rib deflection



(c) Thorax rib V\*C



(d) Abdominal force and pubic force

**Figure 9. Comparison of injury criteria between EuroSID-1 and ES-2 in car A struck by ECE/R95 MDB.**

**Rear seat dummy (SID-IIs)** The injury criteria of the rear seat dummy (SID IIs) in car A impacted by ECE/R95 MDB and AE-MDB were compared from the results of Test No.1, 3, and 4.

Figure 10 shows the HPC of SID-IIs. The HPC was inclined to be higher in the AE-MDB test than ECE/R95 MDB. In Test No.4, the head made contact with the C-pillar, which led to high HPC because the AE-MDB impacted toward the rear of the car compared with other tests.

The shoulder rib deflection and thorax rib accelerations of SID-IIs are compared in Figure 11. The shoulder rib deflections are similar among the three tests. The upper and middle rib accelerations are lower in Test No.3, and higher in Test No.4 compared with the ECE/R95 MDB test (No.1). The lower thorax rib accelerations are similar in the two AE-MDB tests, and they are far higher than in the ECE/R95 MDB test.

Figure 12 shows abdominal rib deflections of SID-IIs. Compared with the ECE/R95 test, the abdominal upper rib deflection is small in Test No.3, and is large in Test No.4. The abdominal lower rib deflection in the AE-MDB tests (Test No.3 and 4) is larger than that in the ECE/R95 MDB test (Test No.1).

The pubic force, iliac force and acetabulum force are shown in Figure 13. The pubic force is similar in the three tests. The iliac force is significantly greater in the AE-MDB tests (Test No.3 and 4) than in the ECE/R95 MDB test (Test No.1). On the other hand, the acetabulum force in the AE-MDB test is high in Test No.3 and is low in Test No.4 compared with that in the ECE/R95 MDB test.

In the present research, the impact location of the AE-MDB tests was changed, therefore, the vehicle deformation and door impact velocity became different from that of ECE/R95 MDB, which affected the injury criteria of the dummy in the front seat. In Test No.4, since the vehicle deformation around the rear seat was large and the injury criteria of the rear seat dummy in this test tended to be higher than in the other tests, the effects of MDB were large compared with the front seat dummy.

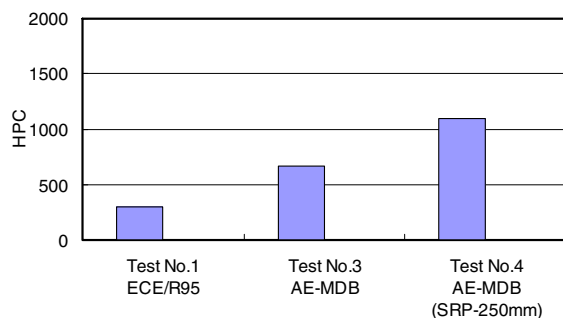


**Figure 10. HPC of rear seat dummy (SID-IIs) in car A struck by ECE/R95 MDB or AE-MDB.**

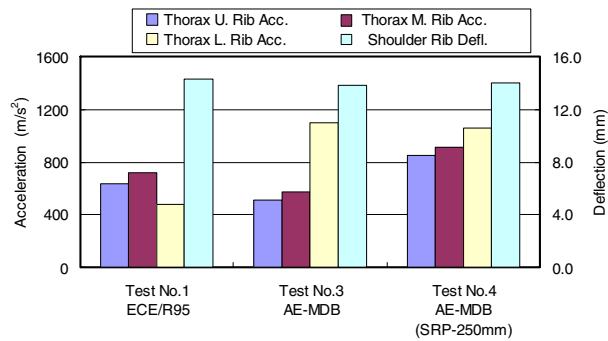


**Figure 11. Shoulder rib deflection and thorax rib accelerations of rear seat dummy (SID-II) in car A struck by ECE/R95 MDB or AE-MDB.**

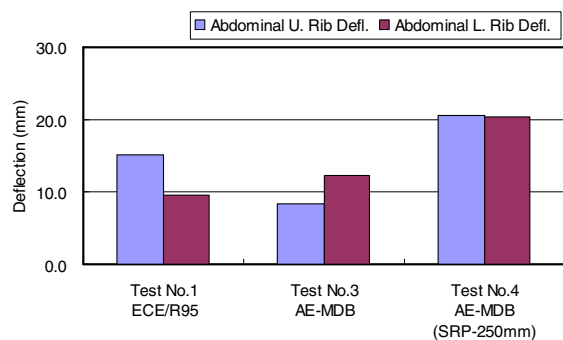


**Figure 12. Abdominal rib deflection of rear seat dummy (SID-II) in car A struck by ECE/R95 MDB or AE-MDB.**

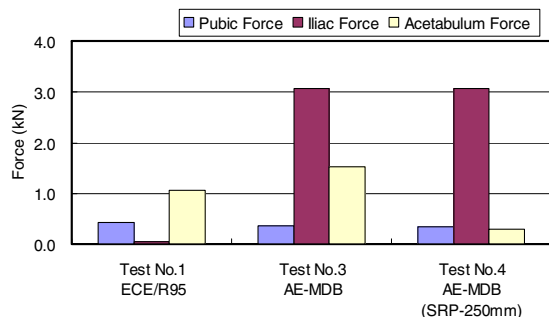


**Figure 13. Pubic, iliac and acetabulum force of rear seat dummy (SID-II) in car A struck by ECE/R95 MDB or AE-MDB.**

### Dummy Injury Criteria in Car B

Based on Test No.5, 6 and 7, the injury criteria of the dummy in car B were examined. The car exterior deformations at the ground clearance level of H.P., thorax, and side sill in the pole test (Test No.6 and 7) are shown in Figure 14. The vehicle deformation at each location is similar in these tests. The deformation of car B in Test No.6 is relatively large compared with that in Test No.7.

The injury criteria of the dummy in car B were compared between the ECE/R95 MDB test and pole test. Figure 15 shows the HPC of the dummy.

Although the curtain airbag deployed, the HPC of the dummy was higher in the pole test compared with the ECE/R95 MDB test. The HPC of ES-2 in the pole test was especially large. Thorax rib deflection is compared in Figure 16. The thorax upper, middle and lower rib deflections were larger in the pole test than in the ECE/R95 MDB test because the door intrusion at the thorax was large in the pole test. The thorax upper, middle and lower rib deflections showed similar tendencies between ES-2 and ES-2re. However, in general, the ES-2re showed higher thorax deflections than ES-2. Thorax rib V\*C of the dummy in car B is compared in Figure 17. The V\*C is higher in the pole test than in the ECE/R95 MDB test. Abdominal force and pubic force of the dummy are shown in Figure 18. The abdominal force is higher in the pole test whereas the pubic force is higher in the ECE/R95 test.

The ES-2 and ES-2re were compared in the pole test (Test No.6 and 7). The thorax upper rib V\*C is similar between ES-2 and ES-2re. The thorax middle rib V\*C of ES-2re is higher than that of ES-2, and the lower rib V\*C of ES-2 is higher than that of ES-2re. Abdominal force and pubic force are similar between ES-2 and ES-2re.

It is difficult to directly compare dummy injury criteria between the pole test proposed by NHTSA and the ECE/R95 test since the test configurations were different. However, the pole test is very severe for the injury criteria of the head and chest of the dummy. In comparing the ES-2re with ES-2, the thorax rib deflection and thorax rib V\*C showed higher values in ES-2re since the ES-2re was improved against oblique impacts.

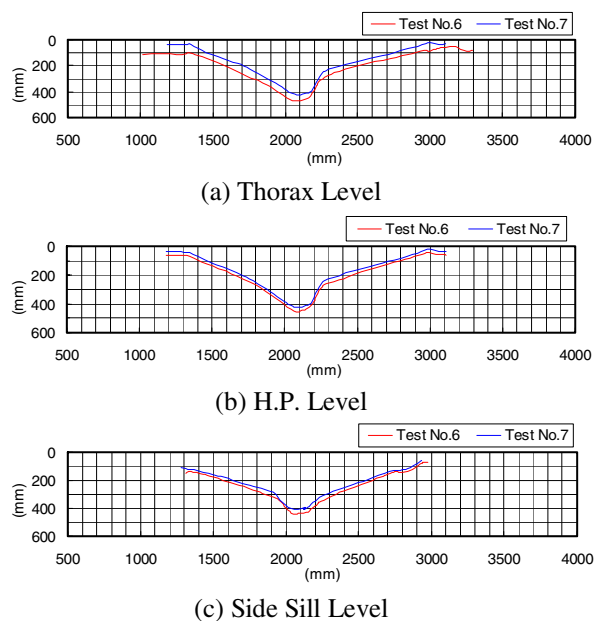


**Figure 14. Deformation of outer panel of car B in the pole test (Test No.6 and 7).**

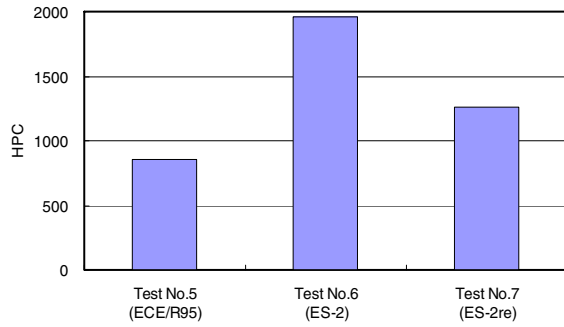


Figure 15. HPC of ES-2 and ES-2re in car B in the ECE/R95 test and pole test.

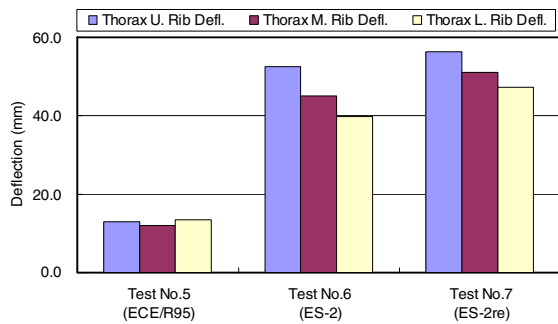


Figure 16. Thorax rib deflection of ES-2 and ES-2re in car B in the ECE/R95 test and pole test.

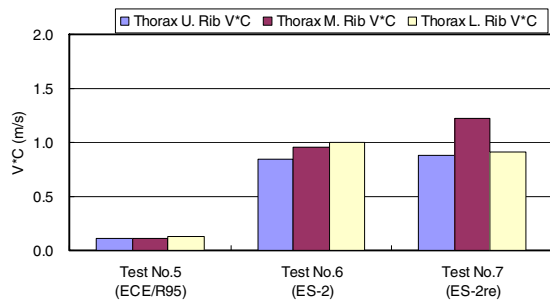


Figure 17. Thorax rib V\*C of ES-2 and ES-2re in car B in the ECE/R95 test and pole test.

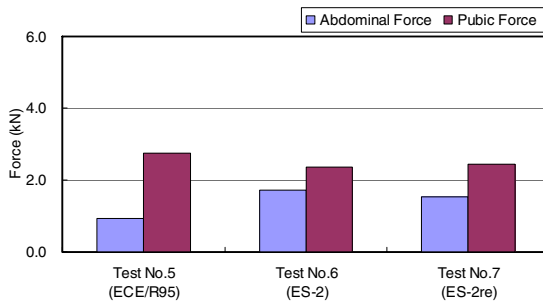


Figure 18. Abdominal force and pubic force of ES-2 and ES-2re in car B in the ECE/R95 test and pole test.

## SUMMARY

The test procedures proposed by IHRA or by NHTSA were compared with the present test (ECE/R95) with respect to injury criteria of the dummy and dummy types. The results are summarized as follows.

### (1) AD-MDB

The tests using AD-MDB, which has been developed to reflect the specifications and stiffness of the present cars, were compared with the ECE/R95 test.

- (i) The vehicle deformation and velocity-time histories were different and could affect injury criteria of the front seat dummy, especially for pubic force.
- (ii) In the AE-MDB test with rearward target point (SRP-250 mm), the deformation in the rear door was large and affected the rear dummy injury criteria. The head made contact with the C-pillar, which led to high HPC.
- (iii) Regarding the injury criteria of EuroSID-1 and ES-2 in the ECE/R95 MDB tests, the thorax deflection and thorax V\*C were higher for ES-2 because the back plate of ES-2 was modified from EuroSID-1.

### (2) Pole impact test

The pole test, which NHTSA is considering introducing in the regulation (FMVSS214 draft), was compared with the ECE/R95 MDB test.

- (i) The injury criteria of the head and chest of the dummy in the pole test were far higher than in the ECE/R95 test.
- (ii) The HPC of the dummy in the pole test could be higher, even though the curtain air bag deployed, depending on airbag deployment timing.
- (iii) ES-2re showed a larger thorax rib deflection and V\*C than ES-2 due to the modification of ES-2re against oblique impacts. However, they showed similar HPC, abdominal force and pubic force.

The MDB prescribed in the present regulation (ECE/R95) was determined on the basis of investigations of vehicles in the 1970s. Recently, there are various vehicle types in the fleet, and it is necessary to develop an MDB (AE-MDB) which reflects the vehicle specifications and front stiffness of the current cars.

In the present research, a series of side impact tests was conducted using the AE-MDB that is under development based on the data of each country in IHRA SIWG. Fundamental research is on-going to develop test procedures with a high level of occupant protection. In addition to car-to-car collisions, occupant protection in single-car crashes is also important. In the present research, the pole test

proposed by NHTSA was carried out and the dummy injury criteria were examined. In Japan, basic research on occupant protection in side collisions will be continued, and side impact test procedures will be developed in the near future.

## REFERENCES

1. Yonezawa, H., et al. "Investigation of New Side Impact Test Procedures in Japan," 18<sup>th</sup> ESV, Paper Number 328 (2003)
2. Yonezawa, H., et al. "Japanese Research Activity on Future Side Impact Test Procedures," 17<sup>th</sup> ESV, Paper Number 267 (2001)
3. Seyer, K., "International Harmonized Research Activities Side Impact Working Group Status Report," 18th ESV, Paper Number 579 (2003)
4. ECE Regulation No.95, "Uniform provisions concerning the approval of vehicles with regard to the occupants in the event of a lateral collision" (1995)

# DELTA VS FOR IIHS SIDE IMPACT CRASH TESTS AND THEIR RELATIONSHIP TO REAL-WORLD CRASH SEVERITY

**Raul A. Arbelaez**

**Bryan C. Baker**

**Joseph M. Nolan**

Insurance Institute for Highway Safety

United States

Paper Number 05-0049

## ABSTRACT

The Insurance Institute for Highway Safety (IIHS) began publishing side impact crashworthiness evaluations for consumer information in 2003. The test on which the evaluations are based uses a barrier representing the ride height and front-end geometry of a pickup truck or sport utility vehicle. In this test a stationary vehicle is struck laterally by a 1,500 kg moving deformable barrier traveling at 50 km/h. In determining the impact severity for the test, the goal was to select an impact velocity that would both drive improvements in side impact protection and discriminate between vehicles in the current fleet offering varying levels of protection.

In the present study the Simulating Motor Vehicle Accident Speeds on the Highway (SMASH) computer program was used to obtain delta Vs for vehicles tested in the IIHS side impacts. These were compared with delta V estimates calculated using the principle of conservation of momentum. The delta Vs calculated from the IIHS tests were compared with those from injury-producing side crashes in the National Automotive Sampling System (NASS) to see how the severity of the IIHS test compares with real-world side crashes.

Analysis of 49 side crashes conducted by IIHS indicates that, overall, SMASH calculations produced delta Vs within 5 km/h of the delta V determined using the conservation of momentum principle. The SMASH delta Vs ranged from 18 to 31 km/h, and the average delta V was 24 km/h. The maximum occupant compartment crush in these tests ranged from 27 to 46 cm. Comparison of delta Vs and maximum crush measures from the 1998-2003 NASS data files indicates that 30-55 percent of real-world front-to-side crashes with seriously injured nearside occupants and 10-25 percent of the crashes with fatal injuries to nearside occupants are less severe than the IIHS side impact test.

## INTRODUCTION

Between 1992 and 2001 the demand for pickup trucks and sport utility vehicles (SUVs) pushed their sales up from 26 to 41 percent of all vehicles sold in

the United States (Automotive News, 1993, 2002). By 2003 pickups and SUVs comprised almost one-third of the registered passenger vehicles in the U.S. fleet (R.L. Polk & Co., 2004). In 2004 these vehicles represented 45 percent of the vehicles sold in the United States (Crain Communications Inc, 2005).

Data from the Fatality Analysis Reporting System (FARS) from 1998 to 2003 show two-vehicle side impact crashes result in approximately 4,000 struck vehicle occupant fatalities per year in the United States (National Highway Traffic Safety Administration, 2004). In 2003 pickups and SUVs comprised 59 percent of the striking vehicles in these fatal crashes. Real-world crash investigations also have shown that pickups, SUVs, and vans are disproportionately involved as striking vehicles in side impact crashes in which the occupants of the struck vehicle sustained serious and fatal injuries (Augenstein et al., 2000; Lund et al., 2000; Thomas and Frampton, 1999; Zaouk et al., 2001). Previous research by Nolan et al. (1999) and Rattenbury et al. (2001) suggests the elevated ride height of pickups and SUVs contributes to their overrepresentation in real-world side impact crashes where the struck vehicle occupants sustain serious or fatal injuries.

In 1999 the Insurance Institute for Highway Safety (IIHS) began developing a new side impact test to evaluate occupant protection in passenger vehicles struck by a truck-like barrier. The moving deformable barrier (MDB) used in this side impact test, the IIHS barrier (Figure 1), was designed to match the front-end geometry and ride height of pickups and SUVs (Arbelaez et al., 2002). By the end of 2002 IIHS began evaluating vehicles in its side impact consumer information program. In the IIHS test a 1,500 kg barrier strikes a stationary vehicle at 50 km/h. The impact severity for the test was established through a series of tests in which the impact angle, velocity, and mass of the striking MDB was varied (Dakin et al., 2003). The impact mass and velocity selected for the IIHS test were chosen to drive improvements in side impact protection while still providing discrimination among vehicles in the current fleet offering varying levels of protection.

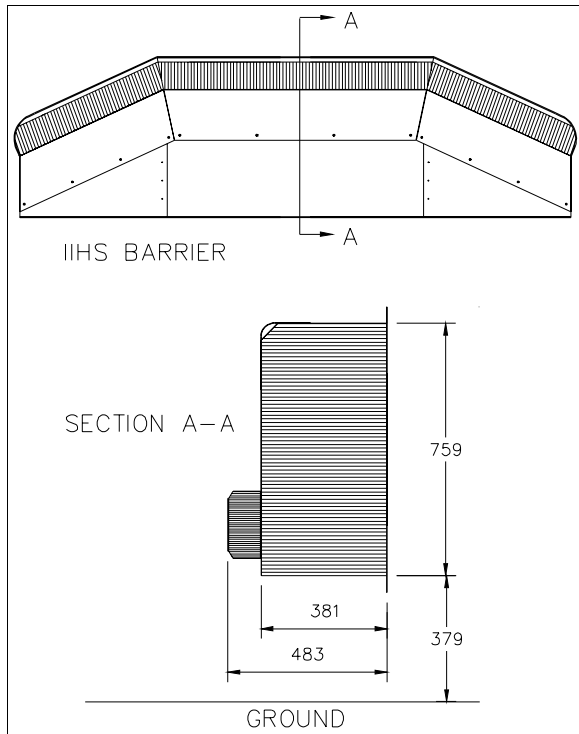


**Figure 1. Top and side cross-sectional views of IIHS barrier; all measurements are in millimeters.**

Crash severity often is described by a vehicle's change in velocity (delta V) during the crash; delta V is the primary metric used to quantify crash severity in the National Automotive Sampling System (NASS) database. Since 1997 delta Vs for crashed vehicles in NASS have been estimated from measures of vehicle crush using the Simulating Motor Vehicle Accident Speeds on the Highway (SMASH) computer program. In the present study SMASH was used to obtain comparable estimates of delta Vs of vehicles subjected to the IIHS side impact test. The purpose was to understand how well these field procedures estimate the actual delta Vs calculated using the conservation of momentum principle and, by comparison with NASS cases, to see how the severity of the IIHS test compares with real-world side impact crashes.

To obtain another perspective on how the IIHS test relates to real-world side impacts, maximum occupant compartment crush measures from the IIHS test were compared with crush distributions for injury-producing crashes in the NASS database.

## METHODS

A total of 37 different vehicle models were subjected to 49 side impacts with the IIHS barrier at 50 km/h. These impacts were conducted according to the IIHS "Crashworthiness Evaluation Side Impact Crash Test

Protocol" (IIHS, 2004). Delta Vs for these vehicles were calculated using the NASS measurement protocol and the SMASH (Version 1.3) damage-only algorithm. SMASH results were averaged for each of the 12 models subjected to repeated tests. The vehicle and barrier crush specifications and crush measures used in the SMASH program are shown in Appendices A, B, and C. The SMASH size category used to describe each vehicle was based on its wheelbase, and the SMASH stiffness value was set equal to the size category, per NASS protocol. The size and stiffness categories for the IIHS barrier were set to the values used in SMASH for "movable barriers" (size and stiffness = 10). In SMASH there is no deformation energy attributed to vehicles categorized as movable barriers (i.e., for a side impact test the delta V estimate for the struck vehicle does not take into account the deformation of the striking barrier). To correct the delta V output for the known deformation of the barrier, the energy absorbed by the deformable barrier was calculated using the measured crush at the height of the barrier's bumper element along with the known crush strength of the barrier's main core (310 kPa). The adjusted delta V for the struck vehicle,  $\Delta V_2$ , was calculated using the following delta V-energy relationship:

$$\frac{\Delta V_1^2}{\Delta V_2^2} = \frac{E_1}{E_2}$$

where,

$\Delta V_1$  = SMASH-calculated struck vehicle delta V (MDB size and stiffness = 10);

$\Delta V_2$  = energy-adjusted delta V for struck vehicle;

$E_1$  = SMASH-calculated energy for struck vehicle (MDB size and stiffness = 10); and

$E_2 = E_1 +$  barrier energy calculated from crush measures.

The adjusted delta V estimates from SMASH then were compared with the delta V calculated using the principle of conservation of momentum and the maximum vehicle delta V recorded by on-board vehicle accelerometers.

Delta Vs from real-world crashes were extracted from the 1997-2003 NASS data files for side impacts involving two vehicles in which there were no ejections of struck vehicle occupants or rollovers. NASS cases were selected based on the following criteria:

- Struck vehicles were restricted to 1990+ model years;
- Collision Deformation Classification (CDC) coding that represents crashes with struck vehicle damage distribution to the occupant compartment;

this includes CDC lateral damage classifications areas D (distributed), P (occupant compartment), Y (occupant compartment and front one-third of vehicle), and Z (occupant compartment and rear one-third of vehicle);

- Principle direction of force was limited to 8-10 o'clock for impacts to the left side of the vehicle and 2-4 o'clock for the right side impacts; and
- Crashes in which struck-side occupants sustained injuries.

The 1997-2003 NASS data contained a total of 9,993 vehicles with reported side structure damage, of which 1,799 met the crash conditions described above. Of those 1,460 vehicles had delta Vs computed using the SMASH damage-only algorithm. In this study the NASS data were used to relate SMASH delta Vs to injury levels.

## RESULTS

Delta Vs calculated using the SMASH damage-only algorithm for the IIHS side impact crashes are listed by vehicle type in Tables 1-3, along with delta Vs calculated using conservation of momentum and actual delta Vs recorded by vehicle accelerometers. Figures 1-3 show postcrash side deformation on vehicles from each of the three vehicle categories used in this study. For all but two of the vehicle models tested, the delta V calculated using the principle of conservation of momentum was within 1 km/h of the maximum lateral delta V recorded by on-board vehicle accelerometers. Overall, the SMASH delta Vs computed for the vehicles in this study were within 5 km/h of the delta Vs calculated using the conservation of momentum and those recorded by the accelerometers mounted in the occupant compartment of the struck vehicles. The SMASH delta Vs for the small and midsize cars and small SUVs tested in the IIHS side crashworthiness evaluation program ranged from 18 to 31 km/h; the average SMASH delta V was 24 km/h.

**Table 1.**  
**Delta Vs calculated for small four-door cars in side crashes with a 1,500 kg IIHS barrier at 50 km/h**

Year, make, and model	Delta V (km/h)		
	Conserv. of momentum	Vehicle accel.	SMASH
2004 Kia Spectra	25	25	29
2004 Nissan Sentra	26	26	31
2005 Dodge Neon	26	26	28
2005 Ford Focus	26	27	26
2005 Saturn Ion*	26	27	24
2005 Toyota Corolla*	26	27	28
<b>Average</b>	26	26	28

\*Based on average results of two tests

**Table 2.**  
**Delta Vs calculated for midsize four-door cars in side crashes with a 1,500 kg IIHS barrier at 50 km/h**

Year, make, and model	Delta V (km/h)		
	Conserv. of momentum	Vehicle accel.	SMASH
2004 Acura TL	23	23	24
2004 Chevrolet Malibu*	24	24	24
2004 Dodge Stratus	24	21	26
2004 Honda Accord*	24	24	25
2004 Hyundai Sonata	24	24	27
2004 Jaguar X-Type	23	23	24
2004 Lexus ES 330*	23	22	21
2004 Mazda 6	24	24	28
2004/05 Mitsubishi Galant*	23	24	22
2004 Saab 9-3	24	25	22
2004 Saab 9-5	23	22	23
2004 Saturn L Series	24	24	25
2004 Suzuki Verona	23	23	26
2004 Toyota Camry*	24	25	26
2005 Mercedes C 240	23	24	20
2005 Nissan Altima	24	23	28
2005 Subaru Legacy*	24	25	21
2005 Volvo S40	24	24	21
<b>Average</b>	24	24	24

\*Based on average results of two tests

**Table 3.**  
**Delta Vs calculated for small SUVs in side crashes with a 1,500 kg IIHS barrier at 50 km/h**

Year, make, and model	Delta V (km/h)		
	Conserv. of momentum	Vehicle accel.	SMASH
2002/03 Land Rover Freelander*	23	24	24
2003 Ford Escape*	23	24	20
2003 Honda CR-V*	23	25	21
2003 Honda Element	23	23	21
2003 Hyundai Santa Fe	22	22	18
2003 Mitsubishi Outlander	23	23	22
2003 Saturn VUE	23	24	20
2003 Subaru Forester*	24	25	23
2003 Suzuki Grand Vitara	24	25	24
2003 Toyota RAV4	24	25	24
2004 Toyota RAV4	24	24	23
2005 Ford Escape	23	24	19
2005 Honda CR-V	23	24	20
<b>Average</b>	23	24	21

\*Based on average results of two tests



**Figure 1.** Example of postcrash deformation of small car (2005 Dodge Neon) following IIHS test



**Figure 2. Example of postcrash deformation of midsize car (2004 Toyota Camry) following IIHS test**



**Figure 3. Example of postcrash deformation of small SUV (2003 Ford Escape) following IIHS test.**

Maximum struck vehicle crush measured in the IIHS crash tests ranged from 27 to 46 cm, with an average maximum crush of 37 cm for all vehicle models. Table 4 shows the crush ranges for the small and midsize cars and the small SUVs tested.

**Table 4.**  
**Distribution of maximum vehicle crush**

Vehicle type	Maximum crush (cm)		
	Range	Average	± st. dev
Small cars	37-42	40	2
Midsize cars	27-46	38	6
Small SUVs	29-40	34	4
<b>All IIHS tests</b>	<b>27-46</b>	<b>37</b>	<b>5</b>

The delta Vs, maximum vehicle crush, and occupant injury data from the 1997-2003 NASS data files were weighted according to NASS guidelines. Figure 4 shows the cumulative distribution of the delta Vs from the weighted NASS cases by maximum abbreviated injury scale (MAIS) level for nearside struck occupants. The average delta V for the vehicles tested was 24 km/h; the calculated delta V for the IIHS test using the principle of conservation of momentum would be 25 km/h, assuming that both vehicles are of the same mass and the striking vehicle is traveling at 50 km/h. Based on a 25 km/h delta V reference, the IIHS test is more severe than 45 percent of the crashes with MAIS 2+ injuries, 30 percent of the crashes with MAIS 3+ injuries, and 10 percent of the real-world front-to-nearside struck occupant fatalities (Figure 4).

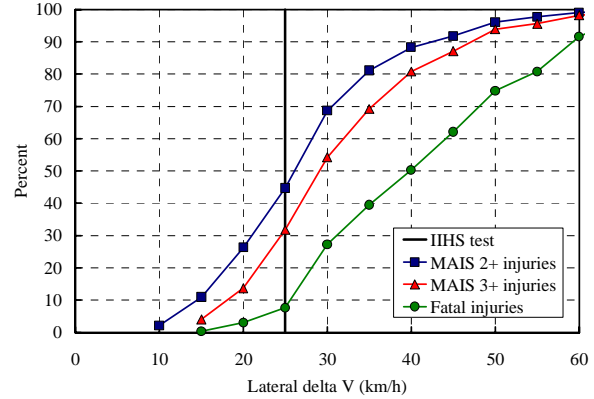


**Figure 4. Cumulative distribution of delta Vs in two-vehicle front-to-nearside crashes; highlighted IIHS test delta V of 25 km/h represents the delta V for striking and struck vehicles of equal mass.**

Figure 5 shows the cumulative distribution of the maximum struck vehicle crush from the weighted NASS cases by MAIS level for nearside struck occupants. The NASS cases considered for the maximum crush versus injury comparison were not restricted to cases in which delta V was determined; this restriction was used only for the delta V versus injury comparison. Given a maximum crush value of 37 cm as a reference value for the IIHS test, the IIHS side crash test is more severe than 60 percent of the crashes with MAIS 2+ injuries, 55 percent of the crashes with MAIS 3+, and 25 percent of the real-world front-to-nearside crashes with struck occupant fatalities.

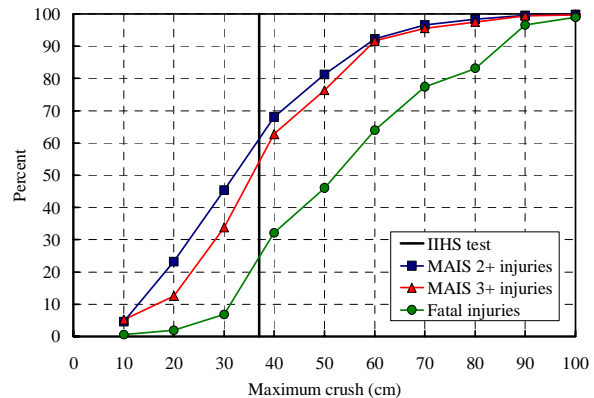


**Figure 5. Cumulative distribution of maximum struck vehicle crush in two-vehicle front-to-nearside crashes; highlighted 37 cm maximum crush line represents the average maximum crush from IIHS side impact tests.**

## DISCUSSION

On average the SMASH delta Vs for vehicles subjected to the IIHS side impact differed from the delta Vs calculated from conservation of momentum and those recorded by vehicle accelerometers during each crash test by only 1-2 km/h. However, the SMASH

delta Vs had a much wider range (18-31 km/h) than the delta Vs based on the conservation of momentum (22-26 km/h) The SMASH reconstructions in this study indicate that the SMASH damage-only algorithm can be off by as much as 20 percent for an individual vehicle.

Analysis of delta Vs and maximum crush values from the IIHS tests indicates the test severity is on the low end of real-world crashes resulting in fatalities (75-90 percent of fatal crashes appear to be more severe), but it is well into the distribution of crash severity resulting in serious injury (30-55 percent of serious injuries occur in less severe crashes). These results indicate that the majority of serious injury and fatal side impact crashes are occurring at significantly higher crash severities than currently are being evaluated in either federal regulation or consumer information tests. Of the NASS cases included in this study with fatal nearside occupants, more than half have maximum deformation of the vehicle side structure of at least 50 cm, which corresponds to approximately one quarter of a typical vehicle width.

#### ACKNOWLEDGMENT

This work was supported by the Insurance Institute for Highway Safety.

#### REFERENCES

Arbelaez, R.A.; Dakin, G.J.; Nolan, J.M.; Dalmotas, D.J.; and Tylko, S. 2002. IIHS side impact barrier: development and crash test experience. *IMEchE Conference Transactions: International Conference on Vehicle Safety 2002*, 73-88. London, United Kingdom: Professional Engineering Publishing Ltd.

Augenstein, J.; Bowen, J.; Perdeck, E.; Singer, M.; Stratton, J.; Horton, T.; et al. 2000. Injury patterns in near-side collisions (SAE 2000-01-0634). *Side Impact Collision Research* (SP-1518), 11-18. Warrendale, PA: Society of Automotive Engineers.

Automotive News. 1993. *1993 Market Data Book*, p. 26. Detroit, MI: Crain Communications Inc.

Automotive News. 2002. *2002 Market Data Book*. Detroit, MI: Crain Communications Inc.

Crain Communications Inc. 2005. *Automotive News*, no. 6129, January 10. Detroit, MI.

Dakin, G.J.; Arbelaez, R.A.; Nolan, J.M.; Zuby, D.S.; and Lund, A.K. 2003. Insurance Institute for High-

way Safety side impact crashworthiness valuation program: impact configuration and rationale. *Proceedings of the 18th International Technical Conference on the Enhanced Safety of Vehicles* (CD-ROM). Washington, DC: National Highway Traffic Safety Administration.

Insurance Institute for Highway Safety. 2004. Crashworthiness evaluation side impact crash test protocol (version IV). Arlington, VA.

Lund, A.K.; O'Neill, B.; Nolan, J.M.; and Chapline, J.F. 2000. Crash compatibility issue in perspective (SAE 2000-01-1378). *Vehicle Aggressivity and Compatibility in Automotive Crashes* (SP-1525). Warrendale, PA: Society of Automotive Engineers.

National Highway Traffic Safety Administration. 2000. NASS Crashworthiness Data System 2000 Coding and Editing Manual. Washington, DC: U.S. Department of Transportation.

National Highway Traffic Safety Administration. 2004. Fatality Analysis Reporting System. Washington, DC: U.S. Department of Transportation.

Nolan, J.M.; Powell, M.R.; Preuss, C.A.; and Lund, A.K. 1999. Factors contributing to front-side compatibility: a comparison of crash test results (SAE 99SC02). *Proceedings of the 43rd Stapp Car Crash Conference* (P-350), 13-24. Warrendale, PA: Society of Automotive Engineers.

Rattenbury, S.J.; Gloyns, P.F.; and Nolan, J.M. 2001. Vehicle deformation in real-world side impact crashes and regulatory crash tests. *Proceedings of the 17th International Technical Conference on the Enhanced Safety of Vehicles* (CD ROM) Washington, DC: National Highway Traffic Safety Administration.

R.L. Polk & Co. 2004. National vehicle population profile database. Southfield, MI.

Thomas, P. and Frampton, R. 1999. Injury patterns in side collisions – a new look with reference to current test methods and injury criteria (SAE 99SC01). *Proceedings of the 43rd Stapp Car Crash Conference* (P-350), 1-12. Warrendale, PA: Society of Automotive Engineers.

Zaouk, A.K.; Eigen, A.M.; and Digges, K.H. 2001. Occupant injury patterns in side crashes (SAE 2001-01-0723). *Side Impact, Rear Impact, and Rollover* (SP-1616), 77-81. Warrendale, PA: Society of Automotive Engineers.

**APPENDIX A. Specifications for vehicles subjected to IIHS side crash test**

<b>Test ID</b>	<b>Vehicle type</b>	<b>Vehicle year, make, and model</b>	<b>Wheelbase (cm)</b>	<b>Length (cm)</b>	<b>Width (cm)</b>	<b>Mass (kg)</b>
1	Small	2004 Kia Spectra	261	448	174	1,484
2	Small	2004 Nissan Sentra	254	452	171	1,375
3	Small	2005 Dodge Neon	267	444	171	1,396
4	Small	2005 Ford Focus	262	445	169	1,412
5A	Small	2005 Saturn Ion	262	469	171	1,432
5B	Small	2005 Saturn Ion	262	469	171	1,424
6A	Small	2005 Toyota Corolla	260	453	170	1,372
6B	Small	2005 Toyota Corolla	260	453	170	1,360
7	Midsized	2004 Acura TL	274	481	184	1,798
8A	Midsized	2004 Chevrolet Malibu	270	478	178	1,656
8B	Midsized	2004 Chevrolet Malibu	270	478	178	1,657
9	Midsized	2004 Dodge Stratus	274	486	179	1,612
10A	Midsized	2004 Honda Accord	274	481	182	1,635
10B	Midsized	2004 Honda Accord	274	481	182	1,615
11	Midsized	2004 Hyundai Sonata	270	475	182	1,674
12	Midsized	2004 Jaguar X-Type	271	467	179	1,816
13A	Midsized	2004 Lexus ES 330	272	486	181	1,754
13B	Midsized	2004 Lexus ES 330	272	486	181	1,747
14	Midsized	2004 Mazda 6	268	475	178	1,616
15A	Midsized	2004 Mitsubishi Galant	275	484	184	1,730
15B	Midsized	2005 Mitsubishi Galant	275	484	184	1,731
16	Midsized	2004 Saab 9-3	268	464	175	1,635
17	Midsized	2004 Saab 9-5	270	483	179	1,781
18	Midsized	2004 Saturn L Series	271	484	174	1,635
19	Midsized	2004 Suzuki Verona	270	477	182	1,721
20A	Midsized	2004 Toyota Camry	272	480	180	1,636
20B	Midsized	2004 Toyota Camry	272	480	180	1,626
21	Midsized	2005 Mercedes C 240	271	453	173	1,708
22	Midsized	2005 Nissan Altima	280	488	179	1,613
23A	Midsized	2005 Subaru Legacy	267	473	173	1,683
23B	Midsized	2005 Subaru Legacy	267	473	173	1,685
24	Midsized	2005 Volvo S40	264	447	177	1,654
25A	SUV	2002 Land Rover Freelander	256	445	180	1,780
25B	SUV	2003 Land Rover Freelander	256	445	181	1,805
26A	SUV	2003 Ford Escape	262	439	178	1,723
26B	SUV	2003 Ford Escape	262	439	178	1,736
27A	SUV	2003 Honda CR-V	262	454	178	1,703
27B	SUV	2003 Honda CR-V	262	454	178	1,700
28	SUV	2003 Honda Element	258	430	182	1,773
29	SUV	2003 Hyundai Santa Fe	262	450	182	1,955
30	SUV	2003 Mitsubishi Outlander	263	455	175	1,731
31	SUV	2003 Saturn VUE	271	461	182	1,759
32A	SUV	2003 Subaru Forester	253	445	174	1,613
32B	SUV	2003 Subaru Forester	253	445	174	1,610
33	SUV	2003 Suzuki Grand Vitara	248	418	178	1,680
34	SUV	2003 Toyota RAV4	249	425	174	1,592
35	SUV	2004 Toyota RAV4	249	426	174	1,629
36	SUV	2005 Ford Escape	262	444	178	1,800
37	SUV	2005 Honda CR-V	262	460	178	1,760

**APPENDIX B. Struck vehicle crush measures for vehicles subjected to IIHS side crash test**

Test ID	Vehicle year, make, and model	Struck vehicle crush measures (cm)						Damage length (cm)
		C1	C2	C3	C4	C5	C6	
1	2004 Kia Spectra	7	33.5	41	41	37	0	194
2	2004 Nissan Sentra	11	35.5	41	41.5	37.5	7	171
3	2005 Dodge Neon	16	33	40.5	40	34	0	177
4	2005 Ford Focus	16	31	36	37	30	14	164
5A	2005 Saturn Ion	5	36.5	39.5	34.5	26	0	161
5B	2005 Saturn Ion	6	33	40	25.5	15	0	182
6A	2005 Toyota Corolla	17	33	38	38	32	0	176
6B	2005 Toyota Corolla	16	32	37.5	38	35	4	175
7	2004 Acura TL	0	34.5	38	38	26	0	204
8A	2004 Chevrolet Malibu	2	31	37	38	29	0	182
8B	2004 Chevrolet Malibu	6	32	37	38	32	0	182
9	2004 Dodge Stratus	20	38	40	38	27	0	180
10A	2004 Honda Accord	7	36	43	39	33	3	185
10B	2004 Honda Accord	8	38	42	39	31	0	185
11	2004 Hyundai Sonata	8	38	44	43	33	0	187
12	2004 Jaguar X-Type	10	37	40	41	29	0	183
13A	2004 Lexus ES 330	4	27.5	38	30	25	0	186
13B	2004 Lexus ES 330	4	30	38	30	28	0	175
14	2004 Mazda 6	26	41	45	42	37	12	163
15A	2004 Mitsubishi Galant	2	24	30	31	29	15	177
15B	2005 Mitsubishi Galant	13	28	30.5	33	26.5	0	186
16	2004 Saab 9-3	0	24	31	32	24	6	184
17	2004 Saab 9-5	0	35	42	37.5	31.5	0	177
18	2004 Saturn L Series	8	36	42	31	20	0	173
19	2004 Suzuki Verona	3	36	43	41	32	0	190
20A	2004 Toyota Camry	10	34	42	41	31	0	188
20B	2004 Toyota Camry	7	27	37	36	30	1	194
21	2005 Mercedes C 240	0	22	24	27	21.5	0	184
22	2005 Nissan Altima	8	38	44	46	36	0	178
23A	2005 Subaru Legacy	4	26	27	26.5	23.5	0	184
23B	2005 Subaru Legacy	6	27.5	29.5	29	24.5	15	177
24	2005 Volvo S40	8	24.5	33	33	29	0	177
25A	2002 Land Rover Freelander	19	33	39	37	23	2	181
25B	2003 Land Rover Freelander	19	32	41	38	27	3	169
26A	2003 Ford Escape	10	24.5	30.5	29	22	0	176
26B	2003 Ford Escape	11	24	31	29	21.5	0	178
27A	2003 Honda CR-V	12	28	32	28	20	1	193
27B	2003 Honda CR-V	0	19	30	32	21	0	191
28	2003 Honda Element	5	22	29	29	19	0	193
29	2003 Hyundai Santa Fe	10	24	32	31	22	0	176
30	2003 Mitsubishi Outlander	15	31	38	36	28	0	185
31	2003 Saturn VUE	19	28	33	28	19	0	180
32A	2003 Subaru Forester	10	28	30	30	19	2	195
32B	2003 Subaru Forester	10	29	30	28	18	4	195
33	2003 Suzuki Grand Vitara	21	38.5	40	36	25	0	163
34	2003 Toyota RAV4	19	30	28	37	23	1	192
35	2004 Toyota RAV4	15	28.5	30.5	31.5	28	0	171
36	2005 Ford Escape	12	24.5	30	28	21.5	0	171
37	2005 Honda CR-V	8	24	34	32	26.5	15.5	172

**APPENDIX C. Moving deformable barrier crush measures for IIHS side crash tests**

Test ID	Moving deformable barrier crush measures (cm)						Damage Length (cm)
	C1	C2	C3	C4	C5	C6	
1	11	6	8	6	3	2	160
2	8	3	5	5	6	9	160
3	8	2	2	0	0	6	160
4	9	6	8	8	5	10	160
5A	5	4	4	4	4	6	160
5B	7	6	6	4	5	8	160
6A	6	5	6	6	5	3	160
6B	5	5	7	6	4	4	160
7	10	9	8	8	8	5	160
8A	10	8.5	9	8	9.5	17	160
8B	10	5.5	6	5	6.5	11	160
9	8.5	4	5	5	2	6	160
10A	3	1	0	2	-1	1	160
10B	7.5	3	5	7	7	7.5	160
11	12	7	6	5	5	8.5	160
12	9.5	4	7	8	8	14	160
13A	6	5	8	9	10	13.5	160
13B	4	4	6	8	9	12	160
14	6	7.5	8.5	10	9	10	160
15A	10	13.5	16	16	13.5	10	160
15B	10	11	13	14	12	10	160
16	13	8	10	10	10	13	160
17	16	6	7	6	8	10.5	160
18	7	4.5	4.5	5	8	17	160
19	8.5	6.5	7.5	7.5	5.5	9.5	160
20A	8.5	6	7	8	8	8.5	160
20B	8.5	9.5	11	11	10.5	11	160
21	15	12	14	17	14	13	160
22	6	3.5	2	1.5	2	3	160
23A	8	10	14.5	14	9	8	160
23B	2	7	11	11	6	9	160
24	12	6	8	8	8	5	160
25A	6	2.5	2	3.5	4.5	7	160
25B	10.5	4.5	3.5	4.5	7	8	160
26A	6	5.5	10.5	13	14.5	14.5	160
26B	5.5	5.5	9	11.5	13.5	14.5	160
27A	8.5	10	11	12	13	10	160
27B	7.5	9	10.5	12	13.5	13	160
28	12	7.5	11	13	9.5	16.5	160
29	6.8	4	8.5	10.5	12	13.5	160
30	4.5	1	1	1.5	3.5	10.5	160
31	3.5	3	5	7	8.5	8.5	160
32A	6	4	4.5	6	8.5	10.5	160
32B	6	3	4	4.5	7	12	160
33	6.5	1	0.5	0	3	12	160
34	0	-1	0.5	2	5	4.5	160
35	8	5	6	6	8	6	160
36	11	10	16	16	15	10	160
37	0	0	2	4	6	3	160

# WORLDSID RESPONSES IN OBLIQUE AND PERPENDICULAR POLE TESTS

Suzanne Tylko  
Dainius Dalmotas

Crashworthiness Division, Transport Canada  
Canada

Paper Number 05-0256

## ABSTRACT

The International Harmonized Research Activities (IHRA) Side Impact Working Group is proposing a 15-degree oblique pole test as part of a comprehensive side impact evaluation protocol. Since collision data from around the world indicate that young males are overrepresented in single vehicle collisions into fixed objects (women tend to be over-represented in vehicle-to-vehicle crashes), a side impact anthropometric test device representative of a 50<sup>th</sup> percentile adult male is believed to be the most appropriate dummy size to evaluate the protective capabilities of vehicles subjected to pole impacts.

In support of the IHRA Side Impact working Group activities, Transport Canada conducted a series of paired vehicle tests to compare the responses of WorldSID in 15-degree oblique pole tests to those observed in a perpendicular pole test. Vehicles included small North American vehicles equipped with head-thorax seat mounted side airbags and mid-size and SUVs equipped with both seat mounted thorax airbags and curtain technology.

While the oblique test configuration tended to result in more elevated responses a number of test parameters including side airbag deployments, dummy arm kinematics and dummy position were found to significantly affect dummy responses. WorldSID performance and thoracic measurement sensitivity in the oblique loading environment observed in the 15-degree pole test are discussed and compared to that of the ES-2re.

## INTRODUCTION

The Transport Canada Side Impact Research Program was initiated in 1999 to identify factors contributing to serious injuries among women involved in vehicle-to-vehicle side impact crashes and to evaluate the appropriateness of new barrier designs and crash configurations. In the latter half of 2003 members of the IHRA Side Impact Working Group (SIWG) identified that laboratory data comparing oblique to perpendicular pole impacts were needed to help the SIWG define a harmonized test protocol for pole impacts that could be scientifically corroborated. Transport Canada began a pole test program in 2004 to compare the effects of oblique and perpendicular strikes. This paper presents the results of three paired oblique and perpendicular pole impacts conducted with the 50<sup>th</sup> percentile world harmonized side impact dummy, WorldSID. Two additional paired oblique pole tests, carried out to compare the response of the WorldSID and ES-2re in oblique pole testing conditions, are presented. Given the preliminary character of these results, parameters to be monitored and recommendations for further testing are discussed.

## METHODOLOGY

### Vehicle Selection

Three different model year 2004 vehicle types were selected for the comparison. These included a small North American 4-door sedan with seat mounted combination (head/ thorax) side airbags identified as 'model A'; a mid-size Japanese 4-door sedan with seat mounted thorax side airbags and curtain identified as 'model B' and a European SUV with seat mounted thorax side airbags and curtain identified as 'model C'. Vehicles selected for the WorldSID and ES2-re comparison included two model year 2003 vehicles identical to 'model A' but without side airbags and two small 4-door German sedans equipped with seat mounted thorax

airbags and curtains and identified as Model 'D'. The test matrix is presented in Table 1.

**Table 1: Test Matrix**

Vehicle	Test Mass kg	Impact Angle	
		90°	15°
<u>Model A</u>	1427	WS	
<u>Model A</u>	1427		WS
<u>Model B</u>	1642	WS	
<u>Model B</u>	1662		WS
<u>Model C</u>	2521	WS	
<u>Model C</u>	2520		WS
<u>Model A '03</u>	1429		WS
<u>Model A '03</u>	1430		ES2-re
<u>Model D</u>	1752		WS
<u>Model D</u>	1772		ES2-re

**Data Acquisition and Videography**

The WorldSID dummy instrumentation included a nine accelerometer cluster in the head; a 6-axis load cell at the upper and lower neck; an InfraRed Telescoping Rod for Assessment of Chest Compression (IRTRACC) (Rouhana, 2002) at the shoulder, each of the three thoracic and two abdominal ribs; tri-axial accelerometers at the upper, mid and lower spine and pelvis; accelerometers at each rib and on the spine box opposite each rib; and single axis load cells at the acetabulum, pubic symphysis and iliac.

The ES-2re included a tri-axial accelerometer at the head CG; a 6-axis load cell at the upper and lower neck; a linear potentiometer at the shoulder and each of the three thoracic ribs; tri-axial accelerometers at the upper, mid and lower spine and pelvis; accelerometers at each rib and on the spine box opposite each rib; and single axis load cells at the acetabulum, pubic symphysis and iliac.

All data recording and filtering was performed in accordance with SAE J211. Collisions were filmed at 1000 frames / second from multiple views.

**Dummy Positioning**

The WorldSID and ES-2re were both positioned in the driver seat as per the University of Michigan Transportation Research Institute (UMTRI) procedure, now referred to as the IIHS/UMTRI seating procedure. This procedure places the dummy in a seat track location and in a seat orientation believed to be statistically representative for a mid-size male and just forward of the B-pillar [2]. A common seating procedure was required for both dummies to facilitate comparison. Precautions were taken to ensure that the outboard arm was in place at 45° to the spine prior to impact.

**Vehicle Preparation and Launch**

Uni-axial accelerometers are generally installed in the driver-side door sill, in the four quadrants and centre of the driver door, at the base of the B-pillar and at the side rocker panel on the passenger side. A tri-axial accelerometer is installed at the vehicle centre of gravity. The driver-side window is taped to prevent glass splatter from interfering with camera views.

The tires are removed and the wheels placed on small trolleys as shown in Figure 1. The vehicle is aligned with the dummy head CG and launched at 29 km/h for perpendicular impacts. The 15° oblique impacts are aligned through the driver's head cg and launched at 32 km/h.

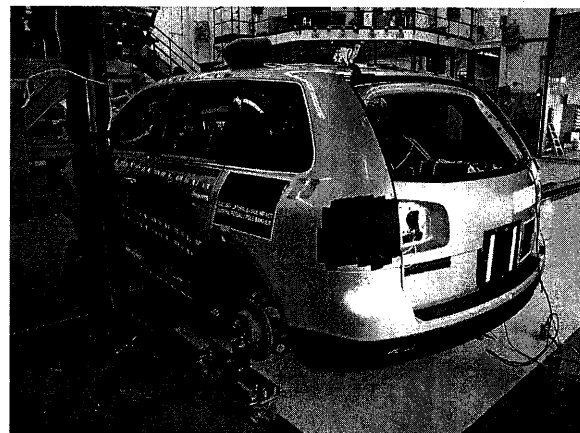


**Figure 1: Photo of test set-up.**

## RESULTS BY TEST CONFIGURATION

**Airbag Performance** There were two incomplete deployments of the seat mounted head torso airbag in model 'A'; one instance of a curtain deploying behind the B-pillar trim in the perpendicular impact of model 'C' and one occurrence of punch through during the oblique impact of model 'B'. In both the perpendicular and oblique modes, the head thorax bag became entrapped by the intruding door trim and was deviated rearwards behind the driver seat. Timing during the perpendicular crash was such that the upper portion of the bag had just enough inflation to cradle the neck as the head rotated outboard and to prevent head contact with the pole. During the oblique crash, the impact point was 128 mm forward of the perpendicular impact point and though the bag became entrapped in a similar way, it was ineffective in preventing the head from striking the pole. Given the airbag deployment problems in the perpendicular mode, it is likely that the impact point alone (independent of the angle) affected the dummy head kinematics.

In model 'B' there were no problems with deployment path or timing; however punch-through occurred because the head impact was centered on a seam between two fully inflated chambers. Again, the more anterior impact point, located 132 mm forward of the perpendicular target affected the head trajectory.

Incorrect deployment of the curtain as observed in the perpendicular test of model 'C' has also been observed in other testing involving the IIHS barrier. It would appear that early onset deformation of the roofline causes disruption of the interior roof and/ or B-pillar trim leading to entrapment of the curtain. It was not possible to accurately compare deployment timing in oblique and perpendicular modes due to instrumentation and measurement limitations. Unlike frontal or seat mounted airbag openings, which can be accurately tracked with a simple filament switch the length of the curtains and variety of deployment patterns preclude the use of these non-intrusive methodologies.

At present it is not possible to employ more accurate techniques without tampering with the trim and electrical conduits. The extent to which deployment timing is affected by the pole impact angle is therefore not quantifiable at this time.

The results for the vehicle acceleration and intrusion profiles are presented first and followed by the WorldSID responses.

**Vehicle accelerations** for the center of gravity of the vehicle are presented in Figures 2 through Figure 4. It should be noted that the oblique configuration was characterized by higher impact energies: model 'A' was exposed to approximately 3% more energy in the oblique test; model 'B' to approximately 10% more energy and model 'C' had 5 % more energy in the oblique test.

Acceleration comparisons could only be carried out for models 'B' and 'C'. During the oblique test of model 'A' the undercarriage of the vehicle was struck by the towing cables causing erroneous measures to be recorded in all 3 axes.

Longitudinal accelerations at the cg of model 'B' and 'C' were not significant. As illustrated in Figure 2, the longitudinal component of acceleration during the first 22 msec of pole crush in the oblique loading condition was of the order of 3 g, indicating that there was very limited forward motion of the vehicle. In comparison, the perpendicular test vehicle acceleration trace displays a flat profile until structural deformation of the vehicle has been initiated.

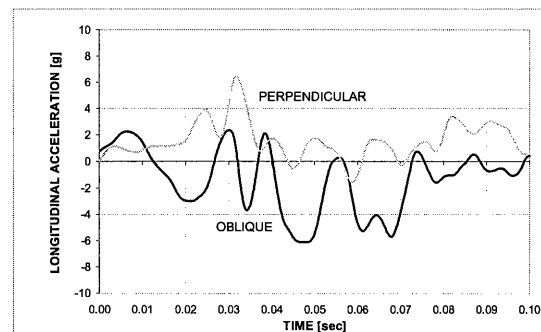


**Figure 2: Longitudinal acceleration traces at the CG of Model 'B' for the two test conditions.**

Lateral accelerations for model 'B' in the two test conditions are shown in Figure 3. The oblique pole test trace displays a 10 msec delay in onset compared to the perpendicular test and a greater magnitude reflective of the increased energy associated with this impact.

A comparison of the vertical acceleration components for Model 'B' is presented in Figure 4. Vertical accelerations were more prominent in the oblique test condition. This was observed for both Models 'B' and 'C' where peak vertical accelerations

were of the order of 21 to 23 g in oblique compared to 9 to 10 g in the perpendicular mode.

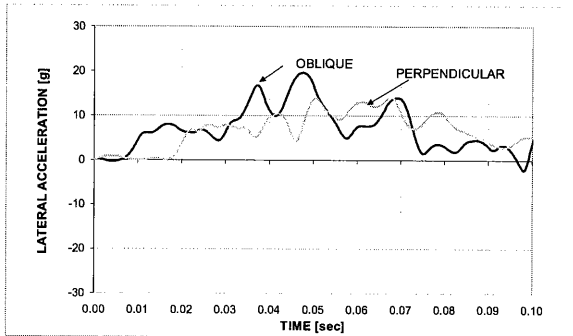


**Figure 3: Lateral CG acceleration traces for Model 'B' in the two test conditions.**

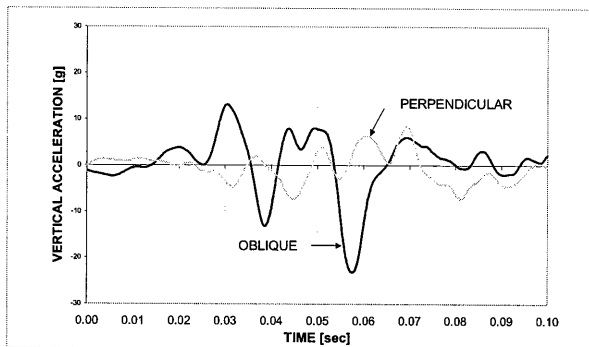


**Figure 4: Vertical CG acceleration traces for Model 'B' in the two test conditions.**

Vehicle intrusion patterns measured at the mid-door are shown for Model 'B' in a full size plot in Appendix A. The impact point for the perpendicular pole impact is aligned with the WorldSID lateral head CG and is located approximately 100 mm forward of the B-pillar. In the oblique alignment the target impact point was obtained by passing a plane through the true CG of the head at a projected angle of 15 degrees; placing the actual impact point 135 mm forward of the perpendicular impact point or 235 mm forward of the B-pillar. Peak intrusion at the mid-door for 'Model 'B' in the oblique mode attained 450 mm compared to a peak intrusion value of 410 mm in perpendicular. The oblique intrusion pattern was shifted some 100 mm forward of the perpendicular intrusion trace. The intrusion profiles were similar for all three model types. The oblique pole always resulted in greater intrusion where peak intrusion at the mid-door ranged from 352 to 431 mm for Model 'C' and 'A' respectively. In contrast, peak intrusion for the perpendicular mode ranged from 310 mm for Model 'C' to 361 mm for 'Model 'A'

WorldSID responses are presented for the head, thorax and abdomen. The elevated head

accelerations observed for the oblique tests and shown in Figure 5 were due to the punch through that occurred with the Model 'B' curtain and the unsuccessful deployment of the seat mounted combination airbag in Model 'A' described earlier. Since both curtain and seat mounted airbag entrapment have been observed in IIHS tests and in SUV-to-car tests the inflation problems illustrated here can not readily be attributed entirely to impact angle. Given the insignificant longitudinal component of acceleration detected in the vehicle it is assumed that the forward motion of the head, defined by the longitudinal head acceleration trace illustrated in Figure 6, was due to the shift of the pole impact point, 132 mm forward, rather than the 15 degree impact angle. This forward displacement of the head towards the pole was sufficient to cause the head to impact a seam in the curtain located 20 mm beyond the fully inflated section impacted during the perpendicular crash.

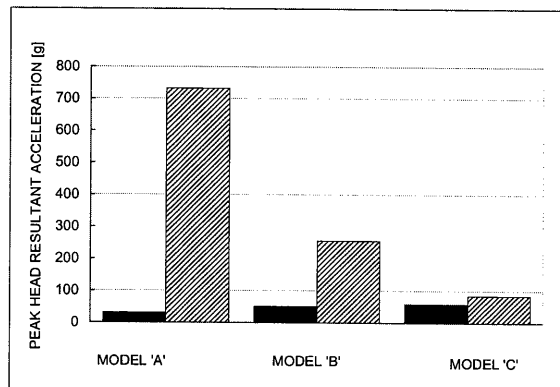


**Figure 5: Peak resultant head acceleration for the WorldSID in three paired tests perpendicular and oblique.**

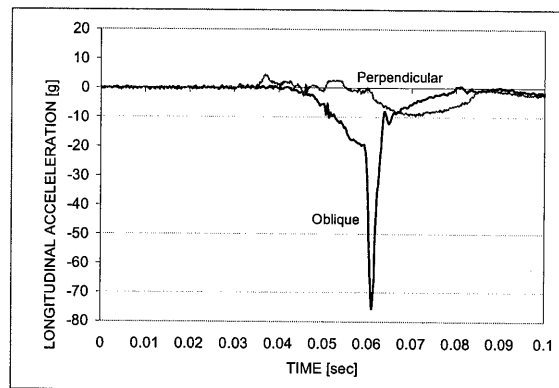


**Figure 6: Longitudinal component of the WorldSID head acceleration in Model 'B'.**

The WorldSID shoulder, thorax and abdominal peak rib deflections for models 'A' 'B' and 'C' are presented in Figures 7 though 9 respectively. Deflections were generally higher in the oblique pole

impacts than in the perpendicular impacts. Shoulder and rib 1 deflections were twice as high in the oblique condition for both Model 'A' and 'B'; while the increase in deflections for the remaining thoracic and abdominal ribs was greatest in the oblique test of model 'B'.

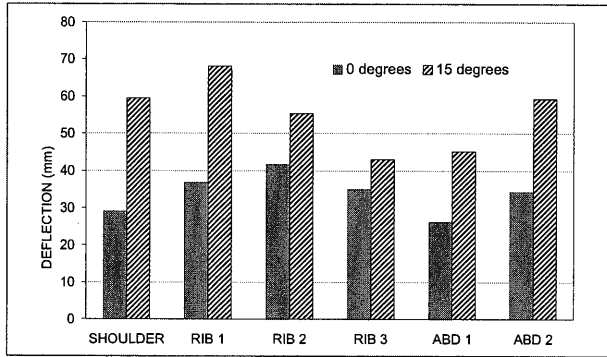


Figure 7: WorldSID thorax and abdominal responses for Model 'A'.

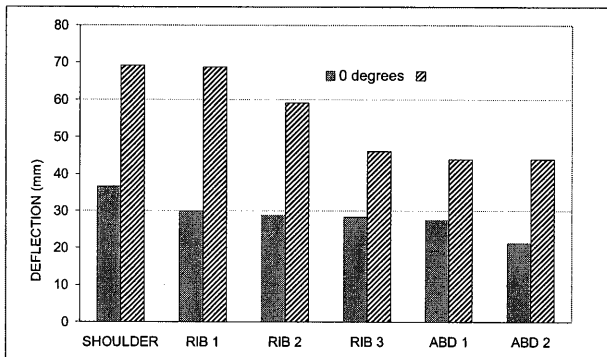


Figure 8: WorldSID thorax and abdominal responses for Model 'B'.

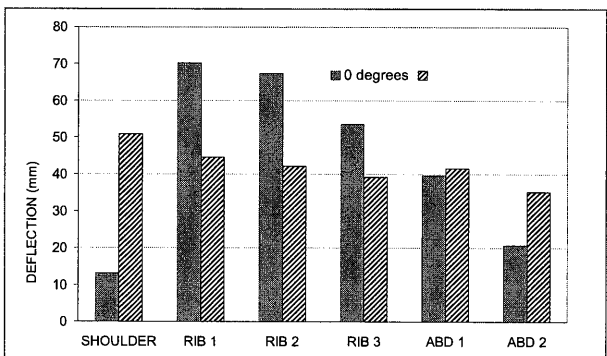


Figure 9: WorldSID thorax and abdominal responses for Model 'C'.

In the Model 'A' perpendicular test a peak deflection of 42 mm was recorded at the second thoracic rib dropping off on either side at rib 1

and rib 3 and rising again slightly in the second abdominal rib. In the oblique mode the loading pattern was similar however, the peak deflections were greater, 68 mm and were localized at rib 1. The seat mounted airbags in models 'A' and 'B' became entrapped by the door trim and could not be seen interacting with the driver in any camera view. They are therefore not considered to have influenced the deflection pattern of the thorax to any great extent.

The airbag performance and dummy kinematics observed in Model 'C' were quite different than the outcomes recorded for the other 2 models. In the perpendicular mode the seat mounted airbag was not obstructed and had sufficient force to rotate the driver arm upwards just high enough for the intruding door to dislodge the shoulder and arm complex into the window opening, further exposing the chest to the intruding structure. In the oblique mode, the thorax airbag initiated arm rotation as well, however the motion of the arm was stopped when the intruding door structure, now more forward, entrapped the arm and the shoulder. The shoulder became wedged in the rear lower corner of the window trim.

Examination of remaining responses including T1, T4 and T12 accelerations indicated that the peak values in all three axes were all greater in the oblique mode with Model 'C' being the exception.

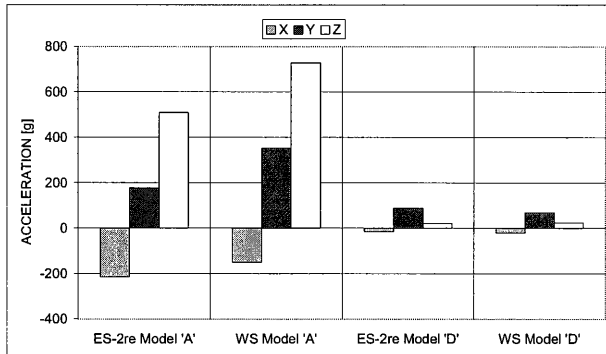
## RESULTS BY TEST DUMMY

WorldSID (WS) and ES-2re comparison in Oblique Test Conditions is based on two vehicle models which included a pair of 2003 Model 'A' vehicles without side airbags and a pair of 2004 Model 'D' vehicles equipped with both curtain and seat mounted airbags.

The dummies were seated using the same seating procedure as described for the previous analysis except that special attention was given to matching key landmark locations to ensure that placement was comparable. All four dummy comparison tests were conducted in the oblique configuration.

**Table 2: Overview of test parameters**

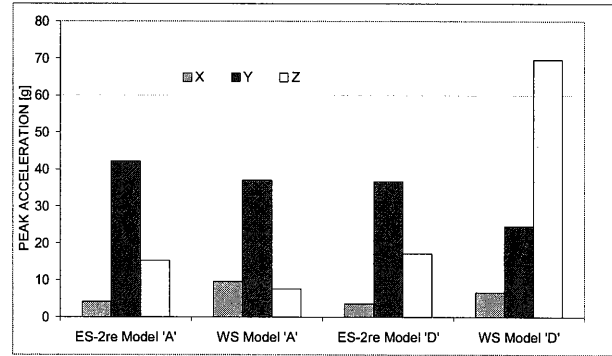
MODEL	MASS Kg	VELOCITY Km/h	IMPACT POINT mm
'A' WS	1428.8	32.61	12 right
'A' ES-2re	1429.9	32.54	0
'D' WS	1752.1	32.7	7 right
'D' ES-2re	1771.5	32.99	18 right



**Figure 10: Comparison of paired vehicle cg accelerations.**

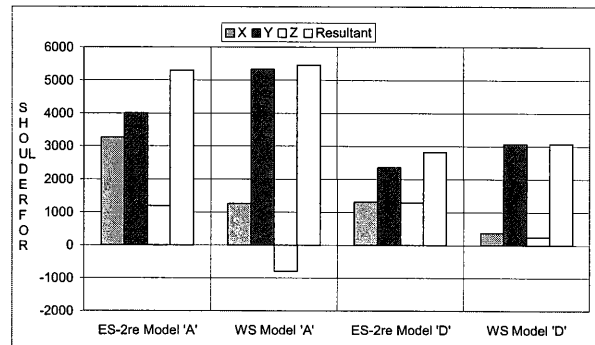
Test mass, impact velocity and impact points were matched as closely as possible. The impact point measurements shown in Table 2 reflect the distance from the intended target. For example in the test of Model 'A' with the ES-2re the intended vehicle target was struck, however in the test with Model 'D' the actual impact point was 18 mm to the right of the intended location.

Figure 10 illustrates a comparison of the accelerations measured at the cg of each vehicle. Both tests of Model 'A' had comparable responses in all three axes. The large vertical acceleration recorded for the Model 'D' test with the WS was actually due to the towing cables striking the undercarriage of the vehicle.



**Figure 11: Comparison of peak head accelerations measured in the WS and the ES-2re.**

Head responses shown in Figure 11 indicate that for the vehicle equipped with an effective side curtain (Model 'D') the translations are comparable for both dummies. In the absence of head protection, however the WS motion surpasses that of the ES-2re in both the lateral and vertical directions.



**Figure 12: Comparison of peak shoulder force measured in the WS and ES-2re.**

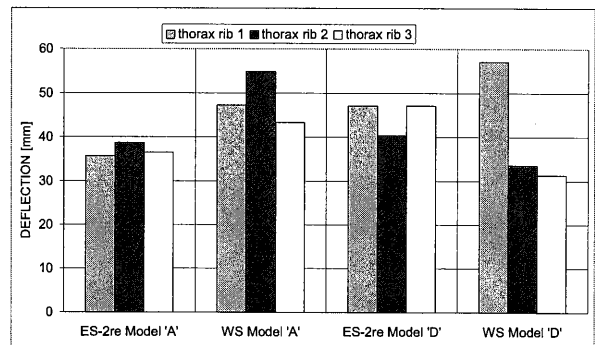


**Figure 13: Comparison of peak thoracic rib deflections measured in the WS and ES-2re.**

The previous test results indicated that for the WS dummy, shoulder, thorax and abdominal response were influenced by the impact location and airbag interaction with the arm. The results obtained from the comparative dummy testing help to quantify the effect that dummy design, specifically shoulder design, can have on shoulder and thoracic rib responses. Figure 12 illustrates the components and resultant shoulder force measured in both dummies. It should be noted that while the resultants are equivalent, the components of force are quite different for the ES-2re and the WS. In Model 'A' for example, the ES-2re longitudinal force component is almost equal to the lateral component, suggesting that the peak load is being transmitted at an angle approaching 45 degrees. The peak value of the longitudinal force in the ES-2re is three times the magnitude of the longitudinal forces measured in WS. In contrast, the WS shoulder is characterized by a predominantly lateral force component. A similar observation can be made in Model 'D' where the ES-2re shoulder response is characterized by strong longitudinal and vertical components whereas the WS shoulder response is again predominantly lateral. The measured shoulder deflection for WS attained the maximum excursion of 70 mm in both Models 'A' and 'D' signaling the location of an important load path at the shoulder complex.

Deflections for the upper, mid and lower thoracic ribs are shown in Figure 13. In Model 'A' the ES-2re deflections were characterized by a flat profile, ranged from 36 mm to 39 mm and were all lower than the corresponding WS rib deflections. In Model 'D' the first and third ribs of the ES-2re deflected 47 mm while the centre rib deflected marginally less at 40 mm. In WS the first rib tracked the shoulder and deflected 57 mm while the remaining lower ribs deflected between 31 mm and 36 mm. Based on the combined load and deflection measures it appears that in Model 'D' the load was transferred primarily through the shoulder and first rib, essentially sparing the remaining ribs of significant contact with the door. While the deflections measured in the ES-2re ribs were elevated it was not able to localize the load path.

The components and resultant lower spine (T12) accelerations for the ES-2re and WS are shown in Figure 14. In Model 'A' the WS accelerations are lower than those of the ES-2re whereas they are equivalent in Model 'D'. In all cases the resultant accelerations fall below the proposed limit of 82 g cited in the Notice of Proposed Rulemaking.

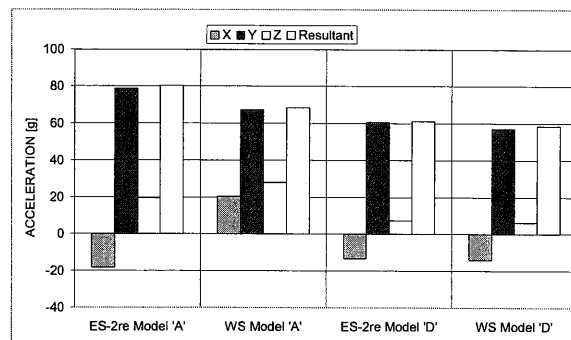


**Figure 14: Comparison of T12 lower spine acceleration measured in the WS and ES-2re.**

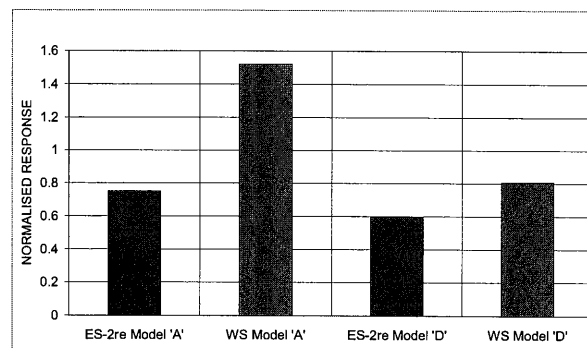


**Figure 15: Comparison of the normalized abdominal responses for the WS and ES-2re.**

Abdominal response in the ES-2re is measured with 3 load cells located in the anterior, mid and posterior pelvic cavity. In the WorldSID abdominal injury risk is determined from two abdominal rib deflections. Figure 15 compares the ES-2re abdominal force response normalized to the NHTSA Notice of Proposed Rulemaking abdominal injury criterion of 2,500 N. The WS response represents the maximum abdominal rib deflection normalized to 42 mm. Though injury criteria have yet to be specified for WorldSID abdominal responses a value of the order of 42 mm of deflection is anticipated. Based on the normalized responses of Figure 15, the ES-2re predict an acceptable level of injury risk for both Model 'A' and Model 'D'; the WorldSID rib deflections however, predict an unacceptable level of abdominal injury risk for Model 'A' where the maximum deflection, occurring in rib 2, surpassed 60 mm. Indeed it appears that the ES-2re is not sufficiently sensitive to differentiate between an aggressive armrest and a more compliant armrest combined with an effective thorax airbag.

## DISCUSSION

Oblique and Perpendicular Tests. WorldSID responses were generally higher in the 15 degree oblique pole impact test when compared to a paired perpendicular pole test. Besides the obvious difference in orientation of the vehicle with respect to the pole, an oblique pole test differs from a perpendicular pole test in three ways:

- a) The impact location is dependant on a plane drawn through the true cg of the dummy head and projected 15 degrees onto the curved surface of the vehicle door and therefore quite sensitive to dummy positioning;
- b) The impact point is shifted forward of the perpendicular impact point by a distance of approximately 130 mm.
- c) The impact energy is 2% higher due to the increased impact velocity. However when combined with test track accuracy, oblique pole tests were up to 10 % higher in this small sample.

The analysis of the vehicle acceleration response describes an impact event principally characterized by a lateral component of force suggesting that the approach angle alone is not sufficient to cause observable differences in the vehicle motion. Dummy kinematics are nevertheless affected by the three differences cited above. Video analysis and accelerometer data suggest the occurrence of a small but important forward motion of the dummy toward the impact point. This displacement influences the location of head strike as well as the exposure of the shoulder and thorax ribs. In the Model 'B' comparison for example, the impact point was situated 132 mm forward, which corresponded to less than a 20 mm shift in the head contact point and was just enough to place the head beyond the protective limits of the curtain. The forward motion added to the inertial loading of the dummy and placed the chest in an area of greater intrusion.

In the interest of future harmonized side impact test protocols it may be advantageous to consider a perpendicular pole test with an impact location defined by a specified distance forward of the dummy head CG. This way the complexity of alignment is removed.

The kinematics of the dummy arm and shoulder in Model 'C' were sufficiently unique to warrant further study. At present, little is understood of the interaction between an inflating thorax bag and the arm (human or otherwise) in the crash environment. Is it possible that the airbag contribute to injury by

exposing the chest? Would a human arm stay in place during the loading phase and protect the chest? The need for in-depth field accident investigations and further laboratory crash testing is clear.

### WorldSID and ES-2re Responses

Vehicle impact conditions and acceleration responses were sufficiently comparable to assume that the paired tests were equivalent and amenable to the comparative analysis of dummy responses. Important differences were observed in the shoulder responses of the ES-2re, designed to rotate out of the way when struck, and the compliant WorldSID shoulder. The components of force measured at the shoulder of the ES-2re describe a combined loading characterized by equivalent longitudinal and lateral forces whereas the WorldSID forces are purely lateral. The non-compliant shoulder of the ES-2re is seen to lead to a rotation of the thorax, displacing the side of the dummy inboard. This inherent rigidity of the shoulder was observed to cause a reduced excursion of the head when compared to the WorldSID head kinematics. The rotation of the chest was also responsible for altering the deflection pattern of the ribs, resulting in lower rib deflections that were evenly distributed across the three ribs. In the case of WorldSID the shoulder flexes and shrugs and stabilizes in position to transmit the lateral load through the thorax.

Comparative tests of the ES-2 and ES-2re carried out within the WorldSID Task Group activities found that the oblique test configuration led to reduced rib deflections when compared to the perpendicular configuration. Simulations carried out by Subaru in support of the IHRA side impact working group activities suggest that the performance of the ES-2 is more sensitive to the location of the impact point than to the angle of impact. This finding is consistent with the findings reported for the oblique and perpendicular comparison with WorldSID.

The measurement capability of the WorldSID shoulder rib in combination with the rib deflection measurements of the three thoracic ribs and two abdominal ribs provides a continuous region of measurement capability making it possible to identify and localize load paths, an advantage not available in the ES-2re. This was demonstrated in the responses of Model 'D' where an important load path present at the shoulder went undetected by the ES-2re. The spine accelerations at T1 and T12 the upper and lower levels of the spine, respectively were insensitive to the shoulder loads described.

In the pelvis the load plates of the ES-2re were unable to detect abdominal penetrations caused by the intruding armrest of Model 'A'. Video analysis of the pole tests show evidence of the intruding door penetrating into a region of the ES-2re dummy abdomen, above the pelvis, that is devoid of instrumentation. The corresponding region in the WorldSID is encompassed by two abdominal ribs and instrumented by IRTRACCs and accelerometers. As a result abdominal deflection response in Model 'A' signaled the potential risk of serious injury to the abdomen where the ES-2re did not.

## CONCLUSION

Three paired pole tests were conducted to compare the differences between a perpendicular pole test and a 15-degree oblique test. Vehicle acceleration responses were not significantly affected by the 15-degree angle though the intrusion profile and maximum residual deformation were exacerbated by the forward shift of the impact point and the increase in impact energy.

The WorldSID head was observed to display slightly greater forward displacement in the oblique tests prior to contact with the curtain or pole. Shoulder, thorax and abdominal rib deflections were greater in two of the three oblique tests conducted. The forward shift of the impact point, which was up to 135 mm forward of the seating reference point in the oblique tests, played a significant role in the overall response of the dummies. In the single paired test where the perpendicular test responses were greater than the corresponding oblique condition the seat mounted thorax airbag deployment was found to adversely affect the protection of the ribs by rotating the arm upwards and exposing the chest to the intruding door.

Further testing is necessary to investigate the interaction between complete airbag deployment and the dummy arm during the loading phase of door intrusion. The feasibility of replacing the angled pole test with a perpendicular pole test shifted forward may well be a viable option for a world harmonized pole test procedure.

Two paired oblique pole tests were conducted to compare the WorldSID and ES-2re responses. The inherently stiff shoulder design of the ES-2re caused rotations of the shoulder and thorax, influencing both the head trajectory and the deflection pattern of the thorax ribs. In contrast the

WorldSID shoulder design responded in a humanlike fashion, shrugging and deflecting to a maximum stroke of 70 mm.

The ES-2re failed to identify principal load paths through the shoulder and elevated intrusions in the abdomen producing dummy response values below the proposed injury criteria. Further investigation should be conducted to more completely quantify the ES-2re limitations prior to adopting this dummy into regulation.

## ACKNOWLEDGEMENT

The authors would like to acknowledge the significant contribution made by Alain Bussières and the staff of PMG Technologies.

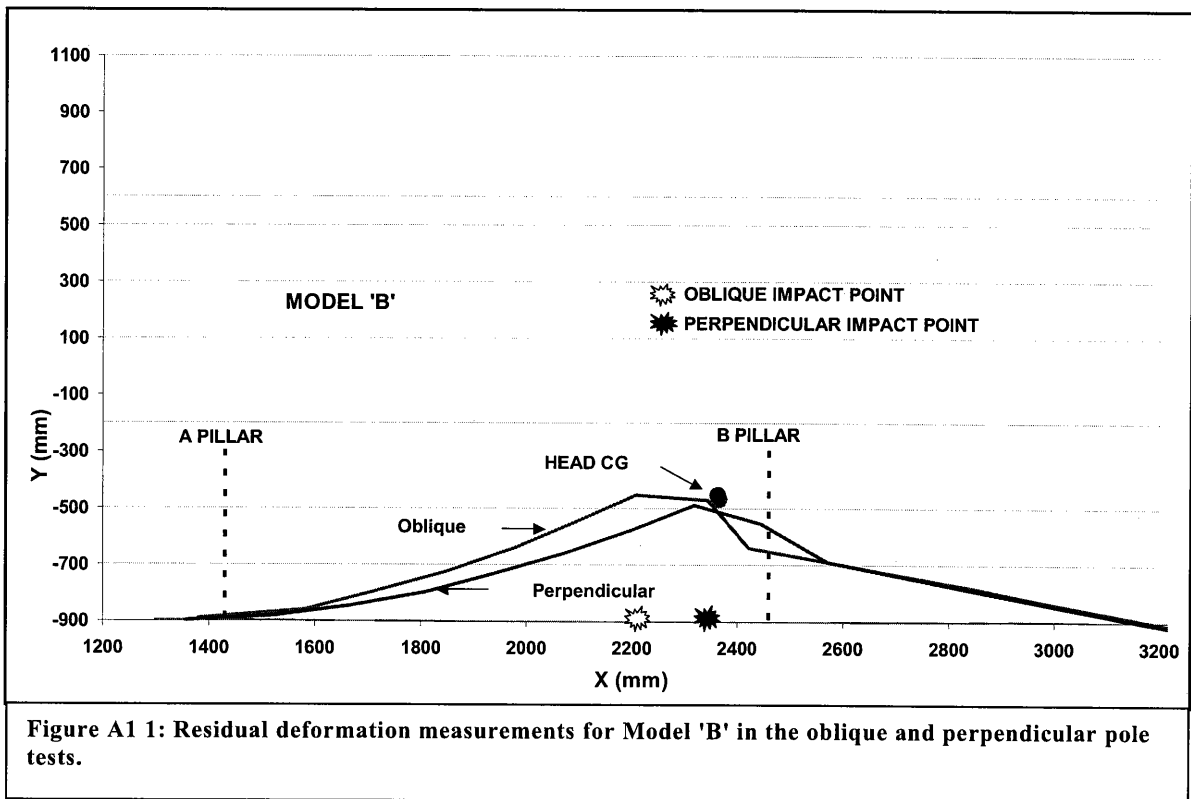
The opinions expressed and conclusions reached are solely the responsibility of the authors and do not necessarily represent the official policy of Transport Canada.

## REFERENCES

1. Arbelaez, R.A., Dakin, G.J., Nolan, J.M., Dalmotas, D.J., Tylko, S., "IIHS side impact barrier: Development and crash test experience." Proceedings of the 2002 Vehicle Safety Conference, May 2002. Institute of Mechanical Engineers, London, England.
2. Dalmotas, D., German, A., Tylko, S., "The crash and field performance of side-mounted airbags". 17<sup>th</sup> International Technical Conference on the Enhanced Safety of Vehicles, Amsterdam, Netherlands, June 2001.
3. Reed, M.P., Manary, M.A., Flannagan, C.A.C., Schneider, L.W., Arbelaez, R.A., "Improved ATD positioning procedure." SAE Technical Paper Series 2001-01-0118. Warrendale, PA: Society for Automotive Engineers.
4. Rouhana, S.W., Elhagediab A.M., Twisk, D., Berliner, J., Baayoun, E., Dalmotas, D., Tylko, S., "Laboratory experience with the IRTRACC chest deflection transducer." SAE Paper 02B-209 Warrendale, PA: Society for Automotive Engineers.
5. Seyer K., "International Harmonized Research Activities Side Impact Working Group Status Report." Proceedings of the 18<sup>th</sup> International Technical Conference on the Enhanced Safety of Vehicles, Nagoya, Japan, May 2003.

6. Tylko, S. & Dalmotas, D.J. (2004) SID-IIs response in side impact testing. *SAE 2004-01-0350, SP1880*.
7. Federal Motor Vehicle Safety Standards; Side Impact Protection; 49 CFR Parts 571 and 598[Docket No. NHTSA-2004-17694] RIN 2127--AJ10. Department of Transportation, National Highway Traffic Safety Administration

APPENDIX A



## **EEVC Research in the Field of Developing a European Interior Headform Test Procedure**

**T. Langner,**  
**Bundesanstalt für Strassenwesen (Germany)**  
**M.R. van Ratingen, T. Versmissen,**  
**TNO Automotive Safety (The Netherlands)**  
**A. Roberts, J. Ellway,**  
**TRL (United Kingdom)**

**on behalf of EEVC WG13**

Paper No. 158

### **ABSTRACT**

The European Enhanced Vehicle-safety Committee (EEVC) Working Group 13 for Side Impact Protection has been developing an Interior Headform Test Procedure to complement the full scale Side Impact Test Procedure for Europe and for the proposed IHRA test procedures. In real world accidents interior head contacts with severe head injuries still occur, which are not always observed in standard side impact tests with dummies. Thus a means is needed to encourage further progress in head protection. At the 2003 ESV-Conference EEVC Working Group 13 reported the results on Interior Headform Testing. Further research has been performed since and the test procedure has been improved. This paper gives an overview of its latest status. The paper presents new aspects which are included in the latest test procedure and the research work leading to these enhancements. One topic of improvement is the definition of the Free Motion Headform (FMH) impactor alignment procedure to provide guidelines to minimise excessive headform chin contact and to minimise potential variability. Research activities have also been carried out on the definition of reasonable approach head angles to avoid unrealistic test conditions. Further considerations have been given to the evaluation of head airbags, their potential benefits and a means of ensuring protection for occupants regardless of seating position and sitting height.

The paper presents the research activities that have been made since the last ESV Conference in 2003 and the final proposal of the EEVC Headform Test Procedure.

### **INTRODUCTION**

Beside the frontal crash the side crash is the most common crash causing severe injuries. The side impact is loading various body parts. The intruding car structure hits the occupant and can cause severe injuries. In side impact tests in laboratories direct contacts mainly occur with the torso of the dummy. Accident analyses have shown that in real world crashes also head contacts occur with the interior structure of cars. These are only very rarely observed in side impact tests according to European Regulation ECE-R95.

One reason is that real world accidents occur in various impact configurations, which cannot be represented in only one test. To overcome this deficiency in Type Approval evaluations, EEVC WG13 was tasked by the EEVC Steering Committee to develop an Interior Headform Test Procedure for Europe. There already exists a test procedure for head contacts in the interior of cars in the USA (FMVSS 201). The European proposal includes latest research results, in order to obtain a modern test procedure.

It was planned to proceed in four phases to develop this Interior Headform Test Procedure, starting with the selection of the headform impactor. At this time the FMH (Free Motion Headform) was also used in FMVSS 201. No significant advantages were identified in selecting either of the three impactors available. The US FMH, was selected as it was already in use in FMVSS 201. This was presented at ESV 1996. Current research suggests that the use of a symmetrical headform may have a number of advantages in simplifying the procedure and improving test reproducibility. WG13 is not currently in a position to make such a decision and the test procedure still uses the FMVSS 201 headform.

Following the second phase of the research it was decided to specify a non guided / free flight headform impactor. This was presented at the 16<sup>th</sup> ESV Conference.

After the decision of the impactor type and test method correlation between EuroSID and FMH responses were analysed, resulting in a formula to calculate HIC FMH to HIC EuroSID. Additionally an accident analysis study for side impact crashes was made to identify potential head impact areas. This was presented as result of phase three at the ESV 2001.

A first draft test procedure was developed and its feasibility, reproducibility and repeatability was checked. Several tests in different European and World cars were performed by TRL, TNO, Volvo and BAST. This was published at ESV 2003.

The experience obtained in these tests lead to several further investigations to optimise the test procedure. In the following paragraphs the major investigations and most important changes to the draft test protocol version of ESV 2003 are presented.

### DEFINITION OF CLEAN CONTACT AND HEAD ALIGNMENT

It was observed in many cases, that the FMH contacted the interior structure twice, firstly with the calibrated zone (see figure 1) and secondly with the nose or chin part. To avoid or minimise the risk and severity of contact with an uncalibrated area a “clean contact” had to be defined (figure 2)

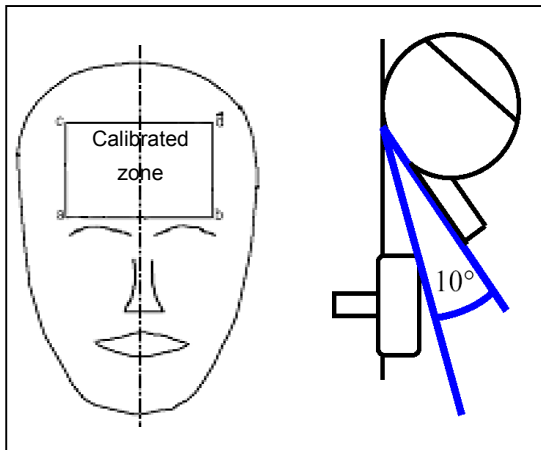


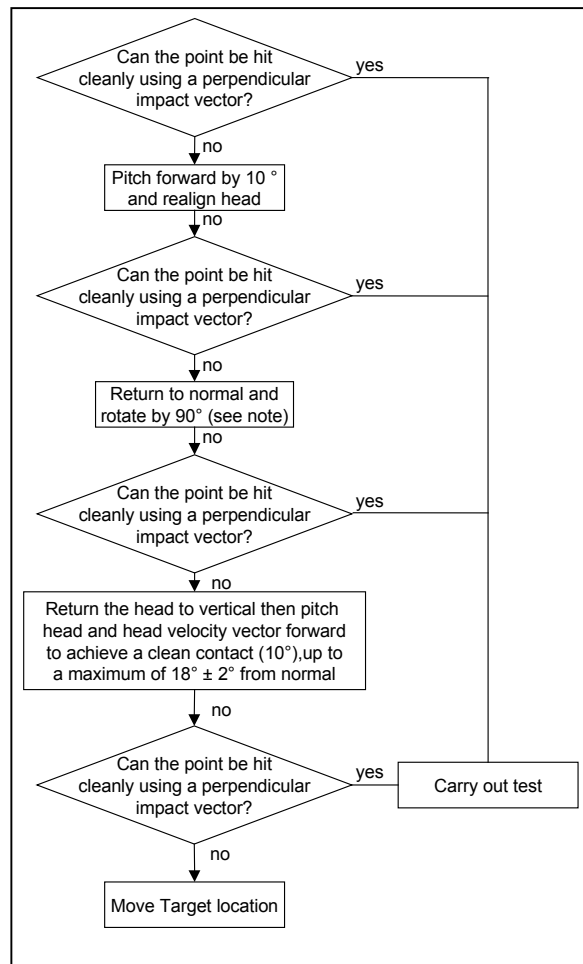
Figure 1: Calibrated zone of FMH

The former draft test procedure proposed to turn the head by up to  $\pm 90^\circ$ . With the possibility to turn the head to any angle between  $0^\circ$  and  $90^\circ$  the definition could be interpreted in several different ways.

As a result the following flow chart was developed to minimise problems of misinterpretation.

This flowchart was checked by TNO and BAST by aligning FMHs in several cars. Most of the head alignments in same cars at same targets were identical.

Another possibility is to reduce the flow chart in figure 2 by excluding the  $90^\circ$  rotation steps. At this point of time WG13 is not in a position to recommend one as being better than the other.



note: Clarification note on headform rotation  
FMH axial rotation about the impact vector facing towards the target point.

Target area	Left hand side of the vehicle	Right hand side of the vehicle
A post target points	90° clockwise	90° anticlockwise
Roof rail target points	90° clockwise	90° anticlockwise
B post target points	90° anticlockwise	90° clockwise

Figure 2: Flow chart to obtain “clean contact”

The two proposed possibilities to obtain “clean contact” are more detailed shown in ANNEX A.

Even with this proposed methodology it is possible that secondary impact could still occur. One possibility to minimise further secondary impacts would be to eliminate the flow chart avoiding different interpretations, by the use of a symmetrical impactor as currently used for pedestrian testing in Europe. This has not been investigated further and can not yet be recommended by WG13

### NON FRONT SEATING POSITION

The initial WG13 research focused on frontal seating positions. To contribute a proposal for IHRA (International Harmonisation Research Activities) SIWG (Side Impact Working Group) the test procedure was extended to cover “non front seating positions”.

The testing zone for the front seating position was limited to a zone constructed from the CoGs (Centre of Gravity) of a large male in the most rearward and a small female in the most forward seating position.

The procedure to define a limitation zone for the rear seating positions was changed due to different types of seats since rear seats are not usually adjustable at the seat back. Therefore the position of the CoG of different sized occupants could be more easily defined.

Figure 3 explains the procedure:

- 1) The dimensions from the H-point to the CoG for 5<sup>th</sup> female and 95<sup>th</sup> male are known.
- 2) The torso angle can be determined by the H-point-manikin.
- 3) The position of the CoGs can now be defined in the car.
- 4) The four limitation planes are constructed in the car (marked green in figure 3).

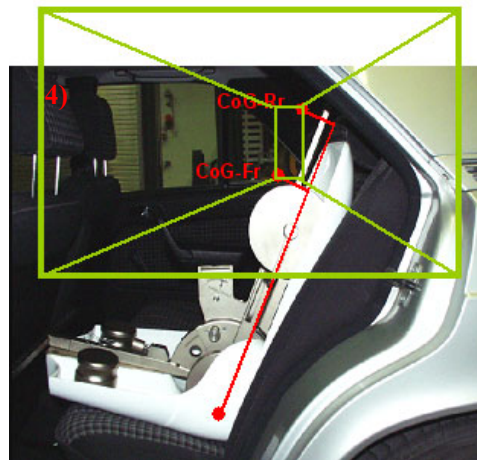
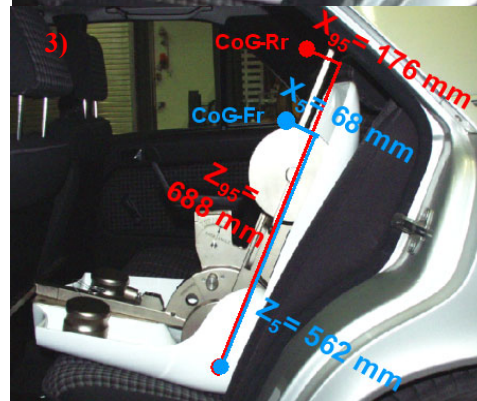
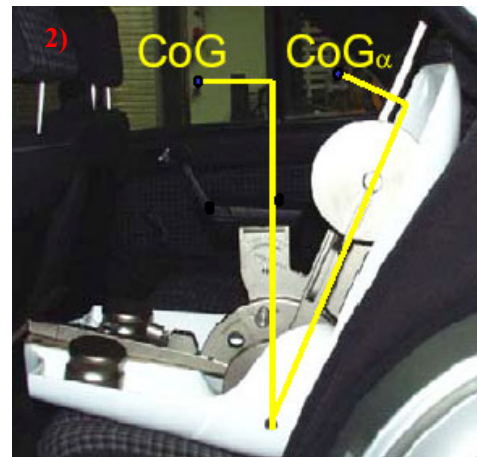
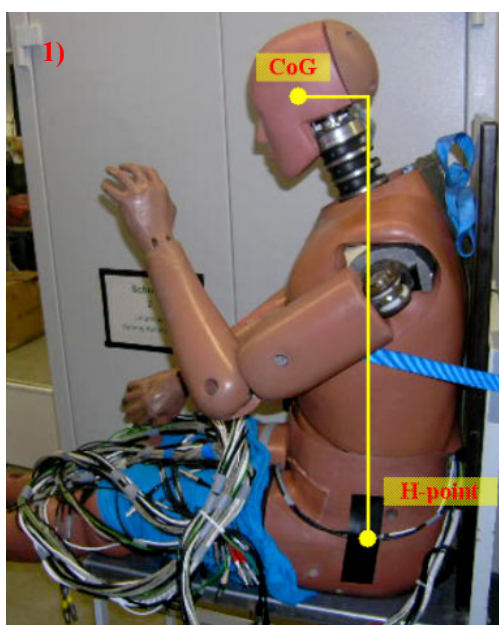


Figure 3: Construction of testing limitation zone for rear seating position

The planes are constructed through the CoGs at the same angles as for the front seating position (see figure 4)

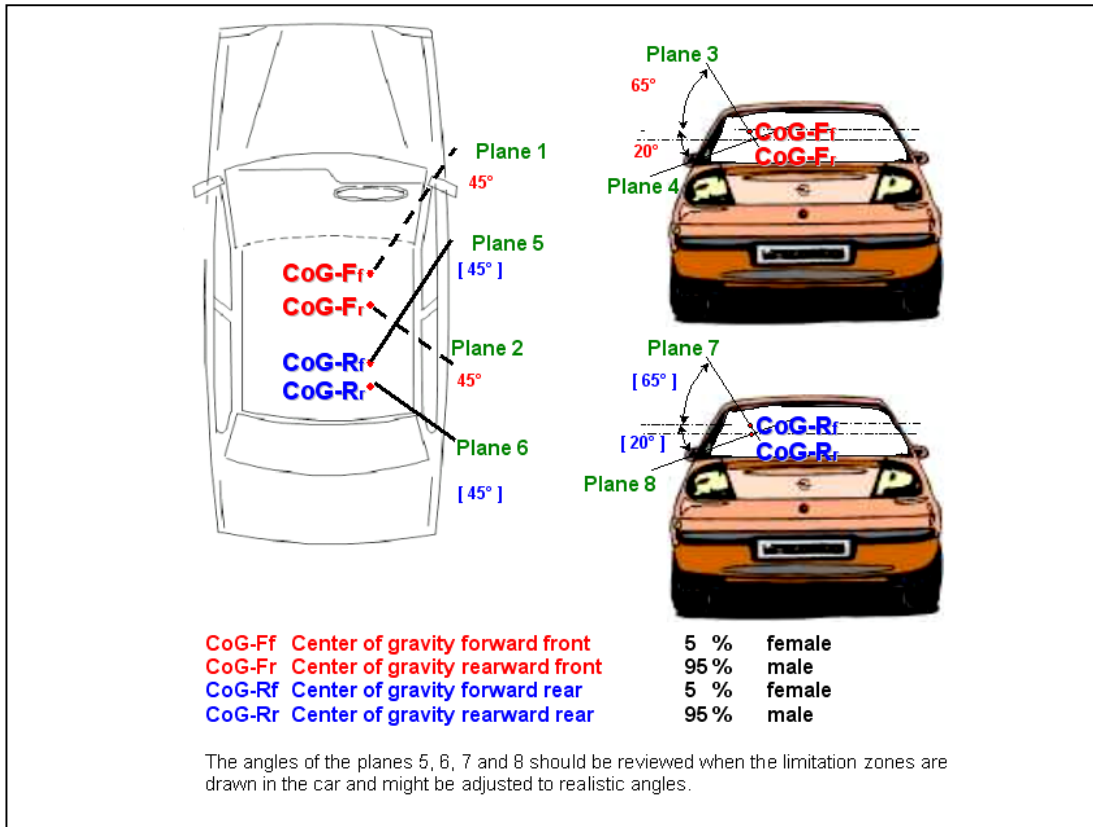


Figure 4: Planes for limitation zone

The interior testing zone is limited by the yellow line. The areas outside this line are excluded from testing.



Figure 5: Limitation zone in the car

These zones and the methodology to create them will need to be validated in broader based programmes, e.g. the European APROSYS project.

**ADDITIONAL TARGET LIMITATION POSITIONS**

In addition to the mentioned limitation zones further limitations are necessary since several of the surfaces and possible targets in the limitation window cannot be reached because of the shape of the vehicles interior. It is proposed that any surface within 165 mm of a glazed surface should be excluded from evaluation. This is diagrammatically

shown by the application of a sphere of 165 mm diameter in figure 6.



figure 6: additional limitation zone

**BENEFIT OF HEAD AIRBAGS**

**a) Tests outside the car / basic tests**

The former test procedure presented at ESV 2003 already included a part dealing with reduction of test velocity due to airbag installation covering the

mounting area around the stowed head airbag. The test velocity being 5.3 m/s instead of 6.7 m/s.

WG13 believe that active head protection systems can offer many benefits and should be encouraged as they can give additional head protection. It therefore seems reasonable to enlarge the exception zone to all areas that are adequately protected by head airbag systems, only requiring lower velocity testing to the covered areas. An investigation into methods of evaluating airbags and encourage appropriate performance has been carried out by BAST, within WG13. More details of the BAST study are presented in Appendix 1.

First of all it was analysed whether these tests should be performed on a permanently inflated airbag or a fired airbag. Tests have shown that the variability in performance is marginal if the static pressure is the same as in the fired airbag at the moment of head contact. The adequate airbag pressure (about 0,5 bar) of the different airbags was provided by the airbag manufactures.

Basic tests were made on different designs of head airbags to analyse the different airbag characteristics. All tested airbags and all tested points are shown in figure 7.

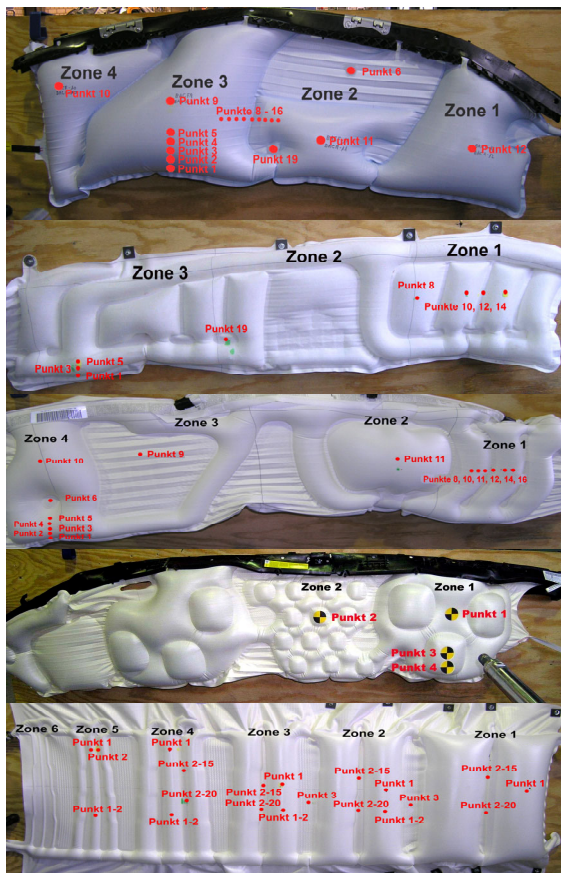


Figure 7: Tested airbags and target points

To eliminate the influence of the vehicle structure behind the bag the airbags were mounted on a homogeneous plate. Therefore a rigid wooden plate was fixed on a rigid steel wall (figure 8). In the research testing in some cases additional foam was attached to the plate, to reduce the HIC to an appropriate level.

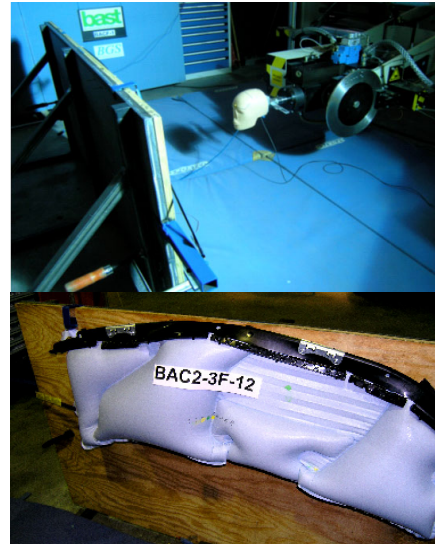


Figure 8: Test set-up – rigid wall

First of all the influence of the impact direction on the airbag was investigated. Figure 9 shows that the influence of the impact direction is marginal, within the range of angles tested, as long as the impactor does not strike through the airbag.

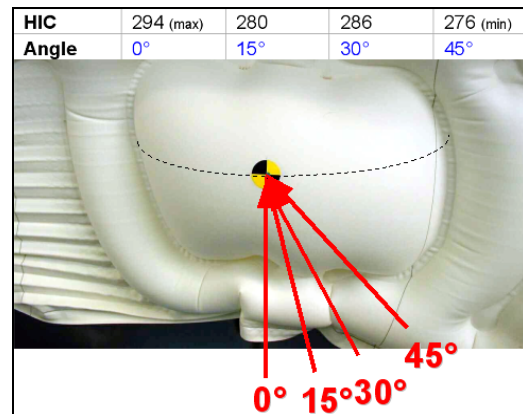


Figure 9: Different impact angles on airbag

To simplify the test procedure into an airbag, it was decided to test perpendicular to the surface below the airbag. The results on the inflated airbags are significant lower than in the tests without inflated airbags on the homogenous plate.

The following figure 10 shows an example of a test on the plate compared to tests on different cushions. The red values are tested with the head at 0° and the yellow values at 10° pitch (see clean contact definition) of the head and velocity vector.

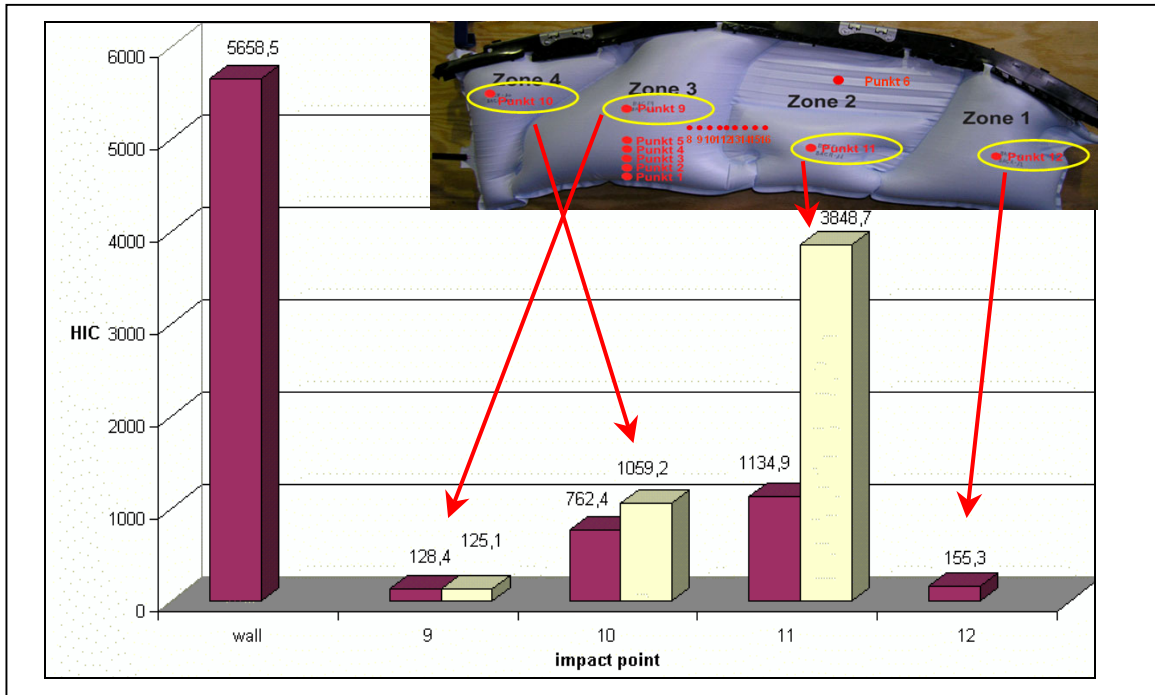


Figure 10: Protection level of different cushions

The critical areas of the airbag where evaluated as indicated in figure 11

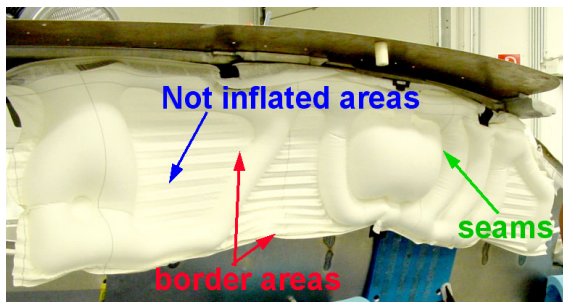


Figure 11: Critical airbag areas

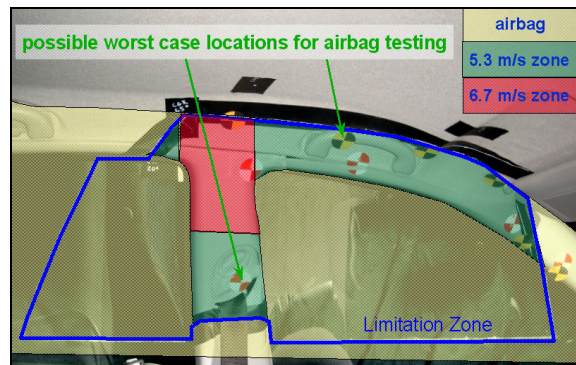


Figure 13: Marked protection level of an airbag on the interior surface

The airbag procedure has been incorporated in the draft EEVC procedure.

- The car would first have to pass a pole test to ensure head airbag triggering.
- The manufacturer has to provide a drawing of areas where the airbag would give the correct level of protection, for example green for adequate protection and red for inadequate protection (see figure 12 and 13)



Figure 12: Marked protection level on airbag

- According to the marked zones the interior structure will be tested at 6.7 m/s in red areas and 5.3 m/s in green areas, without inflated airbag.
- To check whether the determination of the airbag areas in green and red zones is adequate, a minimum of two worst case tests would have to be performed in the green zones on an inflated airbag at 6.7 m/s, in the car. The manufacturer would have to provide information on deployment test pressures and prove compliance.
- The HIC has to be below 1000 in all these tests.

The complete head airbag test proceeding is summarised in the following figure.

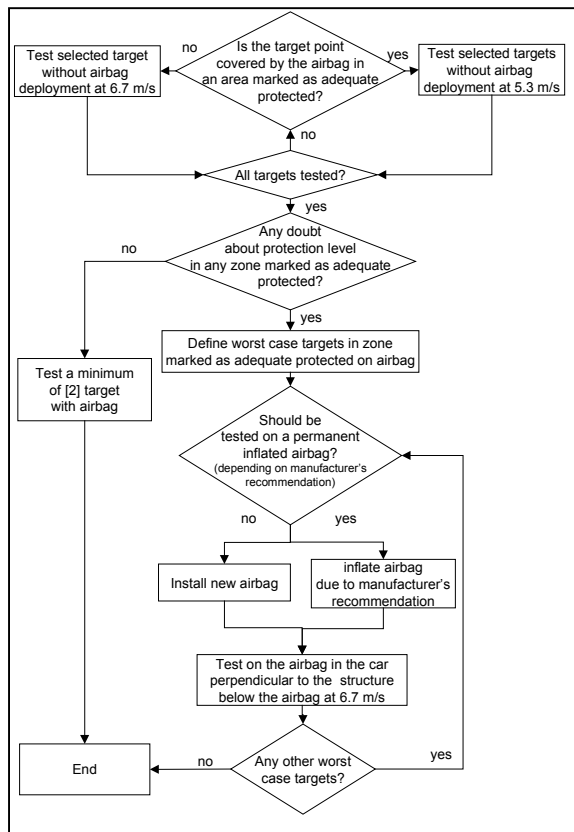


Figure 14: Flow chart for testing with head airbag tests systems

The airbag test procedure is already included in the latest version of the EEVC WG 13 test procedure for interior headform testing.

## HEAD IMPACT ANGLE

TNO have carried out a modelling study to investigate reasonable impact directions in side impacts. The testing protocol requires testing of target points perpendicular to the surface structure as worst case direction. It is noted that in some cases this might lead to testing alignments which are very unrealistic compared to real world accidents. Limitation angles had been given in the test procedure, but no closer investigation had been made before the study of TNO to determine impact angles.

Various accident scenarios have been taken into account. More details of this study are given in APPENDIX 2.

Transferred to a general co-ordinate system of a car, this study proposes the following angles:

- $50^\circ < \text{horizontal angle} < 115^\circ$
- $-12^\circ < \text{vertical angle} < 18^\circ$

The EEVC headform test procedure currently indicates the angles as defined in figure 15, but it does mention the results of the TNO study. It is not yet decided which angles should be recommended in

a final European test procedure. The EEVC WG13 test procedure is suggesting that the impact limitation angles should be limited to those shown in Figure 15. In a broader based practical analysis of the test procedure these angles should be examined and verified. This will be done in the European APROSYS project and other evaluation programs.

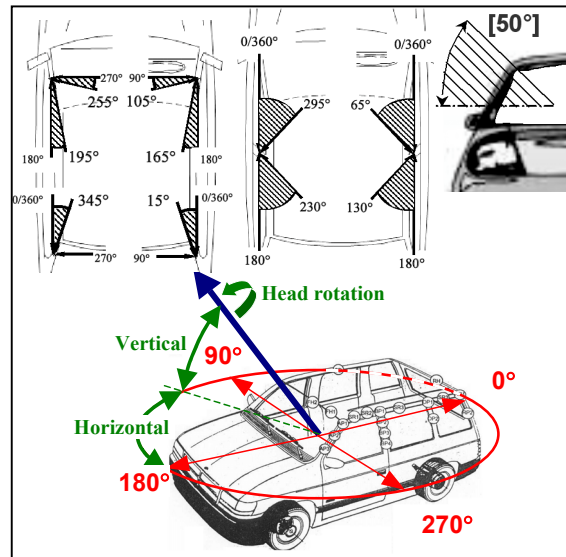


Figure 15: Additional limitation angles co-ordinate system

## CONCLUSIONS

It is the aim of EEVC WG 13 to create a robust test procedure that would lead to reduction in injury in real life accidents to all statures of occupant, sitting in realistic seating positions. On one hand the procedure has to test nearly all injury causing possibilities but on the other hand it has to eliminate unrealistic or extreme unlikely tests, without imposing an unmanageable burden on test authorities and vehicle manufacturers.

Repeatability must be ensured in any test procedure that could be used in an approval process. It is also advisable to have a procedure that does not encourage 'single point' optimisation. This means that worst case target point selection should be encouraged and will be the task of the test house, with sound supporting guidance. In addition head alignment should be the same in all test laboratories.

The EEVC WG13 protocol has changed since the last ESV paper in 2003, due the WG13 members research investigations to improve the repeatability of the procedure. A better definition of head alignment has been included to eliminate unrealistic testing conditions.

The test procedure has been extended to evaluate head airbag systems and give credit to manufacturers who fit such systems, by reducing the severity of the test to areas of the vehicle that are covered by an appropriate head airbag. Such areas being tested at a lower velocity due to reduced injury risk when undeployed.

The draft test procedure is now at a high stage of maturity.

The procedure will need to be revised further following more extensive evaluations as it includes some alternative testing strategies.

WG13 is of the opinion that it is now at a stage whereby it can be evaluated by the border research community.

### RECOMMENDATIONS

Further improvements in repeatability and more realistic kinematics may be possible with the use of a symmetrical headform. Head alignment steps as presented in figure 2 would be reduced to a minimum and contacts with uncalibrated zones eliminated. Unrealistic dynamic head rotation would be minimised since the CoG of the test device would be aligned with the target point. Harmonisation in headform impactors in Europe could be achieved if the same impactor were to be adopted, as for pedestrian testing. No tests have been performed in cars with such a test device. Further investigations need to be performed if a symmetrical headform would be preferred to ensure that other unforeseen problems were not introduced. It is noted that a new headform would mean two different test devices for Europe and the United State.

### ACKNOWLEDGEMENT

The author thanks the EEVC WG13 members for their support to this research.

EEVC WG13 members are:

A K Roberts TRL (Chairman); J Ellway United Kingdom TRL (Secretary); R W Lowne TRL (former Chairman, retired); S Southgate Ford; L Martinez Spain INSIA; G Antonetti Italy Fiat; J-P Lepretre France UTAC; J Faure Renault; D Pouget Renault (retired end of 2004); M van Ratingen TNO The Netherlands; T Versmissen TNO; T Langner Germany BAST; C Müller DaimlerChrysler

## APPENDIX 1 Airbag Testing (BAST studies)

### Investigations of border areas

An important aspect was the protection level at the border areas of an airbag. All the airbags of figure 7 were tested. Figure A1.1 shows a border marked by the dotted line.

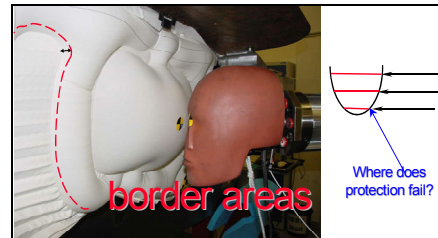


Figure A1.1: Border areas at airbags

An example for border area testing is given in figure A1.2. The result was that at the outer parts of the airbag protection is still provided. It was tested with two different head alignments: 0° (blue) to the horizontal plane and 10° (red) referring to the clean contact definition.

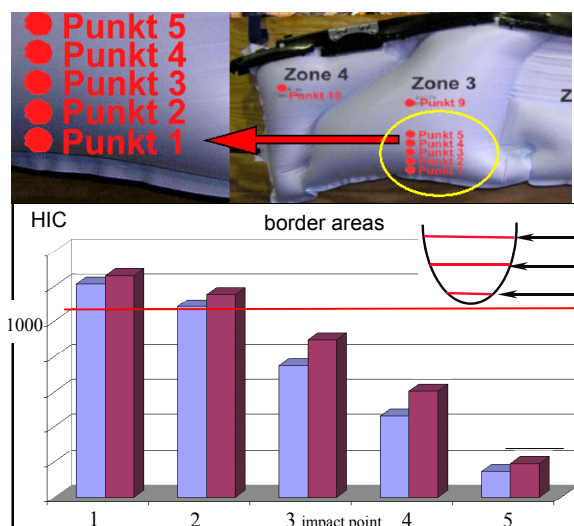


Figure A1.2: Protection level of border areas

Compared to the HIC of about 6000 in figure 10 the HIC values of less than 1300 at the lowest point 1 is quite moderate.

### Investigations of seams

Head airbags are made of several airbag cushions to create an adequate shape. Therefore airbags have seams with an airbag thickness of 0 mm (see figure A1.3)

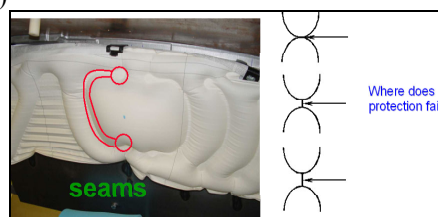


Figure A1.3: Seams at airbags

The questions were: What is the influence of these seams? Is this an area without protection? Several tests have been performed on all airbags of figure 7. Testing was done step by step from one cushion to another cushion by crossing the seam. An example is shown in figure A1.4 testing from a big cushion to a small cushion.

It is surprising that the value of point 12 at the seam with a thickness of 0 mm is still low. The location of the seams cannot be identified by the diagram. The HIC value is rising almost linear.

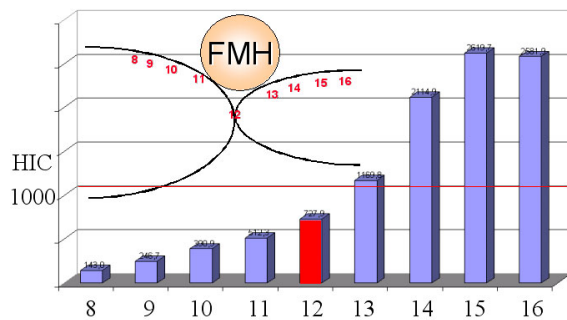
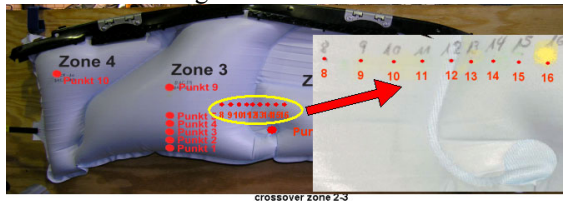


Figure A1.4: Protection level at seams

The explanation for this is: When shooting at the seam, the kinetic energy of the FMH is absorbed by the two bordering cushions (see figure A1.5)

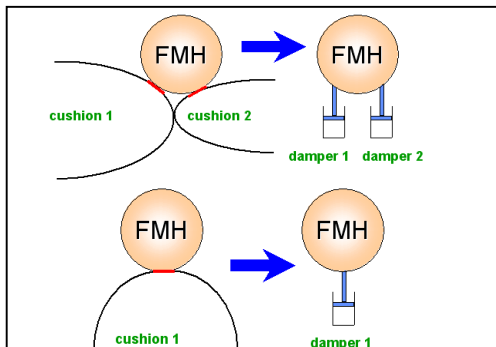


Figure A1.5: Damping effect of cushions

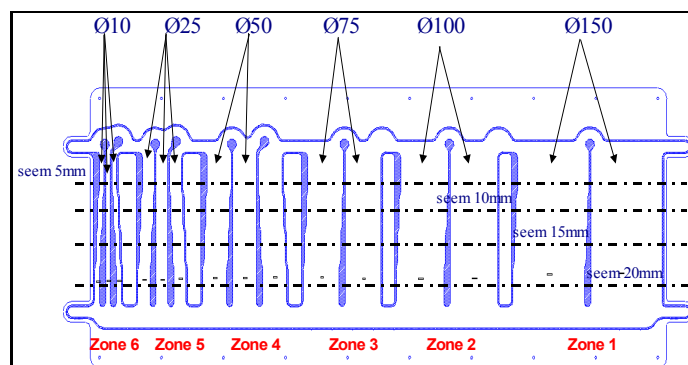


Figure A1.7: Special airbag

Nevertheless it is possible to avoid 0 mm thickness at airbag cushions. A new weaving technique with multi layer is used in some modern cars (see figure A1.6).

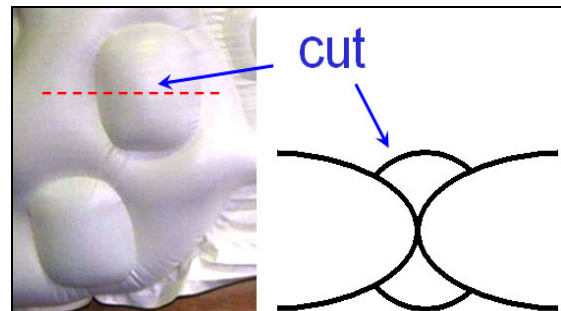


Figure A1.6: Multi layer weaving technique airbag

### Special airbag

Further investigations were made of the above mentioned characteristics: cushion thickness and seams. A special woven airbag as shown in figure A1.7 was produced. Here the geometric characteristics could be tested completely isolated in the most comparable way. As shown in figure A1.7 the thickness of the cushion rises from left with Ø 10 mm to right with Ø 150 mm and the seam width from top to bottom from 5 mm to 20 mm.

### Influence of airbag thickness at special airbag

First it was investigated whether there is a critical airbag thickness by testing the marked points on the airbag in figure A1.8.

Tests from zone 1 to zone 5 were performed. Point 1 is always the point at the top. Point 1-2 is always at the lower part of each cushion. The thickness is always the same for point 1 and 1-2 on the same cushion. Only the seam width between the cushions is 5 mm for point 1 and 20 mm for point 1-2.

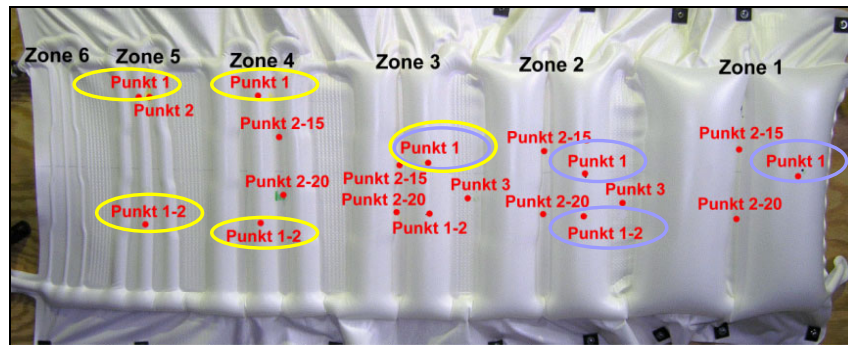


Figure A1.8: Tested points on cushions

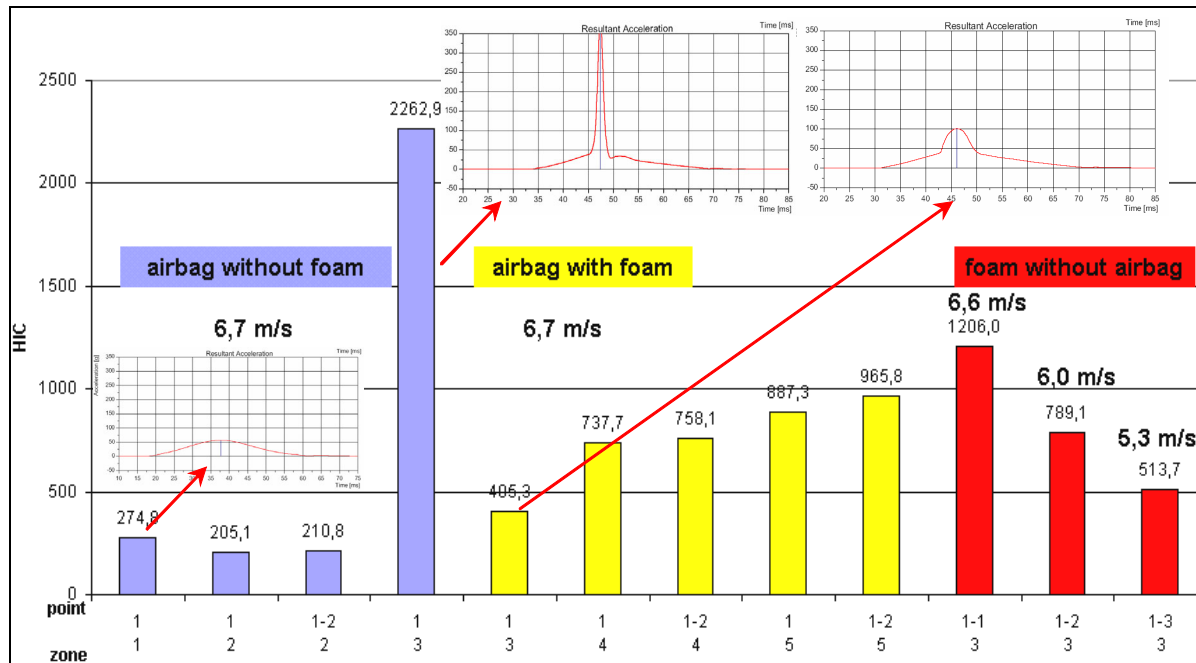


Figure A1.9: Results of cushions testing

The results in zone 1 and 2 show that the airbag thickness has no influence as long as the impactor does not strike through the cushion. The reason is that the kinetic energy was completely absorbed by the cushion. At point 1 in zone 3 the impactor starts to strike through. The critical airbag thickness is under-run. This is visible in the sudden peak in the acceleration curve in figure A1.9. To reduce HICs to an adequate level, further investigations were made with foam underneath the airbag (foam as used in pedestrian testing). Therefore the bars in figure A1.9 are coloured blue when testing without foam and yellow when testing with foam.

After retesting this point with foam underneath, the sudden peak is still visible but is moderated. Further tests from zone 3 to zone 5 show: The thinner the cushion is, the less kinetic energy is absorbed before hitting the structure underneath the airbag.

This study investigated the influence of the thickness completely isolated from any other airbag characteristics. Nevertheless it is impossible to define a certain thickness value where protection fails. There are several other important factors to be taken into

account: Volume and air permeability of the cushion, pressure, number of overflow canals, shape and the kind of cushions connected to the tested cushion. Additionally low protection level may be sufficient for a soft structure underneath.

#### Influence of seam width at special airbag

Now the influence of seams between cushions was investigated.

It was tested from zone 1 to zone 5 at the marked points in figure A1.10, again with foam under the airbag (yellow) and without foam under the airbag (blue).

Only the size of the seams is changing in one zone from top to bottom, indicated by the prefix -15 and -20.

As assumed, the results from zone 1 and 2 are almost identical because the kinetic energy of the head is completely absorbed by the airbag. Therefore it does not make much of a difference if the seam is wide or narrow in this case. In zone 3 the FMH begins to strike through. From here onwards the width of the seams has an influence as shown by point 2-15 and 2-20 in zone 3.

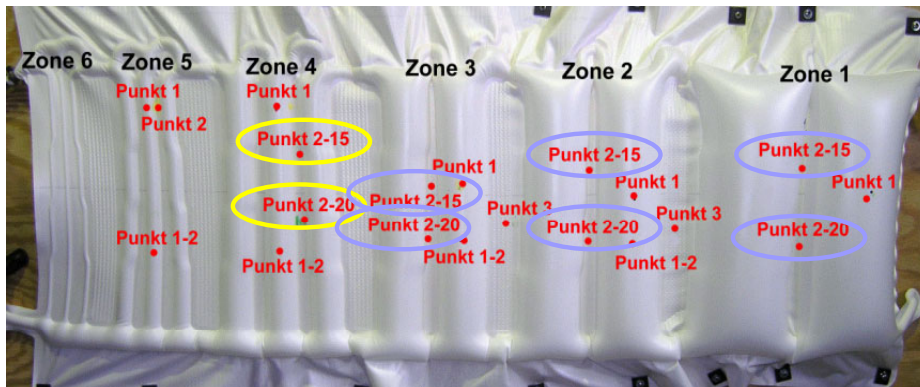


Figure A1.10: Tested points on seams

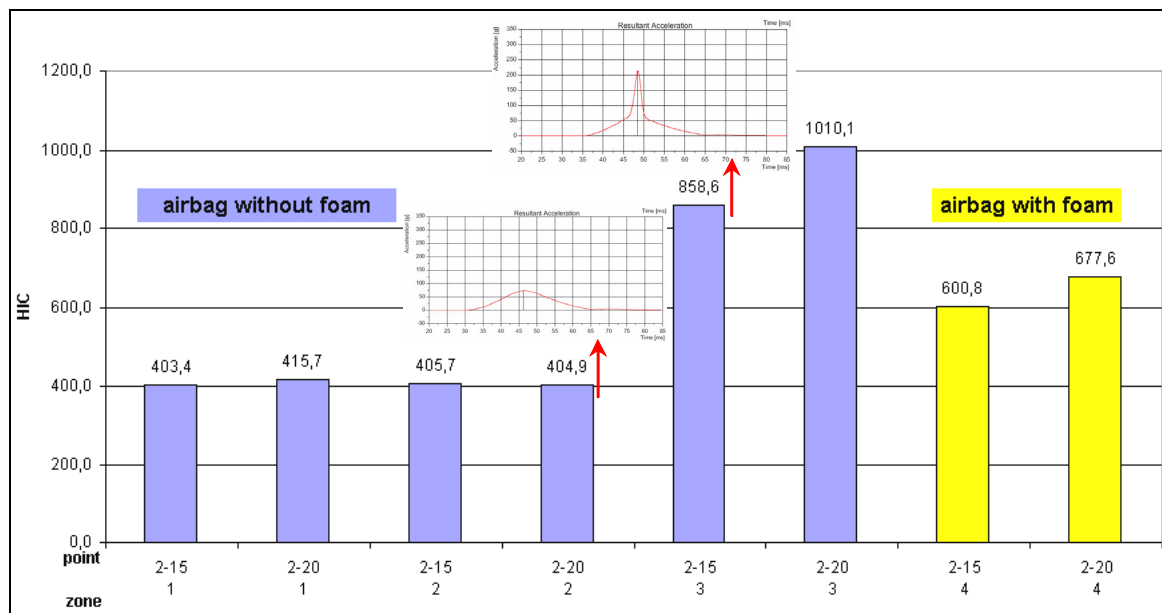


Figure A1.11: Results of seam testing

Looking at figure A1.9 and figure A1.11 it is extremely surprising that the HIC values are higher for zone 1 and zone 2 and lower at zone 3 and 4; tests at seams compared to the cushion values. This indicates that in thin areas where the impactor strikes through, seams offer a better protection than the cushion. The answer is already given in figure A1.5. When shooting at seams the impactor contacts two cushions and is therefore decelerated more effectively.

This means that more energy is absorbed at seams at the same intrusion distance than at cushions.

Result: As long as the impactor does not strike through, the higher deceleration capability of the two cushions leads to higher HICs. In this case the lower deceleration capability with one cushion leads to lower HICs. But more interesting is what happens when the impactor strikes through. The higher deceleration capability by two cushions can absorb more energy before striking on the underlying structure. With only one cushion the HIC value will

now be higher because the impactor is hitting the underlying structure with a higher velocity than with two cushion protection.

This should not imply in general that seams are safer than cushions. It always depends on seam width, shape, volume, radius of the bordering cushions etc. It is been shown that head airbags offer a very good level of protection for head contacts.

#### Tests inside the car

In this test phase it was analysed how to give benefit to head airbag systems in an “interior headform test procedure”.

Originally the idea was to test the car interior at 6.7 m/s with an exception zone of 5.3 m/s tests, in the area where the head airbag is stored. It is reasonable to enlarge that exception zone to all areas where the head airbag provides adequate protection. This motivates the manufacturers to improve their airbags.

To analyse the effect of airbags in cars, several points on the B-pillar in two different cars where

investigated. Three different test scenarios were analysed:

- 1) without inflated airbag -> 5,3 m/s
- 2) without inflated airbag -> 6,7 m/s
- 3) with inflated airbag -> 6,7 m/s

A typical result is shown in figure A1.12.

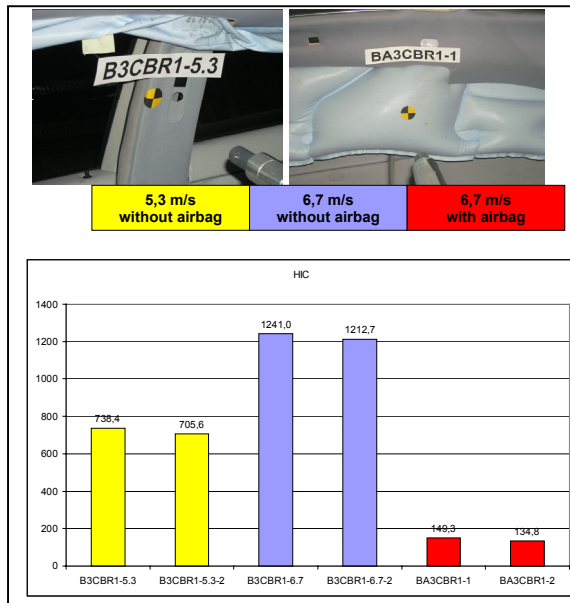


Figure A1.12: Comparison of testing at different velocities and different protections

In some cases the results with 5,3 m/s testing directly on the interior structure were higher than the results with 6,7 m/s testing on the airbag above the interior structure and vice versa, depending on the tested airbag thickness.

Nevertheless again it shows that head airbags can provide a high level of protection.

It should be mentioned that in most tests the airbags were not mounted in their designed positions, because current head airbags are often not equipped with cushions at the B-pillar. The thickest cushion is usually at the position where the pole hits the car in a pole crash according FMVSS 201. Therefore the head airbags have been mounted further backwards. A procedure which gives benefit to head airbags providing an adequate protection, would lead to a better level of protection in the majority of cars.

## APPENDIX 2 Impact Angles (TNO studies)

In the TNO study of impact angles in side impacts various accident scenarios were taken into account. The size of cars is responsible for different kinematics and therefore for different severity of accidents. As first scenario a heavy bullet vehicle (Honda Accord) against a relatively light target vehicle (Chrysler Neon) was selected. The second scenario was performed with two heavy vehicles, Honda Accord against Ford Taurus. For mass and size information see figure A2.1.

Model	Category	Test mass [kg]	Length [m]	Width [m]
Chrysler Neon	Medium size	1381	4.36	1.71
Honda Accord	Medium Family car	1636	5.06	1.90
Ford Taurus	Large	1776	5.07	1.86

Figure A2.1: Mass and size information

Additionally different seating positions and occupant sizes were taken into account as described in figure A2.2.

	Target vehicle	Occupant	Initial position occupant
1	NEON	5 <sup>th</sup> percentile female HBM	Normal (fully forward)
2	NEON	95 <sup>th</sup> percentile male HBM	Normal (fully rearward)
3	NEON	50 <sup>th</sup> percentile male HBM	Normal (mid)
4	NEON	50 <sup>th</sup> percentile male ES-2 dummy	Normal (mid)
5	NEON	5 <sup>th</sup> percentile female HBM	Fully rearward *
6	NEON	50 <sup>th</sup> percentile male HBM	Focus on side rail **
7	TAURUS	5 <sup>th</sup> percentile female HBM	Fully rearward *
8	TAURUS	95 <sup>th</sup> percentile male HBM	Normal (fully rearward)

\* such that there is highest likelihood of contact with B-pillar (representing a passenger).

\*\* such that there is highest likelihood contact with roof rail.

Figure A2.2: Different seating positions and occupant sizes

Impact angles from 30° to 120° and various impact location at 50 km/h were taken into account (see figure A2.3).

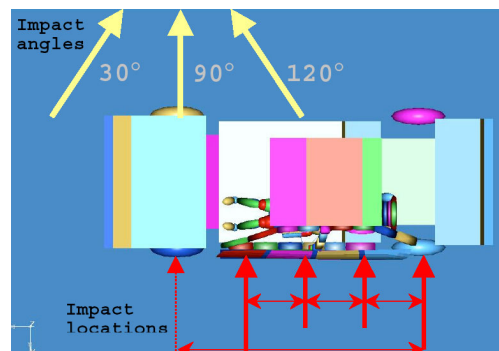


Figure A2.3: Angles and impact locations (top view)

For virtual testing the MADYMO human body occupant model was used because it is more biofidelic than dummy models.

To detect contact between the occupant's head and the interior of the vehicle, a plane was constructed in the car interior by three points. Two points were at the B-pillar and one point at the side roof rail. The plane was not deformable in the simulation but was moved inwards by the crash according to the structure deformation.

For each target car three different planes were used to represent variation in car geometry.

First the base plane was rotated 23° to the vertical and then in addition ± 6° (see figure A2.4)

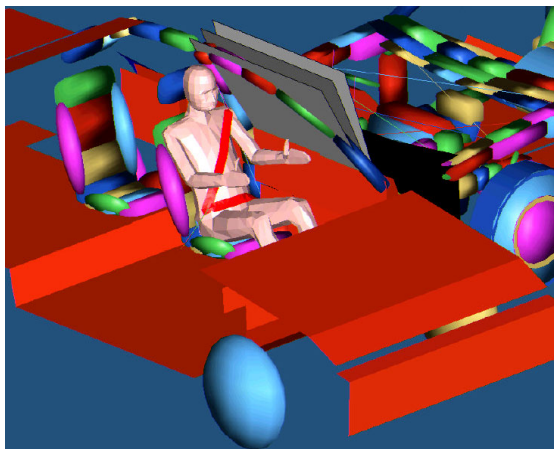


Figure A2.4: Base plane for head contacts

The impact angles are defined according to the constructed plane as shown in figure A2.5.

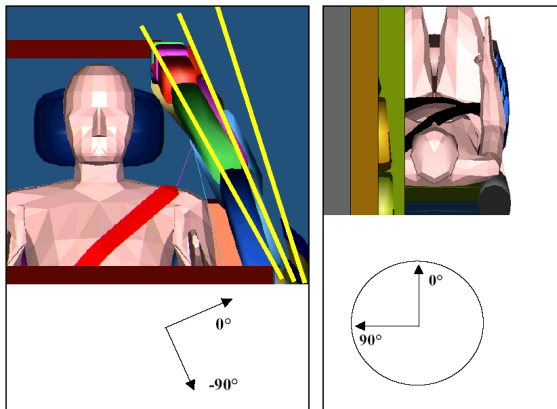


Figure A2.5: Co-ordinate system referred to base plain

Altogether eight scenarios were simulated: seven with three different sized human models and one with a dummy model in different seating positions. Finally 432 simulations were run.

An example of the head contacts is shown in the following figure A2.6 for different occupant sizes and seating positions for the middle plane (see plane in figure A2.4 and A2.5 rotated at 23°).

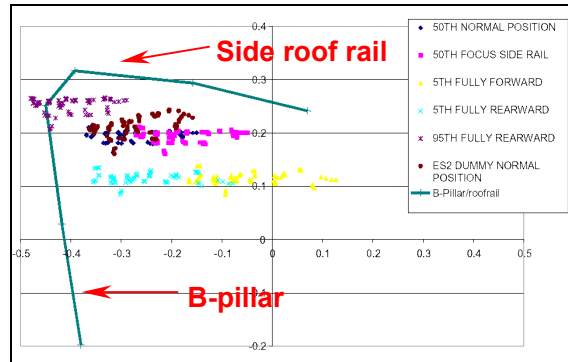


Figure A2.6: Allocation of head contacts for different human sizes

As expected the 95<sup>th</sup> percentile male has got the highest risk to contact the B-pillar region whereas the 5<sup>th</sup> female would contact the window area.

The received head impact velocities differ according to occupant size and car mass. The impact velocity is the difference between the velocity of the impact plane and head CoG. A range of 3 to 9 m/s appeared in the simulation. The average was 6.7 m/s, the same as in the interior headform test procedure.

The horizontal and vertical impact angles according to the co-ordinate system in figure A2.7 and A2.8 are also influenced by the seating position and occupant size.

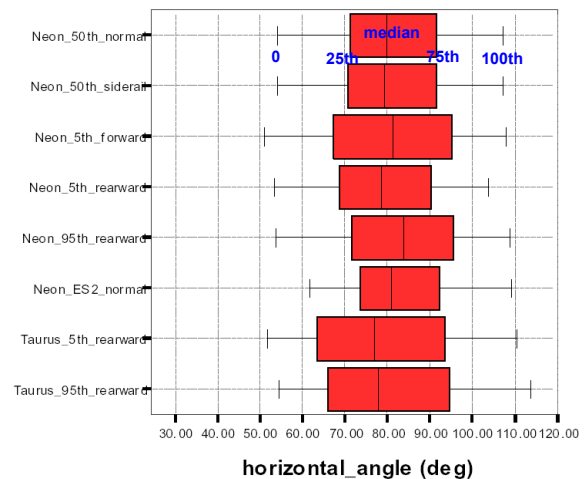


Figure A2.7: Range of horizontal angles

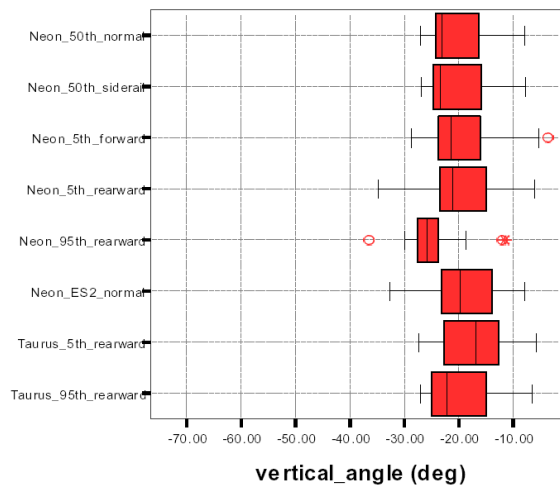


Figure A2.8: Range of vertical angles

The horizontal impact angle is between  $50^\circ$  and  $115^\circ$  and the vertical between  $-5^\circ$  and  $-35^\circ$  as shown in figure A2.9.

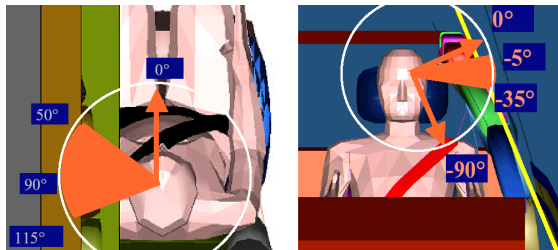


Figure A2.9: Maximum of observed angles

Transferred to a general co-ordinate system of a car, this study proposes the following angles:

- $50^\circ < \text{horizontal angle} < 115^\circ$
- $-12^\circ < \text{vertical angle} < 18^\circ$

## ANNEX A SUMMARY OF TEST PROTOCOL

### Headform – US Free Motion Headform FMH

Text and values between squared bracket are proposed and to be confirmed before the final issue of the protocol. (Example: [255] degrees)

The headform used for testing conforms to the specifications of FMVSS-201 (part 572, subpart L “Free motion headform”)

#### NOTE:

The headform shall be re-certified:

- after every [10] tests,
- after each test in which  $HIC_{dummy} > 1000$
- after any test in which damage to the head-form flesh is suspected

#### Forehead impact zone

The forehead impact zone of the headform is determined according to the procedure specified in sections i to vi below.

- i. Position the headform so that the baseplate of the skull is horizontal. The midsagittal plane of the headform is designated as Plane S.
- ii. From the centre of the threaded hole on top of the headform, draw a line 69 mm forward towards the forehead, coincident with Plane S, along the contour of the outer skin of the headform. The front end of the line is designated as Point P. From Point P, draw a line 100 mm forward toward the forehead, coincident with Plane S, along the contour of the outer skin of the headform. The front end of the line is designated as Point O.
- iii. Draw a 125 mm line which is coincident with a horizontal plane along the contour of the outer skin of the forehead from left to right through Point O so that the line is bisected at Point O. The end of the line on the left side of the headform is designated as Point a and the end on the right as Point b.
- iv. Draw another line 125 mm which is coincident with a vertical plane along the contour of the outer skin of the forehead through Point P so that the line is bisected at Point P. The end of the line on the left side of the headform is designated as Point c and the end on the right as Point D.
- v. Draw a line from Point a to Point c along the contour of the outer skin of the headform using a

flexible steel tape. Using the same method, draw a line from Point b to Point d.

- vi. The forehead impact zone is the surface area on the FMH forehead bounded by lines a-O-b and c-P-d, and a-c and b-d.

#### Free flight trajectory

The FMH must be accelerated under linear control and released for free flight between 25 and 100mm from the point of first contact.

#### Impact Velocity

Two headform impact velocities are specified, the higher one for the evaluation of all target points not possessing and covered by active Head Protection Systems, and the lower one being used for defined areas of the of vehicle, which are covered by approved areas of an active Head Protection System.

- The standard impact speed is  $6.7 \text{ m/s} \pm 0.2 \text{ m/s}$  measured  $\leq 100 \text{ mm}$  from the contact point for ‘normal’ surfaces.
- For areas covered by ‘active head protection systems’, the impact speed is  $5.3 \text{ m/s} \pm 0.2 \text{ m/s}$  measured  $\leq 100 \text{ mm}$  from contact point

#### Impact location accuracy

- The impact alignment accuracy shall be within a radius of  $\leq 10.0 \text{ mm}$  of the selected target point.

#### Impact Environment

- The test temperature range shall be between 19 and  $26^{\circ}\text{C}$
- The relative humidity shall be between 10 to 70%
- The environment shall be stabilised for a period  $\geq 4$  hours prior to test
- Time period between repeated tests using the same headform shall not be less than 3 hours

#### Test location and Head-form orientation

One FMH test should be performed to each test location. These are then restricted to those that lie within the ‘defined’ target area i.e. within an area defined by four planes, two passing through horizontal axes defined by the locations of the heads of large male and small female occupants and two passing through vertical axes also defined by the locations of the heads of large male and small female occupants.

In addition, tests are performed at certain defined structures (taken from FMVSS201u):

- Upper seat belt anchorage
- Seat belt adjustment device, if located above the anchorage point

- Grab handle (located within the defined header rail distance)
- Lighting control unit, coat hook or other such 'fixed' vehicle furniture.

Tests at one position must not compromise a test at an adjacent position due to 'pre-damage'. Although testing will be performed with adjustable windows in the open position, only those contact points, which can be contacted by the headform with the windows closed, will be tested. The impact angle, defined as the angle of the impact velocity vector with respect to the plane tangential to the surface at the point of contact, shall be selected to be the "worst case" as close as possible to perpendicular to the impact surface.

#### Method 1

Then, for each selected target location, the headform orientation and actual impact location for each test is determined according to the following procedure. For clarity this procedure is illustrated by means of a decision making flow chart in Figure a.

- With the mid-sagittal plane vertical, should coincide with the impact velocity vector through the contact target.
- If a clean contact is not possible without contacting other noncertified parts of the FMH, then the headform and impact velocity vector should be pitched forward with respect to the normal by  $10^\circ \pm 2^\circ$  and realigned with the target, figure b.
- If a clean contact cannot be made with the head mid-sagittal plane, aligned vertically following this adjustment then the FMH and velocity vector should be returned to normal to the surface and the FMH be rolled by  $90^\circ \pm 2^\circ$  around the velocity vector, as described in the note.
- If the target location point still cannot be hit cleanly, then the headform should be rotated back to its original vertical position and the headform and impact velocity vector should be pitched forwards, with respect to normal, until a clean contact is established up to a maximum allowable pitch of  $18^\circ \pm 2^\circ$  to normal. A pitch of  $18^\circ$  reduces the lateral component of the impact vector by approximately 5%.
- If the selected point still cannot be impacted cleanly, then the target point should be moved within the limits defined in Appendix 1, Section 1.3 while still seeking a worst case contactable position.

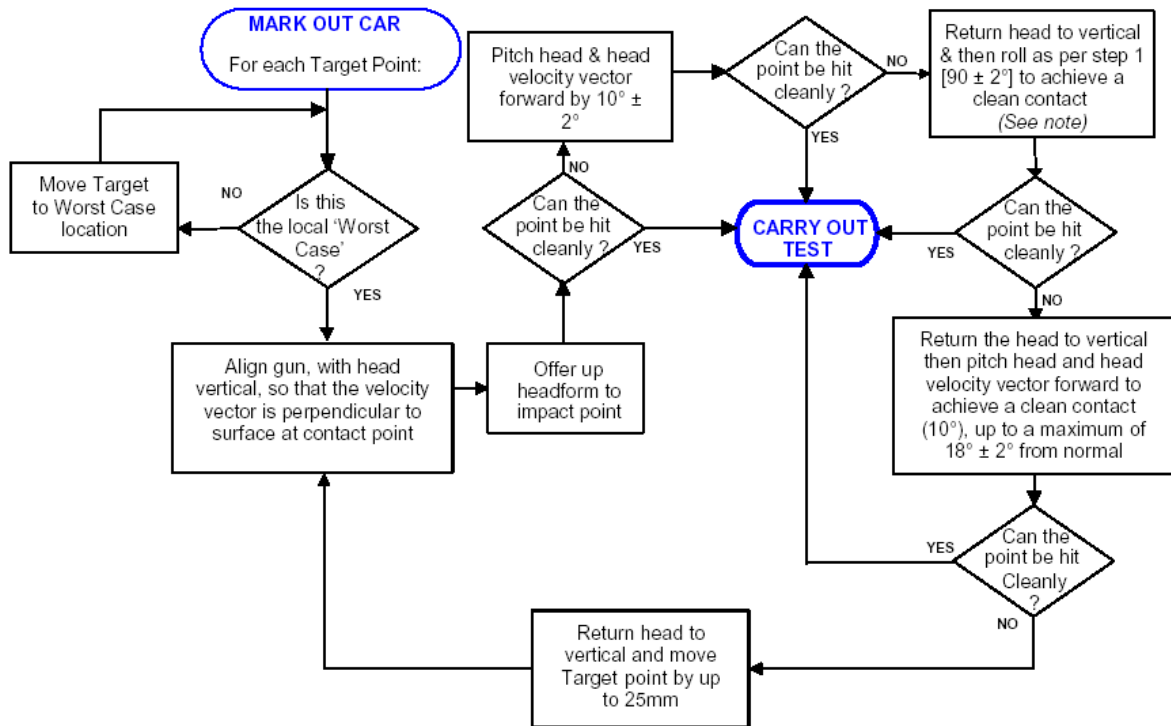
#### Method 2

Then, for each selected target location, the headform orientation and actual impact location for each test is determined according to the following procedure.

- With the mid-sagittal plane vertical, the impact velocity vector shall be perpendicular to the surface through the contact target.
- If a clean contact is not possible without contacting other noncertified parts of the FMH, then the headform and impact velocity vector should be pitched downward with respect to the normal by  $10^\circ \pm 2^\circ$  and realigned with the target, figure b
- If the target point still cannot be hit cleanly, again the headform and impact velocity vector should be pitched downwards, with respect to normal, until a clean contact is established.
- If the selected point still cannot be impacted cleanly, then the target point should be moved within the limits still seeking a worst case contactable position.

For any method the following exceptions will apply:

- (a) Vertical approach angles will be limited to no more than [50] degrees (as is used in FMVSS 201) for all impacts. (Recent computer simulations has suggested that Vertical approach angles of [-10 to +20] degrees may be more appropriate, see TNO study above)
- (b) When testing the A-pillar, the horizontal approach angle will be limited to between [195] and [255] degrees for the left hand side, and [105] to [165] degrees for the right hand side. Figure c. For impacts on the A-pillar only the longitudinal vertical plane passing through the forehead impact zone points O and P shall be perpendicular to the primary axis of the A-pillar at the impact point. Figure d.
- (c) When testing side roof structures, B-pillars and other pillars (where applicable), the horizontal approach angle will be limited to between [230] and [295] degrees for the left hand side, and between [65] and [130] degrees for the right hand side. Figure e.
- (d) For point BP2, the horizontal approach angle will be limited to [270] degrees for the left hand side and [90] degrees for the right hand side.
- (e) When testing the rearmost pillar, the horizontal approach angle will be limited to between [270] and [345] degrees for the left hand side and [15] to [90] degrees for the right hand side. Figure c.



note: Clarification note on headfrom rotation  
 FMH axial rotation about the impact vector facing towards the target point.

Target area	Left hand side of the vehicle	Right hand side of the vehicle
<b>A post target points</b>	90° clockwise	90° anticlockwise
<b>Roof rail target points</b>	90° clockwise	90° anticlockwise
<b>B post target points</b>	90° anticlockwise	90° clockwise

Figure a: Method 1, headform alignment flow chart

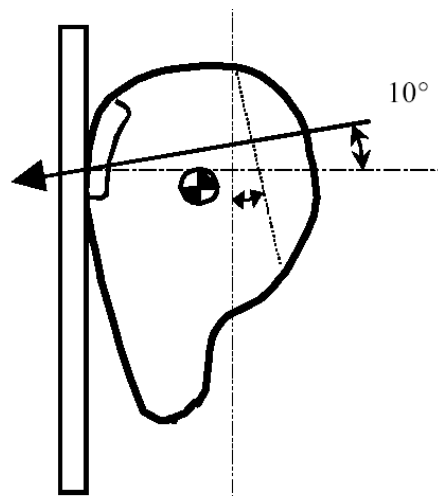


figure b: 10° pitch to the normal

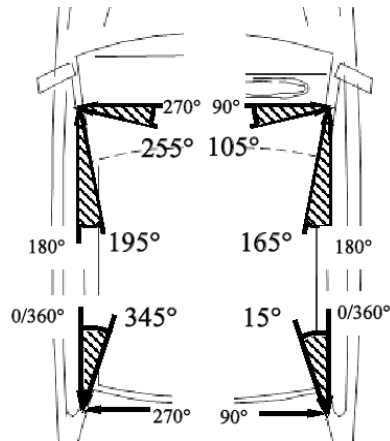


figure c: Horizontal approach angle limitation for A- and rearmost pillar

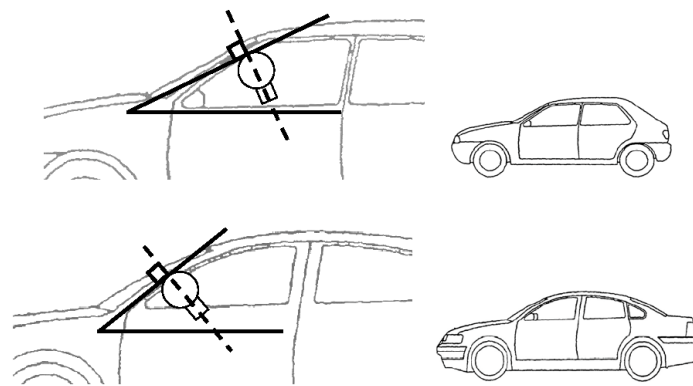


figure d: Perpendicular impact to the A-pillar

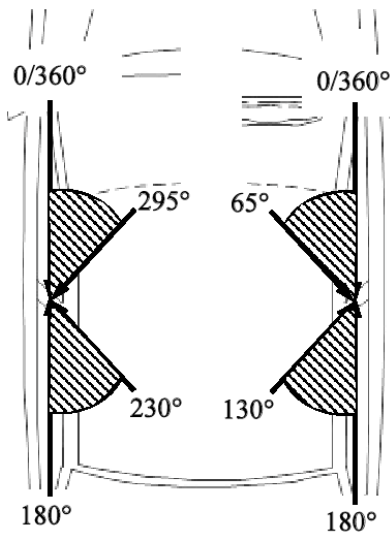


figure e: B-pillar and other pillar horizontal approach angle limitations

**Note:**

During the first phase of the WG13 research the US FMH was selected as the preferred impactor, thus all of the reported WG13 research has focussed on the use of this test device.

## General guidance

### • ‘Worst Case’ impacts

It is expected that ‘worst case’ will differ between vehicles, thus each vehicle should be assessed, by examining the drawings or physical inspection, before assuming the padding, fixing or other structure would be a worst case position. An inspection of the trims and underlying structure should be carried out to look for:

- Where the crush depth of padding is minimal.
- The location of fixings and bolts.
- The position of welds, joints or internal webs in the chassis.
- The attachment of padding or other components

The presence of such features could be used to guide a test authority regarding focal point for ‘worst case’ impacts.

### • Closeness of repeated test

- Multiple impacts

A vehicle being tested may be impacted multiple times, subject to the limitations given below

- Impacts within 300 mm of each other may not occur less than 30 minutes apart.
- No impact may occur within 150 mm of any other impact. The requirement within

FMVSS 201 has been increased to 200 mm between points for what is believed to be technical reasons.

The distance between impacts is the distance between the centres of the target circle for each impact, measured along the vehicle interior.

### • Examination of collateral damage

If other impacts are to be carried out within a 200 mm radius of a previous impact point then any structural damage around and beneath the target point must be assessed. If damage is noted and full repair is not possible then no further adjacent impacts should be performed within the area of damage extended by 200 mm from the target point. Tests at the adjacent points would have to be performed in a different vehicle.

**Note** – the chin of the headform can contact parts of the vehicle structure 150 mm from the contact point.

## Damage assessment

- If any trim or padding has been permanently deformed or show signs of elastic distortion, including attachment points within a 100 mm radius of the target points then the padding must be replaced for adjacent tests. The 100 mm radius could be increased if it is considered that the damage might affect the stiffness of the padding structure in any adjacent impact. All padding and trim attachment points should be examined and assessed for possible collateral stiffness.
- The extent of damage/deformation to structures underlying the padding should be assessed. If any permanent damage is detected the limit of the damage must then be quantified. No adjacent test should be carried out within 200 mm of the edge of the identified structural damage.

## Vehicle preparation, including support

The vehicle should be rigidly supported off its wheels with the principle axes of the vehicle being aligned with ground reference co-ordinates. The maximum displacement of the exterior surface of the vehicle, along the axis of the impact adjacent to the point of contact, shall not exceed 10 mm. If necessary, the exterior of the vehicle may be ‘additionally’ supported to limit exterior movement to 10 mm.

If the side window can be opened, tests should be performed with the window fully open.

### Pole impact test Procedure.\*

The vehicle impacts a fixed 254 mm diameter rigid vertical pole at an impact speed of  $29 \pm 2$  km/h. The pole is aligned with the centre of gravity of the head of the ES-2 dummy. In order to achieve this impact, the vehicle is placed on a carrier, which can translate freely in the direction perpendicular to the vehicle’s longitudinal vertical plane.

\* NOTE: The pole impact test procedure is based on that specified in FMVSS 201 with the ES-2 dummy. The specifications for the test procedure defined in Annex 1 have been taken from an edited version of the Euro NCAP protocol, since this also uses ES-2. Elements only used in the derivation of Euro NCAP ratings and items not appropriate for this draft procedure have been removed.

The impact angle should be  $90^\circ \pm 3^\circ$ .

The dummy's seating position should be adjusted, if necessary, to ensure that the head presents a target through the side glazing and is not obscured by the B-pillar.

The active system FMH tests and active system sub-structure FMH tests will only be performed where the requirements of the pole impact test are satisfied. The procedure is shown in figure f.

### Performance criteria

#### FMH Head Injury Criterion

The Head Injury Criterion for the head-form (HIC<sub>FMH</sub>) is calculated according to the following formula:

$$HIC_{fmh} = \left( \frac{1}{(t_2 - t_1)} \int_{t_1}^{t_2} a d(t) \right)^{2.5} (t_2 - t_1)$$

where 'a' is the resultant head-form acceleration, expressed as a multiple of 'g' (the acceleration due

to gravity), and t1 and t2 are any two points in time during the impact, which are separated by not more than a thirty-six millisecond time interval.

$$HIC_{dummy} = 0.75446 HIC_{FMH} + 166.4 * 1000$$

#### Pole Test Head Injury Criterion

In the pole impact test, the Head Injury Criterion (HIC) must not be more than 1000. The HIC is the maximum value of the expression:

$$HIC_{fmh} = \left( \frac{1}{(t_2 - t_1)} \int_{t_1}^{t_2} a d(t) \right)^{2.5} (t_2 - t_1)$$

where 'a' is the resultant head-form acceleration, expressed as a multiple of 'g' (the acceleration due to gravity), and t1 and t2 are any two points in time during the impact, which are separated by not more than a thirty-six millisecond time interval.

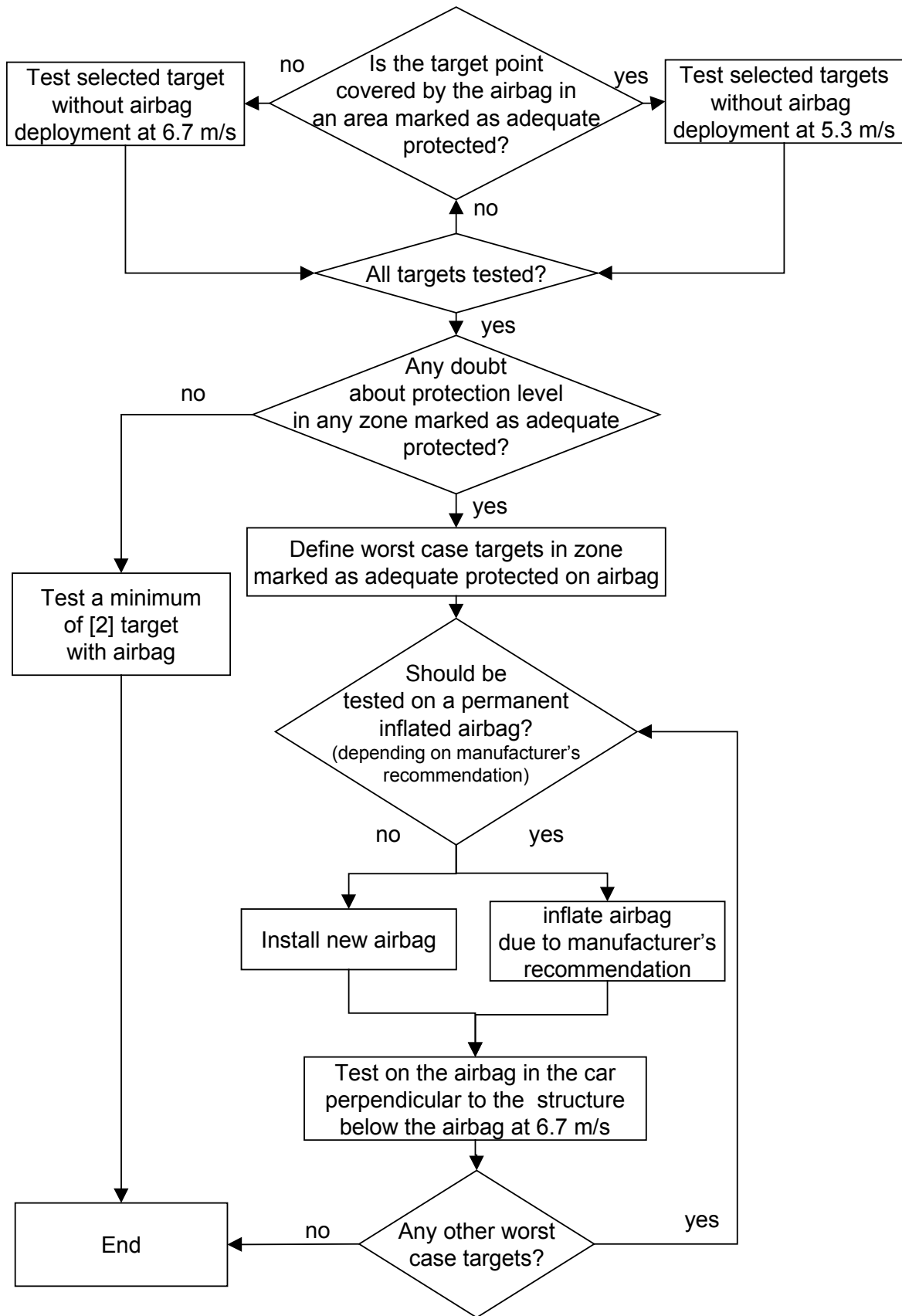


figure f: Flow chart for testing with head airbag systems

## CURRENT WORLDWIDE SIDE IMPACT ACTIVITIES – DIVERGENCE VERSUS HARMONISATION AND THE POSSIBLE EFFECT ON FUTURE CAR DESIGN

A. McNeill, J. Haberl, BMW AG  
Dr. M Holzner, Audi AG  
Dr. R. Schoeneburg, Daimler Chrysler AG  
Dr. T. Strutz, Volkswagen AG  
U. Tautenhahn, Porsche AG

Paper Number: 05-0077

### ABSTRACT

Car manufacturers design vehicles and side impact restraint systems to protect passengers from the risk of serious injury in the event of a side impact. In each of the major markets of the world, the side-impact testing requirements as set by the regulatory and the consumer interests are generally different. This paper will document and compare the international side impact regulatory and consumer test requirements of now and the future.

Using a sample of results from vehicles tested in accordance with the discussed future regulations and consumer tests, it is shown that vehicles currently “best rated” for side-impact protection in consumer tests need to be redesigned in order to meet the prospective regulatory requirements. This paper will discuss the vehicle structural, interior and restraint design changes, which could be required.

The global side-impact tests and requirements are diverging, and not converging towards a harmonized Side-impact Testing Protocol as presented by the IHRA at the 2003 ESV Conference. It is our goal that side-impact requirements and procedures should become less diversified and more harmonized as we continue to improve side-impact protection for all customers worldwide.

### INTRODUCTION

Global accident statistics show that side impacts account for approximately 30 % of all impacts and 35 % of the total fatalities (Source – German In Depth Accident Study - GIDAS, National Automotive Sampling System - NASS & BMW accident databases).

It is essential for us as vehicle manufacturers to provide adequate protection in order to minimize the potential negative effects of such impacts on our customers.

Most side impacts can be classified into two impact types. Either a “Car to Car” or a “Car to narrow object” (tree, lamp post etc).

Side impact protection forms a very important part of any total vehicle protection system. To design, develop and test the optimum level of protection into a vehicle these two impact types are generally used.

A “Car to Car” impact is simulated with a stationary target vehicle being hit sideways by a moving bullet vehicle or barrier. In the event of “Car to narrow object” impact, a moving target vehicle comes into contact with a stationary pole, simulating a post or tree. A schematic showing a barrier and pole type crash test can be seen in Figure 1.

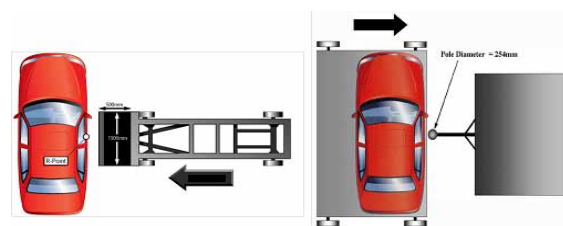


**Figure 1. Barrier and pole crash test schematic.**

The following describes the mechanism of a “Car to Car” impact:

- Contact occurs between the two vehicles.
- The outer skin of the target vehicle is accelerated to the velocity of the outer surface of the intruding surface of the bullet vehicle. The lateral velocity of the occupant is zero. The airbag sensing system detects a crash and ignites the countermeasures.
- The body structure of both vehicles is increasingly loaded and deformed. Airbags deploy.
- The kinetic energy of the bullet vehicle is dissipated by elastic and plastic deformation of each partner.
- The countermeasures dampen the effect of the intruding structure.

- The vehicle and occupant reach the same velocity. The peak dynamic deformation and injury results are reached. Further energy is absorbed through the kinetic energy change of the target vehicle.

The art of side impact protection is about ensuring that the intruding velocities are kept to a minimum through a suitable vehicle structure and deploying an appropriate restraint system to dampen the effect of the intruding structure, thus reducing the effect of the impact on the occupants.

Vehicle manufacturers have made great leaps in terms of side impact protection over the last 10 years. Protection has been steadily increasing as technology has allowed. Most vehicles are now equipped with thorax airbags, head airbags, interior padding and an optimized vehicle structure. A total vehicle protection system is shown in Figure 2.

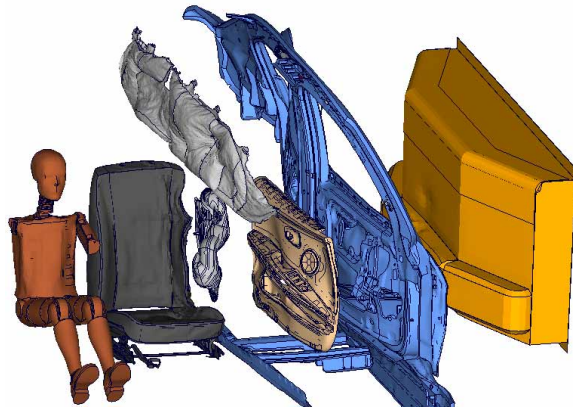


**Figure 2. Side impact countermeasures & small female dummy.**

In order to assess the likelihood of injury during a given crash scenario, several different anthropomorphic test devices, so called crash test dummies, are used. They simulate a human occupant, and are designed to reflect injuries in important regions of the human body, such as head, thorax, abdomen and pelvis. See Figure 2.

### **SIDE IMPACT - CURRENT, FUTURE & HISTORICAL SITUATION**

The worldwide activities to improve passive safety in side impact, started in the 1980's with research work at the National Highway Traffic Safety Administration (NHTSA). A static side intrusion test was developed. This became the Federal Motor Vehicle Safety Standard No. 214 (FMVSS 214).

In 1990 FMVSS 214 was extended to include the dynamic crabbled barrier test. This was the first side impact regulation that included a side impact

dummy (SID) and was enacted in 1993, with a phase in of three years.

In 1997 NHTSA included a lateral impact consumer test known as SINCAP. This was an additional test to the frontal NCAP. Instead of the FMVSS214 speed of 53 km/h, the rating test is completed with a velocity of 61 km/h. The rating is based on acceleration measured in the thorax region of the dummy. More than 40 cars were tested in the first year, none obtained the best score of 5 stars. In the following year two cars achieved a 5 star rating for the driver. Following a further 2 years the first passenger car improved to point of earning a double 5 star rating (for the first two seating rows). Today most cars have a 4 to 5 star rating and only one car in 2004 earned only a two star rating.

Parallel in Europe the European Enhanced Vehicle Safety Committee Working Group 13, (EEVC WG13) started their research activities to create a European wide regulation – ECE-R95. This included a new European barrier and a new generation of dummy, EuroSID1 (ES1). The implementation date for new type approvals was October 1998.

During 1997 prior to this regulation taking effect, Euro NCAP decided to implement the research work of the EEVC WG13 into their program. The more stringent targets at Euro NCAP, especially rib intrusion and abdominal forces, were set at a higher level than current European legislation. Most models earned less than 10 out of 16 points. Today more than ½ of all cars tested achieve the maximum 16 points for the side impact barrier test.

In 1995 NHTSA issued an amendment to FMVSS 201 to include upper interior head impact protection using a 'Free Motion Head Form' (FMH). During 1998 a further final rule was issued, this allowed a reduced impact speed for FMH testing in the area where a head protection was packaged. The head protection system's effectiveness needed to be proved through a dynamic pole crash test. This enabled car manufacturers to implement side impact curtains whilst still meeting the upper interior head protection requirements. For this test the Side Impact Dummy was redeveloped in the neck and head area and called SIDHIII. This dummy was also integrated in the SINCAP procedure.

Euro NCAP implemented the lateral pole test procedure in the year 2000 similar to the US standard, but using the ES1 dummy. The test is voluntary and awards two extra points towards the side impact score. With the implementation of the pole impact, Euro NCAP changed the highest

possible score from four to five stars. Today many manufacturers are able to achieve the Euro NCAP goals for pole impact (even with the new 2002 head acceleration limits and the modifier for improper airbag deployment). Many manufacturers now build head protection airbags into their vehicles as standard. This provides the best possible protection for customers whilst also achieving a 5 star rating.

During 2003 an EEVC proposal for an updated barrier was implemented into the existing ECE-R95 requirement. This was closely followed in 2004 with a change to the dummy from ES1 to Euro SID 2 (ES2). ES2 was shown to have a slightly higher biofidelity rating compared to ES1. See Figure 3.

Again Euro NCAP decided to implement these changes from WG13 into the rating in 2003. This was four years before the changes became mandatory for new vehicle type approvals.

In June 2003 the Insurance Institute for Highway Safety focused on the predominately North American issue of heavy SUVs involved in side impact. A new barrier was designed to duplicate the front-end stiffness and overall size of a typical North American SUV (Sport Utility Vehicle). The 5%ile female dummy SIDII (SID II) was used as the occupant for both seat rows.

Looking forward to the next 3 years the following regulations will influence the design of cars:

Firstly: “The Procedure for evaluating occupant injury risk from deploying side airbags”, as developed by the Technical Working Group (This includes manufacturers, government, special interest groups and OEM suppliers). The requirement has a phase in starting from 2000 with 100% of all 2007 model year cars needing to meet this procedure. The target is to reduce the chance of injuries to small occupants and children from deploying side airbags.

Secondly: The memorandum of understanding for “Front to Side Compatibility” (F2S) signed by most of the vehicle manufacturers within the Alliance. This has a dual stage phase in. During the first phase manufacturers can choose to assess the likelihood of head injury, with either a FMVSS201 pole impact or an IIHS barrier side impact. In phase 2 only the IIHS barrier test can be used.

Current research work for regulations in the next three to seven years includes the upgrade of the US regulation FMVSS214. A notice of proposed rulemaking was published by NHTSA in spring 2004 and proposes four full-scale side impact tests instead of the current, one. The main differences to the existing regulation is the replacement of the

dummy: ES2 modified with a rib extension kit (ES2re), this replaces the SID and a new dummy SID IIs modified with a floating rib guide (SIDIIsFRG). Both will be used in the barrier test (unchanged crabbed barrier) and in a newly developed 75° pole impact.

Phase 3 of the F2S voluntary agreement is currently being discussed. It is possible that further injury limits will be agreed using the IIHS side impact test configuration.

In Europe the EEVC WG13 is working closely together with the Japanese authorities to develop an Advanced European – Mobile Deformable Barrier (AE-MDB). The target for the barrier is to better represent the current fleet of European vehicles.

The WG13 is also close to finalizing a “European Interior Head-Form Test Procedure” for lateral collisions. This is an expected addition to the ECE-R95 regulation. This procedure differs immensely to the US FMVSS201 standard.

Since 1997 the “ISO World Side Impact Dummy Task Group” has been developing a new dummy (WorldSID). The design and development of this dummy, a 50% male side impact dummy was completed in March 2004.

The funding for this programme was achieved through a worldwide consortium from the vehicle industry, research institutes and government agencies. The WorldSID heralds a significant improvement in the ability of crash dummies to duplicate human motions and responses in side impact tests. The use of this dummy should lead to improved vehicle designs and occupant protection. Based on the ISO/TR9790 rating scale, the WorldSID biofidelity rating is 7.6 (“Good” on a 10 point rating scale). In comparison to other side impact dummies currently in use, WorldSID has a far superior biofidelity rating. See Figure 3.

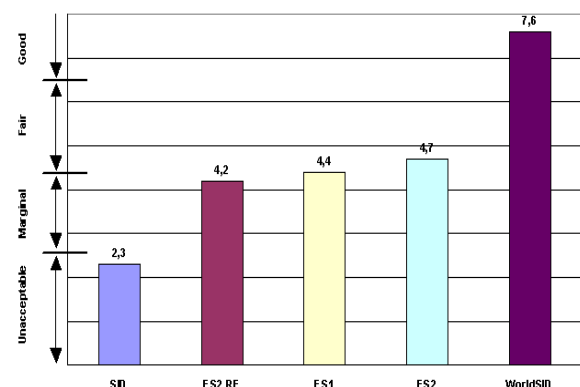


**Figure 3. Dummy biofidelity ratings to ISO/TR9790**

Five working groups were established after the 15<sup>th</sup> ESV 1996 conference, as “The International Harmonisation Research Association” (IHRA). Their aim was to provide the automotive community with harmonised research to develop test procedures, which could then become the basis for global regulations and consumer tests. At the 18<sup>th</sup> ESV conference in 2003, the IHRA Side Impact Working Group (SIWG) presented an outline for a possible Global Technical Regulation (GTR) for Side impact protection.

The proposals main points are simplified below:

- MDB barrier test to simulate “Car to Car” impacts (up to 2 tests to cover worldwide fleet differences).
- Oblique pole test to simulate “vehicle to narrow object impacts”.
- Upper interior head impact test.
- OOP side airbag tests.

Summarising the current and future side impact requirements means over the next 7 years there may be 5 additional test configurations and two additional dummy types. Manufacturers developing world vehicles whilst also providing good side impact protection will have to certify using a total of 7 different barrier configurations:

IIHS, FMVSS 214, Multi 2000 Advanced, AE MDB, Oblique Pole 5%ile, Oblique Pole 50%ile and 90° Pole.

And a total of 6 different dummies:

ES2, ES2re, SIDIIs, SIDIIsFRG, WorldSID, SIDHIII

The total side impact requirements including both legal and consumer tests can be seen in Figure 4.

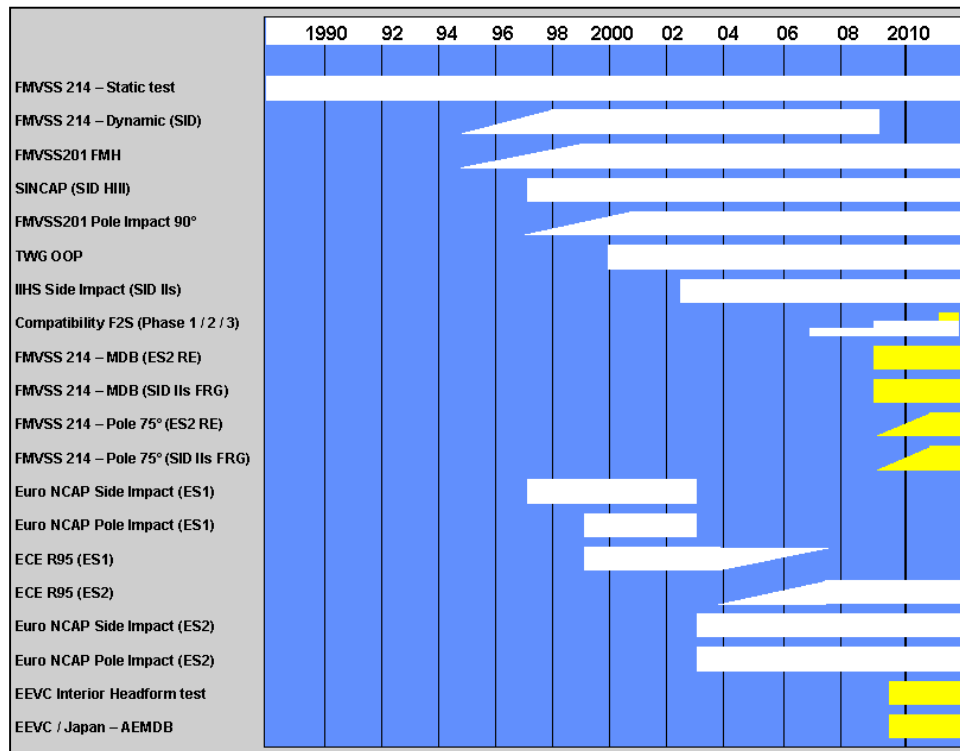


Figure 4. Side impact requirements (proposed new requirements shown in yellow)

# NEW LEGISLATIVE PROPOSALS – VEHICLE BASED ANALYSIS

## Advanced European Mobile Deformable Barrier

The currently proposed design of the AE-MDB (Version 2) has been investigated with full-scale crash tests and simulation. Special emphasis has been given to the stiffness distribution of the particular blocks (D, E, F). See Figure 5. The different barrier versions have then been compared to the front-end structures of typical current vehicles.

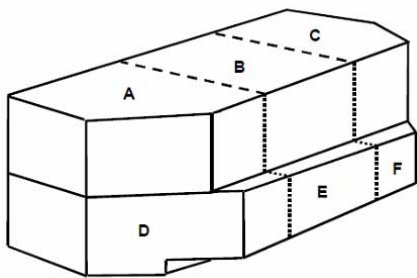


Figure 5. AE-MDB schematic

The stiffness (100% - ~40% - 100%) of the lower row of blocks (D – F) has been criticized for not reflecting the stiffness distribution of modern car front ends (The percentage stiffness values relate to the stiffness of block D). The outer blocks of the barrier have a high stiffness relative to the middle block. This stiffness distribution was supposed to better represent the front longitudinals of vehicles.

However, modern cars are being designed to have an even stiffness distribution of the front end. This is achieved through bumper crossbeams of high stiffness for compatibility and offset impact reasons. Vehicles designed in such a way are able to load struck vehicles with a more homogenous loading pattern.

The discussion of this discrepancy resulted in various proposals for changing the stiffness setup of the lower row of blocks. Figure 6 summarises the simulation carried out by the German Alliance in order to support the barrier development.

Bullet Vehicle	Barrier Specification	Remarks	Target Vehicle			
			VW Golf V	Audi A6	Mercedes E-class	BMW 3-Series
ECE R95	Multi 2000 Advanced		X	X	X	X
AE-MDB v2	(100% - ~40% - 100%)	Reference	X	X	X	X
AE-MDB v3.1	(100% - ~40% - 100% + Bumper)	Japanese Proposal	X	X	X	X
AE-MDB v3.5	(40% - 60% - 40%)	German Alliance	X	X	X	X
AE-MDB v3.6	(70% - 60% - 70% + Bumper)	Task Force - WG13	X	X	X	X
AE-MDB v3.9	(55% - 60% - 55% + Bumper)	BAST Proposal	X	-	X	X
VW Golf V	-	-	X	X	-	-
Audi A6	-	-	-	X	-	-
Mercedes E-class	-	-	-	-	X	-
BMW 3 Series	-	-	-	-	-	X

Figure 6. Matrix of simulations completed with different AE-MDB Specifications and modern vehicles.

For this example the simulation from the VW Golf 5 has been analysed, specifically the following:

- Deformation distribution (homogeneity).
- Intrusion depth.
- Intrusion velocities.

Figure 7 shows the deformation profiles of the AE-MDB version compared to Multi 2000 advanced barrier, AE-MDB (40% - 60% - 40%) and VW Golf 5 “Car to Car”. The AE-MDB (40% - 60% - 40%) best represents the deformation distribution of the “Car to Car” test.

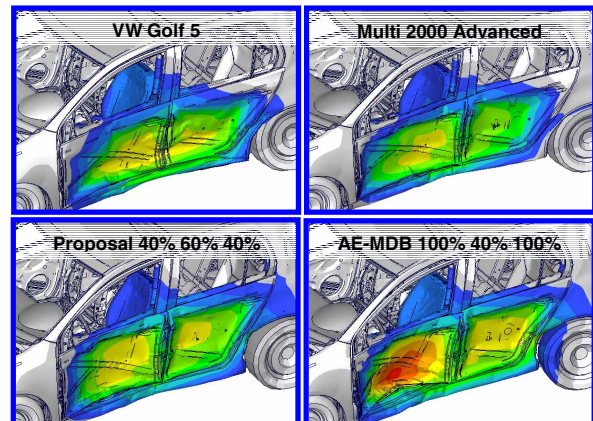
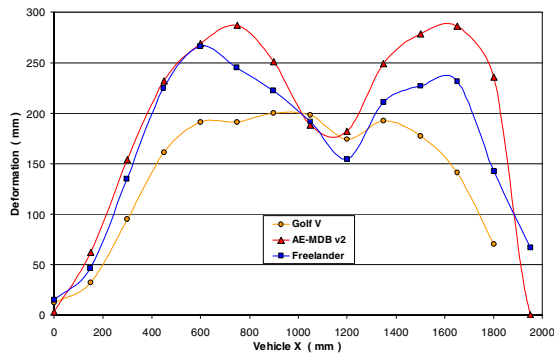


Figure 7. Comparison of deformation profiles (90° Side impact with MDB at 50 km/h & target vehicle at 0 km/h; VW Golf 48 km/h to VW Golf 24 km/h)

In addition to the crash simulations various vehicle tests have been performed. Figure 8 shows the static deformation profiles, recorded at the pelvis height of the dummy. Bullet vehicles included were:

- AE-MDB v2.
- “Car to Car” VW Golf 5.
- “Car to Car” Land Rover Freelander.



**Figure 8. Deformation profiles**

The Land Rover Freelander represents a European SUV and is agreed in WG13 to be the upper limit for consideration in the development of the AE-MDB.

The crash tests results concur with the simulation that the deformation characteristics made by the AE-MDB are not as homogenous as the “Car to Car” test, particularly the VW Golf 5.

It is noted that the total deformation depth with the AE-MDB v2 is even higher than with the suggested “worst case” Land Rover Freelander.

The same trend is seen in Figure 9. This shows the results with Audi A6.



**Figure 9. Deformation characteristics AE-MDB V2 to Audi A6 & “Car to Car” Audi A6**

The intrusion velocities show the same tendency as the static deformations recorded.

Considering the results of the investigations, the stiffness distribution of the blocks of the AE-MDB

needs to be reconsidered in order to be more reflective of real world crashes. If the current barrier is used as a basis for a new legal requirement, this will undoubtedly lead to unnecessary reinforcements being added to future vehicles. Using the results as presented this can in no way be justified from a “Real World” viewpoint.

### FMVSS214 NPRM

The proposed upgrade of US-standard for side impact crash tests with four different configurations, two oblique pole tests (75-degree, 32km/h) and two tests with the “crabbed” mobile deformable barrier (MDB). Each test, pole and MDB, is to be performed with both, ES2RE (50% male) and SID2sFRG (5% female) dummy.

When performing an oblique pole test, the vehicle impacts with an angle of 75°. Most vehicles are currently developed using a 90° pole as specified by Euro NCAP and FMVSS 201. The centre line of the pole is aligned with the Centre of Gravity of the dummy head. See Figure 10.

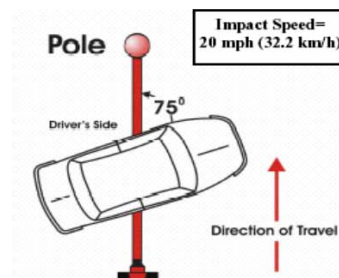


**Figure 10. Oblique pole test schematic**

The level of understanding is somewhat limited regarding the FMVSS 214 NPRM. This is due to lack of dummy availability and the incomplete pre development programs. However through the first investigations a number of issues become apparent.

Is it possible to develop a restraint system, (thorax airbag, head airbag and interior padding) which can fulfil all the requirements? This may be the case for the FMVSS 214 NPRM but when other test configurations are taken into account, such as IIHS or SINCAP this seems unlikely.

It could be that we are on the verge of requiring more adaptive restraint systems for side impact with the associated airbag and sensing technology.

With Cabriolet / Convertible vehicles, the current state of the art system is a head thorax airbag. This offers combined head and thoracic protection. In order to meet the oblique pole requirements such airbags will need to be designed to cover a

significantly larger area. A larger airbag and therefore aggressive deployment will then be required. This will be a clear conflict to the requirements of TWG (Technical Working Group) voluntary agreement “Procedure for evaluating occupant injury risk from deploying side airbags”.

## CONCLUSIONS

Due to the “disharmonisation” between governments and consumer test organisations, there is a real potential for an ever-increasing number of tests and dummies. Each individual test is always justifiable, but together from a global perspective this is not the case.

Are accidents and people the world over so different to warrant a potential of seven different test configurations and six different dummies?

In order for a vehicle manufacturer to meet the different requirements increasingly complex safety systems and vehicle structures will be required.

It cannot be proven whether such systems will provide any real world benefit other than satisfying “disharmonisation” and increasing vehicle weight, with the corresponding negative effect on vehicle emissions & fuel consumption.

The goal for all parties involved must be that safe vehicles are produced in the most efficient way, to ensure that all consumers are able to enjoy the best possible protection. Harmonisation of global side impact requirements would make a large contribution towards this.

Lastly, the IHRA has been pushing worldwide harmonisation with an enormous investment and engagement of its members. The output from this group in our opinion is not being taken seriously enough. This can be seen with the new legislative proposals currently being published.

## RECOMMENDATIONS

Worldwide harmonisation is not receiving adequate consideration. The vehicle manufacturers AUDI, BMW, DaimlerChrysler, Porsche and Volkswagen strictly support all ongoing harmonisation activities and particularly the work of the IHRA. The following needs to be considered:

- “Global Technical Regulation Side Impact Protection” with a timing plan for introduction.
- World NCAP based on a future GTR

## REFERENCES

National Highway Traffic Safety Administration Federal Motor Vehicle Safety Standards; *Occupant protection in interior impact*, Part 571. (FMVSS 201 Revision 2004)

National Highway Traffic Safety Administration Federal Motor Vehicle Safety Standards; *Side Impact Protection*, Part 571. (FMVSS 214 Revision 2004)

National Highway Traffic Safety Administration Federal Motor Vehicle Safety Standards; *Side Impact Protection*, Parts 571 and 598 (FMVSS 214 upgrade NPRM 2004)

ECE Regulation No. 95 - *Uniform provisions concerning the approval of vehicles with regard to the protection of the occupants in the event of a lateral collision* (Revision 2004)

Side Airbag OOP Injury Technical Working Group - *Recommended Procedures for Evaluating Occupant Injury Risk from Deploying Side Airbags* (Revision 2003).

International Organisation for Standardisation - *Anthropomorphic side impact dummy - Lateral impact response requirements to assess the biofidelity of the dummy* ISO/TR 9790 (Revision 1999)

Dakin, - *Insurance Institute for Highway Safety Side Impact Crashworthiness Evaluation Program: Impact Configuration and Rationale*, Paper No. 172, 18<sup>th</sup> ESV Conference, Nagoya, 2003.

Roberts, A. - *The Development of the Advanced European Mobile Deformable Barrier Face (AE-MDB)*, Paper No. 126, 18<sup>th</sup> ESV Conference, Nagoya, 2003.

Seyer, K. - *International Harmonised Research Activities Side Impact Working Group Status Report*, Paper No. 579, 18<sup>th</sup> ESV Conference, Nagoya, 2003

Van Ratingen, M.R. et al, *Development of a European Side Impact Interior Headform Test Procedure*, Paper No.138, 18<sup>th</sup> ESV Conference, Nagoya, 2003.

GIDAS: German In Depth Accident Study [www.gidas.org](http://www.gidas.org)

NASS: National Automotive Sampling System [www-nrd.nhtsa.dot.gov](http://www-nrd.nhtsa.dot.gov)

EEVC – European Enhanced Vehicle Safety Committee [www.eevc.org](http://www.eevc.org)

Euro NCAP – European New Car Assessment  
Program [www.euroncap.com](http://www.euroncap.com)

IIHS – Insurance Institute for Highway Safety  
[www.hwysafety.org](http://www.hwysafety.org)

## OCCUPANT PROTECTION IN FAR SIDE CRASHES

**Brian Fildes, Astrid Linder, Clay Douglas,**  
Monash University Accident Research Centre, Melbourne, Australia

**Kennerly Digges, Rick Morgan,**  
George Washington University (NCAC), Virginia

**Frank Pintar, Narayan Yogandan,**  
Medical College of Wisconsin, Wisconsin

**Hampton Clay Gabler, Stefan Duma, Joel Stitzel,**  
Virginia Tech – Wake Forest, Center for Injury, Virginia.

**Ola Bostrom,**  
Autoliv Research, Sweden

**Laurie Sparke, Stu Smith,**  
Holden Innovation, Melbourne, Australia

**Craig Newland,**  
Dept. Transport and Regional Services, Canberra, Australia

Paper No. 05-0299

### ABSTRACT

Regulations and interventions to protect far side occupants in side impact crashes do not currently exist, even though these occupants account for up to 40% of harm in real world side impact crashes. To address this, a comprehensive international research program has been assembled involving many of the world's experts in side impact protection and biomechanics. Seven work-tasks are outlined for conducting this research, which is due to be completed by the end of 2007.

### INTRODUCTION

Side impacts are frequent and extremely harmful crashes. The likelihood of being killed or seriously injured is very high in side impact crashes. Twenty five percent of vehicle casualties (28 percent of fatalities) occur from these crashes, accounting for roughly one-third of occupant Harm on our roads (Fildes, Lane, Lenard & Vulcan, 1994).

Current side impact regulations in Europe, the USA, Japan and Australia specify acceptable performance levels for a single crash configuration and impact speed for near side occupants. This is appropriate as near side crashes are extremely common and harmful to occupants involved in side impact collisions. Fildes, et al, 1994; Frampton, Brown, Thomas and Fay (1998); and Digges and Dalmotas (2001) all reported that near side occupants account for up to 70% of all side impact injuries. However, far side occupants are involved

in 30% of injuries and up to 40% of occupant Harm in real-world side impact crashes (Fildes, Gabler, Fitzharris. & Morris, 2000). This seating position is currently not addressed by existing vehicle safety initiatives around the world. It is critical therefore to address all side impact types and speeds in future designs and safety regulations.

The in-depth study findings reported by Fildes et al. (1994) showed that the frequency and rate of head injury was greater in far side than near side impacts with fewer chest and abdominal injuries. The head injuries resulted from contact with the far side door, the impacting vehicle or object or other occupants. Dalmotas (1983) reported earlier on injury mechanisms for occupants in real world crashes restrained in 3-point seat belts in side impacts in Canada. While they noted different mechanisms for near and far side occupants, they claimed that both would benefit from improvements in side door integrity and interior padding.

Kallieris and Schmidt (1990) conducted simulated far side impacts using cadavers seated in the rear seat with inboard-anchored shoulder belts. They reported no head injuries for far side occupants with these belt configurations compared with those of near side occupants and lower angular head/neck velocities and accelerations. However, most of the PMHS showed AIS1 injuries to the neck, which in the light of recent whiplash research corresponds to a high probability of disabling injury outcome (i.e. hemorrhages in the inter-vertebral discs).

There has been extensive work completed on near side impacts to define injury tolerance and biofidelity requirements (Cavanaugh Walilko, Malhotra, Zhu and King (1990a,b); and Pintar et al., 1997). In recent work, Pintar and his colleagues conducted 26-side impact sled tests with PMHS impacting a sidewall with a range of different surface conditions. They investigated a number of biomechanical responses and injury tolerances from these tests for occupants involved in near side crashes. Because injury criteria and biofidelity requirements for near side occupants are dependent on a direct impact to one whole side of the body, these results are not directly applicable to far side crashes. Additional far side impact tests are critical for understanding occupant kinematics, forces and accelerations for occupants involved in these kinds of real world crashes. Stolinski, Grzebieta and Fildes (1999) undertook a series of crash tests in Australia focussing on near and far side occupant outcomes. From far side HIII and US-SID full-scale crashes, they showed that deploying belt pretensioners could significantly reduce lateral excursion of the far side occupant and reduce lap belt loads. However, there is reason to question whether current side impact test dummies, designed for near side impacts can accurately reflect far side kinematics and injuries.

Previous far side research undertaken in Australia (Fildes, Sparke, et al 2002) identified a number of strengths and weaknesses with existing side impact test dummies for far side occupant protection. They concluded there was scope for improving dummy design in far side crash testing, and that a comprehensive research program into far side crashes, occupant injuries and countermeasures was warranted to address this severe trauma.

### THE RESEARCH PROGRAM

To address these concerns, an international collaborative research program into increased protection for far side occupants in a crash was developed and commissioned at the start of 2004. The research involves a consortium of universities, auto manufacturers, and part suppliers as shown in Table 1.

The study was funded through a number of contributions from government and industry sponsors, comprising the Australian Research Council in Australia, Ford USA through GWU, Holden Australia, and Autoliv in Sweden. Considerable in-kind contributions were also provided from these sponsors as well as all the participants.

**Table 1: Consortium Members**

Institution	Participants
Monash University Accident Research Centre, Australia	B.Fildes, A. Linder, C.Douglas
George Washington University (NCAC), Virginia	K.Digges, R. Morgan, B. Alonso
Virginia Tech (CIB)	S. Duma, E. Kennedy, J. Stitzel
Virginia Tech (Mech. Eng.)	H.C. Gabler
Medical College of Wisconsin, Wisconsin.	F. Pintar, N. Yoganandan, B. Stemper
William Lehman Trauma Center, Miami	J. Augenstein
Wayne State University, Detroit	King Yang
Holden Australia	L. Sparke, S. Smith
Dept. Transport & Regional Services, Australia	C. Newland
Human Impact Engineering Sydney, Australia	T. Gibson
Autoliv AB	O. Bostrom, R. Judd
Ford USA	S. Rouhana

### Research Objectives

There were three objectives associated with this research program:

- To obtain a more detailed understanding of far side crashes, injuries and injury mechanisms;
- To develop suitable test procedures and injury criteria; and
- The identification of a range of generic far side injury countermeasures to address this trauma.

In addressing far side occupant injuries, it was obvious from previous testing that the appropriate strategy would be to attempt to restrain the occupant in the seat to prevent contact with the struck side of the vehicle. Current restraint designs fail as the sash portion of the 3-point belt offers little restraint to movement away from the D-ring in a side impact. Fildes et al (2003) showed that a supplementary belt on the inside while offering a degree of restraint in this direction, also posed a potential problem of neck loading from the belt and potential problems for the carotid artery. Hence, there was also a need to examine this issue during the research program.

### RESEARCH DESIGN

Seven research tasks were prescribed to address these objectives.

- Task 1- to obtain a more detailed understanding of far-side injuries and Harm in real-world crashes
- Task 2 - to undertake a comprehensive laboratory biomechanical test program using PMHS (cadavers) specimens
- Task 3 – to identify injury criteria and risk functions for neck injury
- Task 4 – to develop a suitable crash test program and suitable injury criteria
- Task 5 – to revisit the suitability of current side impact test dummies in this crash mode;
- Task 6 – to develop suitable computer models for generating far side occupant kinematics and injury parameters; and
- Task 7 – to identify a range of generic countermeasure options for mitigating injuries and Harm.

Research participants were assigned to each task and a work task leader took responsibility for overseeing the research, achieving the prescribed deliverables and outcomes and reporting on progress and any problems encountered. Each of the work tasks is described in more detail below.

### **Task 1 – Problem Identification**

Two sub-tasks were identified for this research.

Initially, an examination was to be conducted from in-depth data in the USA and Australia of the level of Harm to far side occupants in side impact crashes by body region, injury source, crash direction, crash severity, intrusion extent, crash partner, occupant characteristics, and injury lesions. This would be used to focus the research program on major injury and Harm issues, as well as gaining a more detailed understanding of these crashes for addressing countermeasure strategies.

Towards the conclusion of the program, additional Harm analyses would be conducted to illustrate the potential Harm benefits of generic counter-measure strategies to reduce far side injuries.

### **Task 2 - Biomechanical Test Program**

The biomechanical test program is designed to provide a range of human-like kinematics and injury responses under controlled conditions to use for comparing with test dummy responses as well as in developing computer models to simulate occupants in far side crashes. The priority crash types, impact speeds and restraint conditions identified in Task 1 would form the basis for conducting these tests.

Pre-modeling of dummy/cadaver performance using existing computer models of side impact

dummies was to be undertaken prior to these tests to minimize any potential problems or difficulties and ensure a satisfactory outcome

Follow-up PMHS tests at the conclusion of the research may be required as final validation of the countermeasure strategies.

### **Task 3 - Soft Tissue Injury of the Neck**

This task has a number of sub-tasks associated with it. At the outset, a literature review will help identify current knowledge and best practice in neck injury causation and computer modeling with particular attention to carotid arteries.

Following this, a series of tests of neck soft tissue injuries will be conducted to determine constitutive properties and failure conditions. With the assistance of specimen testing to be conducted at MCW, a computer model of the carotid artery will then be developed and validated against biomechanical test data and if possible, real world crash data.

Finally, the model will be exercised to determine injury criteria, injury risk functions, and propose surrogate injury measurements for use on dummy outcomes to gauge the potential for serious neck injuries associated with any restraint solutions.

### **Task 4 - Test and Injury Criteria**

As there are no agreed far side test or injury criteria, the fourth task is aimed at addressing these issues (Gibson et al, 2001).

Through a review of existing literature and the injury and Harm analysis in Task 1, preliminary test criteria will be specified for improved far side impact protection. In addition, acceptable injury criteria for use in far side testing will be arrived at predominantly from current biomechanical tolerance knowledge and additional analyses of existing biomechanical test data where available.

Throughout the research program, these will continue to be evaluated for their suitability for providing adequate protection for these occupants and if required modified in the light of more recent evidence. The findings at the end of the research program will be provided to auto manufacturers and governments around the world to encourage them to give greater attention to preventing these injuries.

### **Task 5 - Far Side Test Dummies**

Previous work by Fildes, Sparke, Bostrom, Pintar, Yoganandan and Morris (2002) and Bostrom and Haland (2002) showed that existing side impact test dummies did not produce accurate occupant kinematics in a far side test. While a modified

BioSID fitted with a new design spring spine was found to be an improvement, it was solely a research instrument and had no role to play in regulation. Furthermore, the WorldSID test dummy included in this test program failed because of a problem between the dummy and the restraint.

The WorldSID appeared to have the potential for simulating far side occupant movements in a far side crash because it contains a more human-like spine. It has been developed by an ISO WorldSID Task Group in anticipation that it may be the appropriate test device for use as a side impact regulation. Hence, further testing of this dummy (now modified to overcome the restraint problem) would be undertaken in this research program.

From these tests, it should be possible to determine its suitability and the need for any modifications in this crash mode. It is planned to conduct a series of tests to validate the dummy responses against cadaver and injury outcomes (5 or 6 restraint combinations expected) and identify areas requiring further attention.

If found to be suitable, WorldSID will be used to conduct any additional tests required for far side model development and countermeasure evaluation.

#### **Task 6 - Computer Model Development**

Biomechanical and physical tests are limited by the time required to conduct these and their associated costs. Given recent developments in sophisticated computer models of occupants, the next task will be to develop such a human model for use in this test program and beyond.

The model will be developed from the biomechanical and test data collected during the program as well as in consultation with model developers around the world. A PhD scholarship has been provided by the Australian Research Council for a student to develop such a model at Monash University as part of his or her research study program.

The model development program will contain a number of associated activities. Initially, existing models of vehicles and dummies will be used to study intrusion, crash pulse, and kinematics in far side crashes. Subsequently, an improved human model will be developed using FEM technology and validated against test and real-world crash data.

It is expected that the model will be useful for examining a range of different crash types, impact angles and crash severities and also hopefully for different sexes and sizes of occupants in single and two-occupant interactions. The model will also

eventually be used to predict injury reduction of generic countermeasures in real world crashes for Harm benefits analysis.

#### **Task 7 - Countermeasure Development**

The final work task in this study is aimed at providing a range of suitable in-vehicle solutions and strategies to improve protection for far side occupants in a side impact crash. Generic in-vehicle countermeasures will be identified, tested and evaluated for their likely benefits and any associated disbenefits. It is expected that a range of potential generic far side protection strategies and countermeasures will be identified to encourage manufacturers to include these in future car models.

The countermeasures will be subject to rigorous testing both with the computer and physical models to illustrate their effects. These will be in terms of their likely kinematics and injury assessment benefits. In addition, Harm analyses will also be conducted to demonstrate potential benefits and costs for implementing fleet-wide. Optimum solutions and/or countermeasure packages will also be identified to help guide manufacturers and regulators in future initiatives.

#### **EXPECTED PRODUCTS**

The sponsors require that the outcomes of the research be made freely available for all to use as required. Hence, a number of products (deliverables) are expected from this research activity, as listed below.

- A paper on the frequency and severity of casualties in far and nearside crashes for restrained occupants in both the USA and Australia is to be presented at the ESV 2005 international conference.
- The results of the comprehensive test program using PMHS will be available on request to technicians for use in helping to further far side occupant protection.
- The identification of a suitable far side test dummy with appropriate kinematics, and injury response is expected for the far side environment (Max Harm and 75% of MAIS 3+ Injuries).
- Suitable injury criteria and injury risk functions for soft tissue neck injury will be published and a recommended test program and injury criteria will be available for use by governments and industry engineers.

- An FEM human computer model will be developed and validated for use in countermeasure determination and evaluation.
- Generic countermeasure strategies will be established to reduce head, neck, chest, abdomen and pelvic injuries in these crashes
- Harm benefits analysis of alternative generic countermeasures will be conducted.

## RESEARCH TIMETABLE

A preliminary timetable for the research was established at the commencement of the research program, as detailed below.

Year 1 – To conduct various reviews, undertaken data analyses and priorities, and commence biomechanical testing.

Year 2 – To continue the laboratory test program, initiate dummy development and test procedures, and establish first estimates of injury criteria and assessment functions.

Year 3 – To commence computer modelling of various crash configurations and develop generic countermeasures to address these.

Year 4 – To conduct benefit-cost analyses of countermeasure options, complete final validation testing of these and write reports and papers.

## PROGRESS SO FAR

Good progress has been made during the first year of the program. A Harm analysis of NASS crashes in the US and similar crash data at MUARC in Australia has been carried out revealing some interesting and unexpected results. A paper on these findings and areas of similarity and difference between these two data sets is to be presented in the side impact session of this conference. These findings are useful in helping to identify priority crash and occupant issues for research to follow.

Details for the biomechanical test program have been worked through following the Harm analysis. Focus for the PMHS testing will be on relevant injuries and seat areas most likely to be amenable to intervention in the conduct of this research. Testing facilities have been agreed upon and developed and it is expected that testing will commence at the Medical College of Wisconsin early in 2005.

A comprehensive literature review of neck trauma, especially that involving the carotid artery, and suitable modelling techniques has been conducted and will be ready for publication soon. In addition, researchers at Virginia Tech's Center for Injury Biomechanics have commenced modelling these

injuries using biomechanical results from sub-system tests. Early results appear promising and subsequent research is focussed on improving these models for later inclusion into the far side occupant protection program.

Research at George Washington University has focussed initially on pre-modelling of occupant kinematics in a far side crash using a range of existing dummy models to provide guidance for the biomechanical test program. In addition, a literature review of injury assessment functions and other relevant data is currently underway to help address the issue of suitable injury and test criteria for improved protection of far side occupants.

Efforts are also underway to construct comparative tests of side impact dummies to show whether any of the existing side impact test dummies are capable of simulating real world occupant kinematics and injuries in a far side crash configuration.

A student has been recruited into a PhD research program at MUARC in Australia to help develop a suitable far side human model. Four working group meetings were held during 2004 and the early part of 2005 to review research efforts and prescribe directions for future research. In addition, briefing sessions and early finding from this research have been presented to the IHRA Side Impact committee for feeding into their research program as well. The enthusiasm and support among the researchers involved in this program is especially noteworthy and there is high expectation that the outcomes and deliverables specified for the research will be achieved, leading to significant improvement in far side occupant protection in the years ahead.

## CONCLUSIONS

The research commenced in January 2004 and a number of key research components are already well underway. Preliminary findings in the area of priority crash configurations, injuries and injury mechanisms have already been identified.

It is expected that through a comprehensive test schedule, this research will lead to a better understanding of occupant biomechanics and injury mechanisms during far-side collisions. Current dummy bio-fidelity can then be assessed and improved, appropriate far-side test measures developed, and recommendation for regulations made. It is anticipated that application of these test procedures will allow the development of innovative and world-leading far-side countermeasures that will ultimately improve vehicle occupant safety.

## Acknowledgement

The funding for this research has been provided by private parties. Dr. Kennerly Digges and the FHWA/NHTSA National Crash Analysis Center at the George Washington University has been selected to be an independent solicitor of and funder for research in motor vehicle safety, and to be one of the peer reviewers for the research projects and reports. The Australian Research Council awarded Grant No. LP0454122 to Professor Brian Fildes at the Monash University Accident Research Centre. Neither of the private parties have determined the allocation of funds or had any influence on the content of this report.

## REFERENCES

- Bostrom O, Fildes B, Morris A, Sparke L, Smith S, & Judd R. (2003). A cost effective far side crash simulation” *International J. Crashworthiness*, 8 (3).
- Bostrom O. & Haland I. (2003). Benefits of a 3+2 point belt and an inboard torso side support in frontal, far-side and rollover crashes, Paper 451, Proceedings of the 18<sup>th</sup> ESV Conference, Nagoya, Japan, NHTSA, Washington DC.
- Cavanaugh JM, Walilko TJ, Malhotra A, Khu Y and King AI (1990a). Biomechanical response and injury tolerance of the pelvis in twelve sled side impacts, SAE Paper No. 9020305.
- Cavanaugh JM, Walilko TJ, Malhotra A, Khu Y and King AI (1990b). Biomechanical response and injury tolerance of the thorax in twelve sled side impacts, SAE Paper No. 9020307.
- Dalmotas D. (1983). Injury mechanisms to occupants restrained by three-point seat belts in side impacts, Pepr 830462, SAE Technical Paper Series, International Congress & Exposition, Detroit, Michigan.
- Digges K & Dalmotas D. (2001). Injuries to restrained occupants in far-side crashes, Proceedings of the 17<sup>th</sup> ESV Conference, Amsterdam June 2001, National Highway Traffic Safety Administration, Washington DC.
- Fildes B., Lane J., Lenard J. & Vulcan, A.P., (1994), Passenger cars and occupant safety: side impact crashes. Report CR134, Australian Transport Safety Bureau (formerly the Federal Office of Road Safety), Canberra, Australia.
- Fildes B., Sparke L., Bostrom O., Pintar F., Yoganandan N. & Morris A. (2002). Suitability of current side impact test dummies in far-side impacts, Proceedings of the 2002 International IRCOBI Conference on the Biomechanics of Impact, Munich, Germany, September 2002.
- Fildes B.N., Gabler H.C., Fitzharris M. & Morris A.P. (2000). Determining Side Impact Priorities Using Real-World Crash Data and Harm, Proceedings of the 2000 International IRCOBI Conference on the Biomechanics of Impact, Mont Pellaire, France, September 2000.
- Fildes B, Bostrom O, Haland Y & Sparke L. (2003). Countermeasures to address far side crashes: first results, Paper No. 447, Proceedings of the 18<sup>th</sup> ESV Conference, Nagoya, Japan, NHTSA, Washington DC
- Frampton R.J., Brown R., Thomas P. & Fay P. (1998). The importance of non struck side occupants in side collisions, Proceedings from the 42<sup>nd</sup> Annual Conference of the Association for the Advancement of Automotive Medicine, Charlottesville, Virginia.
- Gabler H.C., Fildes B.N. & Fitzharris M. (2000). Improved side impact protection: a search for systems modelling priorities, Proceedings of DETR 2000 – ASME 2000 Design Engineering Technical Conferences on Computers and Information in Engineering Conference Baltimore, Maryland, USA P109.
- Gibson, T., Fildes, B.N., Deery, H., Sparke L.J., Benetatos E., Fitzharris M., McLean J. & Vulcan AP. (2001). Improved side impact protection: a review of injury patterns, injury tolerance and dummy measurement capabilities, Report No. 147, Monash University Accident Research Centre, Clayton, Victoria, Australia.
- Kallieris D. & Schmidt G. (1990). Neck response and injury assessment using cadavers and the US-SID for far-side lateral impacts of rear seat occupants with inboard-anchored shoulder belts, Proceedings of the 34<sup>th</sup> STAPP Car Crash Conference, Orlando, Florida, November 1990.
- Pintar F.A., Yoganandan N., Hines M.H., Maltese M.R., McFadden J., Saul R., Eppinger R., Khaewpong N., Kleinberger M. ““hestband analysis of human tolerance to side impact”” 41<sup>st</sup> Stapp Car Conference Proceedings, p63-74, November 1997.
- Stolinski R., Grzebieta R., Fildes B. et al “Response of far side occupants in car-to-car impacts with standard and modified restraint systems using HIII and US SID”, SAE paper 1999-01-1321, 1999.

# **FAR SIDE IMPACT INJURY RISK FOR BELTED OCCUPANTS IN AUSTRALIA AND THE UNITED STATES**

**Hampton C. Gabler**

Virginia Tech  
United States

**Michael Fitzharris**

**James Scully**

**Brian N. Fildes**

Monash University Accident Research Centre  
Australia

**Kennerly Digges**

George Washington University  
United States

**Laurie Sparke**

Holden Innovation  
Australia

Paper No: 05-0420

## **ABSTRACT**

This paper evaluates the risk of side crash injury for far side occupants in Australia and the United States. The study was based on the analysis of Australian data drawn from the Monash University Accident Research Center (MUARC) In-depth Data System (MIDS) and U.S. data extracted from the National Automotive Sampling System / Crashworthiness Data System (NASS/CDS). Over 100 cases of Australian far side struck occupants were examined from the MIDS database, and over 4500 cases of U.S. far side struck occupants were investigated from NASS/CDS 1993 - 2002. For both data sets, the analysis was restricted to three-point belted occupants of cars, light trucks, and vans. The paper evaluates the risk of far side impact injury as a function of struck body type, collision partner, delta-V, crash direction (PDOF), occupant compartment intrusion, and injury contact source. Injury risk is evaluated using the maximum injury severity for each occupant, by injury severity for each body region, and by Harm, a social cost measure. The goal of this study was to develop priorities for developing far side impact injury countermeasures which would be effective in both countries.

## **INTRODUCTION**

The primary objective of both side impact research and side impact regulation to date has been to protect occupants located on the struck side of a passenger vehicle. However, occupants of the non-struck, or far

side, of the vehicle are also at risk of injury (Digges and Dalmotas, 2001). The mechanism of far side impact injury is believed to be quite different than that for near side impact injury. Far side impact protection may require the development of different countermeasures than those which are effective for near side impact protection.

In early 2004, an international consortium of universities and crashworthiness research groups, led by the Monash University Accident Research Centre (MUARC), began to examine the problem of far side impact injury risk (Fildes et al, 2005). The goal of this research program is to investigate far side impact injury to occupants of passenger cars, light trucks and vans. The specific objectives of the project are to establish an improved understanding of the biomechanics of far side impact injury, develop a test procedure for evaluating the potential of injury in a far side impact, and explore new countermeasure approaches for far side impact injury prevention. This paper presents some of the first findings of this project.

## **OBJECTIVE**

The goal of this study is to determine the risk of injury from far side impact crashes in Australia and the United States. The specific objectives are to determine the priorities for injury countermeasure development, and to characterize those impact conditions which lead to far side impact injury as a

first step toward the development of a far side impact test procedure.

## APPROACH

The analysis presented in this paper was based on the examination of Australian data drawn from the MUARC In-depth Data System (MIDS) and U.S. data extracted from the National Automotive Sampling System / Crashworthiness Data System (NASS/CDS) files from 1993 - 2002.

## DATA SOURCES

The MUARC In-depth Data System (MIDS) is comprised of in-depth accident investigation data from four crashed vehicle studies conducted by the MUARC: the Crashed Vehicle File (CVF) collected from 1989 – 1993; the study funded by FORS (now the Australian Transport Safety Bureau, ATSB) to evaluate ADR69 and conducted from 1995 – 2000, the Holden Crash Investigation project (1993 onwards) and the current Australian National Crash In-Depth Study (ANCIS)<sup>1</sup> from 2000 onwards.

The MIDS database contains weights which, when applied to individual cases, permitted national estimates of traffic crash injury in Australia. The MIDS weighting system uses key crash parameters that when used in combination result in 4032 possible covariate patterns, in order to adequately capture crash and injury characteristics. Principal variables for the weighting system are: Year of vehicle manufacture (pre/post-1990); Impact direction (e.g., front, left, or right side of vehicle); Seating position of occupant; Single vehicle crash or multiple vehicle crash; Speed zone (categories:  $\leq 60$ , 70-90, 100+ km/h); Head injury AIS  $\geq 3$ ; Chest or Abdominal injury AIS  $\geq 3$ ; Lower extremity AIS  $\geq 3$ . The year of manufacture is included as advances in vehicle safety have progressed rapidly, and, while crude, serves as a reasonable cut-point as the Australian fleet is on average 10 -12 years of age. The expected number of crashes in each of the 4032 covariate patterns was

---

<sup>1</sup> The ANCIS partners include the Federal Department of Transport and Regional Services; Autoliv Australia; Ford Motor Company Australia Ltd.; Holden Ltd.; Mitsubishi Motors Australia Ltd.; Motor Accidents Authority of New South Wales; National Roads and Motorists' Association, Royal Automobile Club of Victoria Ltd.; Roads & Traffic Authority (New South Wales); Transport Accident Commission (Victoria); Toyota Motor Corporation; and VicRoads. The Federal Chamber of Automotive Industries and the Australian Automobile Association (AAA) are included as Observers.

calculated for all fatality crashes in Australia and Victorian crash statistics for a three year period (1999-2001) with Victorian crashes adjusted and multiplied to approximate and equal, respectively, the Australian serious, minor and non-injury crashes. Weights were determined by expressing expected number of occupants per covariate pattern divided by the number of matching occupants in the MIDS. Analysis was conducted with and without weights applied.

NASS/CDS is a sample of 4,000 to 5,000 crashes investigated each year by the U.S. National Highway Traffic Safety Administration (NHTSA) at up to 27 locations throughout the United States. For a crash to be included in NASS/CDS, at least one of the vehicles in the accident had to be towed from the scene. Each case in NASS/CDS has corresponding weights which allow for computation of national estimates of traffic crash injury outcome.

## FAR SIDE IMPACT DATA SET

The analysis which follows focuses exclusively on occupants of passenger vehicles subjected to far side impact. The analysis was limited to passenger cars, light trucks, and vans subjected to a side impact. For this study, side impact was defined to be a crash in which the general area of damage in the most harmful event was to the left or right side of the car. Any cases in which the vehicle rolled over were excluded.

A far side occupant was defined to be either an outboard occupant on the opposite side of a crash or a center seated occupant. For impacts to the driver side of the car, for example, a front seat passenger would be considered to be on the far side of the car. Likewise, for impacts to the front passenger side of the car, the driver would be considered to be the far side occupant. Only occupants that were restrained by a three-point safety belt were included in the study.

As shown in Table 1 and Table 2, these selection criteria resulted in a final sample of 107 Australian cases and 4,518 U.S. cases of far side struck occupants. 10 of the Australian cases and 281 of the U.S. cases were seriously injured occupants. Seriously injured occupants were defined to be occupants with a maximum injury severity of AIS 3 or greater. Both files contained a small number of fatally-injured occupants which were included in the Harm calculation but not analyzed separately. In addition to the unweighted number of cases, these tables also present weighted counts of the number of occupants in each injury severity category. The

weighted numbers were developed using the multipliers included in both MIDS and NASS to permit national estimates of injury in their corresponding countries. All analyses which follow were performed with weighed accident data.

**Table 1. Number of Australian Belted Far Side Struck Occupants – MIDS**

	Weighted	Unweighted
Occupants	5,894	107
Seriously Injured Occupants (AIS3+)	39	10
Fatalities	4	1

**Table 2. Number of U.S. Belted Far Side Struck Occupants – NASS/CDS 1993-2002**

	Weighted	Unweighted
Occupants	2,386,633	4,518
Seriously Injured Occupants	21,982	281
Fatalities	5,175	80

One analytical challenge of this study was how to combine the Australian and U.S. data. The U.S. far side impact data set is many times larger than the corresponding Australian data set. Our approach was to use the Australian and U.S. data to compare and contrast the higher level characteristics of the far side impact problem, e.g. body region priorities for injury reduction. The larger U.S. data set was then used to determine the detailed injury mechanisms of far side impact injury. At the time of this paper, the number of cases from the MIDS database was too small to perform a similar analysis with Australian data alone.

#### MEASURING SOCIAL COST WITH HARM

Our study used the Harm metric to measure the social cost of traffic accidents. The Harm metric was first developed by Malliaris et al (1982) as a means of balancing number of injuries with the severity or cost of an injury. Using the Malliaris Harm metric, each AIS level has a prescribed social cost. This social cost includes both medical costs and indirect costs such as loss of wages. For each injured person, the Harm is the social cost which corresponds to their maximum AIS injury level.

This original Harm metric was a remarkable new method of injury assessment, but had two weaknesses. First, social cost is not a function exclusively of AIS level. The social cost of injury varies by body region as well as by injury severity. For example, an AIS 3 head injury has a higher social cost than an AIS 3 leg injury. Second, the original Harm metric assigned a cost to only the injury of highest severity. This approach can underestimate the total social cost of a person who suffers multiple injuries as multiple injuries can aggravate the total threat to a crash victim's life.

Fildes et al (1994) developed an improved Harm metric which addressed these two issues. The improved method assigns a social cost to each injury, and sums these costs to estimate a total social cost of injury. In this study, Cost<sub>i</sub>, the social cost of an injury *i* as defined by Fildes et al (1994) was used as a measure of social cost. Cost<sub>i</sub> is a function of the injury severity as measured by the AIS scale, and the body region which has been injured. The cost components include not only treatment and rehabilitation costs but also all other costs to society such as loss or wages and productivity, medical and emergency service infrastructure costs, legal and insurance costs, legal and insurance charges, family and associated losses and allowances for pain and suffering.

Our study uses a variation of the Fildes method for computation of Harm. In some cases, there may be multiple injuries to a single body region. In our methodology, the maximum injury to a single body region is used when assigning costs as costs are typically assigned to treat a single body region not individual injuries of that body region. The costs proposed by Fildes et al (1994) were normalized to cost of a fatality and are presented in Table 3.

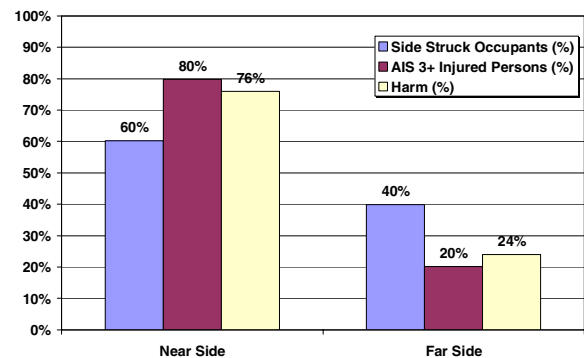
#### COMPARISON OF AUSTRALIAN AND U.S. FAR SIDE CRASHES

The traffic safety environments in Australia and the United States share many common vehicle types and similar safety regulations, but also differ in several important aspects. Differences in fleet composition, driver seating position, and rural-to-urban driving mix may have an influence on the priorities for countermeasure development. Our initial step in the analysis was to compare and contrast the risk of far side impact injury in Australia and the United States.

**Table 3. Average Cost per Injury (Normalized to the Cost of a Fatal Injury)**

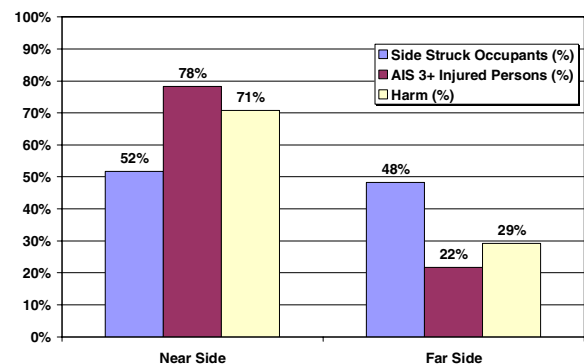
BODY REGION	INJURY SEVERITY						
	Minor (AIS = 1)	Moderate (AIS = 2)	Serious (AIS = 3)	Severe (AIS = 4)	Critical (AIS = 5)	Maximum (AIS = 6)	Unknown
External	0.0045	0.0250	0.0698	0.1135	0.1646	1.0000	0.0045
Head	0.0063	0.0295	0.1213	0.2796	0.9877	1.0000	0.0045
Face	0.0063	0.0295	0.1213	0.1601	0.3277	1.0000	0.0045
Neck	0.0063	0.0295	0.1213	0.1601	0.3277	1.0000	0.0045
Chest	0.0045	0.0250	0.0698	0.1135	0.1646	1.0000	0.0045
Abdomen	0.0045	0.0250	0.0698	0.1135	0.1646	1.0000	0.0045
Pelvis	0.0045	0.0250	0.0698	0.1135	0.1646	1.0000	0.0045
Spine	0.0045	0.0250	0.1631	1.4054	1.6804	1.0000	0.0045
Upper Extremity	0.0063	0.0433	0.1026				0.0045
Lower Extremity	0.0045	0.0433	0.1303	0.1926	0.3277		0.0045

Figure 1 and Figure 2 present the relative injury risk of near and far side impact for Australia and the U.S. As illustrated in Figure 2, a side struck occupant in the U.S. has a nearly equal probability of being seated on the near or far side of the vehicle. Approximately half of the side struck occupants were on the near side, and half were on the far side. In Australia, however, the MIDS database predicts a very different distribution. 60% of side struck occupants were on the near side of the car and the remaining fraction were on the far side of the car.



**Figure 1. Distribution of Australian Near vs. Far Side Impact Injuries for 3-Pt Restrained Occupants**

On the other hand, the ratio of near side to far side occupant injuries was very similar in both countries. Both the Australian and the U.S. accident data show that near side impact carries a significantly higher injury risk. Near side crashes accounted for approximately 80% of the seriously injured side struck persons in Australia and 78% in the U.S. Near side struck occupants incurred 76% of the side impact Harm in Australia, and 71% of the side impact Harm in the U.S.



**Figure 2. Comparison of U.S. Near and Far Side Impact Injuries for 3-Pt Restrained Occupants**

Far side struck occupants have a significant risk of injury in both Australia and the United States. As a fraction of all occupants who experienced a side impact, far side struck occupants accounted for approximately 20% of the seriously injured persons and 24-29% of the Harm.

As seen in Figure 3, the distribution of far side impact injury by body region is very similar in both Australia and the U.S. Head injuries accounted for approximately one-fourth of all Harm, the largest fraction of total Harm. The largest differences in injury outcome were for the chest and the spine. The chest incurred 13% of all Harm in the U.S. and only 7% of all Harm in Australia. Spine injuries accounted for 15% of all Harm in Australia, but only 10% of Harm in the U.S. Protection of the head, chest, and spine are priorities for countermeasure development. These three body regions accounted for approximately half of all the Harm attributed to far side impact in both countries.

Injuries to the upper and lower extremities combined for approximately 40% of the far side impact Harm in both countries – a surprisingly large fraction. These injuries may be due to the flailing motion of the limbs as the occupant is thrown across the car in a far side impact. One difference between NASS and MIDS should be noted here: in the MIDS database pelvic injuries were grouped with the abdominal injuries while in NASS/CDS pelvic injuries were grouped with lower extremity injuries.

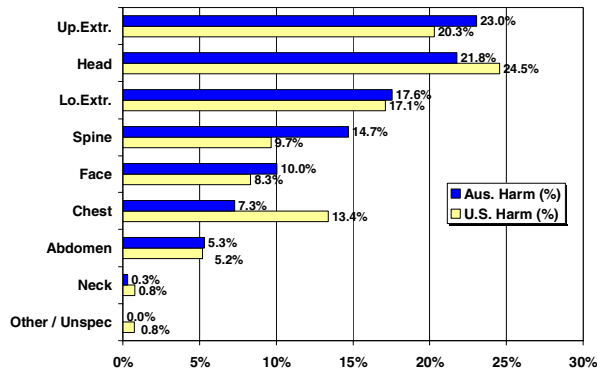


**Figure 3. Distribution of Far Side Impact Harm by Body Region – Australia vs. United States**

In both Australia and the U.S. the distribution of Harm by seating location was very similar. As shown in Figure 4 and Figure 5, in both Australia and the U.S. drivers composed just under three-fourths of the far side struck occupants and incurred just over three-fourths of the Harm. Front passengers accounted for approximately 20% of the far side struck occupants, and 14-20% of the Harm. Rear passengers comprised only 7% of the total far side struck occupants and only 3-6% of the Harm. A test procedure which focuses on the front seat occupants would capture over 90% of the Harm.

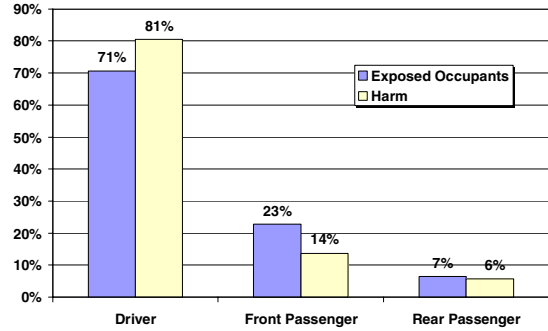


**Figure 4. Australian Far Side Injuries to Belted Occupants by Seating Position**

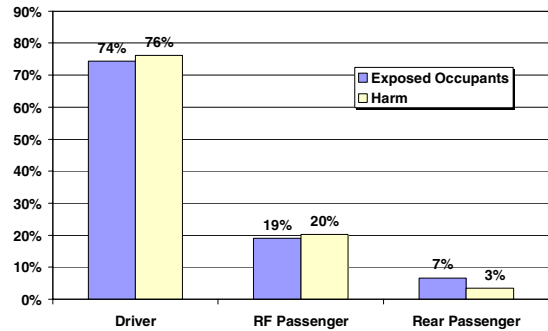


**Figure 5. U.S. Far Side Injuries to Belted Occupants by Seating Position**

The composition of the Australian and U.S. passenger vehicle fleets are very different. The Australian fleet is primarily composed on passenger cars. The U.S. fleet is characterized by a growing segment of light trucks and vans (LTVs) now estimated to account for 40% of registered light vehicles and 50% of all light vehicle sales in the U.S. The LTV category includes pickup trucks, sport utility vehicles, vans, and minivans.

Reflecting this fleet composition, the Australian dataset contained only passenger car data. The U.S. dataset however contained cases of both car and LTV occupants involved in far side impact. Figure 6 presents the distribution of injuries by struck body type in the U.S. Approximately three-fourths (76%) of the side struck occupants in the U.S. were drivers or passengers of a car. The remaining persons were occupants of an LTV. A far side impact is much more dangerous for a car occupant than for the occupant of a light truck or van (LTV). Although car occupants accounted for 76% of side struck persons in the U.S., car occupants accounted for 83% of the seriously injured persons and 84% of the Harm.

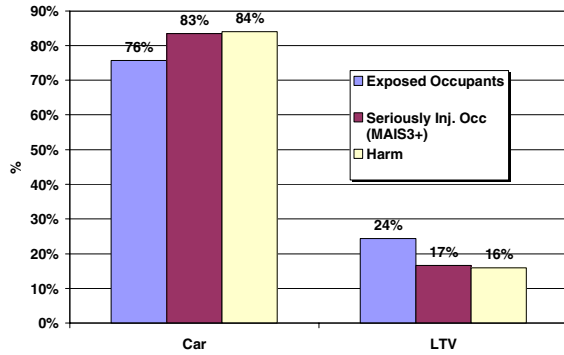


**Figure 6. U.S. Far Side Impact Injuries by Body Type of Struck Vehicle**

Finding that a substantial proportion of the far side harm in the U.S. is incurred by LTV occupants, we next examined whether car and LTV occupants might require different injury countermeasures. As seen in Figure 7, the Harm distributions for car and LTV occupants are not identical. Nevertheless, the head, chest, and spine are still the most urgent targets for Harm reduction. For both car and LTV occupants, the largest contributor to Harm was head injuries. Chest injuries resulted in much more Harm for car occupants (14%) than for LTV occupants (10%). In contrast, upper and lower extremity injuries were somewhat more important for LTV occupants than for car occupants. Injuries to the arms and legs accounted for 44% of LTV occupant Harm, but only 36% of car occupant Harm.

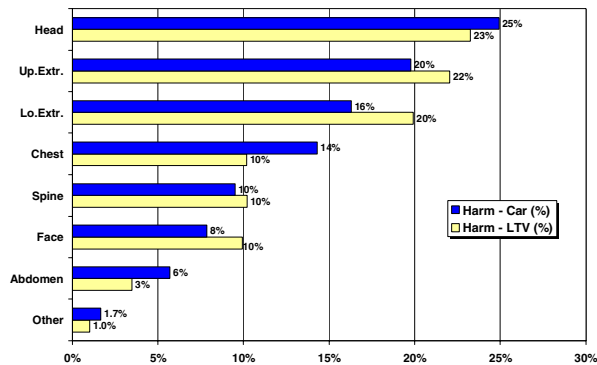


**Figure 7. Distribution of Serious Injuries by Type of Struck Vehicle Type and Body Region Injured in the U.S.**

The distribution of Australian and U.S. far side injuries by striking vehicle were next evaluated to determine the influence of differing fleet composition. As shown in Table 4, however there were too few cases in the Australian data to disaggregate the data to this level. This table does however show that the primary striking vehicle was a

passenger car or a passenger car-derivative denoted as Ute below.

**Table 4. Number of Australian Belted Far Side Struck Occupants – MIDS**

Striking Vehicle or Object	Weighted		Unweighted	
	Occupants	AIS3+	Occupants	AIS3+
Car / UTE	3,892	28	63	5
4WD	264	-	5	
Van	91	-	3	
Hvy Truck / Bus	169	-	4	
Other Vehicle	1,063	-	6	
Pole	139	2	11	2
Tree	251	9	14	3
Other Object	26	-	1	
<b>Total</b>	<b>5,894</b>	<b>39</b>	<b>107</b>	<b>10</b>

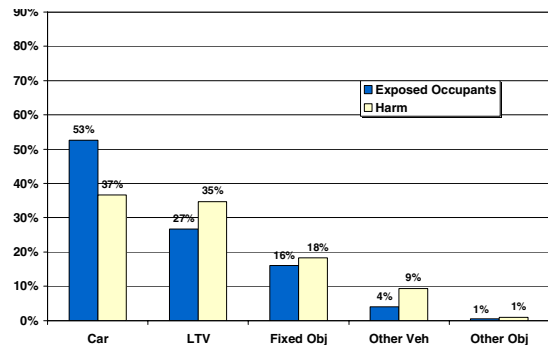


**Figure 8. Distribution of Far Side Injuries by Striking Vehicle Type in U.S.**

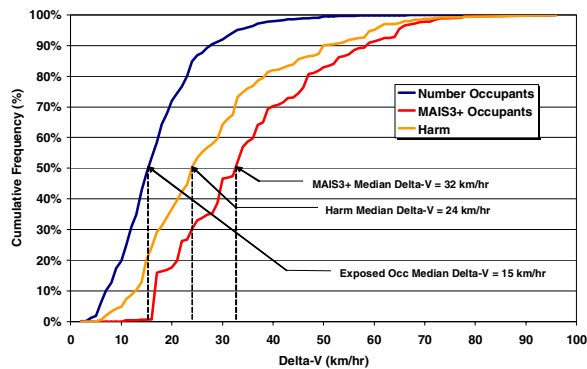
The analysis presented in Figure 8 depicts the distribution of far side injuries as a function of the striking vehicle type in the U.S. Several studies have showed that light trucks and vans are incompatible with cars in traffic collisions [Summers et al, 2001; Gabler and Hollowell, 1998; IIHS, 1998]. The incompatibility is particularly an issue when the striking vehicle is an LTV and the struck vehicle is a passenger car. This observation is confirmed in Figure 8. The striking vehicle for over half of the side struck occupants was a passenger car, yet this collision partner accounted for only 37% of the Harm. In contrast, 27% of the occupants were struck by an LTV, but these collisions resulted in 35% of the Harm. Particularly dangerous, but fortunately

rare, were collisions with ‘Other’ vehicles – a category which includes heavy trucks, buses, and motorcycles. Collisions with fixed objects, e.g. trees and poles, accounted for 16% of the side struck occupants and 18% of the Harm.

## IMPACT CONFIGURATION

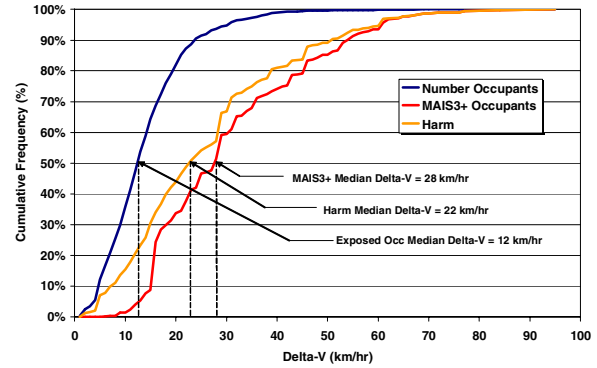
Impact speed, impact angle, and impact location are important parameters which must be identified in order to design a test procedure to evaluate far side impact injuries. This section provides an analysis of the accident data which investigates the impact configuration of a far side crash. Because of the small number of Australian cases, the analysis which follows is based exclusively upon U.S. accident data.

Figure 9 presents the distribution of far side injuries by total delta-V of the struck vehicle. Total delta-V is the resultant change in velocity, and includes both the lateral and longitudinal components of delta-V. The median total delta-V for all far side struck occupants was 15 km/hr. Half of the Harm occurred for total delta-V less than or equal to 24 km/hr. The median total delta-V for occupants with a maximum AIS injury level of 3 or higher was 32 km/hr.



**Figure 9. Distribution of Far Side Impact Injuries by Total Delta-V**

Figure 10 examines the distribution of far side injuries by lateral delta-V of the struck vehicle. The median lateral delta-V for all far side struck occupants was 12 km/hr. Half of the Harm occurred for total delta-V less than or equal to 22 km/hr. The median lateral delta-V for occupants with a maximum AIS injury level of 3 or higher was 28 km/hr.



**Figure 10. Distribution of Far Side Impact Injuries by Lateral Delta-V**

For near side struck occupants, intrusion into the occupant compartment is known to increase the severity of impact injury. The effect of intrusion is not as obvious, however, for far side struck occupants. Our analysis used the SAE collision deformation extent, recorded by NASS crash investigators, as a measure of intrusion. As shown in Figure 11, the SAE collision deformation classification scheme divides the struck side of the car into nine zones. The boundary between the fifth and sixth zone corresponds to the centerline of the car.

As shown in Figure 12, 60% of all far side struck occupants were exposed to crashes with a damage extent involving only the first and second zones. This figure shows that serious injuries are strongly correlated with damage extent. Almost no serious injuries were observed for damage extent limited to the first two zones. However, 60% of the serious injuries were incurred by occupants of a vehicle with a damage extent to zones 3 or 4. However, as damage extent is also correlated with delta-V, it is unclear from this figure if the injury was a result of intrusion or simply a higher inertial loading.

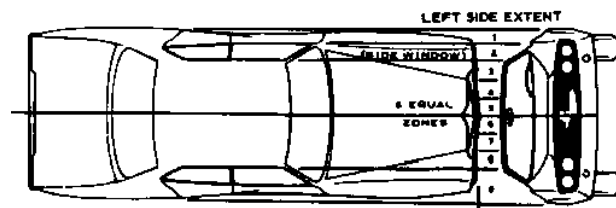


**Figure 11. Side Crash Damage Extent**

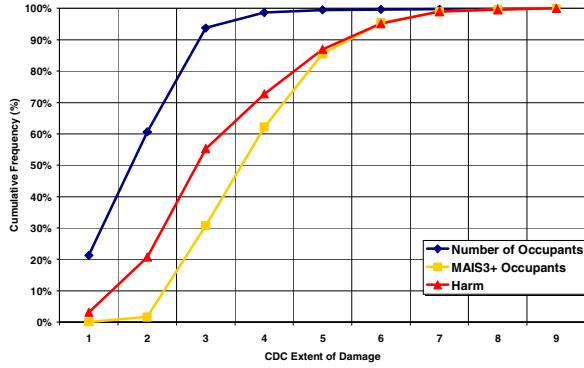


**Figure 12. Distribution of Injuries by Damage Extent**

Figure 13 presents the distribution of injuries by principal direction of force (PDOF). Zero degrees is the front of the struck car, 180 degrees is the rear of the struck car and 90 degrees is normal to the side of the struck car. In NASS, PDOF normally ranges from 0 to 360 degrees. For a side impact, a PDOF ranging from 0 to 180 degrees would correspond to a right side impact, while a PDOF ranging from 180 to 360 degrees would correspond to a left side impact. Note that for this analysis, the PDOF for both left and right side impacts have been collapsed into a set of values ranging from 0 to 180 degrees. Hence, a direction of force perpendicular to the side of either the left or right side of the vehicle would correspond to an angle of 90 degrees.

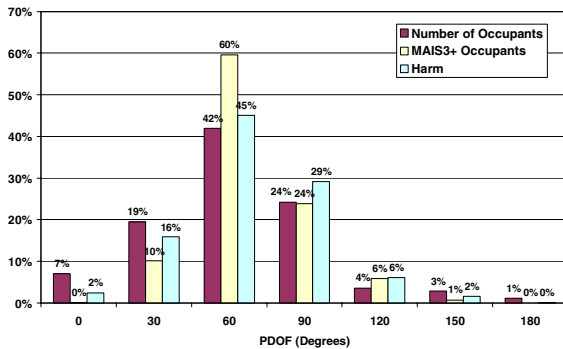


**Figure 13. Distribution of Far Side Impact Injuries by Principal Direction of Force**

As shown in Figure 13, the most likely principal direction of force in far side impacts was 60 degrees. A principal direction of force of 60 degrees, +/- 15 degrees, accounted for 60% of the seriously injured occupants, and 45% of the Harm. Little injury was observed either for PDOF below 30 degrees or for PDOF which exceeded 90 degrees.

Figure 14 shows the definition of impact region used in this analysis. The NASS categories Y (front 2/3 of

the car side), P (center 1/3 of the car side), Z (rear 2/3 of the car side), and D (distributed), all involve impact to the occupant compartment. An impact to the occupant compartment may result in intrusion which is known to increase the injury severity for near side struck occupants. Intrusion may also affect the injury outcome for a far side struck occupant.

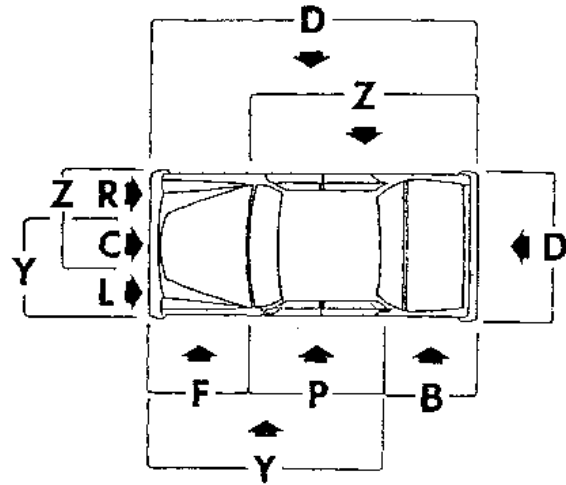


**Figure 14. Side Crash Impact Locations**

Figure 15 shows that the front 2/3 of the vehicle was the most likely damage location for the vehicles in our sample. Impacts to this region also accounted for the largest fractions of seriously injured occupants (42%) and Harm (39%). Collisions which involved the occupant compartment were observed to be result in a disproportionate amount of serious injuries and Harm. The side damage locations P, Y, Z, and D in the figure above accounted for 66% of the side struck occupants, but 86% of both the seriously injured occupants and the Harm.

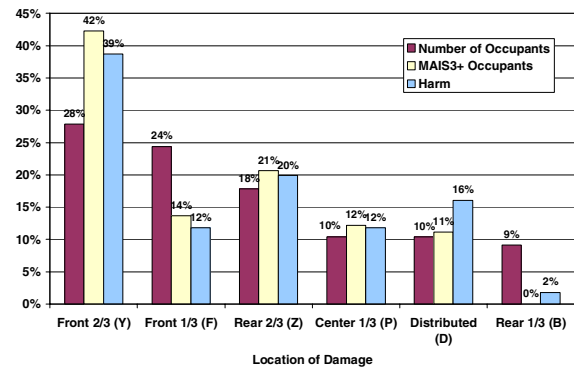


**Figure 15. Distribution of Far Side Impact Injuries by Location of Impact**

## INJURY SOURCES

The following charts present the distribution of far side injuries by injury source. These figures identify potential targets for the development of countermeasures to prevent or reduce the severity of far side injuries. Because the number of AIS3+ cases in each category can be very small when disaggregating the data in this way, these figures report injuries at the AIS 2 level and higher. Harm was computed using only injuries of severity AIS 2 and greater.

As shown in Figure 16, the leading sources of head injury were contact with the right interior, roof, center panel, and right roof rail. Twenty per cent of the head Harm results from contact with the right interior surfaces of the vehicle. Because the head is free to flail about in the vehicle, we also note that unlike other, more constrained body regions, the head suffers impact with a large number of different contact sources.

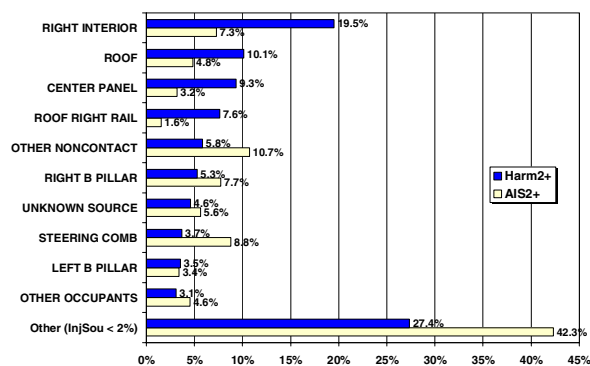


Figure 16. Distribution of Head Injuries by Injury Source

As shown in Figure 17, the leading sources of chest injury were contact with the seat back, the belt webbing or buckle, the right interior, and other occupants. Almost half of the AIS 2+ injuries result from contact with the seat back of the vehicle. Analysis of high speed video of side impact crashes reveals that in a side impact the near side seat is frequently deformed out of position and into the trajectory of a far side occupant. Injuries induced by the safety belt or buckle accounted for approximately one-fourth of AIS 2+ injuries. As shown in Figure 18, most of the serious chest injuries occurred as a result of impacts with a PDOF of 60 degrees.

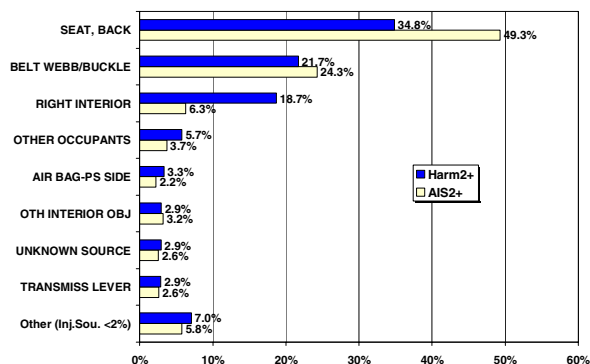


Figure 17. Distribution of Chest Injuries by Injury Source

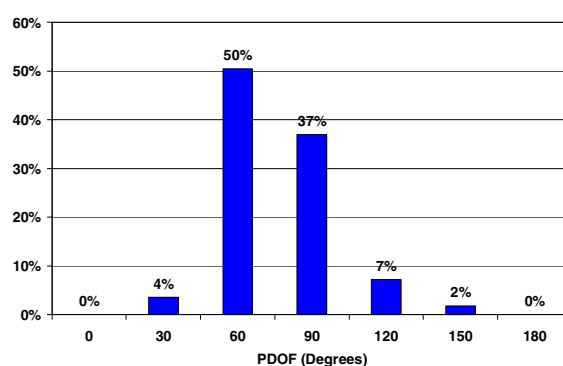


Figure 18. Distribution of Serious Chest Injuries (AIS 3+) by PDOF

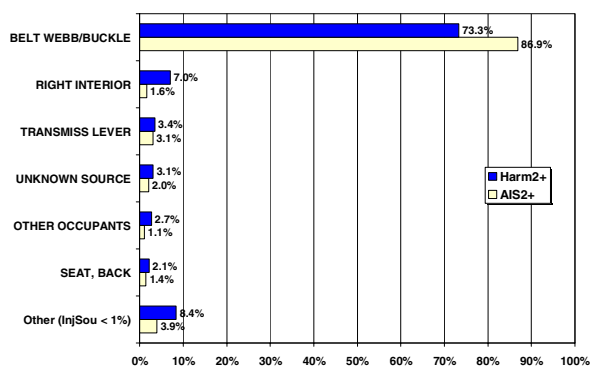
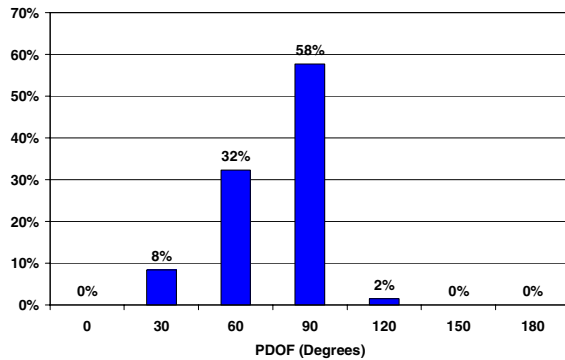


Figure 19. Distribution of Abdominal Injuries by Injury Source

As shown in Figure 19, 86% of the AIS 2+ injuries and 73% of the Harm were the result of abdominal contact with either the safety belt or buckle. These data suggest that current safety belt designs appear to interact very poorly with the abdomen of far side struck occupants. Analysis of high speed video of side impact crashes suggests that some of these abdominal injuries could also be the result of contact with the center console. Because the center console is so much stiffer than the abdomen, it is possible that

impacts with the center console are not always apparent to accident investigators.



**Figure 20. Distribution of Serious Abdominal Injuries (AIS 3+) by PDOF**

## CONCLUSIONS

This paper has evaluated the risk of injury from far side impact crashes in Australia and the United States. Our analysis was based upon an examination of injury outcomes of 107 occupants drawn from the Australian MIDS database, and over 4500 occupants extracted from the U.S. NASS/CDS 1993-2002 crash investigations database. All cases were three-point belt restrained occupants of passenger cars, light trucks and vans who were exposed to a far side impact.

The goal of this study was to establish priorities for injury countermeasure development. Specific conclusions are as follows:

- Far side struck occupants have a significant risk of injury in both Australia and the United States. As a fraction of all occupants who experienced a side impact, far side struck occupants accounted for approximately 20% of the seriously injured persons and 25-29% of the Harm.
- Protection of the head, chest, and spine are priorities for countermeasure development in both Australia and the United States. These three body regions accounted for approximately half of all the Harm attributed to far side impact.
- Injuries to the upper and lower extremities combined for approximately 40% of the far side impact Harm in both countries – a surprisingly large fraction.
- Nearly half of all AIS 2+ injuries to the chest were the result of contact with the seat back.

Analysis of high speed video of side impact crashes reveals that in a side impact the near side seat is frequently deformed out of position and into the trajectory of a far side occupant.

- The accident data suggest that improvement of safety belt loading should be a priority for both abdominal and chest injury reduction. Injuries induced by the safety belt or buckle accounted for approximately one-fourth of AIS 2+ chest injuries. Particularly surprising was the finding that 86% of the AIS 2+ abdominal injuries were the result of contact with either the safety belt or buckle. Future studies will investigate whether some of these abdominal injuries may be the result of undetected contact with the center console.

As a first step toward the development of a far side impact test procedure, the analysis used U.S. data to investigate the impact conditions which lead to far side impact injury. Specific findings are as follows:

- The median lateral delta-V for occupants exposed to far side impact was 12 km/hr. The median lateral delta-V for Harm was 22 km/hr while the median lateral delta-V for serious injuries was 28 km/hr.
- A principal direction of force of 60° was most likely to be associated with serious injury. A PDOF of 60° +/- 15° was experienced by 60% of the seriously injured persons and resulted in 45% of the Harm.
- A vehicle or fixed object striking the occupant compartment of a subject vehicle was most likely to produce far side injuries. Impacts involving the occupant compartment accounted for 86% of the seriously injured persons and 86% of the Harm. Early indications are that this may be due to the effect of intrusion on the far side occupant.

## ACKNOWLEDGEMENTS

The funding for this research has been provided by private parties. Dr. Kennerly Digges and the FHWA/NHTSA National Crash Analysis Center at the George Washington University has been selected to be an independent solicitor of and funder for research in motor vehicle safety, and to be one of the peer reviewers for the research projects and reports. The Australian Research Council awarded Grant No. LP0454122 to Professor Brian Fildes at the Monash University Accident Research Centre. Neither of the private parties have determined the allocation of

funds or had any influence on the content of this report.

Conference on Enhanced Safety of Vehicles,  
Paper no. 249 (2001)

## REFERENCES

1. AAAM. Abbreviated Injury Scale – 1990 Revision, Association for the Advancement of Automotive Medicine, Des Plaines, Illinois (1990)
2. Digges, K., and Dalmotas, D., “Injuries to Restrained Occupants in Far-Side Crashes,” Proceedings of the Seventeenth International Conference on Enhanced Safety of Vehicles, Amsterdam, Netherlands ( 2001)
3. Fildes, B.N., Lane, J.C., Lenard, J., and Vulcan, A.P., Passenger cars and occupant injury: Side impact crashes. Report CR 134, Federal Office of Road Safety, Canberra, Australia (1994)
4. Fildes, B., Linder, A., Douglas, C., Digges, K., Morgan, R., Pintar, F., Yogandan, N., Gabler, H.C., Duma, S., Stitzel, J., Bostrom, O., Sparke, L., Smith, S., and Newland, C., “Occupant Protection in Far Side Crashes”, Proceedings of the Nineteenth International Conference on Enhanced Safety of Vehicles, Washington, DC, USA ( 2005)
5. Gabler, H.C. and Hollowell, W.T., “The Aggressivity of Light Trucks and Vans in Traffic Crashes”, SAE Transactions, Journal of Passenger Cars, Section 6, v.107, Paper No. 980908 (1998)
6. Insurance Institute for Highway Safety (IIHS) “Crash Compatibility: How Vehicle Type, Weight Affect Outcomes”, Status Report, 33(1). (1998)
7. Malliaris, A.C., Hitchcock, R., and Hedlund, J., “A Search for Priorities in Crash Protection”, Crash Protection, SAE SP-513, pp. 1-33, Society of Automotive Engineers (1982)
8. SAE Standard J224, Collision Deformation Classification (1980).
9. Summers, S., Prasad, A., Hollowell, W.T., "NHTSA's research program for vehicle aggressively and fleet compatibility", Proceedings of the Seventeenth International

# KINEMATICS OF THE Q3S ATD IN A CHILD RESTRAINT UNDER FAR-SIDE IMPACT LOADING

**Kathleen D. Klinich**

**Nichole L. Ritchie**

**Miriam A. Manary**

**Matthew P. Reed**

University of Michigan Transportation Research Institute  
United States

**Nicholas Tamborra**

George Washington University  
United States

**Lawrence W. Schneider**

University of Michigan Transportation Research Institute  
United States

Paper Number 05-0262

## ABSTRACT

A series of sled tests was performed using the Q3S anthropomorphic test device (ATD) and the ECE R44 sled buck to study CRS and pediatric occupant kinematics in far-side impacts. Using one model of convertible child restraint system (CRS), tests were performed using a 24 km/hr, 20 g pulse to compare ATD and CRS response to lateral loading in both forward-facing (FF) and rearward-facing (RF) configurations. The effects of initial arm postures on the ATD's motion were examined. Remaining tests examined how various methods of securing the CRS to the vehicle seat affect lateral movement of the CRS and ATD. Tests were run using four tether anchorage locations for the FF configuration and three tether anchorage locations for the rearward-facing configuration. In addition, the CRS was installed using different combinations of vehicle belt restraints and LATCH systems.

Arm position influences ATD kinematics, including head excursion. Placing the arms at the ATD's side, rather than angled or extended forward, reduced lateral head excursions by about 30 mm. In FF tests, using the 3-point-belt with the shoulder belt anchored on the impacted side provided the greatest reduction in lateral head excursion compared to a lap-belt only condition. Using a tether in FF tests also reduced maximum head excursion. In RF tests, using any type of LATCH reduced head excursion compared to conventional installation with only a lap belt. In a RF configuration, some tether configurations reduced head excursion of the ATD. In addition to evaluating head excursion, head retention within the child restraint was also noted. The key to retaining the ATD head within the CRS is to minimize rotation of the CRS about a vertical axis. This was achieved in a FF orientation through rigid

LATCH lower attachments, a 3-point belt with the shoulder belt anchored on the impacted side, or a reverse belt path with a lap belt. The ATD head was not retained within the CRS in any of the RF tests.

## INTRODUCTION

Side impacts are a leading cause of fatalities and injuries to both pediatric and adult occupants in motor-vehicle crashes. In 1999, 32% of children ages 0-12 who died in motor-vehicle crashes were in side impacts (NHTSA 2002). CDS data from 1993-2000 indicate that 16% of nonfatal pediatric crash injuries resulted from side impacts.

Because occupants seated on the struck side of a vehicle in a side impact collision (i.e., near-side occupants) are at the highest risk of serious and fatal injuries because of direct loading by the struck door, most efforts to develop procedures for assessing side impact protection have focused on the near-side occupant. Recent efforts by the ISO/TC 22/SC 12/WG 1 to evaluate CRS performance relative to pediatric injuries in side impacts have concentrated on recreating the occupant loading conditions produced by an intruding door in side impact sled tests (Langwieder et al. 1997, Paton et al. 1998). However, while CRS design is a factor in reducing injuries to near-side pediatric occupants, a significant portion of the near-side injury problem must be addressed through changes in vehicle design rather than CRS design.

Unlike injuries and fatalities caused by door intrusion, preventing injuries from far-side impact conditions is almost exclusively an issue of restraint system design. Key elements for obtaining good CRS performance in side impact are keeping the CRS and ATD within the occupant space, retaining the ATD's head within the CRS, and padding any CRS

surface that the ATD is likely to contact. Kamren et al. (1993) noted that if head retention is a goal of improving CRS side impact performance, simulating an intruding door is less important. Procedures developed to improve impact protection for children under non-contact loading conditions are likely to be less complex than procedures using a simulated intruding door aimed at improving protection of near-side occupants. In addition, designing a CRS to prevent injury to the far-side occupant would likely have some benefit for near-side occupants, but allow separation of CRS-based improvements from vehicle-based improvements in side impact protection.

Crash studies also indicate that a substantial proportion of side impact injuries and fatalities can occur to pediatric occupants not seated directly adjacent to the impact site, and that many injuries occur without vehicle intrusion. Analysis of 1999 FARS data indicated that 45% of pediatric side impact fatalities were to center or far-side occupants (NHTSA 2002). Arbogast et al. (2000) studied 93 children aged 0 to 15 years in 55 side impacts. Crashes with no or minor intrusion produced 42% of significant injuries, including half of serious head injuries. Of the 8 seriously injured children aged 0-4, two were in far-side locations.

Australian regulatory and research testing has focused on evaluating CRS in both far-side and near-side impact conditions without an intruding door. They have examined the effect of different methods of securing the CRS to the vehicle (flexible LATCH, rigid LATCH, 3-point belt) and different tether configurations on CRS performance in side impact (Brown et al. 1995, 1997). NHTSA's preliminary CRS side impact protection research (Esselman 2004, NHTSA 2002) has focused on evaluating ATDs for side impact testing and compared flexible and rigid LATCH anchors and the performance of existing CRS models using both far-side impact conditions and near-side tests with a fixed-position simulated door.

A limitation of previous testing to examine pediatric side impact response has been the absence of pediatric ATDs developed for use in side impact testing. The testing done by ISO and in Australia has used the TNO P series of ATDs, which were designed for frontal impact conditions. NHTSA testing in support of the ANPRM on CRS side impact testing used a Hybrid III 3YO ATD, also a frontal-impact ATD. Adult side impact response corridors have been scaled and used to specify performance standards for pediatric side impact ATDs (van Ratingen et al. 1997, Irwin et al. 2002.) The first

attempt to build a pediatric ATD meeting these specifications was the Q3, which was designed to meet both frontal and side impact requirements (van Ratingen et al. 1999). Initial testing with the ATD indicated that it did not meet all of the specifications, so both frontal and side impact versions of the ATD were developed. The side impact version, the Q3S, was evaluated by NHTSA with fairly good results (Esselman 2004). A few modifications have since been made to improve the neck and shoulder response, and the research program described in this paper uses this latest version of the ATD.

Another limitation of previously published studies is that most tests analyzing the effect of different methods of securing CRS to the vehicle were performed with prototype versions of LATCH anchors and attachments. Because LATCH systems are now required and widely available in the U.S. market, comparison of commercially available LATCH configurations with vehicle belt securement methods is now possible. In addition, some test configurations in the current program were selected to evaluate "misuse" conditions identified in the field for their possible advantages or disadvantages under side impact loading.

The goal of the current research program was to improve understanding of CRS kinematics under non-contact side impact loading using an ATD, the Q3S, designed specifically for this purpose. Key issues examined are the effect of initial arm placement on ATD kinematics and the effects of both primary securement and tether use on ATD and CRS kinematics under far-side impact loading.

## **METHODS**

### **Overview**

A series of sled tests was conducted to examine kinematics of the Q3S and CRS in forward-facing and rear-facing installations during lateral impact loading without contact with the vehicle interior. The ECE R44 buck was chosen for the study because it was easily configurable to a 90 degree impact orientation and has been used for side impact testing by others. A single model convertible CRS with a five-point harness, the Evenflo Titan V, was used in all tests; each CRS was used in one forward-facing and one rear-facing test. This CRS has a rear-facing weight limit of 13.6 kg, so the Q3S, which is just over this limit with a weight of 14.5 kg, could be used in both forward-facing and rear-facing orientations. The 24 km/hr, 20 g pulse proposed by

the NHTSA for side impact testing of CRS (NHTSA 2002) was used in all tests.

Table 1 lists the ATD instrumentation used in the test series. Lateral displacements of the chest and shoulder were measured using an IRTRACC sensor, and the CRS was instrumented with six linear accelerometers mounted on a bar attached to the impacted side of the CRS. All belt loads were measured using webbing load cells. All transducer signals were filtered according to the specifications of SAE J211. Peak lateral head excursion of the leading edge of the head relative to the pre-impact head position was digitized from images collected by an overhead high-speed video camera. Retainment of the ATD head within the seat was evaluated using the overhead camera view by determining if any portion of the CRS was visible beyond the head at the time of peak head excursion. Results presented in this paper are limited to maximum head excursions, head retainment, and evaluation of kinematics from the videos, but the remaining data are included in a final report on the program (Klinich et al. 2005).

Table 1.  
ATD instrumentation

Component	Measurement	Axes
Head	Acceleration	x, y, z
Upper Neck	Force	x, y, z
Upper Neck	Moment	x, y, z
Chest	Acceleration	x, y, z
Pelvis	Acceleration	x, y, z
Lumbar	Force	x, y, z
Lumbar	Moment	x, y, z

### Effect of ATD Arm Position

Table 2 lists the test matrix used to evaluate the effect of initial arm position on ATD kinematics. These tests were performed with the CRS secured in a forward-facing orientation using a lap belt and top tether. Figure 1 illustrates the baseline arm position, as well as two other arm positions tested. In the baseline arm position, the ATD hands were placed on the tops of the thighs. In the second position, the upper arms were placed along the sides of the torso. In the third position, the arms were extended fully forward.

Table 2.  
Matrix of arm position tests

Test	Arm Position
GU0405	Hands on lap
GU0407	Arms extended horizontally
GU0408	Arms at sides



Figure 1. Initial ATD positions for tests varying arm posture: baseline with hands on lap (left), arms at sides (middle), and arms extended (right).

### Securing CRS Forward-Facing

Table 3 lists the tests used to evaluate how different methods of securing the forward-facing (FF) CRS to the vehicle seat affect kinematics during lateral loading. The baseline condition is test GU0420, with the CRS secured by only a lap belt and the belt tension adjusted to the FMVSS 213 requirement of about 50 N. Four other conditions (GU0421 through GU0501) using standard belts without tethers were also tested: higher tension lap belt (roughly double FMVSS 213 specifications), three-point belt (passenger and driver configurations), and a reverse belt path, illustrated in Figure 2. The reverse belt path routes the belt around the front of the CRS on each side and around the back of the CRS. Although the CRS used in these tests is not specifically designed to use this type of belt routing, other CRS are available for which this routing is recommended. The reverse belt path configuration was tested because it was hypothesized that it might reduce rotation of the CRS. For the three-point belt tests, the 3PBL, or driver configuration, anchors the shoulder belt over the left shoulder of a forward-facing ATD (toward the impacted side), while the 3PBR, or passenger configuration, anchors the shoulder belt over the right side of a forward-facing ATD (away from the impacted side).

Table 3.

Matrix of forward-facing securement tests

Test	Main Securement	Tether Anchor
GU0419	Lap belt @ 50 N	Behind seatback
GU0420	Lap belt @ 50 N	None
GU0421	Lap belt @ 110 N	None
GU0422	3PBR	None
GU0423	3PBL	None
GU0501	Reverse lap belt	None
GU0502	Flexible LATCH through belt path	None
GU0506	Attached Flex LATCH	None
GU0504	Flex LATCH through belt path + 3PBL	None
GU0505	Lap belt @ 50 N	Roof
GU0507	Rigid LATCH	None
GU0509	Lap belt @ 50 N	Floor
GU0510	Lap belt @ 50 N	Under seat



**Figure 2. Annotated photo showing reverse belt routing used in test GU0501.**

Four tests were run using different types of LATCH lower attachments. Test GU0502 used the flexible attachment that was provided with the CRS, which is a length of webbing with a hook-on connector at each end that is routed through the belt path of the CRS. Test GU0504 used both a three-point belt (shoulder belt on left side) and the provided flexible LATCH attachment to secure the CRS. This condition has been identified as a common LATCH misuse installation, but was hypothesized to have possible benefits in side impact. In test GU0506, the CRS was modified by clamping short lengths of webbing with LATCH hook-on connectors to each side of the CRS, as shown in Figure 3. It was hypothesized that this configuration might reduce lateral sliding of the CRS. The webbing was attached to the CRS so it would provide the same installed belt angle as when the seat was secured with the flexible LATCH attachment routed through the belt path. Test GU0507 used rigid LATCH attachments, also illustrated in Figure 3, in which the CRS was modified by bolting rigid LATCH attachments from another CRS to each side. The rigid attachments were secured to the CRS so the orientation of the installed CRS matched that of the installation with only a lap belt.

The tether anchor locations tested are illustrated in Figure 4. The baseline location represents a tether anchor location that would typically be found in a sedan, while the roof, floor, and under seat locations represent possible tether

anchor locations in minivans and SUVs. Generic tether anchor hardware was bolted in these locations to rigid structures on the sled buck.

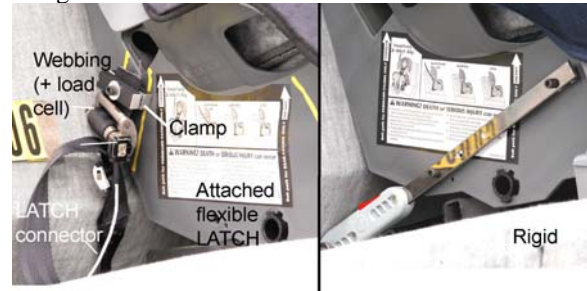


**Figure 3. FF CRS modified with to have attached flexible LATCH attachments (left) and rigid LATCH attachments (right).**

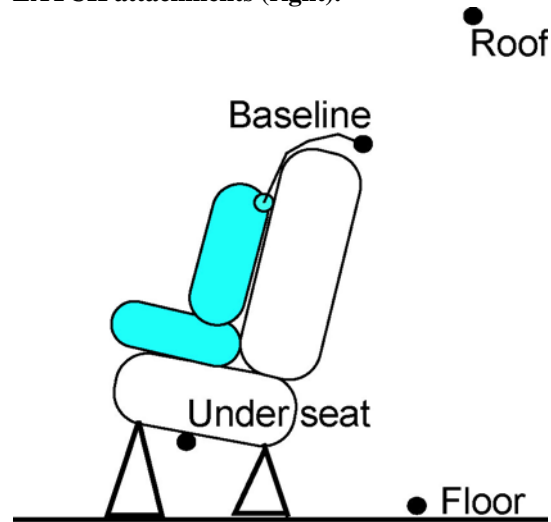


**Figure 4. Illustration of four tether anchorage locations tested with a FF CRS (not to scale).**

### Securing CRS Rear-Facing

Table 4 lists the conditions used to evaluate methods of securing the CRS to the vehicle in the rear-facing configuration. Test GU0511 is considered the baseline test condition, using only a lap belt with the tension set at the FMVSS 213 level of about 50 N. Three other conditions that were tested in FF mode using only vehicle belts to secure the CRS were also tested in RF: higher belt tension and 3-point belt, both passenger and driver configurations. The geometry of this CRS did not allow it to be installed using a reverse belt path in the RF orientation.

The same four installations using LATCH systems that were tested FF were also tested rear-facing. For two tests, attached flexible LATCH attachments or rigid LATCH attachments were added to the CRS as shown in Figure 5. When modifying the CRS to install these LATCH attachments, the

front part of the CRS was trimmed away to avoid interference when connecting the lower LATCH attachments to the lower LATCH anchorages.

Table 4.  
Matrix of rear-facing securement tests

Test	Main Securement	Tether Anchor
GU0511	Lap belt @ 50 N	None
GU0512	Lap belt @ 110 N	None
GU0513	3PB Left	None
GU0514	3PB Right	None
GU0515	Flex LATCH through belt path	None
GU0516	Attached Flex LATCH	None
GU0517	Flex LATCH + 3PBL	None
GU0518	Rigid LATCH	None
GU0519	Lap belt @ 50 N	Over to baseline
GU0520	Lap belt @ 50 N	Down to floor
GU0521	Lap belt @ 50 N	Down under seat



Figure 5. RF CRS modified with attached flexible LATCH attachments (left) and rigid LATCH attachments (right).

Three tether anchorage locations were tested with RF CRS as illustrated in Figure 6, although tether use in a rear-facing configuration is not recommended for this CRS. Test GU0519 used an Australian RF tether configuration, in which the tether is routed over the top of the CRS to a tether anchorage location behind and above the vehicle seat. Test GU0520 used the Swedish RF tether configuration, in which the tether is routed down to the floor in front of the vehicle seat. Test GU0521 used a variation of the Swedish approach, routing the tether down but to a tether anchorage attached to the bottom of the vehicle seat. This type of installation has been identified as a RF misuse of tethers provided with convertible CRS for use in FF installations.

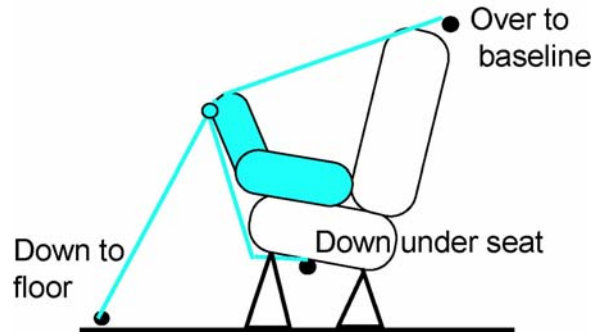


Figure 6. Three tether anchorage locations tested with RF CRS (not to scale).

## RESULTS

### Effect of Arm Position

Figure 7 shows the overhead high-speed video frames at the time of peak lateral head excursion for the three tests comparing initial arm placement, while the maximum head excursion values are plotted in Figure 8. The excursions for the ATD with hands on lap are similar to those with the arms extended, but placing the arms at the sides resulted in almost 30 mm less head excursion.



Figure 7. Peak head excursions with ATD arms initially placed on lap (left), at sides (center), and extended (right).

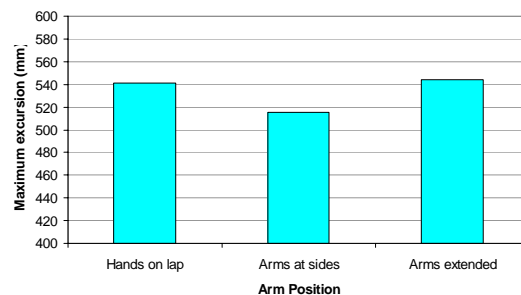


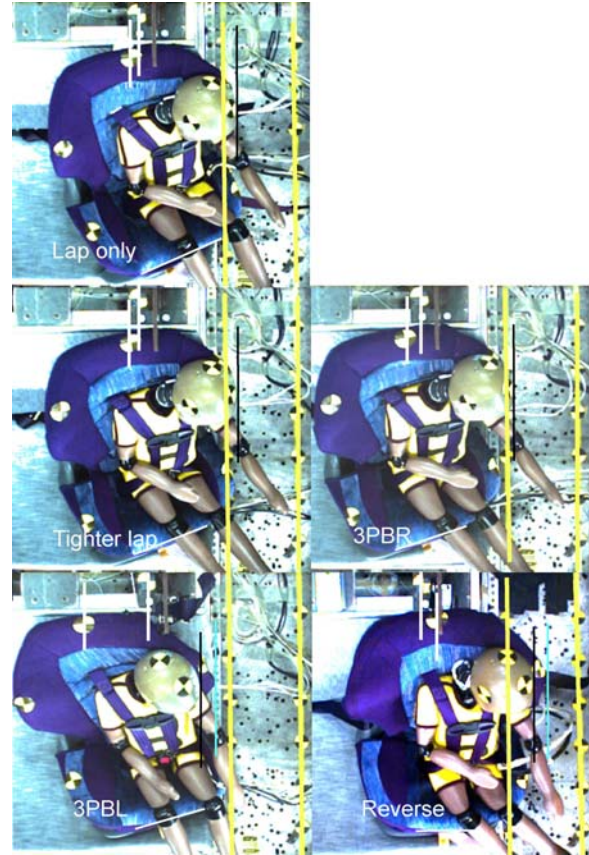
Figure 8. Maximum lateral head excursions for different initial arm positions.

## Securing Forward-Facing CRS

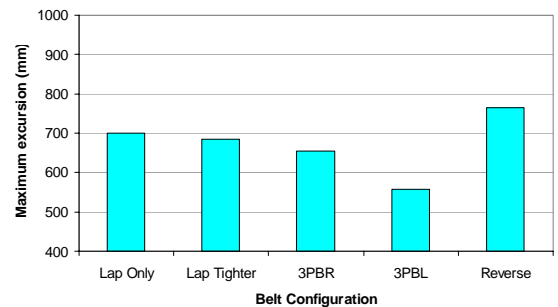
### Variations using Conventional Belts

Figure 9 illustrates the peak lateral head excursions for the five forward-facing tests that secure the CRS with conventional vehicle belts, while Figure 10 plots the magnitudes of these peak head excursions. On Figure 9 (and subsequent illustrations of FF excursion), reference lines on the sled platform have been highlighted on the photos. A black line in each photo indicates maximum lateral head excursion, while a lighter line indicates maximum CRS excursion where visible. A line across the front edge of the CRS has been highlighted in white to indicate the angle of the CRS. White reference lines have also been drawn through targets on the top of the CRS and on the top of the sled buck to assist in visualization of lateral CRS translation.

Compared to the baseline lap-belt-only condition, increasing belt tension and using a right 3-point belt decreased maximum head excursion slightly, but produced kinematics that were very similar to the baseline condition. Using the left (impacted) 3-point belt substantially reduced head excursion (by 142 mm), retained the head within the CRS, and reduced both translation and rotation of the CRS. Using a reverse belt path increased head excursion by allowing greater translation of the CRS, but retained the head and eliminated rotation of the CRS.



**Figure 9.** Peak head excursions of FF tests using lap only (top left), tighter lap belt (mid left), right 3-point-belt (mid right), left 3-point-belt (lower left), and reverse belt path (lower right).



**Figure 10.** Maximum excursions of the head leading edge in FF tests with the CRS secured using different conventional belt configurations.

## Variations using LATCH

The maximum head excursion values in the four FF tests with the CRS secured using variations of LATCH are shown in Figure 11 compared to the baseline lap-belt-only test condition. These maximum head excursions are illustrated in Figure 12. The three tests using just the LATCH system reduced head excursions slightly compared to the lap-belt-only test, but the greatest reduction in head excursion occurred when a left 3-point belt was used in addition to the flexible LATCH attachments routed through the belt path. The kinematics were similar for the two tests run with the flexible LATCH attachments (routed through the belt path or attached to the CRS), although the condition with the attached flexible LATCH appeared to have slightly less CRS rotation. Using both the left 3-point-belt and the flexible LATCH attachments routed through the belt path resulted in the smallest peak head excursion by reducing translation of the CRS back. In this test, the head was not retained. Surprisingly, using rigid LATCH attachments (without a tether) did not substantially reduce head excursion compared to baseline conditions, although it did retain the head within the CRS and eliminated rotation of the CRS. Among all forward-facing tests run, the lateral translation of the top of the CRS was the largest when the CRS was secured by rigid LATCH attachments.

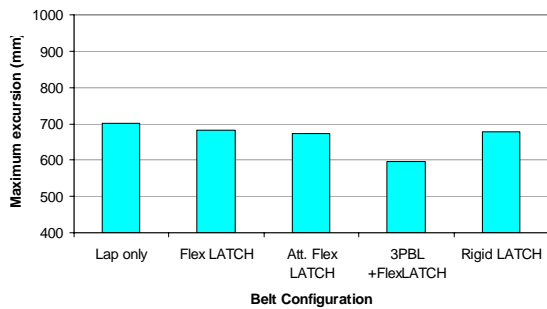


**Figure 11. Maximum excursions of the head leading edge in FF tests with the CRS secured by different LATCH configurations.**

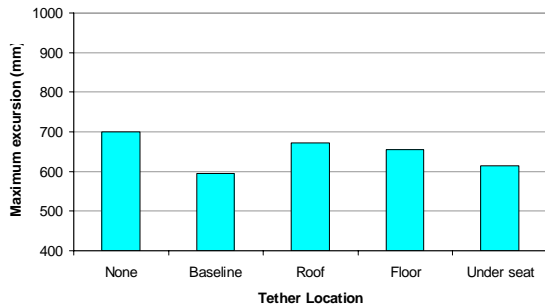


**Figure 12. Peak lateral head excursions of FF tests using lap only (top left), flexible LATCH attachments through belt path (mid left), attached flexible LATCH attachments (mid right), flexible LATCH attachments through belt path plus left 3-point-belt (lower left), and rigid LATCH attachments (lower right).**

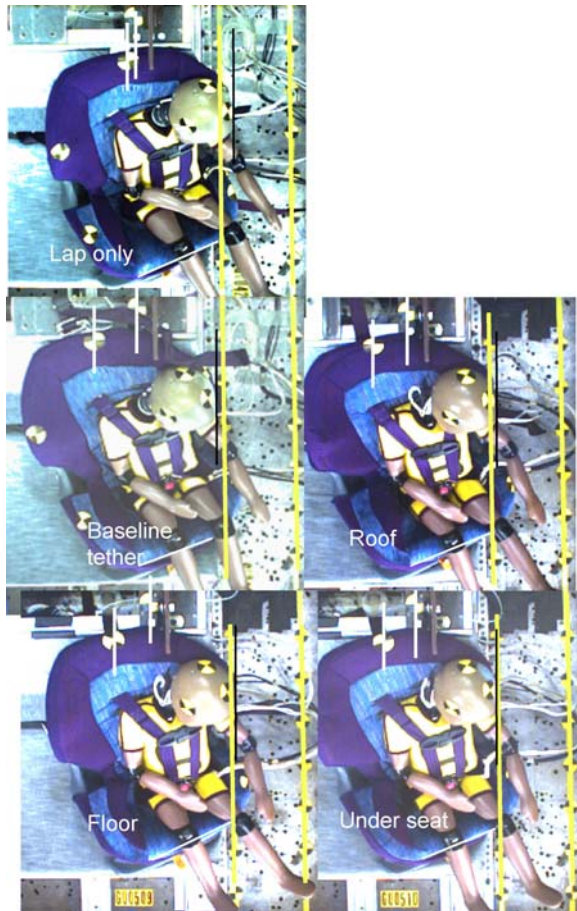
## Tether Effect

Figure 13 compares peak lateral head excursions measured in the four different FF tests run with the CRS secured by a tether and lap belt compared to the baseline FF condition with the CRS secured by only a lap belt. Illustrations of these peak lateral excursions are shown in Figure 14. All tests run with the top tether reduced head excursion compared to the test without. The baseline tether anchorage condition had lower head excursions than the remaining tether anchorage conditions. Of the three remaining tests run with top tethers, peak head excursions were lowest with the tether anchorage under the seat and highest with the tether anchorage mounted to the roof. The kinematics of all the tests with top tethers were similar, in that the tether reduced translation of the CRS seat back, but not

necessarily rotation of the CRS. The head was not retained within the CRS in any of these tests.



**Figure 13. Maximum excursions of the head leading edge in FF tests run with different tether anchorage locations.**



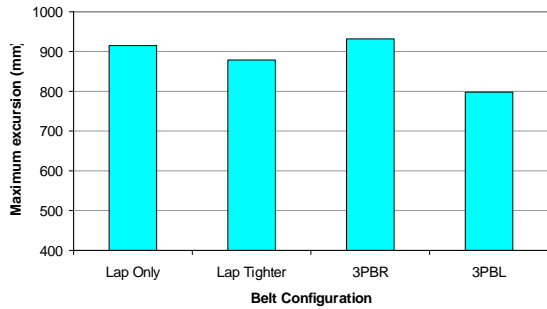
**Figure 14. Peak head excursions of FF tests using no tether (top left), tether anchor behind vehicle seat back (top left), roof tether anchor (mid right), tether anchor on floor (lower left), and tether anchor under vehicle seat (lower right).**

## Securing Rear-facing CRS

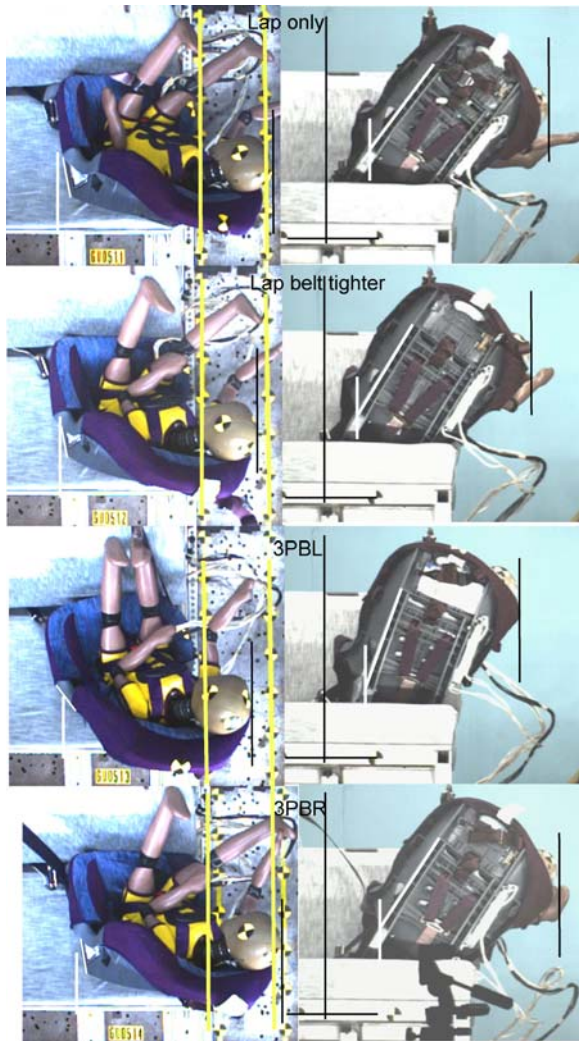
### Variations using Conventional Belts

Figure 15 plots maximum head excursions for the four RF tests run with the CRS secured by conventional belts, while Figure 16 illustrates the overhead and front video frames at the times of maximum head excursion. On the overhead views (for this and subsequent illustrations of RF tests), the reference lines on the floor of the sled buck have been highlighted, and a black line added to indicate maximum head excursion. The angle of the CRS base has also been highlighted and a reference line relative to this angle added. On the front views, a black reference line was added to aid in visualization of CRS lateral translation, and another black line added to indicate maximum head excursion. A white reference line was drawn between two structural points on the back of the CRS to indicate the CRS angle relative to a vertical reference line. For the photo of the 3PBR test, the starting position of the CRS was shifted slightly compared to the other RF tests, so the maximum head excursion photo was shifted relative to the landmarks on the other photos to accurately compare maximum excursion.

Compared to the baseline lap-belt-only condition, using the left 3-point belt reduces head excursion by over 100 mm. As seen in the side view image, the left 3-point-belt reduces the amount that the CRS translates sideways and rolls about the vehicle longitudinal axis. The CRS also has the greatest amount of forward motion toward the front of the vehicle during this test, probably caused by pitching of the CRS about the y-axis. The motion of the ATD was different in this test as well, because the presence of the shoulder belt restricted lower extremity motion. Using a tighter lap belt reduced maximum head excursion slightly compared to the baseline lap-belt-only condition, while use of a right 3-point belt actually increased maximum head excursion slightly. None of the test conditions retained the head within the CRS.



**Figure 15. Maximum excursions of the head leading edge in RF tests run with the CRS secured using different conventional belt configurations.**



**Figure 16. Top and front views of peak head excursions of RF tests using lap only (top), tighter lap belt (second from top), 3-point belt with shoulder belt on left side (third from top), and 3-point belt with shoulder belt on right side (bottom).**

### **Variations using LATCH**

The maximum head excursions of four RF tests run with different types of LATCH securement are compared to the test run with the CRS secured by only a lap belt in Figure 17. Overhead and front views at the time of maximum head excursion are illustrated in Figure 18. All of the RF LATCH conditions reduced maximum head excursion by reducing translation of the CRS, which is most clearly visible on the front views by comparing the amount of vehicle seatback cushion visible between the CRS and a black reference line. Results for the two tests run with flexible LATCH attachments were similar, while adding a left 3-point belt to the flexible LATCH led to further reductions in maximum head excursion. Using rigid LATCH attachments to install the CRS resulted in the greatest reduction in maximum head excursion. None of these tests retained the head within the CRS based on analysis of the overhead views, although the front views indicate that using attached flexible LATCH, flexible LATCH plus left 3-point-belt, and rigid LATCH attachments came close to doing so.

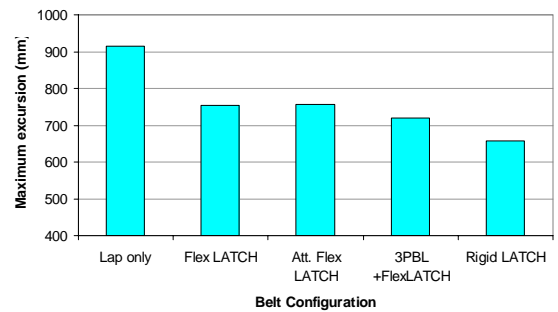


**Figure 17. Maximum excursions of the head leading edge in RF tests run with different LATCH configurations compared to lap only condition.**

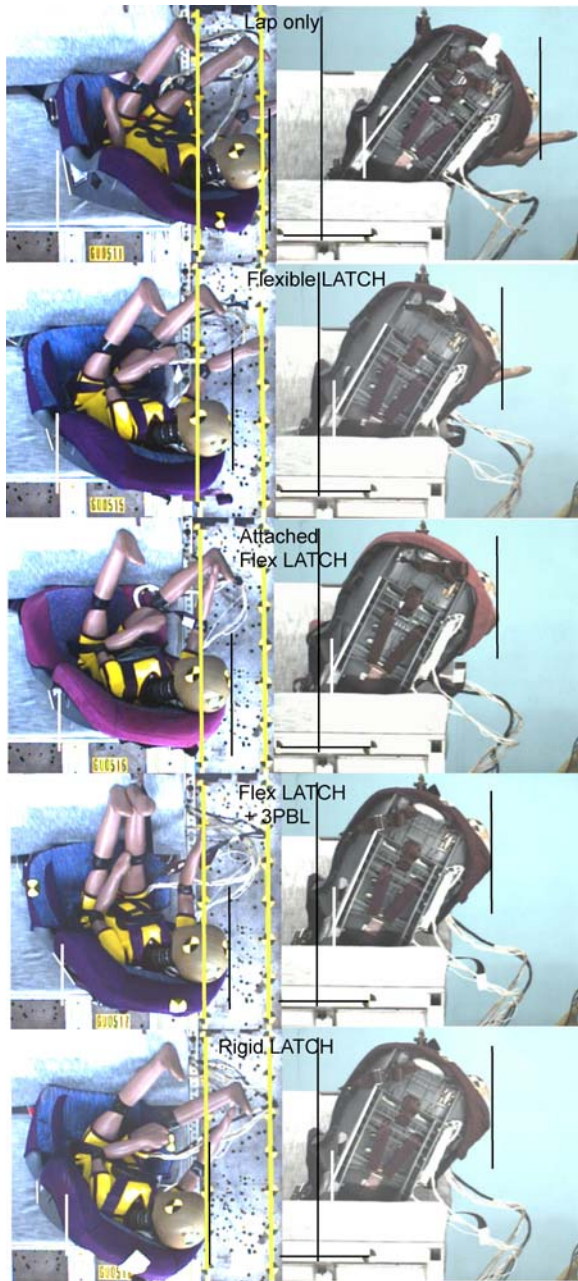


**Figure 18. Top and front views of peak head excursions of RF tests using lap only (top), flexible LATCH attachments routed through the belt path (second from top), attached flex LATCH attachments (third from top), flex LATCH attachments through the belt path plus 3-point belt with shoulder belt on left side (fourth from top), and rigid LATCH attachments (bottom).**

### **Tether Effect**

The peak head excursions for the RF tests run with a tether are shown in Figure 19 and illustrated in Figure 20. For the test with the tether anchored down to the floor, the starting position of the CRS was shifted slightly compared to the other RF tests, so the maximum head excursion photo was shifted relative to the landmarks on the other photos to accurately compare maximum excursion. Routing the tether over the CRS to an anchorage above the back of the vehicle seat reduces head excursion by reducing lateral translation of the CRS, reducing roll of the CRS about the longitudinal axis, and keeping the seat more upright (reduces translation toward the front of the vehicle). When the tether is anchored down to the floor, it increases head excursion by increasing the roll of the CRS about the longitudinal axis and the pitch of the CRS about the y-axis, although it reduces yaw of the CRS about the z-axis. Anchoring the tether down under the seat reduces head excursion by reducing yaw about the z-axis, roll about the x-axis, and lateral translation, although it increases pitch of the CRS about the y-axis, which places the top back of the CRS closer to the front of the vehicle. The ATD head was not retained within the seat for any of these tests, but anchoring the tether over the top to behind the vehicle seatback came closest to doing so.

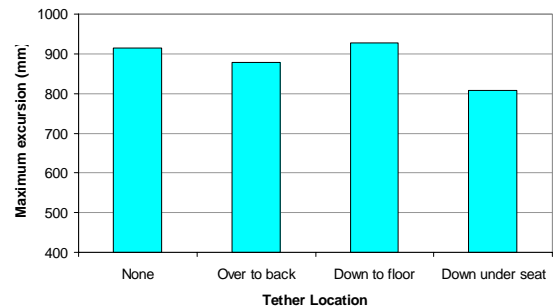


**Figure 19. Maximum excursions of the head leading edge in RF tests run with different tether anchorage locations compared to lap only condition.**

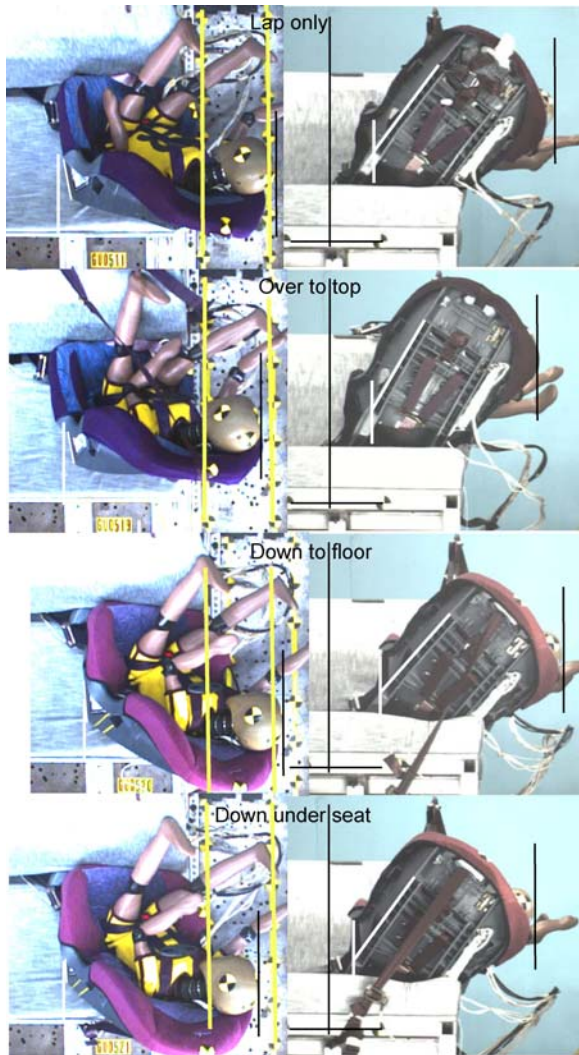


**Figure 20. Top and front views of peak head excursions of RF tests using lap only (top), tether anchored over to behind the vehicle seat (second from top), tether anchored down to floor (third from top) and tether anchored down under seat (bottom).**

## DISCUSSION

### Effect of Arm Position

Arm position was studied in this test program because other users had reported variations in chest displacement and acceleration when arm position was varied under direct contact lateral loading (Tylko 2004). For the less severe noncontact loading conditions of the current study, chest readings did not vary substantially with arm position, but kinematics were affected. Moving the arms from the baseline hands-on-lap position to the arms at the side reduced peak lateral head excursion by as much as changing CRS securement from only a lap belt to

flexible LATCH attachment. In addition, the head was retained when the arms were at the sides but not in the baseline condition.

The Q3S is the only side impact ATD ever designed with complete arm components. None of the adult side impact ATDs have hands or forearms, and often the upper arm component is coupled to the torso to improve response repeatability. Because the arm position of the Q3S affects kinematics under lateral loading, it should be specified when developing a procedure for evaluating CRS in side impacts.

### Securing CRS Forward-Facing

The most interesting finding from these lateral FF tests was that the most effective means of reducing lateral head excursion is securing the CRS with a three-point belt that had the shoulder belt anchored on the left (impacted) side. Prior research evaluating securement techniques under lateral loading has usually compared response of proposed LATCH systems (flexible or rigid) and tether recommendations to the baseline securement used in the regulations of the country (lap belt only in U.S., 3-point belt in Australia). Prior comparison of responses between lap only and three-point-belt has not been reported.

This finding has implications for recommendations about securing FF CRS in the United States. Currently, best recommended practice is to secure CRS with LATCH when possible because it theoretically makes CRS installation easier than when using conventional vehicle belts. In addition, securing CRS with both LATCH and conventional belts is considered misuse. The results of this test series, though preliminary, indicate that use of a 3-point-belt to secure a FF CRS may provide some protection in side impact, even more than adding a tether, and might provide some benefit when used together with LATCH.

Eliminating rotation of the CRS about the vertical axis seems to be the key factor to retaining the head within the CRS. The only three tests that retained the head used securement conditions that substantially reduced rotation of the CRS: rigid LATCH attachments, left (impact side) 3-point-belt, and reverse belt path. While prior research has indicated that making side wings on CRS bigger might be required to retain the head, these tests indicate that controlling rotation of the CRS through different securement methods may also be an effective means of improving head retention.

Using a tether in FF tests reduced head and CRS excursions compared to the lap-belt-only securement test, but did not eliminate CRS rotation or retain the ATD head within the CRS. These findings agree with results of Brown et al. (1995, 1997). The shortest tether length provided the greatest reduction in head excursion among tether conditions.

Using rigid LATCH attachments without a tether reduced head excursion compared to securing the CRS with only a lap belt. However, it was not the best performing securement condition among the forward-facing tests. A possible reason is that the CRS was not equipped with rigid LATCH attachments, and that the modifications made to add rigid LATCH attachments to this CRS may not have been optimal for securing an ATD of this weight, since the rigid LATCH attachments bent about 15 degrees during the test. In addition, most of the motion of the CRS secured by rigid LATCH attachments occurred at the top back of the CRS, which would be reduced by using a tether.

Securing a FF CRS with a reverse belt path led to high head excursions because of large lateral translations of the CRS, even though this securement method did eliminate rotation of the CRS and retain the head. The CRS used in these tests was not designed to use this belt routing, which probably accounts for the large lateral translations. It is possible that redesigning the CRS to allow use of a reverse belt path for either a conventional belt or flexible LATCH attachment may be an effective means of controlling CRS and ATD kinematics in side impact.

Using two variations of flexible LATCH attachments (routed through the belt path or webbing attached to both sides of the CRS) did not lead to substantially different kinematics. However, the short length of webbing used in the attached flexible LATCH test caused interference with the belt load cell, so the belt could not be tightened to FMVSS 213 levels prior to the test and may contribute to the unexpected similarity in performance. Using the attached flexible LATCH attachments reduced rotation of the CRS somewhat compared to using the flexible LATCH routed through the belt path.

The results of this study for FF CRS differ somewhat from results of Australian testing. In the Australian tests, securing FF CRS with rigid LATCH attachments (without a tether) showed superior performance, and flexible LATCH attachments, with and without tether, worked better than the 3-point-belt securement. Results may differ because the

Australian tests used a P3/4 ATD in their evaluations, and their test involved contact with a simulated door, which may disguise differences in kinematics. They noted that the location where the tether is attached on Australian CRS is higher than on North American CRS and may affect evaluation of lateral kinematics.

### **Securing Rear-facing CRS**

In the rear-facing tests, using rigid LATCH attachments provided the greatest reduction in head excursion (over 250 mm) compared to the baseline test in which the CRS was secured by only a lap belt. This substantial reduction might have been even larger if the rigid LATCH attachments had been optimized for this CRS and size of ATD, as they were bent about 15 degrees post-test. However, peak lateral head excursions were lower in all of the tests that used LATCH attachments compared to all of the tests that used only conventional vehicle belts to secure the CRS, possibly because the LATCH anchors are more closely spaced than lap-belt anchors. This appears to have reduced the lateral translation of the CRS. Using the flexible LATCH attachments together with the left (impacted side) 3-point belt led to additional reductions in lateral head excursion. The Australian securement testing of RF CRS (1997, 1995) also found that rigid LATCH provides the best response in side impacts. However, unlike the current study, the Australian testing had better results in securing RF CRS with a 3-point-belt than with flexible LATCH and tether.

Two RF tether anchorage locations reduced maximum lateral head excursion, although they achieved this by different means. The tether anchored over the top of the CRS to behind the vehicle seatback reduced lateral head excursion by reducing pitch and roll of the CRS. The tether anchored underneath the vehicle seat increased pitch of the CRS, but reduced head excursion by eliminating yaw and reducing lateral translation. A possible advantage of the over-the-top tether anchorage position is that it would be more likely to prevent contact of the CRS with the back of vehicle seat in front of it.

An interesting finding of this study of RF CRS kinematics under lateral loading was the pattern of ATD and CRS kinematics. Pioneering testing of CRS in the 1960's indicated that a RF CRS would swing toward the door about a vertical axis under lateral loading (Weber 2005). However, with today's CRS and securement methods, it appears that a greater amount of motion occurs from the CRS rolling about the longitudinal axis towards the impact

side. Figure 21 plots the angle of the CRS back relative to vertical against peak head excursion, at the time of peak head excursion, with a linear fit through all points except for the 3PBL test. Lateral excursion of the head seems to be associated with how much the CRS rolls toward the door rather than rotates toward the door. This may partly result from the choice of the CRS used in these tests or from the CRS approaching the edge of the R44 seat, but the relative contributions of roll and rotation of RF CRS on lateral head excursion should be investigated further in the future.

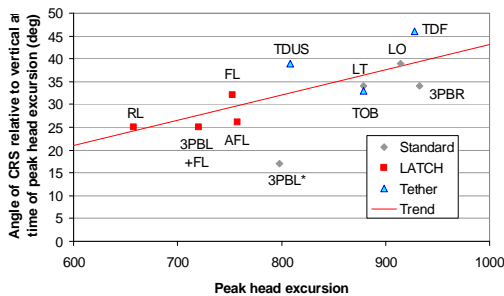


**Figure 21. Angle of the CRS back relative to vertical at time of peak head excursion vs. peak head excursion. \* not included in trendline.**

### Comparing FF and RF Tests

Figure 22 compares the maximum head excursions for the FF and RF tests under each securement condition. The peak lateral head excursions with a single RF CRS range from 657 to 933 mm with a mean value of 821 mm, while the peak lateral head excursions for the FF CRS range from 558 to 764 mm with a mean value of 656 mm. The mean FF head excursion is essentially the same as the best RF head excursion, while the worst FF head excursion is over 50 mm less than the mean RF head excursion. The only condition where the RF CRS test resulted in a lower lateral head excursion than the FF CRS test was when the CRS was secured by rigid LATCH attachments. All of the peak lateral head excursions for RF tests in this program are greater than the excursion limit of 622 mm proposed by NHTSA for a 3-year-old ATD.

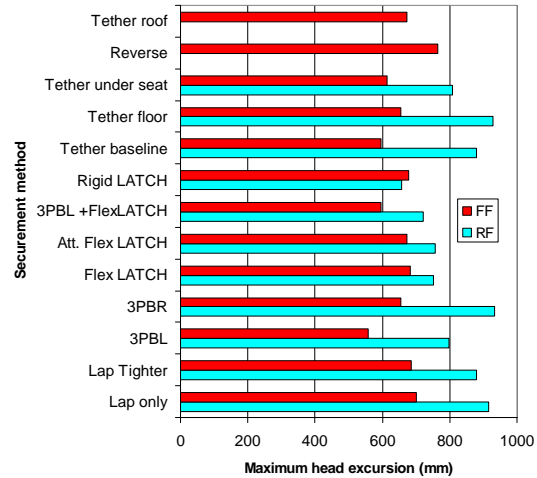


**Figure 22. Comparison of RF and FF head excursions under the same securement conditions.**

Analysis of the kinematics of these tests indicates that FF and RF CRS have different degrees of freedom under lateral loading. FF CRS primarily translate sideways at the top and bottom of the CRS back and rotate about a vertical axis. RF CRS translate laterally and rotate relative to all three axes, which affects the amount of forward and lateral excursion of the CRS back and ATD head.

A concern when evaluating CRS under side impact conditions is how to fairly test forward-facing and rear-facing CRS using the same test procedure. The ISO/TC 22/SC 12/WG 1 has proposed testing FF CRS in a vehicle front seat configuration, and RF CRS in a rear vehicle seat configuration, so both conditions would represent worst case scenarios of intrusion at the B-pillar. This approach presents challenges in the United States, where best practice recommends seating children in the rear seat, and a test procedure that appears to evaluate CRS in the front seat would contradict this best practice. In testing to support their ANPRM, the NHTSA evaluated both FF and RF seats under non-contact and non-intruding door conditions and proposed a single head excursion limit for all types of CRS. However, because lateral loading of RF CRS almost always result in higher lateral head excursions than lateral loading of FF CRS, these criteria would suggest that FF CRS are safer than RF CRS in side impacts. This implication is inconsistent with results from crash investigation studies of side impacts, in which children seriously injured in RF CRS are quite rare. The unintended consequences of making RF CRS appear less protective than FF CRS in side impacts, contrary to field data, should be seriously

considered when developing a side impact procedure for evaluating CRS.

### Study Limitations

This study provided a thorough examination of securement factors that affect ATD and CRS kinematics in non-contact side impacts. The main limitations are that only one test in each configuration was conducted, only one model of CRS was used, and only one size of ATD was used. Also, testing was conducted using a laboratory bench seat that simulates a vehicle seat. Actual rear vehicle seats have contouring, bolsters, and support structures that might significantly alter CRS and ATD kinematics. Additional tests to examine repeatability of test results and confirm trends in this initial set of tests are planned, and other CRS models will be evaluated.

### CONCLUSIONS

- Arm placement of the Q3S affects kinematics and should be considered and specified when developing a CRS side impact test procedure.
- Head retention in FF CRS is associated with reduced CRS rotation about the vertical axis. Rotation is reduced compared to the baseline lap-belt-only securement condition by securing the CRS with a 3-point belt with the shoulder belt on the impacted side, rigid LATCH attachments, and a reverse belt path.
- Using a tether with FF CRS limits lateral CRS translation but does not affect CRS rotation of the CRS nor result in head retention within the CRS. The test with the shortest distance to the tether anchorage had lower peak head excursions than the other tether anchor locations tested.
- Relative to the baseline test with CRS secured by only lap belts, rigid LATCH attachments were more effective in the rear-facing configuration than the forward-facing configuration at reducing ATD head excursion, although rigid LATCH attachments still exhibited good performance in the forward-facing test.
- Securing RF CRS with any type of LATCH attachments results in lower peak lateral head excursions than when securing RF CRS with any variation of conventional belts.

- Peak lateral head excursion of RF CRS is primarily caused by roll of the CRS about a longitudinal axis, not rotation about the vertical axis.
- None of the tests in the rear-facing configuration retained the head within the CRS, but the Australian tether configuration came closest to doing so.

### ACKNOWLEDGEMENTS

The funding for this research has been provided by private parties, who have selected Dr. Kennerly Digges [and FHWA/NHTSA National Crash Analysis Center at the George Washington University] to be an independent solicitor of and funder for research in motor vehicle safety, and to be one of the peer reviewers for the research projects and reports. Neither of the private parties have determined the allocation of funds or had any influence on the content of this report.

The authors would like to acknowledge First Technology Safety Systems for use of the Q3S in this program, and thank Mike Carlson of FTSS in particular for assistance with the dummy. We would also like to acknowledge Brian Eby, Stewart Simonett, Charlie Bradley, and Carl Miller of UMTRI for their assistance in conducting the tests.

### REFERENCES

- Arbogast, K. B., Moll, E. K., Morris, S. D., Anderko, R. L., Durbin, D. R., and Winston, F. K. (2000). Factors influencing pediatric injury in side impact collisions. Proceedings of the 44<sup>th</sup> Annual Conference of the Association for the Advancement of Automotive Medicine. AAAM, Chicago, Ill., p. 407-428.
- Brown, J., Kelly, P., and Griffiths, M. (1997). A comparison of alternative anchorage systems for child restraints in side impacts. Child occupant protection, SAE, Warrendale, p. 87-92. Report No. SAE 973303.
- Brown, J., Kelly, P., Griffiths, M., Tong, S., Pak, R., and Gibson, T. (1995). The performance of tethered and untethered forward facing child restraints. Proceedings of the International IRCOBI Conference on the Biomechanics of Impacts. IRCOBI, Bron, p. 61-74.
- Esselman, K. (2004). Personal communication with authors.

Irwin, A. L., Mertz, H. J., Elhagediab, A. M., and Moss, S. (2002). Guidelines for assessing the biofidelity of side impact dummies of various sizes and ages. *Stapp Car Crash Journal*, 46:297-319.

Kamren, B., Kullgren, A., Lie, A., Skoeld, B.-A., and Tingvall, C. (1993). Side protection and child restraints - accident data and laboratory test including new test methods. Thirteenth International Technical Conference on Experimental Safety Vehicles, Proceedings. Washington, D.C., NHTSA, 1993, p. 341-345.

Klinich, K. D., Ritchie, N., Manary, M. A., Reed, M. P., and Schneider, L. W. (2005). Evaluation of the Q3S under Far-Side Impact Loading. UMTRI final report.

Langwieder, K., Hell, W., and Lowne, R. (1997). Development of a sled-based impact test for child restraints in side collisions. Proceedings of Second Child Occupant Protection Symposium. Society of Automotive Engineers, Warrendale, Pa. p. 207-216. Report No. SAE 973313.

Langwieder, K., Hell, W., and Willson, H. (1996). Performance of child restraint systems in real-life lateral collisions. Fortieth Stapp Car Crash Conference Proceedings. Warrendale, SAE, p. 391-404. Report No. SAE 962439.

Langwieder, K., Hummel, T., and Finkbeiner, F. (1999). Injury risks of children in cars depending on the type of restraint. *Child Occupant Protection in Motor Vehicle Crashes*. Proceedings. Bury St. Edmonds, Professional Engineering Publishing, Ltd., p. 37-56.

National Highway Traffic Safety Administration . (2002). Advanced Notice of Proposed Rulemaking (ANPRM) to Add a Side Impact Test to FMVSS No. 213. Docket No. NHTSA-02-12151,RIN 2127-AI83.

Paton, I. P., Roy, A. P., and Lowne, R. (1998). Development of a sled side impact test for child restraint systems. Sixteenth International Technical Conference on Experimental Safety Vehicles, Proceedings. NHTSA, Washington, D.C., p. 2179-2184. Report No. 98-S10-O-09.

Tylko, S. (2004). Personal communication with authors.

van Ratingen, M. R. and Twisk, D. R. (1999). Comparison of the Q3 and P3 dummy kinematics and

kinetics in frontal and oblique impacts. *Child Occupant Protection in Motor Vehicle Crashes*. Bury St. Edmonds, Professional Engineering Publishing, Ltd., p. 145-158.

van Ratingen, M. R., Twisk, D., Schrooten, M., Beusenberg, M. C., Barnes, A., and Platten, G. (1997). Biomechanically based design and performance targets for a 3-year-old child crash dummy for frontal and side impact. *Child occupant protection*. SAE, Warrendale, p. 243-260.

Weber, K. (2005). Personal communication with authors.

# THE EFFECT OF REAR ROW SEATING POSITION ON THE RISK OF INJURY TO BELTED CHILDREN IN SIDE IMPACTS IN PASSENGER CARS

**Matthew R. Maltese**

**Irene G. Chen**

The Children's Hospital of Philadelphia

**Kristy B. Arbogast**

The Children's Hospital of Philadelphia and

The University of Pennsylvania

United States

Paper Number 05-0281

## ABSTRACT

Several studies have characterized the benefits of rear seating on injury outcome in children. While most studies have focused on frontal impacts, our previous work demonstrated that these benefits apply to side impacts as well. In this earlier study, however, results indicated that among those rear seated, the side impact injury risk did not vary by seat position, i.e. those on the struck side had similar injury risk to those on the non-struck side. In that study, the center rear occupants were grouped with the non-struck side occupants, and compared with the struck side. The present analyses built upon that previous work and sought to further explore and explain those results by studying the effect of the three distinct rear seat positions (struck-side, center, non-struck-side) in side impacts in a sample limited to seat belt restrained children. Data were obtained from a probability sample of 592 children, representing 6370 children, 4-15 years of age who were enrolled in an on-going crash surveillance system which links insurance claims data to validated telephone survey and crash investigation data. The sample was limited to children restrained by seat belts involved in side impact crashes and seated in the rear seating rows. The risk of injury was calculated for each seating position - struck, center or non-struck side of the crash. Injuries were defined as scalp and facial lacerations, facial bone fractures, and all other AIS 2 and greater injuries. Risk of injury was lower to children seated on the non-struck-side (1.4%) as compared to those on the struck-side (2.6%) (OR:0.55 95% CI: 0.33 0.93). Of interest, the injury risk to children seated on the struck side (2.6%) was roughly equal to that of those in the center rear position (3.0 %) (OR: 1.15, 95% CI: 0.50, 2.66). Accounting for differences in child age did not change the aforementioned results. These results highlight the elevated injury risk for children in center rear seating position in side impacts, and suggest that the injury mitigation approach is unique to that of the other rear seating positions.

## INTRODUCTION

Many researchers have examined the role of seat position on injury outcome for children in motor vehicle crashes. In a study of children in the Fatal Analysis Reporting System (FARS), Braver et al [1] concluded that rear seating offered protective benefit over front seats, and children were 10 to 20 percent less likely to sustain fatal injuries in the rear center than in rear outboard seat positions. Berg et al [2], in a study of a single state database of crashes, found that children seated in the front seat positions were 1.7 times more likely to suffer a serious injury or fatality than those in the rear seat, and also found that the mean inpatient hospital charges were greater for front seat child passengers (\$248.18) than children in the rear (\$194.74). More recent studies have examined the role of seat position on injury outcome in side impacts. Durbin et al. [3], in a study of a large child specific surveillance system, examined side impact crashes involving children and found a protective benefit of rear seat struck-side seating as compared to front seat struck-side seating. Others have chosen to study the effect on struck side seating versus non- struck side. In a study focused on adult occupants in the front outboard seat positions, Farmer et al. [4] examined the National Automotive Sampling System: Crashworthiness Data System (NASS/CDS) database and found that, among non-ejected occupants of vehicles which did not roll over, the likelihood of serious injury was only 3% for those on the near side and 2% for those on the far side. Howard et al [5] conducted a study of children aged 0 to 12 years in all seating rows involved in side impacts. Through analysis of the Fatality Analysis Reporting System (FARS), Howard found that for restrained children, the children seated on the near side were 2.5 times as likely to receive a fatal injury than children seated in the center, and also found through analysis of NASS that among children known to be restrained, severe injury (ISS  $\geq$  16) was much more common for those seated in the near-side seat (7 per 1,000) than for those in the center (2 per 1,000). Neither of these analyses accounted for

restraint type. Using the child specific surveillance system as Durbin et al above, but with a side impact population limited to children in forward facing child restraint systems, Arbogast et al<sup>6</sup> found that the injury risk was significantly higher for struck-side occupants in the rear row (8.9 injured children per 1000 crashes) as compared to non-struck-side and center seat occupants combined (2.1 injured children per 1000 crashes).

Most of the above analyses either include children restrained in all types of restraints or are limited to children restrained in add-on restraint systems (i.e. child restraints and booster seats). Vehicle and restraint design techniques to mitigate injuries for children in side impact crashes in these varying restraint systems are likely different. In particular, protection of older children who have outgrown, and therefore do not use, add-on child restraints cannot rely on the presence of an add-on restraint system to modulate impact forces. Understanding the injury risk for these seat belt restrained children is a critical first step in injury mitigation efforts. For this reason, the objective of this paper is to examine the injury risk by rear row seating position for children restrained by seat belts alone in side impact crashes. By defining the unique injury risks for the three-rear row seating positions, vehicle design improvements can be facilitated. We have restricted the analysis to passenger cars only, since there are significant structural differences (sill height, seat location, door design) between passenger cars and other vehicles that commonly carry children, such as sport utility vehicles and minivans.

## **METHODS**

Data for the current study were drawn from the Partners for Child Passenger Safety (PCPS) program, collected from December 1, 1998 to November 30, 2002. A description of the study methods has been published previously [7]. PCPS consists of a large scale, child-specific crash surveillance system: insurance claims from State Farm Insurance Co. (Bloomington, IL) function as the source of subjects, with telephone survey and onsite crash investigations serving as the primary sources of data. Vehicles qualifying for inclusion were State Farm<sup>TM</sup>-insured, model year 1990 or newer, and involved in a crash with at least one child occupant  $\leq 15$  years of age. Qualifying crashes were limited to those that occurred in fifteen states and the District of Columbia, representing three large regions of the United States (East: NY, NJ, PA, DE, MD, VA, WV, NC, DC; Midwest: OH, MI, IN, IL; West: CA, NV, AZ). After policyholders consented to participate in

the study, limited data were transferred electronically to researchers at The Children's Hospital of Philadelphia and University of Pennsylvania. Data in this initial transfer included contact information for the insured, the ages and genders of all child occupants, and a coded variable describing the level of medical treatment received by all child occupants (no treatment, physician's office or emergency department only, admitted to the hospital, or death). A stratified cluster sample was designed in order to select vehicles (the unit of sampling) for the conduct of a telephone survey with the driver. In the first stage of sampling, vehicles were stratified on the basis of whether they were towed from the scene or not, and a probability sample of both towed and non-towed vehicles was selected at random, with a higher probability of selection for towed vehicles. In the second stage of sampling, vehicles were stratified on the basis of the level of medical treatment received by child occupant(s). A probability sample from each tow status/ medical treatment stratum was selected at random with a higher probability of selection for vehicles in which a child occupant died, was admitted to the hospital, or evaluated in a physician's office or emergency department. In this way, the majority of injured children would be selected while maintaining sample representative of the overall population. If a vehicle was sampled, the "cluster" of all child occupants in that vehicle were included in the survey. Drivers of sampled vehicles were contacted by phone and screened via an abbreviated survey to verify the presence of at least one child occupant with an injury. Surveys were conducted only in English. All vehicles with at least one child who screened positive for injury and a 10% random sample of vehicles in which all child occupants screened negative for injury were selected for a full interview. A 2.5% sample of children untreated as of the crash report was included as well. The full interview involved a 30-minute telephone survey with the driver of the vehicle and parent(s) of the involved children. Only adult drivers and parents were interviewed. The median length of time between the date of the crash and the completion of the interview was six days. The eligible study population consisted of all 430,308 children riding in 288,187 State-Farm<sup>TM</sup>-insured vehicles newer than 1990 reporting a crash claim between December 1, 1998 and November 30, 2002.

Claim representatives correctly identified 95% of eligible vehicles, and 73% of policyholders consented for participation in this study. Of these, 18% were sampled for interview and an estimated 81% of these were successfully interviewed. Comparing the included sample with known population values from all eligible State Farm claims, little difference is

noted: in both the sample and the population 42%, 34%, and 24% of the vehicles were located in the East, Midwest, and West regions respectively; 52% of the sampled vehicles were model 1996 or newer, compared with 51% of the population; 55% were passenger cars, 20% passenger vans, 16% SUVs, and 7% pickup trucks, compared with 56%, 19%, 16% and 7% in the population; and 33% were towed away, compared with 32% of the population. The mean age of the child in the sample was 7.0 years, compared with 7.2 years in the population. For a subset of cases in which child occupants were admitted to the hospital or killed, in-depth crash investigations were performed. To date, over 600 cases have had field investigations completed. Cases were screened via telephone to confirm the details of the crash. Contact information from selected cases was then forwarded to a crash investigation firm (Dynamic Science, Incorporated, Annapolis, MD), and a full-scale on-site crash investigation was conducted using custom child-specific data collection forms. Crash investigation teams were dispatched to the crash scenes within 24 hours of notification to measure and document the crash environment, damage to the vehicles involved, and occupant contact points according to a standardized protocol. The on-scene investigations were supplemented by information from witnesses, crash victims, physicians, hospital medical records, police reports, and emergency medical service personnel. From this information, reports were generated that included estimates of the vehicle dynamics and occupant kinematics during the crash and detailed descriptions of the injuries sustained in the crash by body region, type of injury, and severity of injury. Delta  $v$ , (the instantaneous change in velocity) an accepted measure of crash severity, was calculated using WinSmash and crush measurements of the vehicles involved. For the purposes of this analysis, these cases were used to examine the validity of information obtained from the telephone survey.

### **Variable definitions**

Seating location and restraint use of each child were determined from a series of questions in the telephone survey. Among 170 children for whom paired information on seating position (front versus rear) was available from both the telephone survey and crash investigations, agreement was 99% between the driver report and the crash investigator ( $\kappa=0.99$ ,  $p<0.0001$ ). Among 164 children for whom paired information on restraint use was available from both the telephone survey and crash investigations, agreement was 89% between the driver report and the crash investigator ( $\kappa=0.74$ ,

$p<0.0001$ ). Direction of first impact was derived from a series of questions regarding the vehicle parts that were involved in the first collision. Survey questions regarding injuries to children were designed to provide responses that were classified by body region and severity based on the Abbreviated Injury Scale (AIS) score [8]. The ability of parents to accurately distinguish AIS 2+ injuries from those less severe has been previously validated for all body regions of injury [9]. Separate verbal consent was obtained from eligible participants for the transfer of claim information from State Farm to CHOP/Penn, for the conduct of the telephone survey, and for the conduct of the crash investigation. The study protocol was reviewed and approved by the Institutional Review Boards of both The Children's Hospital of Philadelphia and The University of Pennsylvania School of Medicine.

### **Data analysis and study sample**

Data were obtained from a probability sample of 592 children, representing 6370 children, 4-15 years of age. The sample was limited to children restrained by seat belts involved in side impact crashes and seated in the rear seating rows of passenger cars. The risk of injury was calculated for each seating position - struck, center or non-struck side of the crash. Injuries were defined as scalp and facial lacerations, facial bone fractures, and all other AIS 2 and greater injuries.

The robust chi-square tests of association were performed. Odds ratios (OR) were obtained from logistic regressions to approximate the relative risk of serious injury. Results of logistic regression modeling are expressed as unadjusted and adjusted OR with corresponding 95% confidence intervals (CI). Because sampling was based on the likelihood of an injury, subjects least likely to be injured were underrepresented in the study sample in a manner potentially associated with the predictors of interest. To account for this potential bias, data were analyzed by using SAS-callable SUDAAN: Software for the Statistical Analysis of Correlated Data, Version 8.0 (Research Triangle Institute, Research Triangle Park, NC, 2001) to account for sampling weights, sampling strata, and sampling units.

### **RESULTS**

Table 1 shows both distributions of child age group by seat position and seat position by child age group for the study sample. Those 4 to 8 years of age were the most common age group in the study sample. 57.3% of the children in the rear outboard struck-side

**Table 1.**  
**Distribution of child age by seat position for the study sample and crash side proximity.**

	Weighted row % Weighted column % (Unweighted n)			
	4-8 years	9-12 years	13-15 years	Total (seating position)
Rear Outboard Struck-side	57.3 43.7 (112)	29.5 35.4 (90)	13.2 50.1 (45)	100.0 (247)
Rear Outboard Non-struck-side	46.5 34.2 (107)	44.1 51.6 (94)	9.4 34.9 (41)	100.0 (242)
Rear Center	67.1 22.7 (64)	24.1 13.0 (27)	8.8 15.0 (12)	100.0 (103)
Total (age group)	100.0 (283)	100.0 (211)	100.0 (98)	100.0 (592)

position, 46.5% of the children in the rear out-board non-struck side, and 67.1% of the children in the rear center were in the 4 to 8 year old age group (Chi-square test:  $p=0.14$ ). Children seated in the rear center position tended to be younger; 22.7% of 4-8 year olds were seated in the rear center, as opposed to 13.0% of 9-12 and 15.0% of 13-15 year olds.

Table 2 displays both distributions of seat belt type by seat position/crash side proximity, and seat position/crash side proximity by seat belt type.

**Table 2.**  
**Distribution of seat belt type by seat position and crash side proximity.**

	Weighted row % Weighted column % (Unweighted n)				
	Lap only	Lap/ Shoulder	Shoulder	Unknown	Total (seating position)
Rear Outboard Struck-side	8.4 17.1 (29)	87.1 47.4 (208)	4.3 68.2 (5)	0.2 7.2 (5)	100.0 (247)
Rear Outboard Non-struck-side	4.4 8.7 (24)	91.9 48.8 (208)	2.0 31.9 (7)	1.6 50.4 (3)	100.0 (242)
Rear Center	81.4 74.3 (85)	15.6 3.8 (15)	0.0 0.0 (0)	3.0 42.4 (3)	100.0 (103)
Total (belt type)	100.0 (138)	100.0 (431)	100.0 (12)	100.0 (11)	100.0 (592)

Children in the rear outboard seating positions were most frequently restrained in lap / shoulder belts (87.1% to 91.9%, depending on seat position), while children in the rear center position were more frequently in lap only belts (81.4%) (Chi-square test:  $p<0.001$ ).

Injury risk varied by seat position. For all ages combined, those seated in the rear center had similar injury risk (3%) to those in the rear outboard struck-side (2.6%) (Figure 1). These two seating positions were at elevated risk compared to the rear outboard non-struck-side (1.4%). This pattern remained the same for both the 4-8 year olds and the 9-12 year olds. Those 13-15 years, few of which were seated in the center rear, had the highest injury risk when seated on the rear outboard non-struck-side (4.6%) followed by the rear outboard struck-side (3.7%).

Multivariate logistic regression was employed to account for the varying age distribution by seat position highlighted in Table 1. Adjusted for age, the risk of injury was lower to children seated on the non-struck-side as compared to those on the struck-side (OR:0.55 95% CI: 0.33 0.93). Of importance, the injury risk to children seated in the center rear was roughly equivalent to that of those on the struck side (OR: 1.15, 95% CI: 0.50, 2.66).

## DISCUSSION

Based on a study of seat belt restrained children in side impact crashes, results of this study confirm previous reports that children seated on the struck-side of the crash have an higher risk of injury than those seated on the non-struck-side. In particular, of children restrained in seat belts, those on the non-struck-side are at a 45% reduction in injury risk as compared those seated on the struck side, even after accounting for the potentially confounding effects of age.

Of most importance, no statistically significant difference in risk of injury was noted between children seated in the center rear and those seated on the struck-side. This finding was relevant for those 4-12 years of age, an age group in which children are transitioning out of add-on child restraints with significant side structure that can be used to mitigate injuries. Children of this age group are typically using either adult seat belts or belt positioning booster seats for their restraint and have an elevated risk of interacting with the vehicle interior surface than their younger counterparts.

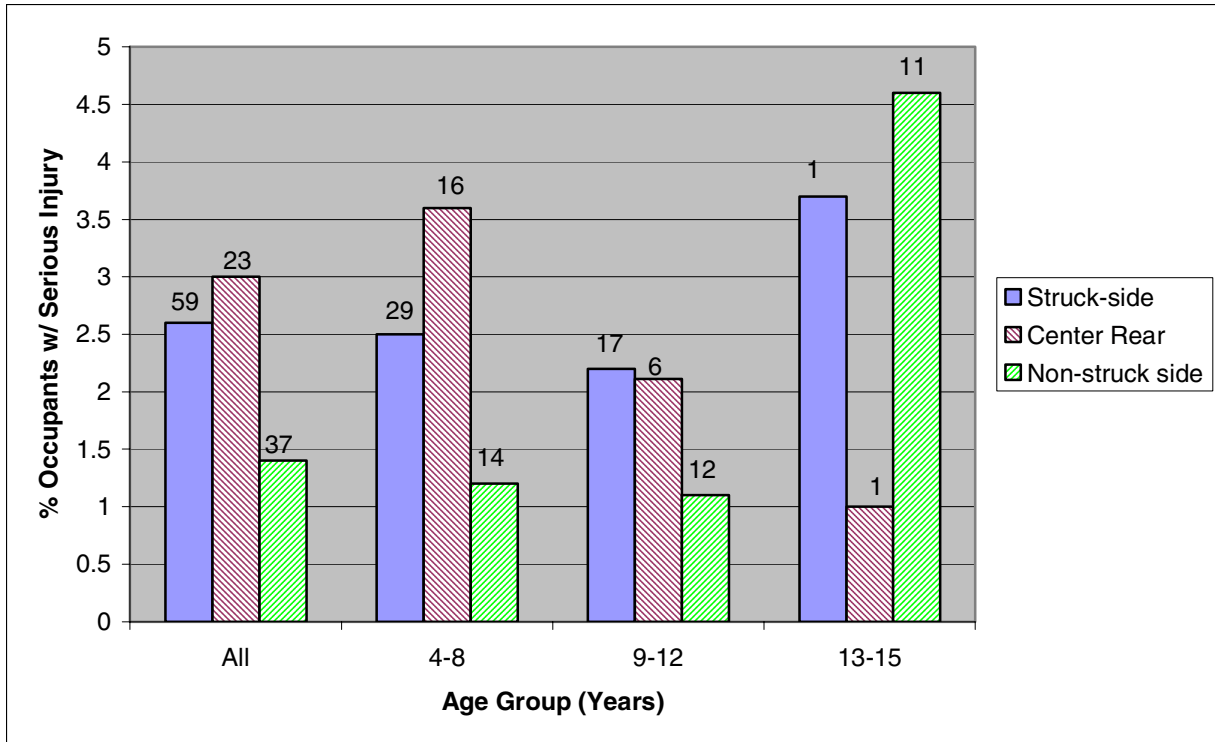


**Figure 1 - Risk of Serious Injury by Occupant Age Group and Seat Position on the Rear Row. Numbers above bars are the unweighted sample size.**

The present analysis is not the first comparison of the struck-side and center rear side impact environments in a nationally representative sample. Howard et al<sup>5</sup> examined the injury risk across the rear seat in restrained children in side impact crashes using NASS-CDS. In contrast to the findings of equal risk between struck-side and center rear in the present study, Howard et al found that serious injury was much more common for those in the struck-side seat position (7 per 1,000 children) than for those in the center (2 per 1,000). There are some methodological differences between the present study and the Howard work that may help explain the contrast in findings. First and foremost, Howard et al included children in all restraint types, whereas the present study includes only seat belt restrained occupants. Research on the effectiveness of child safety seats has found them to reduce fatal injury by 71 percent for infants (less than 1 year old) and by 54 percent for toddlers (1-4 years old) in passenger cars [10], as compared to lap/shoulder belts which reduce the risk of fatal injury to front-seat passenger car occupants by 45 percent [11]. Thus, if the CRS restraint use frequency is higher in the center rear as compared to the outboard rear positions, then the NASS-based finding that the center rear occupant’s risk is less than the struck-side occupants risk may be due to a change

to a safer restraint design, as well as the point of impact proximity factors already delineated by Howard et al. Second, Howard et al utilized the National Automotive Sampling System (NASS) dataset that, as described by Newgard and Jolly [12], contains relatively few children for a population-based sampling system, and these limitations may influence NASS-based results. Third, Howard et al assessed serious injury based upon whether or not the occupants Injury Severity Score (ISS) score exceeded 15, whereas the present analysis assigned serious injury if the occupant received an AIS 2 or greater injury and includes injuries ranging in severity from concussions to more serious brain injuries. Whether the range of injury severity varies by seating position within the outcome category of “injury” cannot be determined in the present study. The methodology used for the PCPS crash surveillance system utilized in the present study allows for the enrollment of large numbers of crashes involving children and thus addresses the second limitation highlighted above, however it precludes determination of specific AIS severity for each injury, and thus ISS, so no precise repeat of the Howard et al methods is possible with the PCPS dataset. Future work will extend the results presented herein by using the crash investigation component of the PCPS study to further

elucidate the effects of seating position on risk of injury suggested in these analyses, and to suggest countermeasures to prevent these injuries. In this approach, more detailed information on the nature and severity of the injuries as well as the location and direction of crash impact and crash severity, a critical factor in side impact protection, is obtained. We hypothesize that this future analysis will elucidate differing injured body region patterns between the center and struck-side seat position.

The role of occupant-to-occupant contact in determining injury outcome cannot be discounted in side impact crashes. Sherwood et al [13], in a case study of 37 child-involved side impact fatal crashes, found two cases where the child fatality was caused by contact with other unrestrained (adult) occupants. Cummings and Rivara [14] found a small fatality risk increase for an adult occupant involved in a side impact if there was another unrestrained occupant seated next to them as compared to another restrained occupant. Future analyses will explore the role of this parameter in injury causation within this study sample.

Results presented herein also have relevance to the proposed upgrade to the US side impact standard [15], which notably includes both the 50<sup>th</sup> percentile male and 5<sup>th</sup> female size crash test dummies. The 5<sup>th</sup> female dummy, in particular, is approximately the same size as 50<sup>th</sup> percentile 12 year old. According to Figure 1 above, the 13 – 15 year old age groups were frequently at the highest injury risk relative to other age groups, and should be similar in size to the 5<sup>th</sup> female and 50<sup>th</sup> male dummies proposed in the side impact standard upgrade. However, the current proposed regulatory upgrade is focused on struck side occupants. This data suggests that for this age group in particular the center and non-struck side occupant should also be considered.

In addition to the side impact standard, the regulatory landscape for the rear seat is changing in that lap shoulder belts will now be required for the center rear. Our data set which includes vehicles from model year 1990 to the present, contains both vehicles with a lap only belt in the center rear as well as those with a lap shoulder belt. Our previous work [16] has highlighted in the benefits of a lap shoulder belt restraint in the center rear for injury mitigation in crashes of all directions. Effects of this technology change on the results of this study will be considered in future work.

## **Limitations**

This research is conducted on crashes involving State Farm Insurance Co. policyholders only. State Farm is the largest insurer of automobiles in the United States, with over 38 million vehicles covered; therefore, its policyholders are likely representative of the insured public in this country. The surveillance system is limited to children occupying model year 1990 and newer vehicles insured in 15 states and the District of Columbia. Our study sample represents the entire spectrum of crashes reported to an insurance company including property damage only, as well as bodily injury crashes. While our sample included a significant number of vehicles with intrusion into the occupant compartment, it is possible that the PCPS study does not have a representative sample of the most severe crashes. Nearly all of the data for this study were obtained via telephone interview with the driver/parent of the child and is, therefore, subject to potential misclassification. On-going comparison of driver-reported child restraint use and seating position to evidence from crash investigations has demonstrated a high degree of agreement. There may be over-reporting of those using both portions of a lap shoulder belt when in fact, the shoulder portion of the belt was behind their back or under their arm.

## **CONCLUSION**

These results highlight the elevated injury risk for seat belt restrained children in center rear seating position in side impacts, and suggest that the injury mitigation approach in the center seat is unique to that of the other rear seating positions. Vehicle manufacturers and researchers should devote resources to understanding injury mechanisms and injury sources for children restrained in this seat position.

## **ACKNOWLEDGEMENTS**

The authors wish to express their thanks to Michael Elliot and Michael Kallan of the University of Pennsylvania, and Kennerly Digges and Nick Tambora of the George Washington University for their contributions to this manuscript. Funding for this work was partially provided by private parties, who have selected Dr. Kennerly Digges (and FHWA/NHTSA National Crash Analysis Center (NCAC) at the George Washington University) to be an independent solicitor of and funder for research in motor vehicle safety, and to be one of the peer reviewers for the research projects and reports.

Neither of the private parties have determined the allocation of funds or had any influence on the content of this report. The authors would also like to acknowledge the commitment and financial support of State Farm Mutual Automobile Insurance Company for the creation and ongoing maintenance of the Partners for Child Passenger Safety (PCPS) program, the source of crash investigation data for this study. The authors also thank the many State Farm policyholders who consented to participate in PCPS. The opinions contained herein are the opinions of the authors and not of State Farm™.

## REFERENCES

1. Braver ER, Whitfield R, Ferguson SA. 1998. "Seating Positions and Children's Risk of Dying in Motor Vehicle Crashes." *Injury Prevention* Vol. 4:181-187.
2. Berg MD, Cook L, Corneli HM, Vernon DD, Dean JM. 2000. "Effect of Seating Position and Restraint Use on Injuries to Children in Motor Vehicle Crashes". *Pediatrics* Vol. 105, No. 4.
3. Durbin DR, Elliott M, Arbogast KB, Anderko RL, Winston FK. 2001. "The Effect of Seating Position on Risk of Injury for Children in Side Impact Collisions." *Annu Proc Assoc Adv Automot Med*. Vol 45:61-72.
4. Farmer CM, Braver ER, Mitter EL. 1997. "Two-Vehicle Side Impact Crashes: The Relationship of Vehicle and Crash Characteristics to Injury Severity". *Accid. Anal. And Prev*. Vol 29 No 3 pp 399-406.
5. Howard A, Rothman L, McKeag AM, Pazmino-Canizares J, Monk B, Comeau JL, Mills D, Blazeski S, Hale I, German A. 2004. "Children in side-impact motor vehicle crashes: seating positions and injury mechanisms." *J Trauma*. Jun;56(6):1276-85.
6. Arbogast KB, Chen I, Durbin DR, Winston FK. 2004. "Injury Risks for Children in Child Restraint Systems in Side Impact Crashes." *Proceedings of International Research Council on the Biomechanics of Impact Conference*.
7. Durbin, DR, Elliott M, Arbogast KB, Anderko RL, Winston, FK. 2001. "The Effect of Seating Position on Risk of Injury for Children in Side Impact Collisions." *Annu Proc Assoc Adv Automot Med* 45: 61-72.
8. Association for the Advancement of Automotive Medicine. 1990. "The Abbreviated Injury Scale, 1990 Revision." Des Plaines, Ill., Association for the Advancement of Automotive Medicine.
9. Durbin, DR, Winston FK, Applegate S, Moll E, Holmes J. 1999. "Development and validation of ISAS/PR: A new injury severity assessment survey." *Arch. Pediatr. Adol. Med* 153(4): 404-408.
10. Traffic Safety Facts 2003 Data - Children. National Highway Traffic Safety Administration, United States Department of Transportation. 2004 DOT HS 809 762.
11. Traffic Safety Facts 2003 Data – Occupant Protection. National Highway Traffic Safety Administration, United States Department of Transportation. 2004 DOT HS 809 765.
12. Newgard C and BT Jolly. 1998. "A Descriptive Study of Pediatric Injury Patterns from the National Automotive Sample System." 42<sup>nd</sup> Annual Proceedings of the Association for the Advancement of Automotive Medicine.
13. Sherwood CP, Ferguson SA, Crandall JR. 2003. "Factors leading to crash fatalities to children in child restraints." *Annu Proc Assoc Adv Automot Med*. 47:343-59.
14. Cummings P and FP Rivara. 2004. "Car Occupant Death According to the Restraint Use of Other Occupants" *J. Amer. Med. Assoc*. Vol 291, No. 3.
15. Federal Motor Vehicle Safety Standard No. 214 "Side Impact Protection" Code of Federal Regulations, 49 CFR 571.214 2004 United States Government Printing Office.
16. Arbogast KB, Durbin DR, Kallan MJ, Winston FK. 2004. "Evaluation of pediatric use patterns and performance of lap shoulder belt systems in the center rear." *Annu Proc Assoc Adv Automot Med*. 48:57-72.

# **CHILD SIDE IMPACTS: SIMULATION OF MID-SIZED SEDAN IN SIDE IMPACT TO DESCRIBE CRASH ENVIRONMENT**

**Nick Tamborra**

FHWA/NHTSA National Crash Analysis Center

The George Washington University

United States

Paper Number: 05-0381

## **ABSTRACT**

A structural and kinematic evaluation of a representative mid-size sedan subjected to lateral impacts with various crash partners is described. A detailed evaluation of the exterior crush, interior intrusion, and vehicle motion is provided using measurements and data from computational simulation. The mid-size sedan is struck by partner vehicles that cover a range of vehicle sizes common in the US fleet. These include a side impact with a small car, a mid-size car, a LTV, and a MDB. Specific focus on the rear seating row is included to develop impact data that will help to describe the crash environment for rear seated child occupants.

This portion of the project builds upon previous work that has examined mid-size sedans involved in real world side impacts and those tested in lateral impacts with regulatory and consumer metric test conditions. The long term goal of this project series is to create a detailed understanding of children involved in side impacts. This report provides insight into the range of possible intrusion patterns for various impact partners that may contact a rear seated child occupant. Future evaluations will then utilize this data to understand the sensitivity of injury for restrained children exposed to these crash conditions.

## **INTRODUCTION**

A cooperative effort by multiple research organizations is being conducted in order to examine child occupants involved in vehicle side impacts. The overall goal of this study is to develop an understanding of how children are being injured in side impacts and what can be done to reduce the risk. This process involves an examination of three fundamental factors of side impacts. These include the behavior of vehicles involved in side impact, the risk and mechanism of injury to children, and the role of countermeasures. A comprehensive understanding of these three

factors is needed prior to proposing and testing improvements that might reduce injury.

As described by previous research of child involved accidents (Arbogast, 2004), child injury in side impact is sensitive to compartment intrusion. Case reviews of accidents with injured children often cite intruding door panels, trim, or other interior components as the injury source. The most common injuries for the children in the age group of 1-3 years old for these crashes are injuries to the head and lower extremities. Farside or middle seated occupants are also subject to intrusion injury, but may be more susceptible to vehicle motion as is seen with farside adult occupants.

In the interest of producing data to support the development of a laboratory test condition that can assess child injuries from side impacts, it was decided that the early stages of the overall research project would focus on rear row crash conditions in side impacts. Children within the United States in the target age group, 1-3 years old, are shown to have high occupancy rates for rear seating rows. These can include nearside, farside, or middle seated children. They are also most commonly transported in sedans. Details are being sought to describe rear row interior intrusion and external crush patterns, and overall vehicle kinematics for various severities of side impacts for sedans. As stated in previous documentation surrounding this project (Tamborra, 2005), the assessment will broaden to other vehicle types at a later point.

## **SIDE IMPACT STUDIES**

A previous report on the topic of child side impacts illustrated the exterior crush patterns for mid-size sedans involved in field accidents and compared these with results of similar vehicles subjected to current side impact test methods (Tamborra, 2005). Additional summaries of similar studies conducted by many researchers were also considered as supporting data for the overall project. Similarities and differences between real world sedans involved in side impacts and those tested against various MDBs were described. The purpose of this

comparison was to start looking for crash conditions for rear seated restrained child occupants involved in side impacts.

In order to complement the data that was obtained from crash investigations and vehicle tests, computer simulation of side impacts is employed in this report. The use of simulation for this stage of the project offers insight into the specific interaction of structural members between the struck car and the striking vehicles. The simulation output can be examined in detail over the entire impact event by using the computational data output and graphics.

With conventional testing it is difficult to illustrate the exact manner in which vehicle structures interact with each other during the impact event. Transient crash data is available through the use of sensors and film analysis, and improvements in miniaturized cameras have expanded visual coverage. Engineers can use accelerometer timing, sensor contacts, and pre-crash geometric measures to understand how the vehicles may interact, but only in limited cases with external fascia removed, can one see exactly which parts are contacting. It remains a challenge in physical crash testing to be fully aware of component interaction and the effect this has on either the structural response of the vehicle or the injury measures captured by the ATDs.

Computer crash simulation has the benefit of being fully illustrated with component interaction clearly shown. In addition, data output for specific areas of interest is neither limited by physical constraints of instrumentation, nor is it influenced by the dynamic event itself, i.e. damaged sensors, rotating axis, channel noise. Researchers are able to view the exact deformation and interaction of any part that has been included in the model.

Simulation is however limited by how well the models are able to predict actual crash outcomes. Complex simulations involving occupants and vehicle interiors, as well as those with complex material models or contacts can be difficult to rely on. Simulation has been in use for several decades though and common practices employed by analysts can help to improve the simulation output.

The most appropriate way to employ simulation is to use it in tandem with physical testing and to draw out whatever information adds value to the research. For the purpose of this study the simulation will be used to examine

the potential structural response of a mid-size sedan impacted by several vehicles using a controlled setup and velocity. The models are able to help understand the potential crash environment that the rear seated child may be subjected to under these conditions. The cause and effect relationship between the crash partner and the crash outcome is illustrated by the simulation output.

## **INJURY AND SIDE IMPACT**

ATD injury response is often sensitive to minute variations in the exterior loading of a vehicle and the resulting impact between dummy and the interior. This is especially true in side impacts where the dummy is in close proximity to the impacting partner. Crash engineers can optimize ATD injury measures by balancing the localized loads that are exerted on the dummy. This often includes shoulder leads, pelvic blocks, arm rest positioning, and more recently airbag interaction. The interior trim that interacts with the ATD in side impact is mounted onto stiffer underlying structural components such as the b-pillar and door. Impacts that might put the dummy and countermeasures out of balance or alignment may subject the dummy to unintended load paths. Although considerable margins of safety can be built into the side impact load paths, deviations can occur due to the influence of the impacting partner.

When considering children restrained in the rear seating row of vehicles, the range of body position is diverse and depends on the type of restraint. Children in child seats may be perched higher and more forward than those seated on bolsters in seatbelts. Differences in head or chest locations can vary for children just a few years of age apart and all of these may differ from adults. It is therefore important to determine the structural response of a vehicle for a range of impacting partners in order to determine an expected boundary of structural deformation. Vehicle reinforcements optimized for specific crash inputs can then be exercised in a variety of impacts and an overall crush and kinematics profile can then be considered for an eventual subsystem test. By looking beyond singular crash events there should be opportunity to develop a robust test methodology that will help to assess injury for a broad range of impacts.

**METHODS**

This report covers the side impact of a mid-size sedan by multiple partner vehicles. These include a small sedan, a mid-size sedan, a LTV, and a MDB. The baseline crash condition is the US side NCAP test methodology using the NHTSA FMVSS-214 moving deformable barrier. The alignment of the barrier to the sedan and the input speeds are controlled for each impact. This process was selected in order to keep several variables common to help facilitate comparison.

The selection of impacting partners gives a satisfactory representation of current fleet vehicles for the United States. The spread in mass and the variation in build provide insight into the effects these have on the structural response of the struck car. Descriptions of the variation in front end construction for the four impacting partners is provided and insight into the cause and effect relationship is shown for how front end construction influences struck vehicle deformation.

The mid-size sedan was modeled with two forward facing child restraints installed in the rear outboard seating positions of the second row. These are models that are currently under development and will be used in future assessments with child ATD models. They were attached to the vehicle model using belt and tethers and are placed in outboard seating positions. The models were not included in the contact of the struck vehicle since the definition of the materials is incomplete. They are instead included to illustrate the kinematics of the child restraints in side impact to help to begin understanding the different challenges that a near and farside seated child may face. The child restraints were weighted to include the mass of a child seated on the restraint and should give an approximate description of how the seat moves during a side impact.

**SIDE IMPACT TEST AND OUTPUT**

The test mode used in this study is based on the US Side NCAP test procedure. The Taurus struck car will be impacted in the side by the four impacting vehicles using positioning and velocity values prescribed by the side NCAP procedure. The three bullet vehicles align themselves relative to the MDB by placing the vehicle longitudinal centerline at the MDB longitudinal centerline.

The following output is recorded for each simulation.

- Exterior maximum and residual crush along the length of the vehicle at four vertical heights
- Interior maximum and residual intrusion along the length of the vehicle at four heights
- Vehicle kinematics measured at various locations
- Interior trim shape and profile for rear seating rows

**MODEL DESCRIPTIONS**

Four different classes of vehicles are represented with finite element models. A brief description of each model is included for reference. Each model has been in existence for several years except for the Taurus model which is a pre-release version. All models were developed by the FHWA/NHTSA National Crash Analysis Center at The George Washington University under funding from the Department of Transportation. Many of the models are publicly available for use in safety research. Figure 1 provides an illustration of the four vehicles used as striking models and Table 1 provides a brief summary on model mass and size.

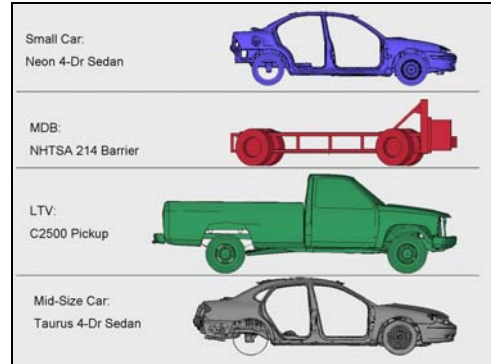


**Figure 1. Striking vehicle finite element models.**

**Table 1. Finite Element Model Summary**

Models	# Elms	Mass
Taurus (Struck)	876k	1462kg
Taurus (Striking)	505k	1476kg
Neon (Reduced)	200k	1242kg
C2500	18.6k	2015kg
214 Barrier	57k	1368kg
Vanguard CRS	19k	19kg

**Small Car**

The small car vehicle class is represented by a 1997 Dodge Neon four door sedan. A finite element model of this vehicle

was created by the NCAC Vehicle Modeling Lab and is publicly available for use in safety research. The vehicle model contains a complete representation of the Neon's body-in-white, mechanical drivetrain, and chassis. Rudimentary interior parts are available, but were not considered for use in the vehicle as a striking partner.



**Figure 2. Dodge Neon Small Car FEA Model (Reduced Striker Version).**

A reduced model was created from the detailed model in order to save simulation resources. Unnecessary components from the model were removed if they were deemed to be insignificant for the frontal impact of the Neon into the side of the Taurus. Adjustments to the vehicle mass were made in order to preserve the Neon's inertial properties.

**Mid-Size Car**

The mid-size vehicle class for this project is represented by a 2001 Ford Taurus four-door sedan. This vehicle served as both the baseline struck vehicle and as a striking vehicle. The Taurus model is an early version of the latest NCAC Vehicle Modeling Lab reverse engineering project. This model is a highly detailed recreation of a production Taurus sedan that features fully detailed structural BIW, interior components, drivetrain components, and suspension systems.

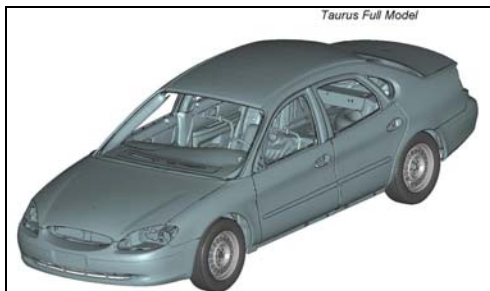


**Figure 3. Ford Taurus Mid-Size Sedan FEA Model (Full Version).**

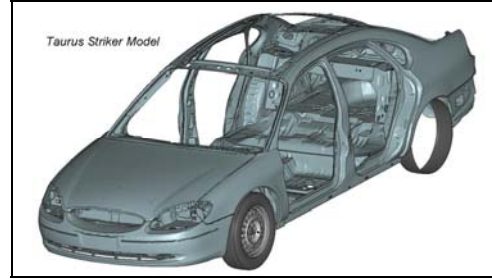


**Figure 4. Ford Taurus Mid-Size Sedan FEA Model (Reduced Striker Version).**

The striking model for the Taurus underwent a similar reduction process as the Neon in order to help reduce simulation time. Removal of rear components and rigidizing certain parts helped to reduce the runtime while having a minimal effect on the frontal performance of the Taurus as a bullet vehicle.

The baseline struck vehicle of the Taurus had several parts removed that were considered insignificant to a side impact vehicle. These included certain engine bay components and front passenger compartment interior components. This effort again helped to reduce the computational time while minimizing the affect on simulation output.

**LTV**

The LTV category is represented by a Chevrolet C2500 pickup truck developed at the NCAC Vehicle Modeling Lab. This vehicle model has been in use for nearly 10 years by researchers studying roadside hardware safety. The truck model features a detailed front end and suspension with a reduced representation of the rear pickup bed and passenger cabin.

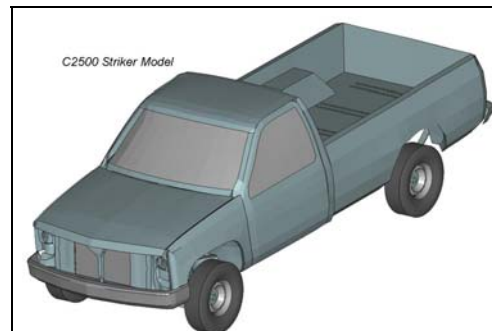


**Figure 5. Chevrolet C2500 Full-Size Pickup FEA Model.**

**Moving Deformable Barrier (MDB)**

The NCAC MDB barrier model was used for the program to represent the NHTSA specified FMVSS-214 impact barrier. The finite element model of the 214 barrier is fully compliant with the design specifications outlined

in the federal register although current efforts are underway to improve the material modeling for the deformable honeycomb elements.

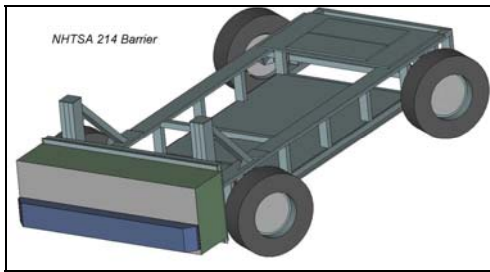


Figure 6. NCAC 214-Barrier MIDB FEA Model.

### Child Restraint

The struck vehicle Taurus is modeled with two forward facing Evenflo Vanguard child restraints installed in the outboard rear seating positions. The Vanguard CRS was reverse engineered in the NCAC Vehicle Modeling Lab and is starting to be used in several child safety research projects. This child seat is a representative example of convertible child seats and features most of the common features including LATCH straps, side wings, top-tether, movable feet, and a one-piece molded shell.

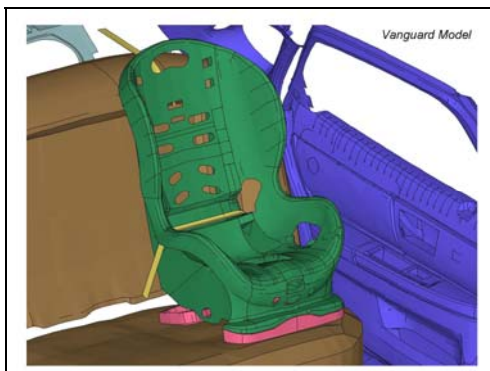


Figure 7. Evenflo Vanguard CRS FEA Model installed forward facing.

The CRS is installed in the two outboard rear seating positions for the Taurus rear bench seat. The child seats were installed assuming a vehicle belt installation. Actual child restraints were installed into a Taurus with measurements taken to approximate the location of the CRS. This location is different in the Taurus than a LATCH installed CRS since the Taurus lower LATCH anchors are shifted slightly inboard. The child seats were attached to the Taurus model using a lap belt routed through the forward facing belt guides and a top-tether strap attached to the upper anchor on the Taurus rear shelf. This is not an exact simulation

of a real installation since the Taurus features three-point belts in the outboard locations. Future simulations will improve the modeling of the belt system to include the upper shoulder belt as sled testing with three point belts has revealed that the movement of the CRS is affected by the shoulder belt depending on load direction.



Figure 8. Twin Vanguard CRS models in Taurus second row.

### DIMENSIONAL COMPARISON

The following series of figures illustrate the dimensions of the struck Taurus and the striking vehicles. Emphasis is placed on underlying structural components that affect performance in the side impact simulations. Illustrations of external sheet metal or fascia show the difference that can exist between components that are often included in external vehicle measurements, but have been shown to have minimal affect on the actual impact.

#### Struck Taurus Dimensions

Structural dimensions of the Taurus and Vanguard child restraint are provided in Figures 9 and 10. An illustration of the relative position of side impact countermeasures relative to the location of the child restraint is provided in Figure 11.

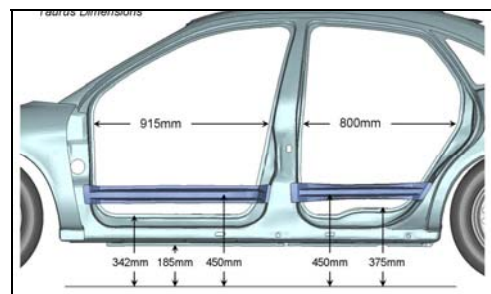


Figure 9. Taurus structural dimensions.

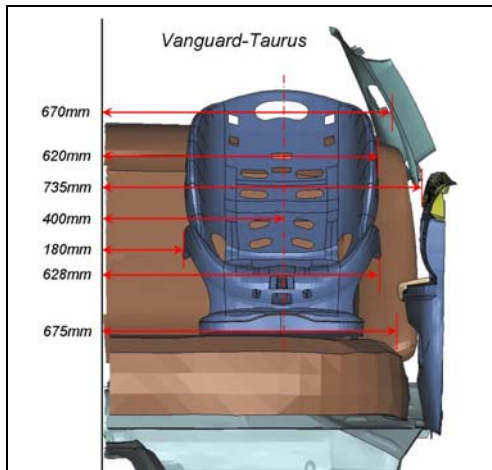


Figure 10. Vanguard/Taurus internal dimensions.

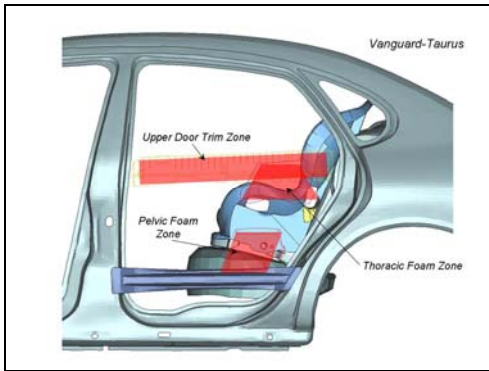


Figure 11. Vanguard/Taurus side impact occupant countermeasure overlap.

The reference system used for measuring external crush and internal intrusion is illustrated in Figure 12 and 13. This system is based on the US side NCAP protocol for pre and post crash test measurements. The system measures crush and intrusion at five levels, rocker, SID H-Point, mid-door, windowsill, and roof. The spacing along the longitudinal axis is 150mm with the origin located approximately 440mm rearward of the front axle centerline.

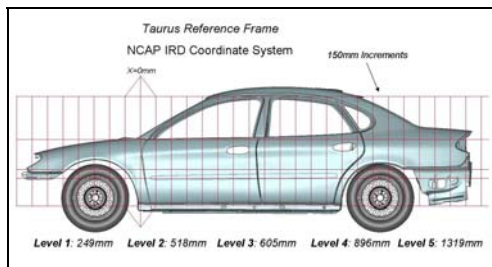


Figure 12. NCAP IRD Coordinate System for measuring external crush.

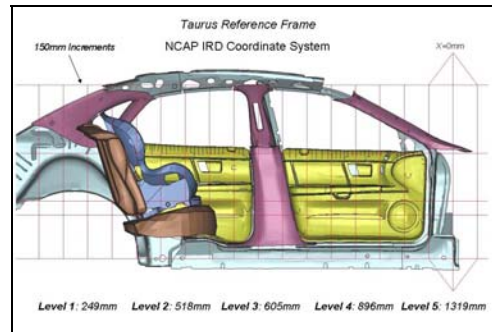


Figure 13. NCAP IRD Coordinate System for measuring internal intrusion.

### Striking Vehicle Dimensions

Figures 14-27 illustrate the dimensions for the striking vehicles used to impact the Taurus. Dimensions of external fascia and underlying structural components are provided. An illustration that compares the relative size of the actual vehicles to the MDB is also given in order to facilitate later discussions of the impact results.

Differences between the structural designs of the four vehicle types are illustrated in the images. The front structural bumper of the Neon and Taurus are narrower in width and height than their outer fascia. This is different from the C2500 whose structural bumper is the outer surface. The differences between the design of the MDB and the structural components of the vehicles are also illustrated. Previous research by many organizations has highlighted this, but these illustrations should provide useful detail on several specific examples.

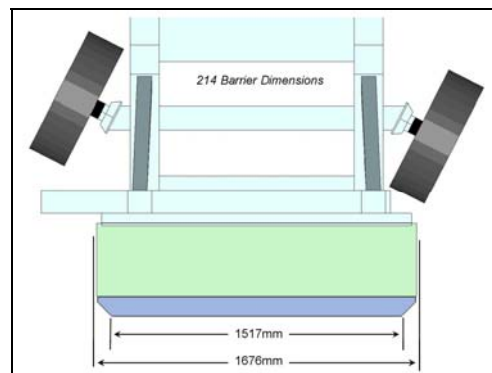


Figure 14. NHTSA 214-MDB dimensions.

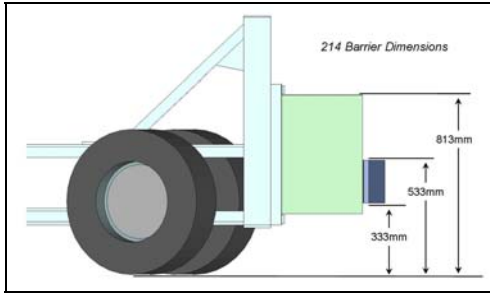


Figure 15. NHTSA 214-MDB dimensions.

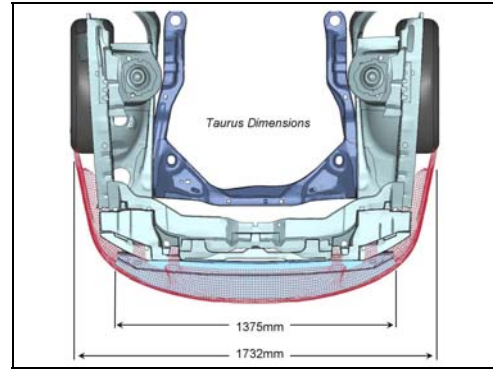


Figure 20. Taurus structural dimensions.

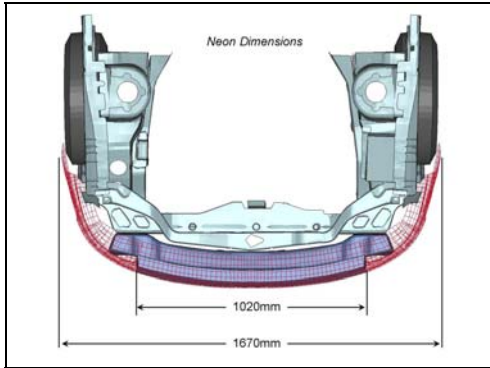


Figure 16. Neon structural dimensions.

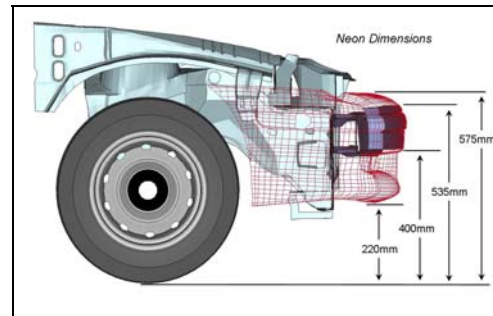


Figure 21. Taurus structural dimensions.

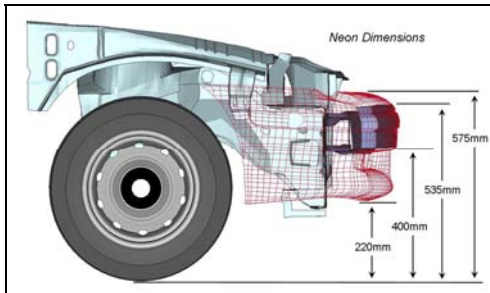


Figure 17. Neon structural dimensions.

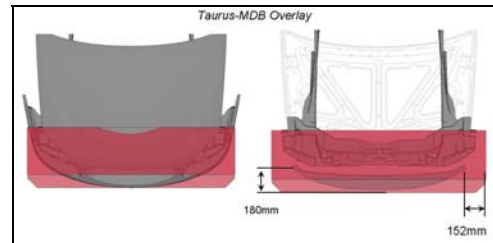


Figure 22. Taurus-MDB dimension comparison.

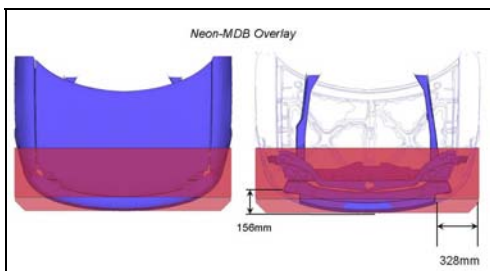


Figure 18. Neon-MDB dimension comparison.

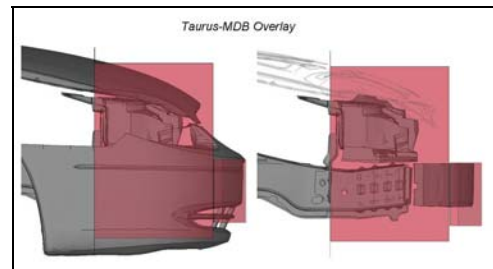


Figure 23. Taurus-MDB dimension comparison.

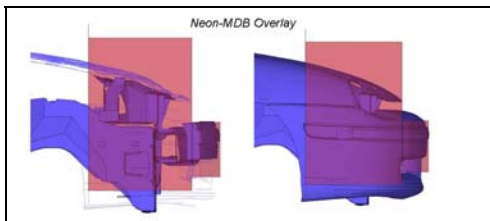


Figure 19. Neon-MDB dimension comparison.

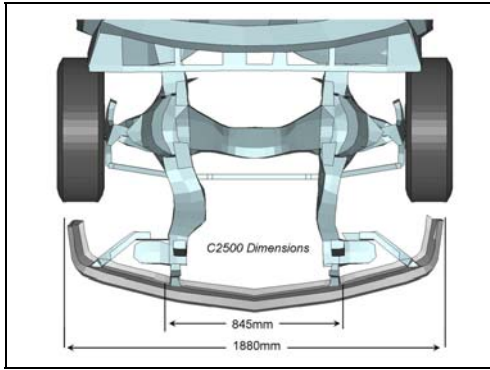


Figure 24. C2500 structural dimensions.

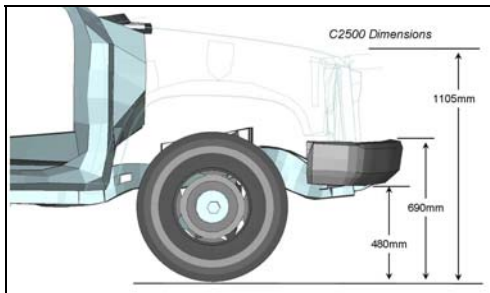


Figure 25. C2500 structural dimensions.

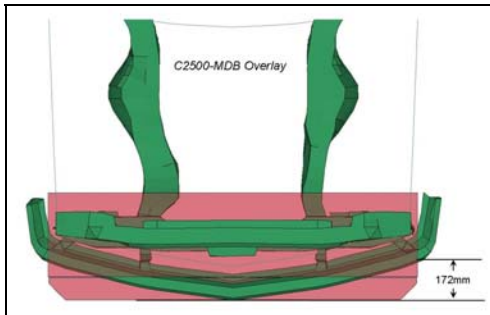


Figure 26. C2500-MDB dimension comparison.

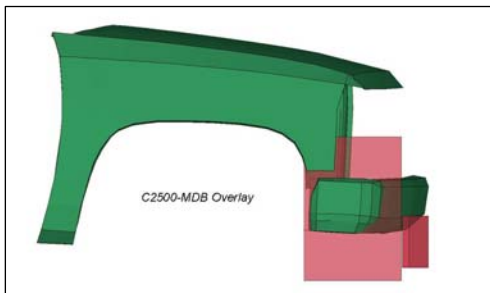


Figure 27. C2500-MDB dimension comparison.

### Vehicle Structural Component Overlap

Figures 28-31 provide an illustration of the overlap of the striking vehicle structural components and the struck Taurus. These images help to show which components of the struck car that are impacted by the striking vehicle. The red areas indicate the underlying components and not the outer fascia.

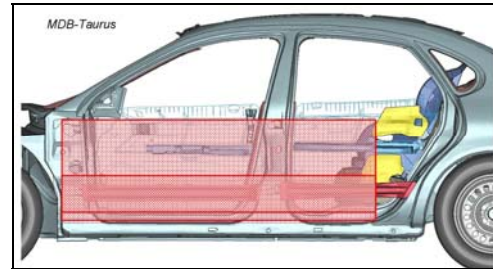


Figure 9. 214-MDB structural overlap with Taurus.

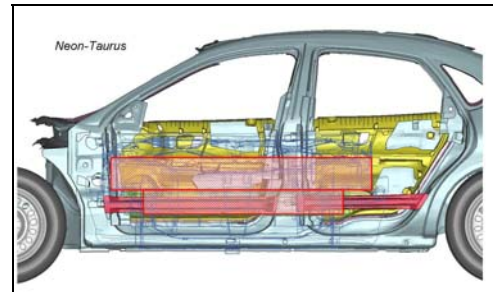


Figure 10. Neon structural overlap w/ Taurus.

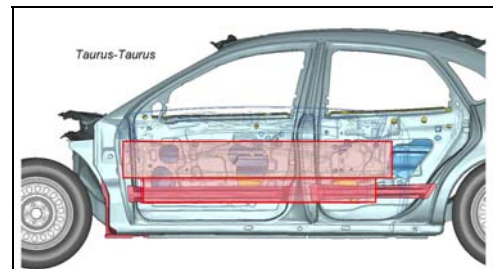


Figure 11. Taurus structural overlap w/ Taurus.

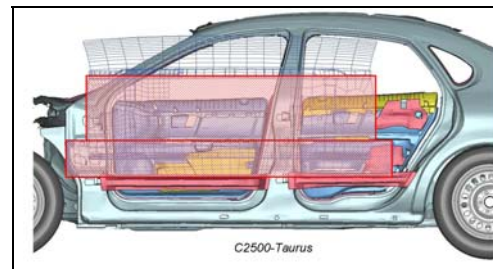


Figure 12. C2500 structural overlap w/ Taurus.

## RESULTS

### Individual Vehicle Crush/Intrusion Profiles

The plots shown in Figure 32-39 represent the residual post-crash position of the exterior sheet metal and interior trim surfaces relative to an exterior X-Z plane located just outboard of the widest part of the Taurus. The actual crush and intrusion values can be obtained by subtracting the ordinate value of the deformed curve from the corresponding original position of either the interior trim or exterior surface.

Tables with the values calculated are included for reference. Level-3 and 4 are only included due to space constraints, but all four levels are tabulated in Table 2.

Table 2 lists both the maximum dynamic values and the post-crash residual values for the crush and intrusion. Differences between the two values can range from 5-15% based on the springback of the Taurus structure. Timing for the peak values can be determined from the simulation results.

Included on each graph is an outline of a seated Q3 child dummy in the Vanguard child restraint. Head, pelvis, and lower extremities are marked with graphics and approximate actual dimensions. The outer edge of the child restraint shell is also depicted. This outline will illustrate the extent that the intrusion may interact with a rear child occupant. Note that the landmarks are in static pre-crash position.

**MDB-Taurus**

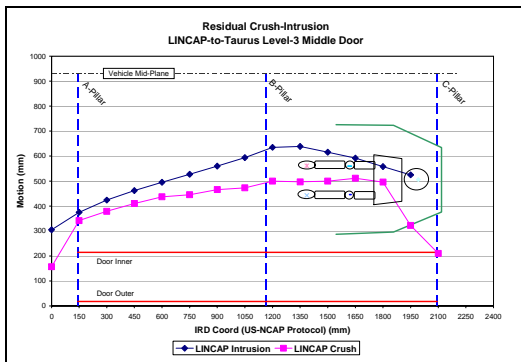


Figure 13. MDB-Taurus Level-3 (Mid-Door).

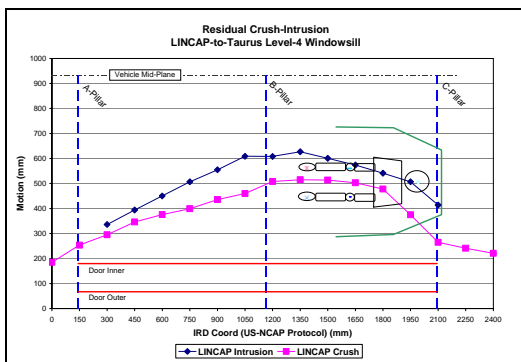


Figure 14. MDB-Taurus Level-4 (Windowsill).

**Neon-Taurus Impact**

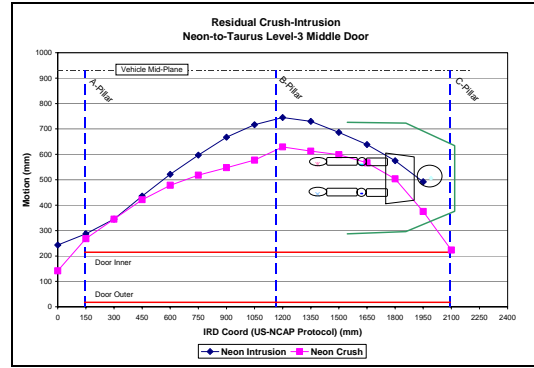


Figure 15. Neon-Taurus Level-3 (Mid-Door).

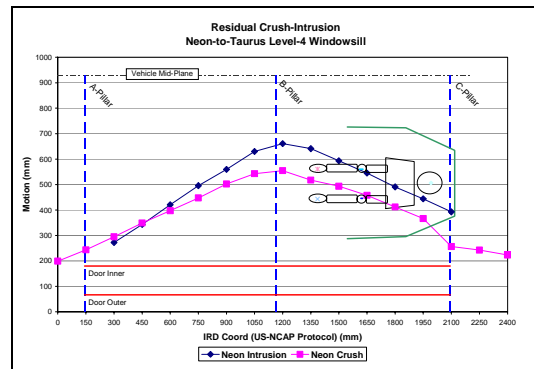


Figure 16. Neon-Taurus Level-4 (Windowsill).

**Taurus-Taurus Impact**

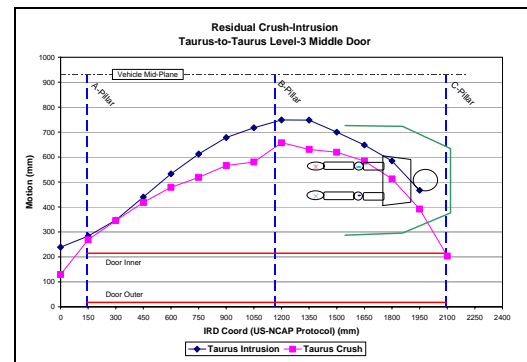


Figure 17. Taurus-Taurus Level-3 (Mid-Door).

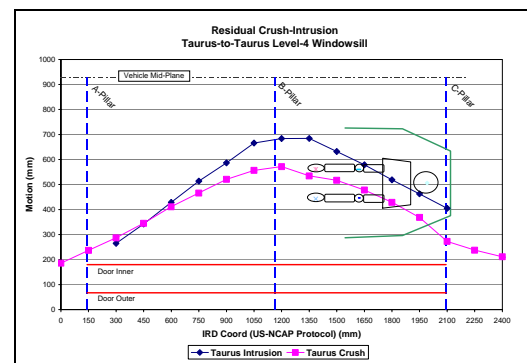


Figure 18. Taurus-Taurus Level-4 (Windowsill).

## C2500-Taurus

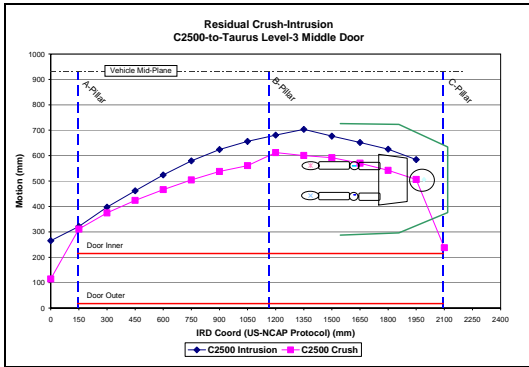


Figure 19. C2500-Taurus Level-3 (Mid-Door).

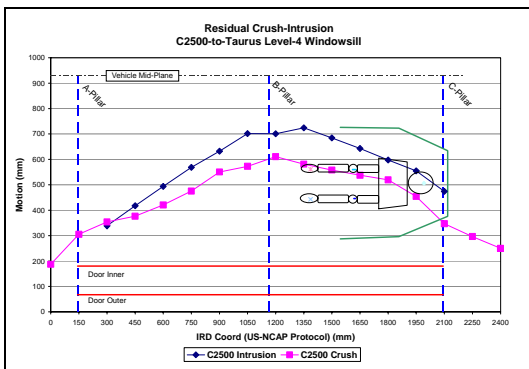


Figure 20. C2500-Taurus Level-4 (Windowsill).

### Total Vehicle Crush/Intrusion Comparison

The following plots shown in Figure 40-47 are presented to show the relative differences in the struck car performance for each impacting vehicle. These graphs help illustrate the different levels of expected exterior crush or interior intrusion for each of the four crash partners.

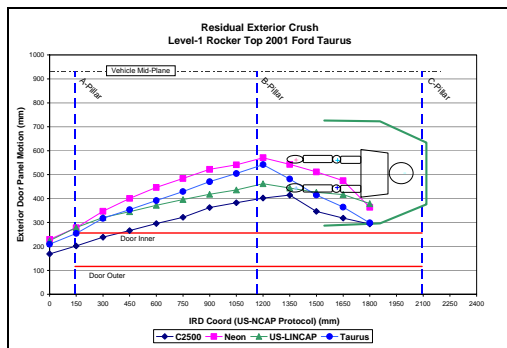


Figure 21. Taurus Level-1 (Rocker) residual exterior crush.

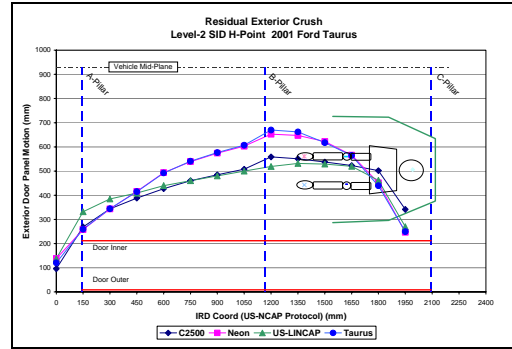


Figure 22. Taurus Level-2 (SID H-Point) residual exterior crush.

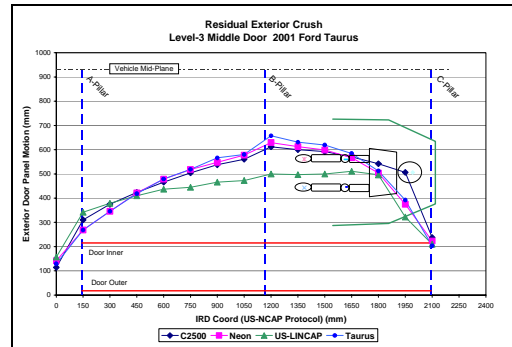


Figure 23. Taurus Level-3 (Mid-Door) residual exterior crush.

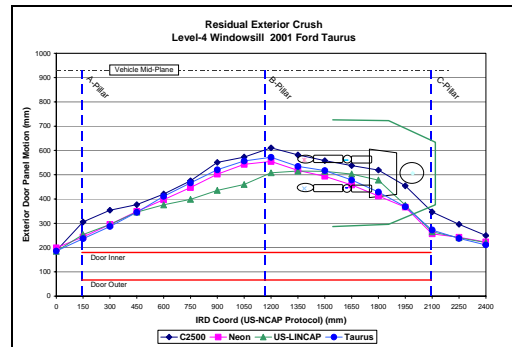


Figure 24. Taurus Level-4 (Windowsill) residual exterior crush.

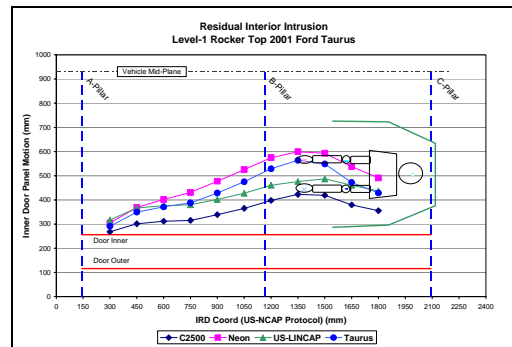


Figure 25. Taurus Level-1 (Rocker) residual interior intrusion.

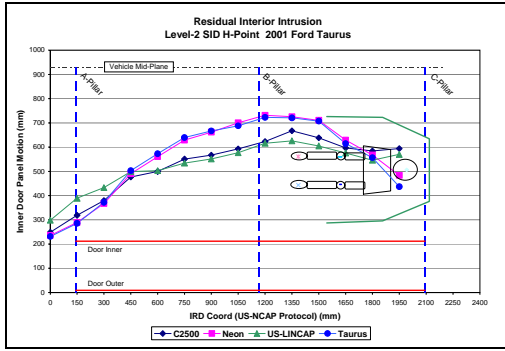


Figure 26. Taurus Level-2 (SID H-Point) residual interior intrusion.

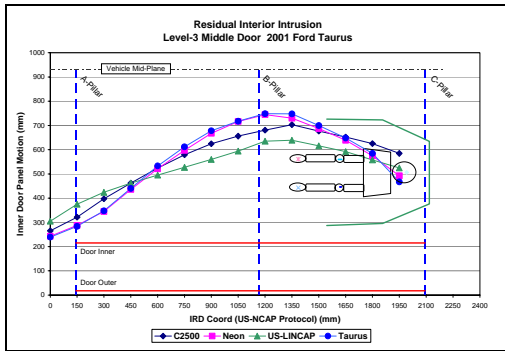


Figure 27. Taurus Level-3 (Mid-door) residual interior intrusion.

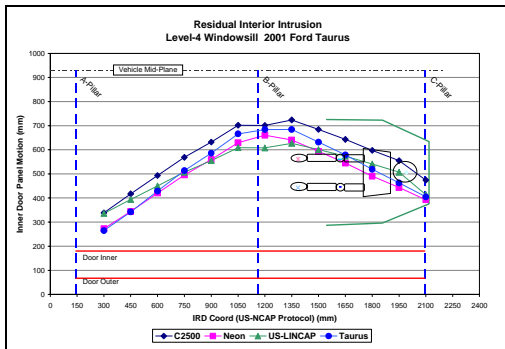


Figure 28. Taurus Level-4 (Windowsill) residual interior intrusion.

Table 2.  
Level 1-4 maximum and residual exterior crush and interior intrusions

Level-1 Rocker		Max (mm)	Residual (mm)
MDB	Crush	457	346
	Intrusion	350	231
Neon	Crush	538	454
	Intrusion	433	343
Taurus	Crush	499	426
	Intrusion	386	308
C2500	Crush	380	298
	Intrusion	253	167

Level-2 SID H-Point		Max (mm)	Residual (mm)
MDB	Crush	612	523
	Intrusion	504	414
Neon	Crush	704	644
	Intrusion	577	520
Taurus	Crush	717	661
	Intrusion	571	571
C2500	Crush	615	550
	Intrusion	521	455

Level-3 Mid-Door		Max (mm)	Residual (mm)
MDB	Crush	569	493
	Intrusion	506	424
Neon	Crush	667	611
	Intrusion	576	530
Taurus	Crush	695	640
	Intrusion	587	534
C2500	Crush	657	594
	Intrusion	554	488

Level-4 Windowsill		Max (mm)	Residual (mm)
MDB	Crush	509	448
	Intrusion	510	447
Neon	Crush	519	488
	Intrusion	498	481
Taurus	Crush	546	505
	Intrusion	546	546
C2500	Crush	595	544
	Intrusion	601	544

## KINEMATICS

Transient kinematic behavior of three struck side accelerometer locations and two non-struck locations are plotted in Figures 49-53. The location of the two rear door mounted accelerometers is shown in Figure 48 for reference.

Dynamic information for several locations is presented. These include the upper rear door beltline, rear door middle, lower struck side b-pillar, rear occupant compartment, and rear non-struck side rocker.

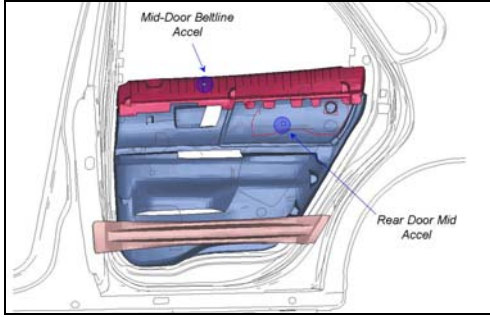


Figure 29. Rear door accelerometer locations.

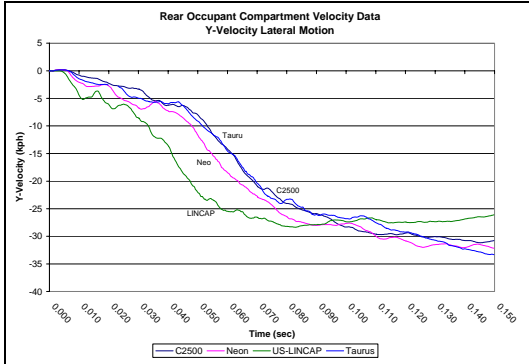


Figure 30. Rear occupant compartment Y-Velocity.

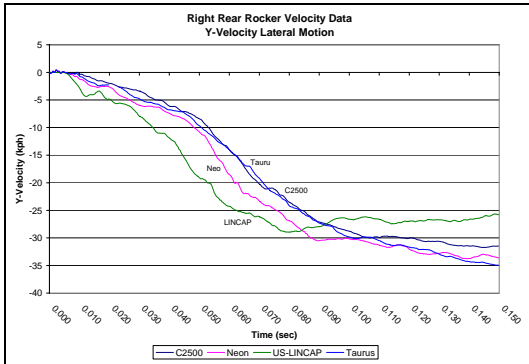


Figure 31. Right rear rocker (non-struck side) Y-Velocity.

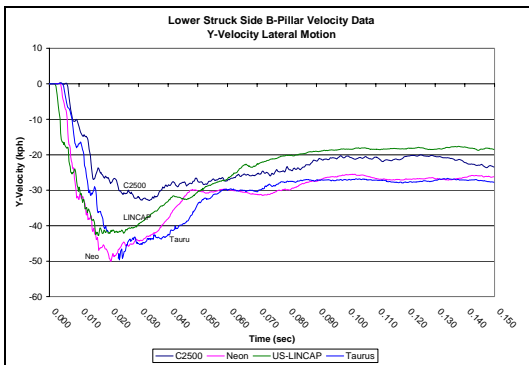


Figure 32. Lower struck side b-pillar Y-Velocity.

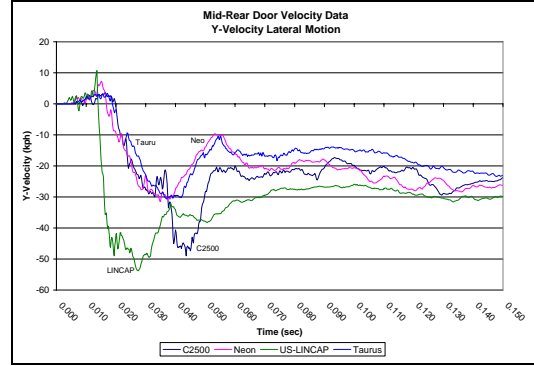


Figure 33. Mid-rear door Y-Velocity.

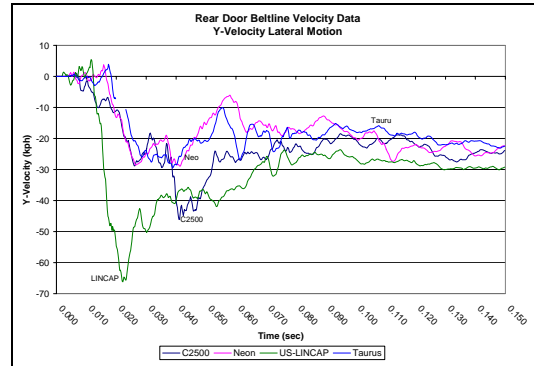


Figure 34. Rear door beltline Y-Velocity.

## STRUCTURAL INTERACTIONS

A brief description of structural interactions is included in the following four sections. The purpose is to describe how the various structural interactions between the struck Taurus and the impacting crash partner produce the varying degrees of external crush, interior intrusion, and vehicle kinematics.

### MDB-Taurus Side Impact

The MDB contacts the side of the Taurus with the broad, flat bumper surface and manages to contact the rocker and lower floor cross-members. The bumper of the MDB lines up exactly with the door reinforcements. The MDB does contact the front hinge pillar early in the event. The prominent structural interaction between the MDB and the Taurus produces high struck vehicle accelerations and results in a broad flat peak and residual intrusion profile. The rear door trim panel is minimally deformed and moves into the cabin in an upright manner.

An interesting result from the two door mounted accelerometers is the early and high reading as compared with the three actual vehicles. The main block of the MDB contacts the upper and mid-door outer sheet metal

approximately 20-30ms earlier than any of the vehicles. This is a result of the upright design of the MDB main honeycomb block versus the sloped hoods of the sedans and to a lesser extent the pick-up truck. In addition the upper beltline accelerometer is almost cantilevered since the upper edge of the MDB contacts outer sheet metal several centimeters rearward of the accelerometer mounting point. This creates a velocity that exceeds the impacting MDB velocity.

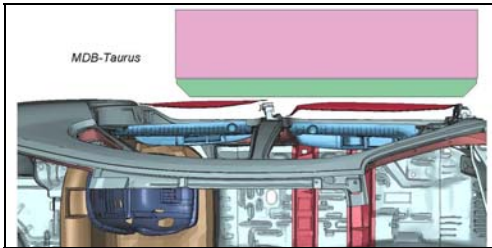


Figure 35. MDB-Taurus structural overlap.



Figure 36. MDB-Taurus post-impact deformations.

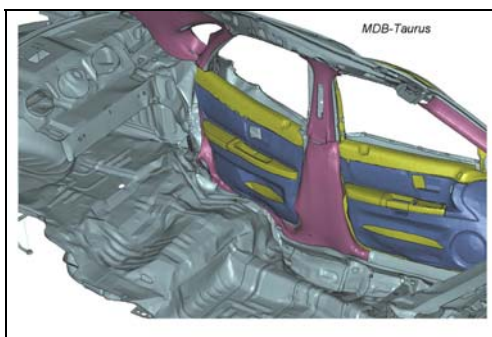


Figure 37. MDB-Taurus post-impact interior intrusion.

### Neon-Taurus Side Impact

The Neon front end is narrower than the other bullet vehicles. During the contact with the Taurus, the front structural bumper misses the rocker and both the front hinge pillar and rear wheel-well, although it does contact the door reinforcements. Later in the event, the lower front sub-frame of the Neon impacts the rocker and cross-members of the Taurus resulting in the delayed acceleration to the overall struck vehicle.

The narrow front end protrudes deeply into the body of the Taurus and results in a noticeable arcing of the inner door panels and b-pillar. The lower sections of the door panels tip inward, but the upper windowsill does remain straight and relatively undeformed. It is interesting to note that at the lower vertical measurement heights, the Neon produces significantly more intrusion than the Taurus, MDB, or C2500

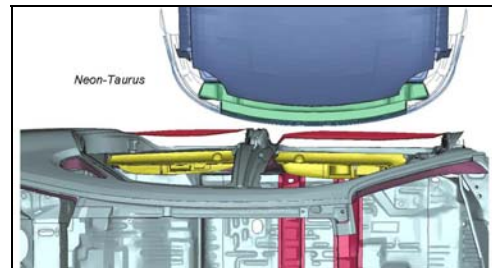


Figure 38. Neon-Taurus structural overlap.

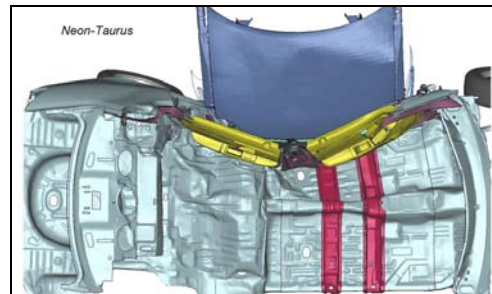


Figure 39. Neon-Taurus post-impact deformations.

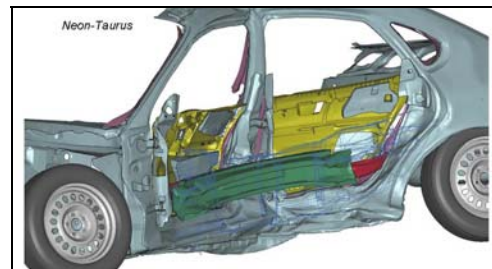


Figure 40. Neon-Taurus structural interaction.



Figure 41. Neon-Taurus post-impact interior intrusion.

### Taurus-Taurus Side Impact

The Taurus impacting vehicle behaves similarly to the Neon except that the front end bumper is wider and the intrusion height seen in the door panels is higher. The intrusion of the rear door is greatest at the mid-height of the door with the upper windowsill remaining straight and undeformed.

The bumper of the Taurus overrides the rocker, but later in the event the lower structure engages the floor and cross-members. The resulting velocity change in the struck Taurus is delayed compared to that of the Neon or MDB, mainly due to the later engagement of lower floor cross-members.

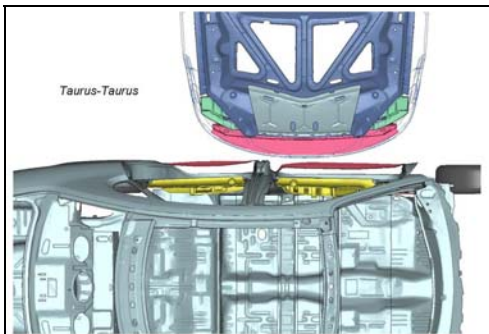


Figure 42. Taurus-Taurus structural overlap.

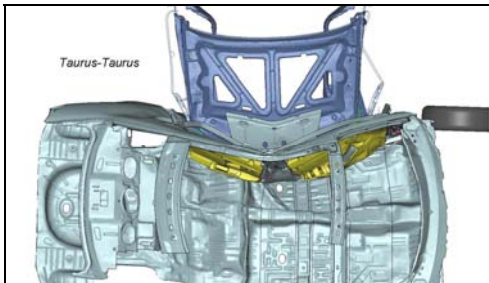


Figure 43. Taurus-Taurus post-impact deformation.

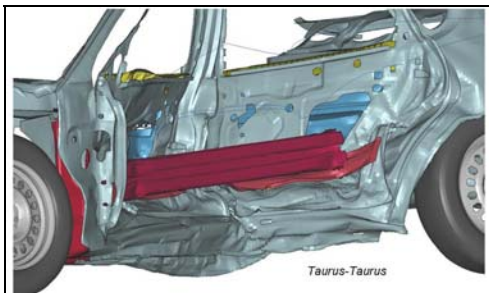


Figure 44. Taurus-Taurus structural interaction.

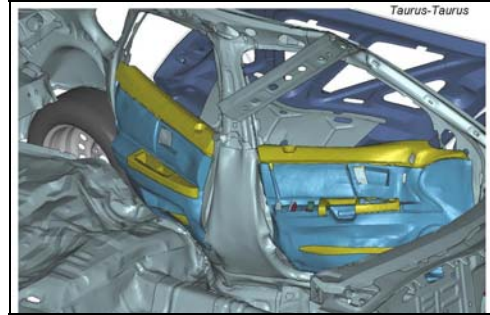


Figure 45. Taurus-Taurus post-impact interior intrusion.

### C2500-Taurus Side Impact

The C2500 features a wide structural front bumper that is rigidly mounted onto the main frame rails and support members. The bumper overrides both the rocker and door reinforcements of the Taurus and causes a tipping of the upper interior door trim and b-pillar. The bumper does however engage the front hinge-pillar and rear wheel-well. This contact with stiff BIW components and the overall width of the bumper helps broaden the shape of the intruding surface and minimize the local punching effect that both sedans exhibit.

The overall acceleration to the struck car is somewhat lower than the MDB and Neon since the lower floor and cross-car members are not engaged as is evident from the low crush at Level-1. The C2500 does produce the greatest amount of intrusion at the windowsill vertical measurement height.

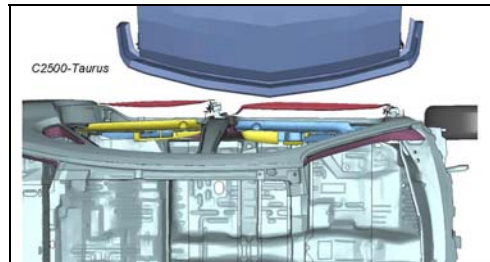


Figure 46. C2500-Taurus structural overlap.

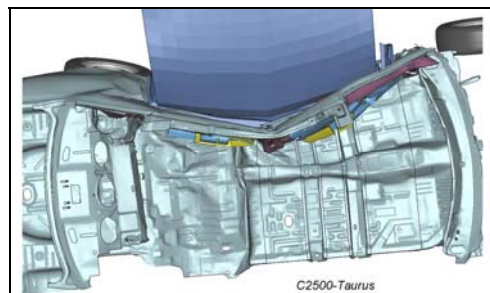


Figure 47. C2500-Taurus post-impact deformations.



Figure 48. C2500-Taurus structural interaction.



Figure 49. C2500-Taurus post-impact interior intrusion.

## DISCUSSION

There are two outcomes from this data that is of interest depending upon the seating location of a restrained child involved in a side impact. For those seated nearside, the rear occupant compartment intrusion and intrusion rate will most likely be the most influential factors in producing injury. Farside occupants and middle row occupants may most likely be sensitive to the struck vehicle overall kinematics.

The results of the simulations help illustrate the effect of the impacting partner on the four parameters of interest. Given that real world side impacts can occur with any type of object or vehicle, having data on crash outcomes for a broad mix of impacting partners will help frame the crash conditions that can be considered for a laboratory assessment.

The benefit of the simulation is a clear illustration of the structural interaction between the two vehicles involved in the impact. Localized damage to specific vehicle parts and the way that these contact a rear child occupant can be examined in detail. Used appropriately in conjunction with data from actual tested vehicles, the simulation serves as a valuable tool for examining alternative crash modes. The vehicle models clearly illustrate the breadth of damage potential and vehicle motion and can be used to further determine the range of damage that a rear seated occupant may be subjected to.

## CONCLUSION

The data briefly described in this report is only a small illustration of the resulting structural deformation of a mid-size sedan subjected to specific side impacts. A child seated in a rear row of a mid-size sedan can find themselves in collisions similar to these. Understanding the potential range of intrusions that the child may contend with can be partially fulfilled with this data. As field investigations have indicated, intrusion is a significant factor leading to injury, being able to describe the range and type of intrusion for a broad spread of striking vehicles is necessary in order to determine injury mechanism and create effective countermeasures.

Additional assessments using non-vehicle striking objects should be added to broaden the data set for single-vehicle side impacts. Once a satisfactory amount of data has been developed to describe the rear seat environment, the project can move from full vehicle assessments into sub-system testing and evaluation. At this point detailed analysis of child restraints and child occupant dummies can be used to help determine injury mechanism.

## REFERENCES

1. Arbogast, K., et al. Child restraints in side impacts. Proceedings of the International Conference on the Biokinetics of Impact Attributes. 2004. Graz, Austria.
2. Tamborra, N., Bahouth, G. Child Side Impacts: Comparison of Vehicle Crush in Side Impacts from Field Investigations and U.S. Consumer Tests. SAE International Congress and Exposition. 2005. Detroit, MI: Society of Automotive Engineers, Inc.

# ACTIVE MAGNETIC FIELD BASED SENSING SYSTEM FOR IMPROVED DETECTION AND DISCRIMINATION OF SIDE IMPACT CRASHES

**Len Cech**

**Todd Watson**

Takata Corporation

United States

**Markus Schiefele**

Germany

**Hiroshi Aoki**

Japan

Paper Number 05-0406

## ABSTRACT

Motivated by the complexity and variety of real-world side impacts, the Magnetic Side Impact (MSI) approach for side-impact crash detection and discrimination is presented. NHTSA has issued a rulemaking proposal that requires improved occupant protection in side impact crashes. It proposes 100% passenger car compliance to a more challenging standard in the near future. OEMs will likely require new sensing technologies and configurations to meet the proposed NHTSA standard.

This paper discusses a sensing technology for improved side-impact crash detection and discrimination. The MSI system induces a time-varying, fixed frequency magnetic field into the vehicle structure using a wire coil transceiver located in the vehicle door or frame. The induced field can also be sensed at other vehicle locations using a second wire coil receiver that detects changes in the magnetic field flowing through it. In normal operation, the transceiver (and receiver) signals are constant amplitude sinusoidal voltages at the transmitted frequency. During a crash, the magnetic path around the transceiver and between the transceiver and receiver is perturbed, and the resulting changes in the magnetic field are superimposed onto the MSI waveform. The received signal(s) are demodulated, leaving a signal whose content is proportional to crash severity and general impact location. The MSI system has shown to provide fast and reliable time to fire (TTF) signals in both laboratory and crash testing.

The MSI uses electromagnetic waves for communicating crash information, resulting in extremely fast detection and clear separation of deploy/non-deploy events. Placing a transceiver and receiver at opposite ends of the door allows wider spatial coverage. This paper describes the model and shows crash-sensing performance and

system benefits based on crashes using a full vehicle Body -in- White platform.

## MOTIVATION

During the years 2000 and 2001, side impact crashes accounted for approximately 37% of driver deaths in the U.S. While the rate of deaths per new registered vehicle (less than 3 years old) in the US from frontal impacts was reduced by 52% over the last 20 years, the rate for side impacts has only been reduced by 24%. Improvements in side impact safety have clearly lagged those for frontal impact safety. A major reason for the lack of progress in side protection is due to the small crush zone. Improved side impact safety can be achieved through improvements to structure, restraint/airbags, and sensing speed/accuracy. Better side airbags are always in development, but without improved sensing these restraints may not provide substantially better occupant protection.

Side impact sensing performance requirements have primarily been driven by regulatory tests (FMVSS 214 and EU 96/EC/27 Side Impact Regulations). Basic sensing requirements have focused on the need to rapidly distinguish severe regulatory developed crash modes from minor crash and abuse events so that restraint deployment will occur in sufficient time to protect occupants only when the crash could result in significant injury. In the past, regulatory agencies and consumers have relied upon OEMs to ensure robust side impact protection in real world conditions; however, newer crash modes have been proposed covering a broader range of real world impact scenarios [1,2] making the minimum sensing requirements more challenging.

Side impact sensing systems designed specifically to meet the existing regulatory crash modes may not perform optimally under a variety of real world crash scenarios [3]. National Highway Transportation and Safety Administration

(NHTSA) crash testing for side impact pole events showed that although several existing sensing systems deploy properly during a standard FMVSS201 pole impact, they do not deploy at all during an oblique pole impact [4]. In comparing these crashes, the lateral impact velocity is the same, only the incident angle is changed from 90 to 75 degrees and the impact location moved from a 50<sup>th</sup> percentile male to a 5<sup>th</sup> percentile female seating position (a separation of perhaps 15 cm or less). These test results imply that existing sensing systems may be inadequate under a variety of real world crash conditions.

### Statistics

Statistics on side impact crashes are generally classified into two categories, car-to-car and car-to-fixed object. (i.e. pole, tree, stationary car, etc.)

Evaluation of the NHTSA National Accident Sampling System (NASS) database for car-to-car side impact crashes between 1998-2002 shows that the angular distribution of relative impact force direction (~ impact angle) has a mean of approximately 63 degrees with the majority of Maximum Abbreviated Injury Score (MAIS) 1-6 injuries falling within 30 and 90 degrees.

Side impact crashes into fixed, narrow objects (e.g. pole, tree) account for about 20% of all deaths and serious injuries in side crashes. The mean impact angle, or principle direction of force, for real world crashes of this type is about 60 degrees and the distribution of angles is quite wide ranging (majority range from 30 to 90 degrees). Current regulatory barrier and pole tests are run at a 90 deg. impact angle, which may provide a good evaluation of restraint performance for severe impacts, however, these test conditions are not the most challenging for evaluating sensor performance.

### Regulatory Testing

NHTSA has issued a notice of proposed rulemaking [4]. The proposed rule suggests that a 75 degree pole impact for the 50<sup>th</sup> % male and a similar test for the 5<sup>th</sup> % female are appropriate test additions to the current FMVSS214 standard. The ideal sensing system will sense the crash for pole impacts occurring over a wide range of angles and impact locations along the door rather than being tailored to perform for regulatory crashes.

The Insurance Institute for Highway Safety (IIHS) has been performing side impact testing to address real world vehicle-to-vehicle compatibility. The IIHS impact sled is heavier, has a higher

bumper area, and has approximately 1/2 the initial contact impact area compared with the NHTSA 214 barrier sled. This barrier reflects the growth in the light truck and sport utility vehicles (SUV) market in the U.S. (~37% of vehicle market share). In the years 2000-2001, 57% of driver deaths during side impact with another vehicle occurred when the striking vehicle was a pickup/SUV [5]. For impact with an SUV, the occupant of the struck vehicle is more likely to sustain severe head injuries due to the higher potential for direct head/upper body contact with the SUV hood. The high intrusion rate of the IIHS side impact test requires faster crash detection times than similar speed crashes with the FMVSS 214 barrier.

The European Union EU 96/EC/27 side impact barrier, compared with the FMVSS 214 barrier, is softer and has a larger initial impact area. The reduced stiffness and wider contact area of the EU barrier leads to significantly different signals for some sensors as the barrier itself absorbs and damps more of the initial impact energy. In this case, the transfer of energy into the impacted car may still cause severe deformation, but it may be more difficult to rapidly separate a more severe EU barrier crash from a less severe 214-barrier crash.

The challenge for next generation side impact sensing systems is to provide wide area coverage, fast response, and good response for severe crashes over a range of impact stiffness, area, location and angle while maintaining immunity to false deployment from abuse events.

### BACKGROUND

The greatest threat to an occupant involved in a side impact crash is the penetration of the internal door structures or the impacting object into the head, thorax or hip of the occupant [6]. For this to occur, sufficient impact energy must be transferred into the impacted car to cause door displacement relative to the frame and door deformation. The function of any side impact crash sensor system is to quickly detect and discriminate the wide variety of potential crash events and deploy airbag restraints in sufficient time to protect the occupant. Typically, the time required to inflate the airbag can be between 10 and 20 milliseconds. For a regulatory high-speed impact, such as an IIHS, the required crash detection time can be less than or equal to 5 milliseconds. During this time, the penetration into the vehicle side structure may be as small as 5 centimeters. Such a relatively minor dent might also be expected for many non-threatening impacts (fender bender). So the ideal

side impact sensing system should be capable of quickly detecting both deformation and deformation rate of the vehicle structures, which threaten the occupant directly and provide resistance between the occupant and the impacting object.

### **Accelerometer Sensors**

The majority of current state of the art side impact sensing systems is composed of one or more lateral axis accelerometers mounted on each vehicle side. These systems evolved from frontal impact systems where a long crush zone and large structural mass help integrate and damp crash energy to the accelerometer; with less dependence on the impact point, area and direction of force. In frontal impacts, the distance between the impact object and the occupant is long and the accelerometer can be placed in a very benign location where it is relatively immune to shock and vibration induced by non-crash events (occupants, rough road and abuse).

However, for side impact crashes, the situation is very different. There is a short crush zone for side impact and the typical occupant compartment is composed of a variety of rigid (A, B, C pillar) and less rigid (door, glass) structures. The energy transfer paths for side impacts varies greatly depending on the crash location, impact angle, contact area and impact energy, making it extremely difficult to select the ideal location for a 1-D point sensor to quickly detect all real-world crash variations (poles, soft and hard barriers, impacting angles) and suppress all non-crash testing variations (abuse, rough road, minor crashes). Often, the only viable method to accomplish faster and reliable detection for the newly envisioned crash modes is to incorporate more accelerometers, which increases system processing complexity and cost.

### **Pressure Sensors**

Several other technologies have been proposed to replace or augment the performance of accelerometers in an attempt to improve side impact crash detection and discrimination. A specific example is the use of a pressure sensor enclosed within a vehicle door cavity. Such a sensor provides a pressure pulse signal upon impact. This signal, combined with those from accelerometers may provide faster response for some crash modes, which are difficult to detect with accelerometers alone. However, for non-cavity applications (3rd row seat, or panel vans), or where the seal integrity of the cavity may be

compromised (e.g. holes in the door, or interior trim or speakers removed), or when impact occurs on the cavity perimeter, a pressure sensor may have difficulty improving detection and discrimination [6].

## **MAGNETIC CRASH SENSING**

The use of electromagnetic physics for crash sensing is an evolution that potentially provides enhancements in the speed of sensing and the wider distribution of response. During the general development of sensing methods in many applications, the sensing technology often evolves from mechanical sensing to electromagnetic field sensing. Field sensing, in general, often provides faster, more accurate, and more reliable sensing where the sensed phenomena can be tailored by sensor design rather than limited by mechanical mounting and mechanical interactions. For metal body cars, or bodies augmented with metal coatings, magnetic field sensing has the potential to provide rapid, wide region sensing of mechanical phenomena at a competitive cost. The MSI system, in its simplest form, consists of a device for creating a known magnetic field near the vehicle metal and a way to detect if this field is rapidly changing due to metal motion and deformation in a crash.

### **Electromagnetic Relations**

The basic physical relations that define all electromagnetic phenomena are defined by Maxwell equations [7]. The primary equations needed to describe the MSI system function can be simply stated as:

**Ampere's law:** the magnetic field in space around an electric current is proportional to the electric current (which serves as its source).

**Faraday's law:** any change in the magnetic environment of a circuit (e.g. coil of wire, conductive sheet) will cause a voltage to be induced in the circuit.

**Gauss's law for magnetism:** The net magnetic flux out of any closed surface is zero such that all magnetic flux lines are closed loops.

### **Creating Magnetic Fields**

Applying a current to a wire is a common method for creating a magnetic field (Ampere's law). By arranging the wire in a loop, the direction of the magnetic field along the loop axis can be controlled. The field magnitude is directly

proportional to the product of the current in the wire and the number of turns in the loop. The current waveform signal applied to the coil will match the induced magnetic field waveform. Applying a discrete frequency sinusoidal current to a coil of wire generates a sinusoidal magnetic field at the same frequency along the coil axis.

### Sensing Magnetic Fields

Faraday's law states that a voltage will be induced in a wire coil if the magnetic field enclosed by the coil changes in time:

$$V_{\text{ind}} = -N \dot{\Phi} \quad (1)$$

Here  $V_{\text{ind}}$  is the induced voltage measured across the coil leads,  $N$  is the number of coil loops, and  $\Phi$  is the magnetic flux that passes through the coil. Accordingly, a coil is also a very simple, but effective sensor for measuring time variant magnetic fields. The MSI uses a sinusoidal magnetic field which is inherently time variant providing the control system with an expected continuous waveform. Changes from the nominal magnitude and phase of this waveform provide information about changes in the vehicle metal.

### Electromagnetic Fields in Conductors

In conductive materials such as steel, aluminium, and copper, an externally applied DC magnetic field will be equally distributed within the cross section of the material. However, as a sinusoidal field is applied at increasing frequency, Faraday's law predicts that induced electric voltage potentials will be produced in the conductor. These voltage potentials cause free charges in the metal to move, forming currents, commonly called eddy currents. These induced currents produce a secondary magnetic field, which opposes the original field according to Lenz's law [7]. These eddy currents extend into the conductor, with the magnetic field created by each deeper eddy current loop adding to the total opposing field. The result of this phenomenon is that the current density increases at the surface of the conductive material and decreases exponentially at greater depths. Skin depth ( $d$ ) is defined for a conductor as the distance from its surface to the depth where the current density is  $1/e$  times the surface current density:

$$d = (\pi f \mu \sigma)^{-1/2} \quad (2)$$

where  $f$ =frequency (Hz),  $\mu$ = magnetic permeability (H/m),  $\sigma$ =electrical conductivity (S/m), and  $\ln(e)=1$ . For standard steel materials, in the

frequency ranges that the MSI operates in, the skin depth is on the order of approximately 0.2 mm.

Magnetic permeability is a physical property that indicates how easily a material will temporarily magnetize in response to an applied magnetic field. For highly permeable materials, such as most steels, it is energetically favorable for the applied magnetic field to stay in the magnetic material. However, the eddy currents attempt to cancel this applied magnetic field. As the frequency of the applied magnetic field increases, the eddy currents constrain the field into an increasingly thinner layer at the surface of the conductive material, increasing the magnetic energy density of the system. Any electro mechanical system will find the state where there is a minimum total magnetic energy and, in this case, achieves this minimum by forcing portions of the magnetic field into the air near the surface of the conductor. For frequencies in the range from approximately 10kHz to 100kHz (MSI operation), it is energetically favorable for the magnetic flux to primarily reside in air more than in steel, but still be bound to a conducting surface. For frequencies above 100 kHz, an electromagnetic wave can develop that is no longer bound to a conducting surface. This is the frequency range where antennas operate.

### Single Coil System (Transceiver)

A functional MSI system can consist of a single coil placed near one or more conducting surfaces that will move and/or deform relative to each other during a crash. This single coil functions as both the magnetic field generator (transmitter) and the sensor (receiver) of magnetic field perturbations and is referred to as a transceiver coil. Changes in the position and shape of metal in proximity to the coil cause detectable changes in the driving circuit impedance. Using Ohm's law, this change in impedance can be measured as a change in applied current for a constant peak voltage driven circuit. The change in impedance results from: 1) changes in coil inductive reactance as the coil inductively couples with nearby metal and 2) changes in coil resistance as the coil interacts with opposing eddy current induced fields in the nearby metal. Deformation and displacement of metal further away than a coil diameter will have less effect on the coil signal unless those motions couple to the nearby metal. The effective use of a transceiver, therefore relies upon proper coil placement relative to mechanical door structures, which cause motion and deformation in the regions near the coil. The transceiver coil is placed where it is certain to

observe metal motion/deformation if the crash severity will warrant restraint deployment.

### Two Coil Systems (Transmitter and Receiver)

A two-coil MSI system is a magnetic device, where one coil is used as a transmitter (or also a transceiver) of the magnetic field and another coil is used for receiving the field at another location. The signal from a receiver coil can add information about the crash.

The basic quantity that describes the transmission of the magnetic field from one coil to another is the complex Reluctance  $R_c$ . It is defined as;

$$R_c = \frac{NI}{\Phi} \quad (3)$$

where  $I$  is the transmit current. The reluctance is a measure of the magnetic “resistance” between two points. A crash event changes the reluctance between two points by altering the geometry of the metal and surrounding air so that the magnetic field paths are altered as a function of time. A system with a receiver coil detects changes in the field as the metal between it and the transceiver is disturbed, changing the amplitude and phase of the magnetic field reaching the receiver location. A two-coil system will have inherently broader area coverage of crash sensing than a single coil system. The magnetic field must travel through/around the vehicle components between the two coils, and the received signal will be dependant on mechanical changes due to a crash anywhere in this path. In addition, the use of a two-coil system provides the potential for a safing function.

We have introduced the concept of a 2-coil MSI system. Such a system has undergone extensive testing at Takata with successful crash discrimination results. However, it is much simpler to directly relate the crash dynamics to the signal response of a 1-coil transceiver. Additionally, a crash sensing system based on transceivers provides a near term solution to improve crash detection in response to new regulatory test modes. As such, the transceiver system will be the focus of the remainder of this paper.

### Sensor Components (Transceiver)

The basic MSI transceiver system consists of the electronics, wiring harnesses, and transceiver coils needed to provide the crash detection coverage desired by the OEM. One transceiver coil for each door on a side could provide crash sensing

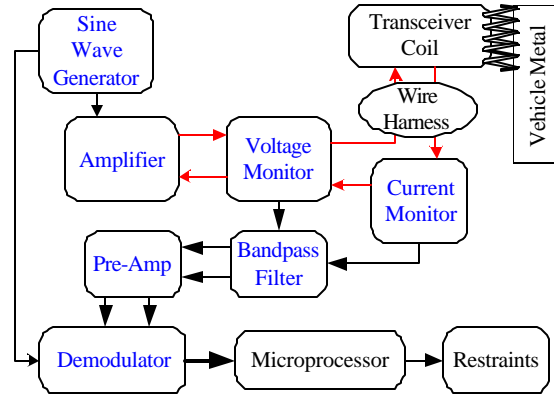


Figure 1. MSI block diagram.

for that side of the vehicle. The centralized electronics consist primarily of power conditioning, a circuit for generating the voltage (or current) supplied to the transceiver coil a circuit for monitoring the current and voltage supplied to the receiver coil and memory and processing capability to extract and process this magnetic signal through a crash discrimination algorithm. Figure 1 shows a block diagram of a basic MSI transceiver system; the red lines identify the excitation path, the black lines show the signal paths, and the blue text indicates functions that could be built into an application-specific integrated circuit (ASIC).

The sine wave generator creates a low distortion sinusoidal signal used to control the drive amplifier exciting the coil. Typically the sine wave will be operated at constant peak voltage and at a fixed frequency chosen from a range of about 20 kHz to 100 kHz. The generated sine wave will operate at frequencies above electric power and audible frequencies (50-60 Hz, 20 kHz) and below AM radio frequencies (>531 kHz), thereby producing an inaudible oscillation that is less likely to have mutual interferences with many existing electromagnetic systems. Because the MSI system uses a sinusoidal field, the field is constantly changing in time in a known way. Deviations from this expected constant-amplitude fixed-frequency sinusoid field are indicative of metal motion. This signal must be demodulated from the sinusoidal to extract the information about changes in the field. Standard techniques exist for removing or demodulating this signal by mixing the signal with the original sine wave generator signal. [8]. Before demodulation, each signal (voltage and current) undergoes band-pass filtering to remove noise and is then amplified to better optimise the dynamic resolution of the system. Demodulation allows measurement of changes in the magnitude and

phase (relative to the sine generator) of the current and voltage signals. After demodulation, the signals are sent to a microprocessor where algorithms determine if the observed changes over time represent a crash of sufficient severity to deploy restraints.

The placement, orientation, and dimensions of a transceiver coil determine the primary metal motions and deformations that influence the sensed signal during the crash detection time (usually 0 to 30ms or less after initial crash contact). Figure 2 shows several candidate locations for the placement of a transceiver coil on a simplified door model. One location is inside the door (blue coil), near the occupant’s hip, oriented to be most sensitive to inward motion of the outer door skin and reinforcement rail during a crash. Such an in-door transceiver coil would be primarily sensitive to door deformation along the axis of the coil in a region within about one diameter of the coil. Another location to place a transceiver coil is in the gap between the door and the frame, possibly on or near the pillar striker (red or green coil). This second transceiver location is sensitive to door deformation, but its response during the crash detection time is indicative of the whole door three-dimensional motion relative to the frame. While the majority of the signal in either of these arrangements is caused by metal motion in the region near the coil, coil locations can be chosen where the door structure and reinforcements will ensure that significant nearby metal displacement or deformation will occur within the required sensing time.



**Figure 2. Candidate transceiver coil locations**

Computer Aided Engineering (CAE) of the electromagnetic field and crash dynamics can be used to better understand the region of sensitivity and the response of the transceiver coil to deforming structures during a crash. As an example, Figure 3 show the computer predicted magnetic field shape within a simple steel box model, intended to approximate the aspect ratio of a vehicle door. A thin, flat coil whose size is approximately 1/2 the width and 1/4 the length of the box is mounted over an access hole in the inside door panel (shown in the cross section as a thin

purple line). The cross section shows that a symmetric field is created within the inner steel and air with intensity contours. The surface view shows the “bull’s-eye” pattern of the magnetic field magnitude superimposed upon the inner door skin. This simple model provides a visualization of the sensing space of a “coil in the door” transceiver

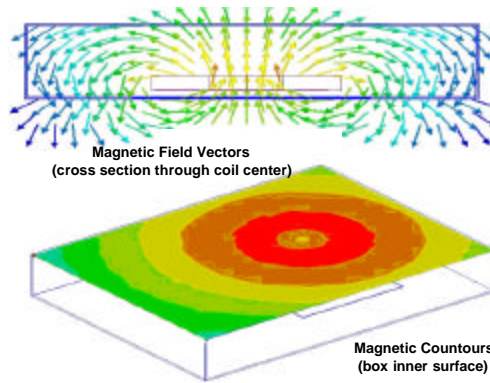
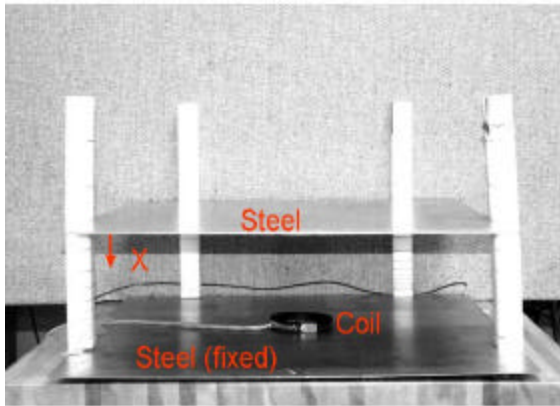


**Figure 3. Magnetic CAE response for coil in door**

### Transceiver sensor response

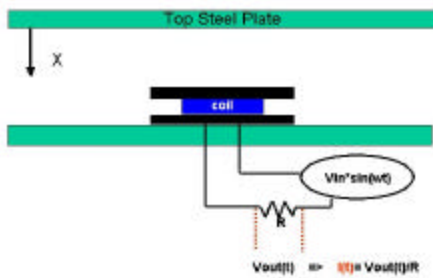
To illustrate the sensing characteristics of the MSI transceiver for a basic in-door coil arrangement, a simple test was performed using 2

steel plates and a transceiver coil. The plates were 60 cm square sheets, 0.16 cm thick, composed of common 1006/1020-carbon steel. The transceiver coil used in these tests was a circular coil with a diameter of about 9.5 cm and an axial coil length of about 5.3 mm. The coil was wound with 88 turns of 22 gauge copper wire. The coil excitation frequency was 35 kHz and was driven at a constant peak voltage. The coil was placed on top of a fixed first plate and a second plate was moved incrementally towards the bottom plate. Figure 4 shows the laboratory set-up for the experiment.



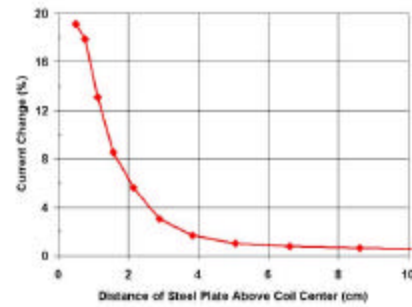
**Figure 4. Transceiver response experiment.**

Figure 5 shows a sketch of the experimental set-up and the transceiver sense circuit. The current in the sense circuit is allowed to vary while the peak voltage and excitation frequency are held constant. The change in current is a measure of the proximity of the top steel plate as it moves toward the coil.



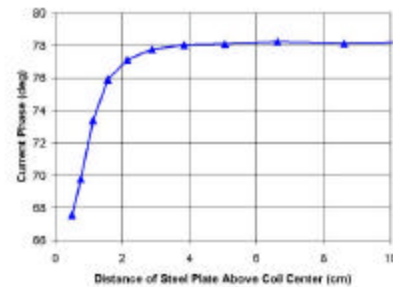
**Figure 5. Transceiver experiment test circuit.**

Figure 6 shows the static MSI transceiver current magnitude response as a function of the distance between the top of the coil plate towards the fixed bottom plate.



**Figure 6. Magnitude response with gap change.**

Note that there is also a phase shift in the measured current as the gap between the coil and the upper steel plate gap closes. This measurement is shown in Figure 7. Accordingly, the demodulated transceiver current and voltage provide both magnitude and phase information, which can be used to discriminate metal body displacement and deformation.



**Figure 7. Phase response with gap change.**

## CRASH TESTING

The crash discrimination capability of the MSI transceiver has been demonstrated in a series of crash tests on a mid-size 4-door sedan Body-in-White (BIW) platform. While several transceiver designs performed well in crash discrimination, the performance response is perhaps best and most simply illustrated for a single coil mounted on the inner surface of the door back wall. In this location, the sensor response is determined primarily by the deformation and deformation rate of the exterior door skin and support beam relative to the coil.

This intrusion is directly related to the potential for occupant injury and *required time to fire* (RTTF).

### Coil Selection

In a production application, the specific mount location for a transceiver coil on a given platform will be based on several criteria, including the vehicle geometry, door structural response to impact, the occupant types, seating locations and seat travel span. Also, the restraint RTTF would affect the sensor mounting location and size as illustrated in Figure 8.

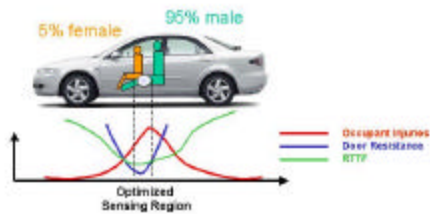


**Figure 8. Occupant vulnerability and coil location.**

The production location of a transceiver coil within the door must also consider the impact points of regulatory crash barriers that are derived from governmental statistics on side impact crashes and vehicle forms. Coil placement that is guided by these crashes does not limit the usefulness of the response in a variety of real world crashes, but rather places some extra sensing emphasis on crash locations where these agencies have determined that the occupant may be more vulnerable. These barrier and pole impact locations span the same region where various drivers may be located front to rear but provide a target height region where initial impact sensitivity may be most desirable. An example of how barrier location can influence coil location is shown in Figure 9.

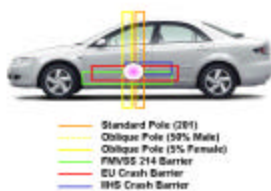


**Figure 9. Barrier impact locations and coil location.**

The selected coil location must also fit within the door mechanical and functional constraints (i.e. window, door locks, etc.). Ideally, the optical coil size, shape, location and mountings should be worked out using CAE tools in coordination with the platform designers.

Testing of the MSI system has shown that non-standard irregular shaped coils can be effectively used (i.e. elliptical, concave, oblong shapes, etc. ). Additionally, PCB and flexible coils could be used when space is limited and conformance to existing structures is required.

The transceiver coil used in these BIW crash tests is a circular coil with a diameter of 17 cm and an axial length of 1.2 cm that was wound with 100 turns of 26-gauge wire. This coil was driven at a frequency of 33.5 kHz.

### Test Matrix

In order to verify the crash discrimination performance of MSI transceivers, a series of crash tests were carried out, including a variety of barrier types and impact speeds. Each test conformed, as close as practical, to the regulatory published standards. Because the tests were carried out on Body-in-White vehicle without dummies, actual required TTFs cannot be determined. To estimate test repeatability, test 2 and test 5 were each executed twice (tests 4 & 6).

Table 1.  
**Crash Test Matrix**

Test	Test Mode	Speed (kph)	Deploy
1	FMVSS 214	53	ON
2	FMVSS 214	19	OFF
3	FMVSS 214	32	ON
4	FMVSS 214	19	OFF
5	European Union	50	ON
6	European Union	50	ON
7	IIHS	50	ON
8	FMVSS 201 (Pole)	21	ON
9	Oblique Pole	23	ON

### ANALYSIS

In each crash test, a high-speed data acquisition system (DAS) is triggered at impact (barrier contact = time zero) and the sensor current is measured as a voltage across a sense resistor at 16 bit resolution. The sensor current was processed using a 2<sup>nd</sup> order band-pass filter with cut-off

frequencies placed at +/- 3 kHz around the drive frequency. The data was then demodulated using the system clock and the complex signal magnitude passed through a 1 millisecond moving average and normalized to the pre-trigger to derive the response in Figure 10. In the Figure, the two black curves are the repeated non-deploy crashes and all other color curves are deploy condition crashes.

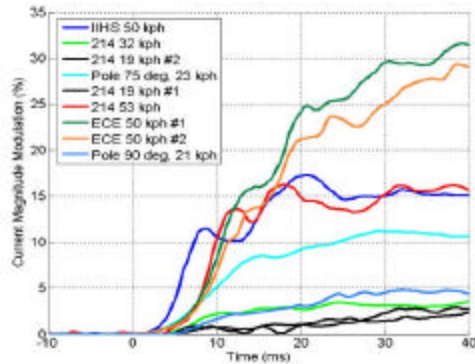


**Figure 10. Coil in front door magnitude response.**

This plot shows that the two OFF condition events can be separated from the remaining ON condition events. The majority of ON condition signals show a high rate of signal change within the first 3-7 milliseconds. Although the coil sensor was not optimised in terms of coil diameter and placement for these Body-in-White crash tests, the response trends are indicative of what would generally be expected from an optimised coil. Coil design, mechanical packaging and CAE can be combined to optimise the coil TTF and ON/OFF separation response for a given platform.

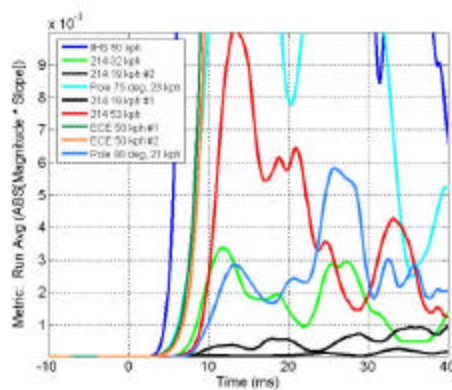


**Figure 11. Simple crash metric (amplitude\*rate).**

In order to evaluate the crash discrimination potential that might be expected from a production intent electronic control unit, the 16 bit data was decimated to 12 bits and the data down-sampled to 3 kHz of bandwidth. The data was processed using a simple mathematical metric and provided the estimated TTF performance shown in Table 2. Figure 11 shows the result of one such simple metric. The magnitude data, shown in Figure 10, has been used to develop a metric that is the low pass filtered result of the absolute value of the product of the local average slope and the local average magnitude.

Using a second simple metric, estimated Time to Fires have been derived for the crash tests and are shown in the following table.

**Table 2. Crash test estimated time to fires**

Test	Test Mode	TTF (ms)
1	FMVSS 214	5.3
2	FMVSS 214	OFF
3	FMVSS 214	6.2
4	FMVSS 214	OFF
5	European Union	6.5
6	European Union	7.0
7	IHS	3.8
8	FMVSS 201 (Pole)	5.3
9	Oblique Pole	7.0

## DISCUSSION/CONCLUSION

The crash detection and discrimination performance has been demonstrated for a single embodiment of an MSI transceiver sensor. The characteristics of this sensor can be controlled to optimally fit the sensing environment. This may be attractive to OEMs. Takata continues to develop an MSI system, initially based on transceivers, with the goal of improving system performance and coverage using a multi-coil system. Such a system has undergone extensive crash testing on several vehicle platforms with excellent results. However, in order to meet the near-term market need for improvements in side impact crash sensing, a first generation magnetic crash sensing system composed of one or two (rear door coverage) transceivers per vehicle side combined with a safing accelerometer mounted on the B-pillar is being developed by Takata.

## ACKNOWLEDGEMENTS

The authors would like to acknowledge Tim Bomya and Dr. John Brauer for theoretical support; Mike Bruce, Benedikt Heudorfer and Noriyuki Kosugi for managerial support; Karen Willis for paper coordination and Takata crash test support engineers who worked so hard to complete the necessary crash testing.

## REFERENCES

- [1] Dakin G.J.; Arbelaez R.A.; Nolan J.M.; Zuby D.S.; Lund A.K. 2003. "Insurance Institute for Highway Safety Side Impact Crashworthiness Evaluation Program: Impact Configuration and Rationale", 18<sup>th</sup> ESV Conference, Nagoya, 2003.
- [2] Samaha R. R.; Elliott D. S. 2003. "NHTSA Side Impact Research: Motivation for Upgraded Test Procedures", 18<sup>th</sup> ESV Conference, Nagoya, 2003.
- [3] Kirk A.; Morris A. 2003. "Side Airbag Deployments in the UK – Initial Case Reviews", 18<sup>th</sup> ESV Conference, Nagoya, 2003.
- [4] Federal Register, Volume 69, No. 95 Monday, May 17, 2004, proposed rules; National Archives and Records Administration.
- [5] "Status Report", Special Issue: Side Impact Crash Worthiness, Insurance Institute for Highway Safety, Vol. 39, No. 5, April 24, 2004.
- [6] Chan, Ching-Yao. "Fundamentals of crash sensing in automotive air bag systems"; ISBN 0-7680-0499-3; Society of Automotive Engineers, Inc.; 2000.
- [7] Halliday D.; Resnick R. "Physics"; John Wiley and Sons Publisher; 1978.
- [8] Bateman A. Paterson-Stephens I. 2002, "The DSP Handbook"; Prentice Hall; 2002.

# REDUCING RIB DEFLECTION IN THE IIHS TEST BY PRELOADING THE PELVIS INDEPENDENT OF INTRUSION

**Greg Mowry**  
**David Shilliday**

Zodiac Automotive US, Inc.  
United States  
Paper Number 05-0422

## ABSTRACT

A cooperative research project with the National Highway Traffic Safety Administration (NHTSA) was conducted to evaluate the capability of a Tubular Thoracic Cushion (TTC) airbag concept to significantly reduce rib deflections for the SID-IIIs dummy in the Insurance Institute for Highway Safety's (IIHS) side-impact barrier test.

The concept of the TTC airbag was to efficiently distribute a majority of the crash force to the pelvis, which is more able to tolerate forces from side-impact crashes. The characteristic of the airbag to develop tension when deployed appeared to offer additional opportunities for occupant restraint in the IIHS side-impact environment.

Computer analysis confirmed that an approach of interposing an inflatable cushion between vehicle occupants at the ribs and a vehicle's intruding side structure may be problematic when attempting to limit rib deflection, particularly for small-stature occupants.

NHTSA analysis of NCAP side-impact tests suggested that pelvic lead (pelvic loading prior to the loading of the rib cage) lessens severity of thoracic injury [1]. Simulations of the IIHS side-impact barrier test utilizing this approach of pelvic lead with the TTC device showed reductions in rib deflection to a 5<sup>th</sup> percentile female dummy when airbag inflation was limited only to the pelvis region.

Due to the characteristic of the TTC airbag to develop tension when deployed, a strategy of applying an inboard lateral "pre" load to the pelvis region of the SID-IIIs dummy prior to intrusion was developed. This further reduced rib deflection in dynamic simulations and was validated in dynamic sled testing. The tensioning characteristic of the TTC airbag concept demonstrated pre-loading the pelvis of an occupant in the IIHS side-impact environment provided significant reduction in injury risk.

## BACKGROUND

Side-impact crashes represent the most hazardous crash mode of all planar crashes. Based on 1999 US NASS data, the frequency of these crashes comprises approximately one fifth of all planar crashes. However, 1999 US FARS data indicates more than a third of all occupants fatally injured are disproportionately represented in side-impact collisions.

There are several reasons why side-impact collisions have the highest injury potential over frontal impact crashes. Unlike frontal crashes, side crashes involve considerably less crush space between the point of impact from the striking vehicle and the struck passenger [2]. Consequently, this very limited crush space increases the protection requirements on the vehicle side-structure, interior padding, and other countermeasures such as side airbags.

During a side-impact crash, the door of the struck vehicle intrudes into the passenger compartment with the velocity of the striking vehicle. The occupant in the struck vehicle remains motionless relative to the intrusion until the distance between the occupant and the intruding door come together and the door accelerates the occupant. The struck vehicle is accelerated as a result of the stiffness of the side structure. The intrusion of the door is complete when the velocity of the door is equal to the velocity of the vehicle. Later in the crash event, the velocity of the occupant becomes greater than the intrusion velocity and the occupant separates from the intrusion. However, the highest risk of injury is likely to occur much earlier in the crash event [3].

## Changes to U.S. Vehicle Fleet

A significant shift in the United States' vehicle fleet composition appears to be greatly increasing the hazards associated with side-impact crashes [3]. This shift is due to increased popularity of sport utility vehicles, vans and light trucks.

Side-impact crashes of light vehicles, i.e. passenger cars and multi-purpose vehicles (MPV's) result in approximately 9,800 fatalities and over 1,020,000 injuries each year (1996 FARS and GES). This corresponds to about 30% of vehicles involved in tow away crashes. Also, over 43% of the fatalities and 37% of the serious injuries (MAIS 3) in U.S. light vehicle side-impact crashes are in side impacts where an MPV is the striking vehicle (based on a yearly average from the current U.S. crash environment (1988-1996 NASS/CDS and FARS).

Based on analysis of Canadian field accident data and crash testing, 67% of passenger car occupants injured at the AIS 3 or greater level, sustained their injuries in impacts where the striking vehicle was an MPV [4]. Additionally, it was observed that female occupants were over-represented among seriously injured occupants.

These recent real-world changes in the vehicle fleet have shown to present technical challenges in protecting occupants in this more difficult circumstance. The hood heights of MPV's such as sport utility vehicles typically correspond with the head of an occupant seated in a passenger car. This situation exposes the occupants in a passenger car to the risk of serious head injuries in a side-impact. However, risk of torso injury to the occupant in the passenger car also increases as a result of the proximity of the hood height of the MPV.

The side-impact test program developed by the Insurance Institute for Highway Safety (IIHS), addresses this real-world scenario. The basis for this side-impact test program is illustrated in figure 1.



Courtesy of IIHS

**Figure 1. IIHS test demonstration for consumer information side crash test**

The design of the IIHS side-impact test is to assess the protection afforded to both the head and torso of small-stature occupants in passenger cars struck in the side by MPV's. Results from tests conducted on a variety of vehicles equipped with and without side airbags has shown the test to be a significant challenge for vehicle manufacturers to demonstrate satisfactory performance especially for torso protection.

## INTRODUCTION

There are several approaches to side-impact protection for passenger vehicles. These generally include vehicle intrusion stiffness, interior geometry, and inflatable devices and padded structures capable of absorbing the impact energy.

Minimal improvements in reducing intrusion velocity are possible through stiffening the vehicle structure, however; sufficient thoracic protection is not likely without additional countermeasures to meet the requirements in the IIHS side-impact scenario.

Investigation into potential safety benefits of padding using constant crush force energy absorbing materials for thoracic protection in side impacts have been studied over several decades [5]. Some analysis indicates 15-30% potential reduction of thoracic injury risk for selected material characteristics as an upper bound [6]. Another study has shown approximately 10% effectiveness for padding in the door and armrest as an injury countermeasure in side crashes [5]. However, reducing the risk of injury to the chest and abdomen in the IIHS situation with padding countermeasures appears more difficult.

## Side Airbag Functions

Most types of side airbags are designed to establish early contact between the door and occupant. This interaction with the airbag accelerates the occupant before the intruding door contacts the occupant. These airbags are designed to distribute the contact forces over a large area of the rib cage to avoid localized loads and reduce the overall risk of thoracic injuries. A critical challenge of an airbag design is to inflate the airbag with sufficient pressure to accelerate the occupant from the intrusion while appropriately cushioning the occupant to minimize the risk of rib fractures.

Loading the pelvis prior to contact with the thorax is a favorable occupant kinematic and is often referred to as "pelvic lead." This occupant motion is indicative of reduced injury risk to the thorax [1] [3].

As such, a strategy of distributing greater contact load to the pelvis region appears appropriate due to higher loading tolerance of the pelvis (Injury Assessment Reference Value 4kN per IIHS evaluation) compared to rib structures. Therefore, padding in the door itself is often used to push the pelvis region to accelerate the occupant with the lowest possible risk. Some side airbags cover not only the thorax but also the pelvis region to minimize potentially injurious loads to the thorax and abdomen.

The interior door trim contour is another important design consideration in addressing the risk of injury in side-impact. The Institute's experience in the development of their side-impact program has identified the abdomen as a critical area of concern [3]. This is an interesting finding, considering that injuries to the spleen are common in serious side impacts. The deformed door can protrude more significantly at the armrest, which can increase the risk of abdominal injury. Some airbag designs fill these irregular contours to provide a large flat contact zone between the intrusion and occupant to avoid localized loads and minimize the risk of abdominal injuries.

### Airbag Deployment Timing

One of the single most important deployment characteristics necessary for inflatable devices to mitigate injury in side-impact crashes has to do with the timing of the airbag. Side collisions require a much faster airbag reaction time compared to frontal collisions [7]. This is due to the limited distance and time to sense the crash and insert the airbag between the occupant and intruding structure. Therefore, deployment time of an airbag is critical, especially in more severe side-impact crashes.

Analysis of thoracic dummy responses from test results in some IIHS side impact tests show more than 42 mm of rib deflection for a SID-II dummy after 25 milliseconds after initiation of barrier impact. This magnitude of rib deflection represents a 50% risk of AIS3+ injury. NHTSA identifies 42mm of rib deflection represents

### PROJECT DESCRIPTION

A cooperative research project with NHTSA was established to evaluate the capability of a Tubular Thoracic Cushion (TTC) concept airbag with a contracting characteristic that offered possibilities to significantly reduce rib deflections of the SID-II dummy in IIHS side-impact environment. The

project was divided into two major tasks. The first task consisted of computational analyses intended for design development of the concept airbag. The second major task for the research project included dynamic tests of prototypes airbags for model validation and evaluation of concept feasibility.

### Model Development

The primary occupant-simulation software used to evaluate various design iterations of the concept airbag was MADYMO (Mathematic Dynamic Modeler). A full-scale crash test identified in the IIHS database (1999 Pontiac Grand Am, test #CS01009) was used for developing the baseline computer model. The model was used to simulate the IIHS Grand Am test and then apply the airbag design iterations based on occupant dynamic responses. The Grand Am vehicle configuration was equipped without deployable side-impact countermeasures. The vehicle test was selected without side airbags to eliminate the complications of other inflatable countermeasures and so design iteration could be based on occupant response interaction with the vehicle's intrusion profile.

This multi-step process consisted of creating a baseline model correlated to the occupant responses measured in the IIHS test. Various airbag designs were created and implemented into the baseline model, and iterated on the designs until occupant response goals were achieved.

A modeling technique called Prescribed Structural Motion (PSM) was used to recreate door intrusion. This technique assigns motion to the nodes of an FEM structure according to 3-D displacements in time. Since the IIHS test procedure includes digitized FARO data of the outer door panel pre and post-test, the door intrusion was recreated by assigning displacement of FEM nodes from the pre-test coordinates to the post-test coordinates. Figure 2 illustrate the outer door mesh at the pre and post-test conditions in the model.



**Figure 2. PSM of outer door structure in MADYMO**

Outer door motion was prescribed for all nodes in the representative mesh. Only the nodes along the perimeter of the inner door mesh were prescribed to transfer this motion to the inner door. This allowed the inner door panel to deform independently from the outer door based on material properties assigned to the inner door surface. The baseline MADYMO model was completed by defining contact between the occupant and door, assigning generic material properties to the inner door surface, and prescribing motion with a rough approximation of intrusion rate. The baseline model was simulated and the occupant responses in the model were compared to the IIHS test results.

Occupant responses used to correlate the MADYMO model and IIHS results included: rib deflection and velocity, pelvic force and acceleration, and shoulder force and deflection. Initial model results showed the magnitude and timing of these responses needed adjustment to match the IIHS test results. Model input parameters used to match occupant responses included, outer door intrusion rate, inner door material properties, seat attachment deformations, and friction coefficients

### Problem Definition & Injury Metrics

Before performing model iterations on the airbag designs, it was necessary to establish injury metrics to measure the effectiveness of each design. An extensive review of the IIHS test data showed severe rib deflection and rib deflection rate above injury tolerance levels for the 5<sup>th</sup> female occupant. Crushing injuries in a chest impact tend to be characterized by extensive rib fractures before soft tissues are involved [8]. Consequently the primary injury metric used to evaluate effectiveness of the airbag design in preventing thoracic injury was rib deflections.

The 5<sup>th</sup> female occupant seated height exposes her to increased risk of abdominal rib deflection due to the location of the armrest in the Grand Am vehicle. This situation is reflected in the data as the lower abdominal ribs show greater deflection (~56mm) than the thoracic ribs (~41mm) and correspond to the armrest location. All rib deflections exceeded the injury assessment reference value (IARV) of 34mm for the thoracic ribs and 32mm for the abdominal ribs. Therefore, an airbag solution would need to be designed to reduce loading to all the ribs and minimize the affects of the intrusion at the abdominal ribs.

Other occupant responses, such as pelvic force and shoulder displacement and force, and spinal acceleration were monitored to ensure injury risks were not induced in other body regions due to the TTC designs.

### Occupant Response Comparison

The SID-IIs dummy utilizes five independent ribs to measure rib deflections during side impacts. The top three ribs represent the thoracic region while the bottom two represent the abdominal region.

The process of establishing a satisfactory baseline simulation consisted of correlating known input variables and comparing occupant response values between the IIHS test data and model simulation. In the IIHS test, individual rib deflection and velocity responses in the thoracic region were all similar in magnitude and timing. Abdominal rib deflections and velocities were also similar, but of a higher magnitude than the thoracic ribs due to the impact from the armrest. Table 1 shows the magnitude of rib deflection and the time of initial contact between the inner door and occupant for both the IIHS test and MADYMO model. The difference in impact severity between the thoracic and abdominal regions prompted separate comparisons of each body region between the model and the test.

**Table 1.**  
**Comparison of peak occupant responses and initial contact timing in IIHS test and MADYMO simulation**

Peak Occupant Response	IIHS Test		MADYMO	
	Value	Time (sec)	Value	Time (sec)
Thoracic Rib Deflection (mm)	41	0.021	34	0.023
Abdominal Rib Deflection (mm)	56	0.018	52	0.022
Shoulder Force (N)	2310	0.019	2090	0.018
Pelvic Force (N)	3300	0.019	3340	0.025

The initial TTC design activities were conducted in a simulated dynamic environment and were important that an acceptable correlation between the baseline model and real-world IIHS data was achieved. It was then determined the baseline MADYMO correlation for timing and magnitude of the occupant responses in multiple body regions was satisfactory for the TTC design effort.

## DESCRIPTION OF AIRBAG CONCEPT

The TTC is a seat-based airbag that utilizes a contracting feature of its design. The TTC design is contoured around the occupant's pelvis and lower back to an attachment point on the inboard seatback structure as shown in figure 3.

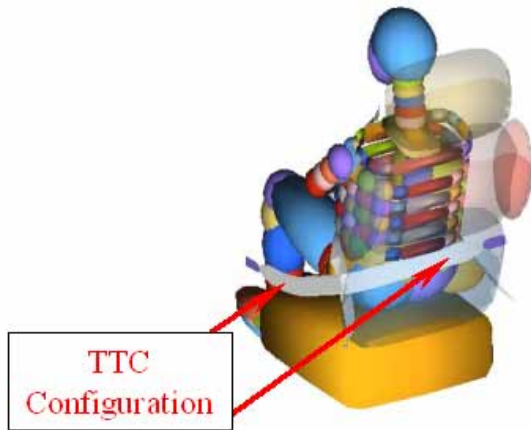


**Figure 3. Model of TTC with seated occupant**

Upon inflation, the tubular airbag increases in diameter while significantly shortening its length. This contracting characteristic can develop significant axial tension between its end attachments, which is used to provide significant occupant restraint in side-impact crashes.

## AIRBAG DESIGN DEVELOPMENT

The capability of MADYMO to accurately simulate airbag deployment characteristics and represent the IIHS dynamic impact event proved ideal for optimizing the TTC design for improved restraint performance. Multiple design iterations were investigated including optimizing airbag coverage, attachment locations, vents, shapes and inflator characteristics.

A prototype TTC was fabricated and attached to a test fixture then deployed with an inflator. The pressure response from this test was used to define the properties of the inflator function and material properties of the simulated TTC. The model correlation of the deployment results is shown in figure 4.

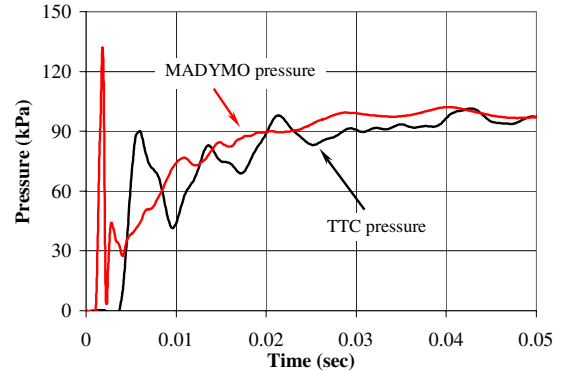


**Figure 4. Model correlated to deployment test data**

## DESIGN SOLUTION

All previous TTC design iterations utilized approaches that interposed the inflatable cushion between vehicle occupants at the ribs and a vehicle's intruding side structure. This approach was unable to sufficiently minimize rib deflections within IARV's. Methods of augmenting additional pelvis interaction while limiting rib interaction demonstrated substantial performance benefits. Nevertheless, these approaches were not within the goals of the IARV requirements.

However, another approach was investigated to better utilize the tensioning characteristic of the contracting TTC feature. A design iteration was developed that consists of an TTC airbag applying a lateral "pre-load" to the pelvis region of the occupant. To accomplish this, the TTC is attached at the front of the seat bottom as previous designs while the rear attachment is routed across the seat back and attached to the inboard seatback structure.

When the TTC is inflated, the tubular airbag contracts between its attachments to create tension. As the TTC contracts to form a straight line between its end attachments, an inboard force is applied against the occupant's pelvis to accelerate the occupant inboard and away from the intruding door. This strategy facilitated inboard movement of the occupant to minimize interaction with vehicle intrusion. A mockup of the TTC is shown in figure 5.



**Figure 5. TTC mockup located with pelvis region**

Thoracic and abdominal peak rib deflections were significantly decreased with the final TTC design iteration. Comparisons of the SID-II's rib deflection responses in crash test simulations with and without the TTC are shown in figures 6 and 7.

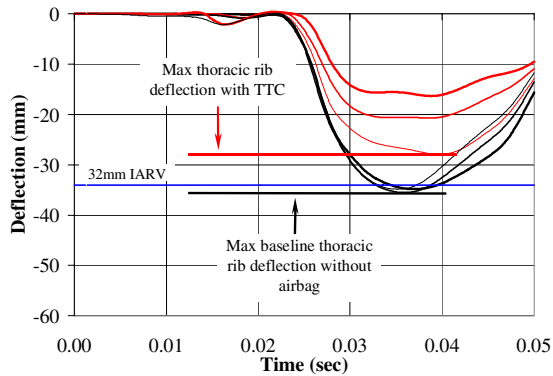


**Figure 6. Comparison of thoracic rib deflection for IIHS simulations with and without TTC**

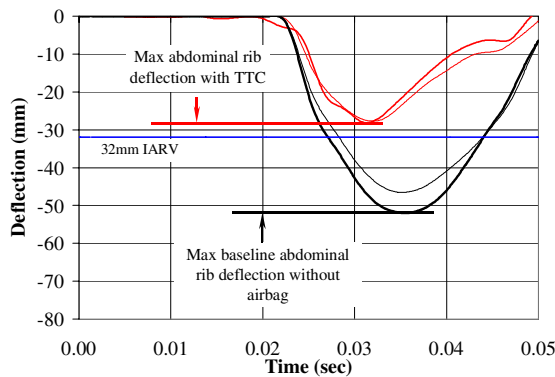


**Figure 7. Comparison of abdominal rib deflection for IIHS simulations with and without TTC**

## PRELOADING THE PELVIS INDEPENDENT OF INTRUSION

The timing of the pelvic response for the baseline test condition was compared to a pelvis-only airbag to identify timing differences when the interaction from the intruding door structure contacts the dummy. The timing of load applied to the pelvis by the pelvis airbag occurs at approximately 14 milliseconds. This contact timing with the pelvis airbag is earlier than the baseline due to the thickness of the airbag. This comparison is shown in figure 8.

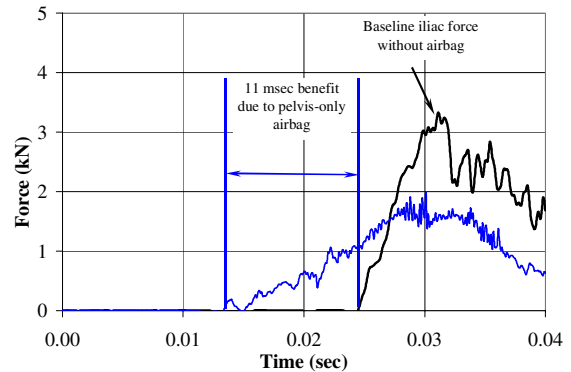


**Figure 8. Difference in pelvis response timing for pelvis-only airbag and baseline condition**

The pelvis force response time shown in figure 9 illustrates a dramatically earlier pelvis response with the TTC than the pelvis only airbag by approximately 9 milliseconds. The inflated airbag thickness of the TTC was the same for the test with pelvis only airbag. Therefore, the earlier response was apparently a result of the contracting feature of the TTC that applied an inboard lateral "pre-load" to the pelvis region of the occupant.

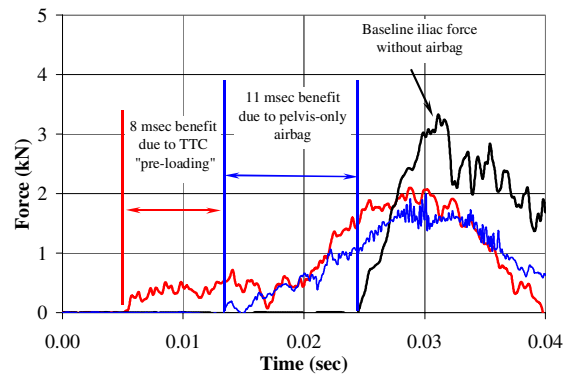


**Figure 9. Timing of TTC pre-loading pelvis**

## PROOF OF PRE-LOAD CONCEPT

The strategy of pre-loading the occupant facilitated inboard movement of the occupant, which minimized interaction with vehicle intrusion in the model simulation. Actual deployment testing of the TTC was then conducted on a rigid seat fixture to validate the model's prediction of pre-loading an inboard motion of the occupant.

Prototypes of the TTC were fabricated and tested with a seated dummy occupant. A 50<sup>th</sup> percentile Hybrid III male dummy was chosen for testing on a surrogate driver's side seat. Tri-axial pelvic acceleration was measured to determine the affect of the TTC loading on the pelvis was not injurious. A Grand Am seat was modified to accommodate TTC attachment locations on the front, bottom of the seat pan and inboard seatback structure. The upper portion of the TTC was placed behind the seatback cushion to investigate its ability to function with cushion interaction. The TTC was routed behind the lower back, over top the lap belt and fixed to the front mount point. High-speed video cameras were placed around the test setup to capture the dummy's kinematic responses during deployment. The overall setup of the static deployment evaluation in a surrogate seat is shown in figure 10.

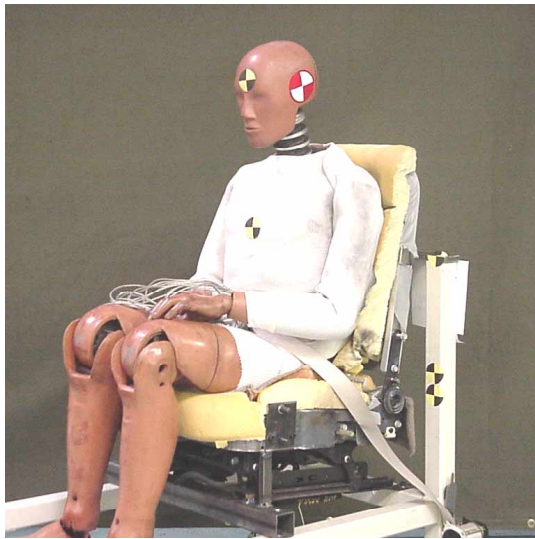


**Figure 10. Hybrid III dummy in seat fixture**

The TTC was deployed as designed. Time-to-position was evaluated from the video to be approximately 4 milliseconds when the TTC coverage was over the pelvis region. Review of the pressure response in figure 11 indicates very little pressure in the airbag during the first 4 milliseconds

due to the remote location of the pressure transducer within the airbag.

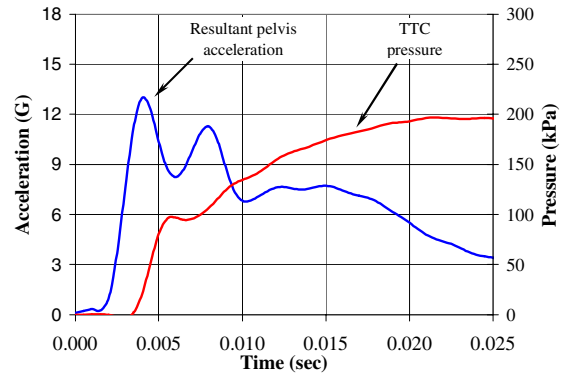


**Figure 11. Timing of pressure response of TTC and pelvis acceleration for Hybrid III dummy**

Maximum pelvis acceleration occurred very quickly due to rapid inflation of the relatively small inflatable volume of the airbag. The pelvis acceleration is due to the inboard movement of the TTC since there wasn't any door or intrusion for the airbag to react against and contact with the dummy. The peak acceleration occurred approximately 4 milliseconds, which corresponds to the time-of-position of the TTC in the video analysis. Peak resultant acceleration was less than 13Gs indicating a minimal injury risk to the lower body during static deployment.

The static deployment test with the 50<sup>th</sup> male dummy demonstrated the TTC was capable of moving an occupant inboard as shown in figure 12. Reference lines are used in the figure to highlight the relative positions of the dummy before and after deployment of the TTC. Alignment of the target on the dummy's chest was used to observe inboard motion. Motion at the pelvis region was likely more substantial than movement observed at the chest target. Nevertheless, this test validated the computer model's prediction of inboard motion of an occupant without interacting with intrusion. The timing response with the TTC in the test further supported timing of occupant interaction in the computer model.

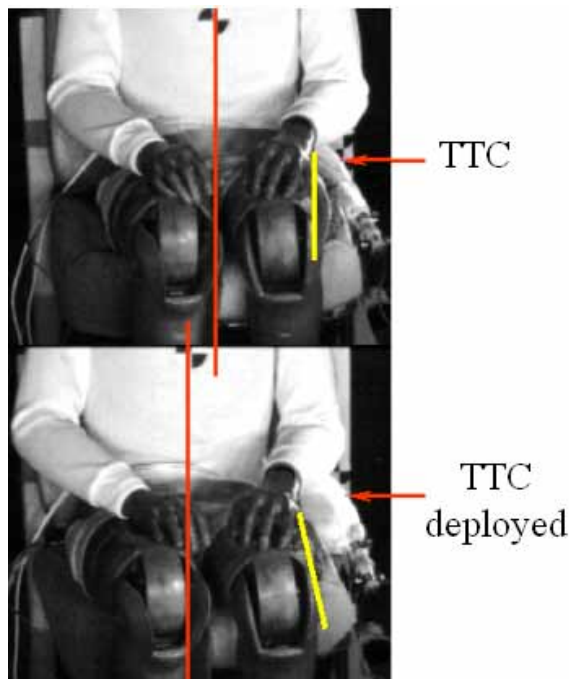


**Figure 12. Video of inboard movement of Hybrid III dummy in seat fixture**

TTC performance and airbag survivability would need to be evaluated in an actual dynamic environment under comparable impact conditions to an IIHS test.

### DYNAMIC EVALUATION OF ITTC

Although the baseline modeling effort yielded a strongly correlated dynamic simulation upon which to design the TTC, concept validation required full dynamic testing.

Dynamic sled testing was designed to allow for repeatable testing at an impact severity equivalent to the full scale IIHS test. The goal was to generate similar rib responses to the baseline model and then evaluate the effectiveness of the TTC in reducing these rib deflections in a dynamic environment.

### Sled Test Setup

A test apparatus was fabricated to allow the occupant to accelerate into a rigidly mounted Grand Am door at an appropriate acceleration pulse in order to evaluate the TTC in a dynamic environment. The occupant was restrained in a sliding seat mounted atop a sled that was allowed to move towards the door upon impact. This setup provided a repeatable test that could utilize the same door trim for multiple tests.

The door was reinforced with welded plates inside the door to support the inner door trim. The reinforced door structure would provide consistent material response and contoured geometry so that multiple tests could be maintained for each test. The height and fore-aft position of the door was positioned relative to the seated location of the SID-II's dummy. Accuracy of the relative position between the armrest and SID-II's abdominal ribs was equivalent to the IIHS test and the computer model setup. Figure 13 shows the SID-II's in the dynamic sled test setup.



**Figure 13. Sled test setup with SID-II's dummy in seat fixture**

A rigid seat was fastened to a sliding base to allow lateral movement of the occupant towards the door upon impact. This motion of the seat towards the door structure simulated intrusion of a vehicle crash.

A baseline test without the TTC was conducted to compare with results from tests conducted with the TTC.

### Sled Test Results

Occupant kinematics of the dummy in the baseline sled test was similar to the dummy kinematics in the test with the TTC with the notable exception of limited motion of the pelvis towards the door fixture. The dummy moved laterally into the rigid door fixture and against the inner door panel as the sled decelerates for each of the two tests. The dummy in the baseline test interacts with the door structure in a relatively upright position exposing the ribs to considerable deflection as shown in figure 14.



**Figure 14. Video frames of baseline sled test without airbag**

However, a space created by the TTC between the dummy's thoracic/abdominal region and the door structure can be seen in the video frame shown in figure 15.



**Figure 15. Video frames of baseline sled test with TTC airbag**

The kinematic difference of the dummy in the TTC test reflected loading of the pelvis prior to contact of the thorax/abdomen with the door. This resulted in a favorable occupant kinematic, which reduced the rib deflection responses in the dynamic test. Also, the strategy of loading the pelvis with the TTC actually reduced the pelvis force as predicted in the computer model.

Thoracic rib deflections were significantly greater in the baseline test than the test with the TTC. The maximum thoracic rib deflections in both tests were the upper thoracic ribs. The maximum rib deflection in the baseline test was 37mm compared to 30mm for the test with the TTC. All of the rib deflection responses are shown in figure 16.

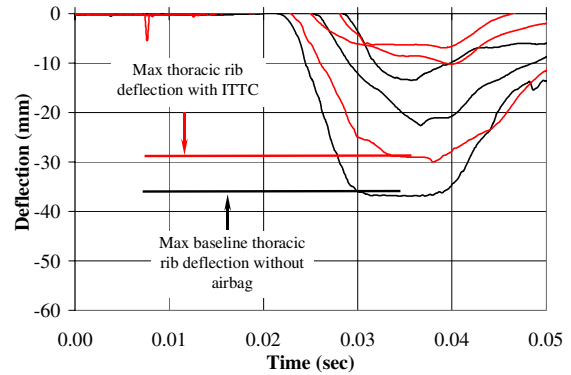


**Figure 16. Comparison of thoracic rib responses in the sled test with and without the TTC**

The responses of the rib deflections in the baseline test compared to the test with the TTC represented a reduction of 21%, 72%, and 31%, for the upper, middle, and lower thoracic rib deflections respectively. The reduced thoracic rib deflections with the TTC indicated a realistic improvement attributable to the airbag system.

However, the data from the baseline test indicated a much more severe impact on the occupant than expected, as shown in figure 17.

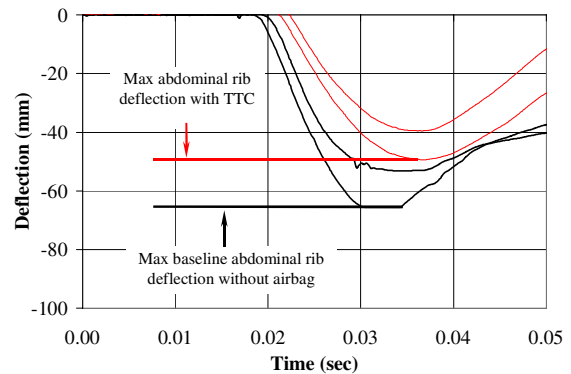


**Figure 17. Comparison of abdominal rib responses in the sled test with and without the TTC**

The upper abdominal rib deflection in the baseline test was 53mm while the lower abdominal rib potentiometer was deflected to its maximum amount of 65mm. The maximum abdominal rib deflection in the test with the TTC was the upper abdominal rib, unlike the maximum deflection occurring at the lower abdominal rib in the baseline test. This represented a 40% improvement between the maximum rib deflections for the upper abdominal rib in the test with the TTC compared to the

maximum deflection for the lower abdominal rib of the baseline test.

Although the baseline occupant responses indicated an impact severity greater than expected, results supported the potential improvement in using the TTC to reduce occupant loading in a dynamic impact scenario. The TTC functioned as designed by preloading the pelvis prior to door impact, applying an inboard lateral force to the occupant inboard, and thus reducing the severity on the thorax and especially the abdominal region. Although pelvic loading was not a primary injury concern throughout this project, the sled testing demonstrated the capability of the TTC to significantly reduce peak lateral pelvis forces. Table 2 is a comparison of the peak occupant responses and percent difference for the tests with the TTC and baseline dynamic sled test.

**Table 2.**  
**Response comparison of maximum occupant responses for baseline and TTC sled tests**

<b>Occupant Response</b>	<b>Baseline</b>	<b>TTC</b>	<b>% Diff</b>
Upper thoracic rib deflection (mm)	37	29	-21%
Middle thoracic rib deflection (mm)	22	6	-72%
Lower thoracic rib deflection (mm)	13	9	-31%
Upper abdominal rib deflection (mm)	53	49	-8%
Lower abdominal rib deflection (mm)	65	39	-40%
Pelvic force (N)	2900	1200	-59%

## DISCUSSION

Computer analysis confirmed that an approach of interposing an inflatable cushion between vehicle occupants at the ribs and a vehicle's intruding side structure may be problematic when attempting to limit rib deflection, particularly for small-stature occupants. However, computer modeling of the TTC airbag have shown to affirmatively load the occupant's pelvis inboard from intrusion during IIHS crash test simulations and subsequently mitigated the effects of contact and interaction between the occupant's rib and the intruding vehicle structure.

A significant reduction in thoracic and abdominal rib deflection as a result of the inboard

pelvis interaction with the TTC airbag was later demonstrated in very severe dynamic sled tests intended to simulate the IIHS side-impact condition. Review of the kinematic response of the SID-II's dummy in the sled test showed noticeable space created by the TTC between the dummy's thoracic/abdominal region and the door structure, which minimized the interaction with the simulated intrusion.

The effect of the deployment timing was illustrated in computer models by comparing the pelvic force time history for the lateral preload system of the TTC and more typical functions of side-mounted airbags, which represents more mainstream designs of current side airbag systems. The inboard lateral preload to the occupant by the TTC would seem to work as well only if the deployment timing of the TTC were sufficiently rapid in order to offer the demonstrated potential increased performance benefit.

Peak pelvis acceleration responses measured in actual static deployment testing occurred very quickly due to rapid inflation of the relatively small inflatable volume of the TTC airbag. The inboard pelvis acceleration of a dummy was created without a door surface to react against as would be required by typical side airbags. The peak acceleration created by the TTC airbag occurred approximately 4 milliseconds, which corresponds to the time-of-position of the TTC in the video analysis. This rapid inflation would be advantageous in real-world side-impacts by quickly positioning the TTC prior to door intrusion.

The current TTC development involved evaluation of design iterations in a simulated dynamic environment. MADYMO was used extensively as the initial tool for optimizing TTC performance and will likely continue, to a lesser degree, to be used to guide design decisions for concept feasibility

## CONCLUSIONS

Feasibility of significantly reducing rib deflection in the IIHS test by preloading the pelvis only, independent of vehicle intrusion, has been demonstrated with a TTC airbag device. Tests with the TTC design at various component and system levels have validated the computer model predictions. Potential benefits due to timing advantage of the TTC in this severe crash environment appear attainable as shown in figure 18.

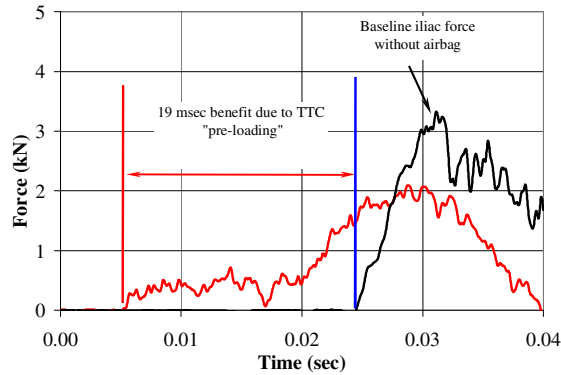


**Figure 18. Potential benefit due to TTC timing**

[8] Chung, J., Cavanaugh, J., King, A., Koh, S., Deng, Y., "Thoracic Injury Mechanisms and Biomechanical Responses in Lateral Velocity Pulse Impacts", 43<sup>rd</sup> Stapp Car Crash Conference Proceedings, October 1999

## REFERENCES

[1] Chan, H., Hackney, J., Morgan, R., "An Analysis of NCAP Side Impact Crash Data", Paper 98-S11-0-12, 16th International Technical Conference on the Enhanced Safety of Vehicles, Windsor, 1998

[2] Sherba, M., "Side Impact Airbags- The General Motors Approach", 17th International Technical Conference on the Enhanced Safety of Vehicles, Paper387, Amsterdam, 2001

[3] Nolan, J., Powell, M., Preuss, C., Lund, A., "Factors Contributing to Front-Side Compatibility: A Comparison of Crash Test Results", 43<sup>rd</sup> Stapp Car Crash Conference Proceedings, October 1999

[4] Dalmotas, D., German A., Tylko, S., "The Crash and Field Performance of Side-Mounted Airbag Systems", Paper 442, 17th International Technical Conference on the Enhanced Safety of Vehicles, Amsterdam, 2001

[5] Monk, M., Sullivan, L., "Side Impact Padding Investigation Study", National Highway Traffic Safety Administration, Department of Transportation Report No. DOT-HS-805-957, March 1981.

[6] Viano, D. "Evaluation of the Benefit of Energy Absorbing Material in Side Impact Protection: Part II", 31<sup>st</sup> Stapp Car Crash Conference Proceedings, November 1987

[7] Friedwald, K., "Design Methods for Adjusting the Side Airbag Sensor and the Car Body", Paper 98-SS-W-17, 16th International Technical Conference on the Enhanced Safety of Vehicles, Windsor, 1998